Developing Tools for Determination of Parameters Involved in CO₂ Based EOR Methods

by © Mohammad Ali Ahmadi

Thesis Submitted to the School of Graduate Studies in partial

fulfillment of the requirements for the degree of

Master of Engineering in Oil and Gas Engineering/Faculty of

Engineering and Applied Science

Memorial University of Newfoundland

September 2017

St. John's Newfoundland and Labrador

Table of Contents

Abstract

To mitigate the effects of climate change, CO_2 reduction strategies are suggested to lower anthropogenic emissions of greenhouse gasses owing to the use of fossil fuels. Consequently, the application of CO_2 based enhanced oil recovery methods (EORs) through petroleum reservoirs turn into the hot topic among the oil and gas researchers. This thesis includes two sections. In the first section, we developed deterministic tools for determination of three parameters which are important in CO_2 injection performance including minimum miscible pressure (MMP), equilibrium ratio (K_i), and a swelling factor of oil in the presence of CO_2. For this purposes, we employed two inverse based methods including gene expression programming (GEP), and least square support vector machine (LSSVM). In the second part, we developed an easy-to-use, cheap, and robust data-driven based proxy model to determine the performance of CO_2 based EOR methods. In this section, we have to determine the input parameters and perform sensitivity analysis on them. Next step is designing the simulation runs and determining the performance of CO_2 injection in terms of technical viewpoint (recovery factor, RF). Finally, using the outputs gained from reservoir simulators and applying LSSVM method, we are going to develop the data-driven based proxy model. The proxy model can be considered as an alternative model to determine the efficiency of CO_2 based EOR methods in oil reservoir when the required experimental data are not available or accessible.

Acknowledgment

My deepest gratitude is to my supervisors, Dr. Sohrab Zendehboudi and Dr. Lesley James, for holding me to a high research standard and teaching me how to conduct successful research. I am especially thankful to Dr. Sohrab Zendehboudi for his friendship and for sharing his vast experience and knowledge over the past year.

Most importantly, none of this would have been possible without the love and patience of my family, especially my mother and father.

Nomenclatures

Abbreviations

AARD = average absolute relative deviation

ACE = Alternating conditional expectations

ARD = Average Relative Deviation

BBU = Bubble Break-Up

BOP = Break-Over Pressure

BRH = Bubble-Rising Height

BRV = Bubble-Rising Velocity

CCE = Constant Composition Experiment

CIT = Critical Interfacial Thickness

CPU = Central Process Unit

EOR = Enhanced Oil Recovery

EOS = Equation of State

ET = Expression Tree

FID = flame ionization detector

GA = Genetic algorithm

GC = gas chromatography

GEMC = Gibbs Ensemble Monte Carlo

GEP = Gene Expression Programming

GOR = Gas to Oil Ratio

GP = Genetic Programming

IFT = Interfacial Tension

LCC = Linear Correlation Coefficient

LM = Levenberg–Marquardt

LPG = Liquefied Petroleum Gas

LSSVM = Least Squares Support Vector Machine

MAE = Maximum Absolute Error

MM = Million

MMP = Minimum Miscibility Pressure

MRI = Magnetic Resonance Imaging

MMSCF = Million Standard Cubic Feet

MSE = Mean Squared Error

M-SIMPSA = Simplex Simulated Annealing Algorithm

NMR = Nuclear Magnetic Resonance

NPV = Net Present Value

OOIP = Original Oil in Place

ORF = Oil Recovery Factor

QP = Quadratic programming

RBA = Rising bubble apparatus

RBF = Radial basis function

RF = Recovery Factor

SCF = Standard Cubic Feet

SLT = Statistical Learning Theory

SR = Standardized Residual

STB = Stock Tank Barrel

SVM = Support vector machine

SVR = Support Vector Regression

SWAG = Simultaneous Water Alternating Gas

TCD = thermal conductivity detector

VIT = Vanishing interfacial tension

VIT = Vanishing Interfacial Tension

WAG = Water Alternating Gas

Variables

P_{ci} = critical pressure of ith component (psi)

P_k = convergence pressure (psi)

ω_i = acentric factor ith component

T_{ci} = critical temperature ith component (^{o}R)

T_b = boiling point temperature (^{o}R)

e_k = the regression error

$x_k = k^{th}$ input data in the input space

α_k = Lagrange multipliers

n = space's dimension

P = Pressure (psia)

T = Temperature (^{o}R)

T = Temperature, (F) (For Swelling Factor)

y_k = output value for a specified input variable (i.e. x_k)

b = a term of bias

w = the vector of weight

γ = the regularization parameter

σ^2 = kernel sample variance

MMP = minimum miscible pressure in MPa

T = the reservoir temperature in $^{\circ}$F

T_{cm} = the pseudo-critical temperature

M_w = the molecular weight of C_{5+} crude

R^2 = Coefficient of determination

Vol. = Volatile components

List of Tables

List of Figures

Chapter one: Introduction

1.1. Background

The oil demand is increasing progressively, mainly in the developing and developed countries for acquiring better living standards. Conversely, crude oil production is steadily decreasing as the reservoirs depletion. After primary production stage practically seventy percent of the initial oil in place in a reservoir is not produced [1-2]. To produce this considerable amount of oil, different Enhanced Oil Recovery (EOR) methods should be applied. There are various methods which are employed for EOR as per the compatibility of the reservoirs and the performance of the method [3-4]. Figure 1-1 depicts the classification of available EOR methods for mature oil reservoirs. Before applying each of EOR methods for increasing the oil production, several studies should be performed. One of these studies is phase behavior investigation which focuses on the behavior of the system including reservoir oil and injected fluid. This investigation helps us to figure out the contribution of different oil production mechanisms and decide which one should be applied. Also, the results from phase behavior study is one of the essential parts for dynamic reservoir simulations [3,5]. CO_2 injection is one of the interesting EOR methods for improving oil production from the matured and depleted oil reservoirs due to promising microscopic sweep through the fine pores of the reservoir and reducing greenhouse gas, especially carbon dioxide, emission into the atmosphere. These characteristics make CO_2 injection as good EOR option, especially in United States [1-5].
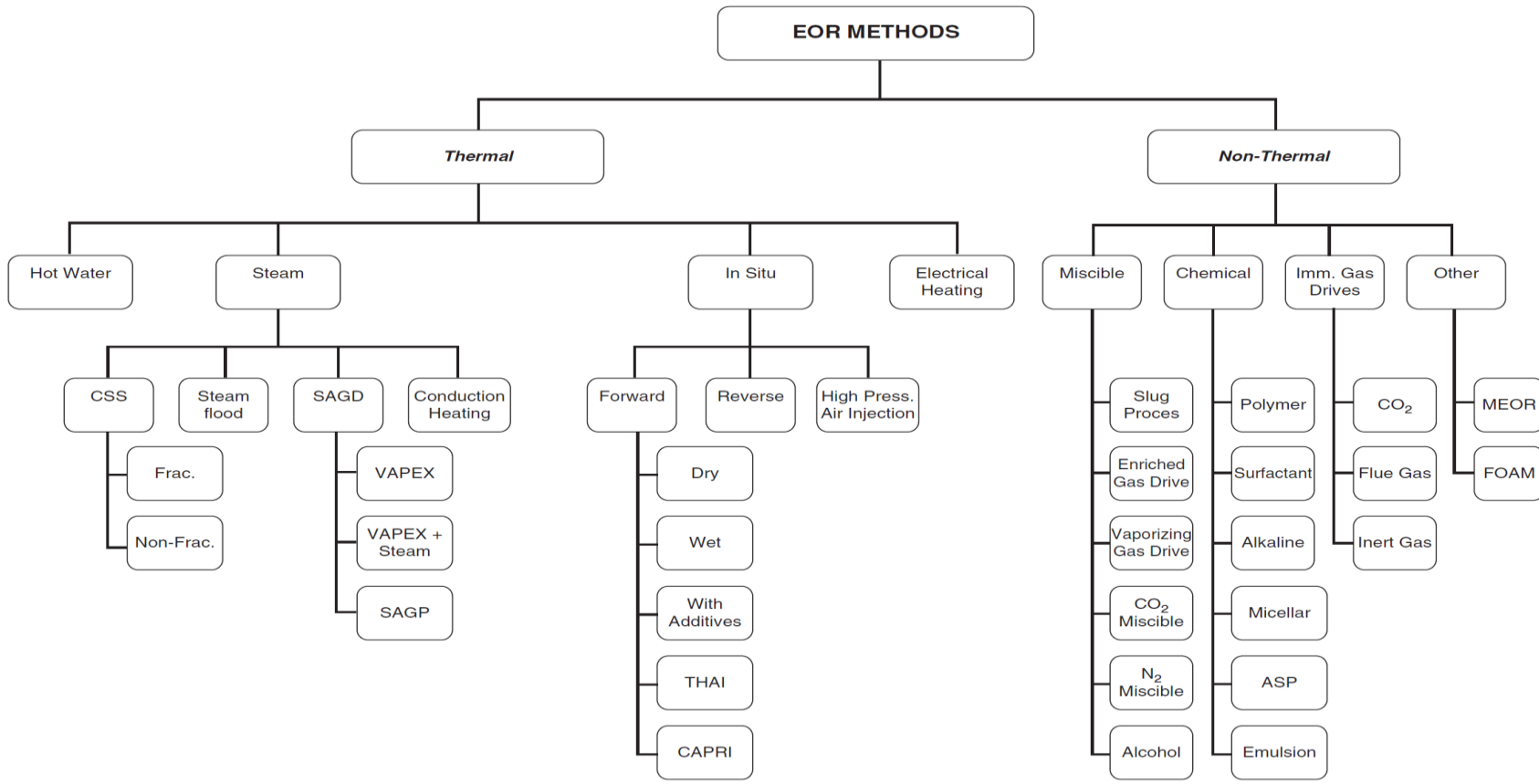
Figure 1-1: EOR classification [5]

1.2. Research Objective and Scope

This thesis includes two sections. In the first section, we developed deterministic tools for determination of three parameters which are important in CO_2 injection performance including minimum miscible pressure (MMP), equilibrium ratio (K_i), and a swelling factor of oil in the presence of CO_2. For this purposes, we employed two inverse based methods including gene expression programming (GEP), and least square support vector machine (LSSVM). In the second part, we developed an easy-to-use, cheap, and robust data-driven based proxy model to determine the performance of CO_2 based EOR methods. In this section, we have to determine the input parameters and perform sensitivity analysis on them. Next step is designing the simulation runs and determining the performance of CO_2 injection in terms of technical viewpoint (recovery factor, RF). Finally, using the outputs gained from reservoir simulators and applying LSSVM method, we are going to develop the data-driven based proxy model. The proxy model can be considered as an alternative model to determine the efficiency of CO_2 based EOR methods in oil reservoir when the required experimental data are not available or accessible.

1.3. Thesis Organization

This thesis is written in manuscript-based format, including five journal papers. Table 1-1 reports the papers published and unpublished during the course of this research. Chapter 2 reviews the previous works done on the CO_2 based EOR methods and the parameters involved in these methods. Besides these parameters, Chapter 2 delve into the proxy model development for EOR purposes.

Table 1-1: Organization of the thesis

Chapter Title	Supporting Paper Title
Chapter 1: Introduction	Not Applicable (NA)
Chapter 2: Literature Review	Worldwide CO2 injection into underground formations: Technical status and Challenges, Submitted to Journal of Petroleum Science
Chapter 3: Equilibrium Ratio of Hydrocarbons and Non-Hydrocarbons at Reservoir Conditions	Equilibrium Ratio of Hydrocarbons and Non-Hydrocarbons at Reservoir Conditions: Experimental and Modeling Study, Fuel (2017), 210, 315-328
Chapter 4: Minimum Miscibility Pressure of CO_2-Oil System in Miscible Gas Flooding Processes	A Reliable Strategy to Calculate Minimum Miscible Pressure of CO_2-Oil System in Miscible Gas Flooding Processes, Fuel (2017), 208, 117-126
Chapter 5: Hybrid Connectionist Model Determines CO_2-Oil Swelling Factor	Hybrid Connectionist Model Determines CO_2-Oil Swelling Factor, Submitted to Journal of Petroleum Science
Chapter 6: Developing a Robust Proxy Model of CO_2 Injection	Developing a Robust Proxy Model of CO_2 Injection: Coupling Box–Behnken design and a Connectionist Method, Fuel (2018), 215, 904-914
Chapter 7: Conclusions and Recommendations	NA

Chapter 3 discusses an easy-to-use and reliable method for calculation equilibrium ratio for both hydrocarbon and non-hydrocarbons, i.e., carbon dioxide, nitrogen, and

hydrogen sulfide. The outputs of the proposed connectionist method were compared to the previously developed models.

Chapter 4 proposes a new method for determination of minimum miscibility pressure (MMP) of the CO_2 injection process using a connections method which is called " Gene Expression Programming (GEP)". The results of the proposed model were compared with well-known empirical correlations.

Chapter 5 presents a novel intelligent based method for predicting CO_2-oil swelling factor using least square support vector machine (LSSVM). To validate the developed connectionist method, an extensive data sample from literature were used and performance of this method were compared with other conventional correlations.

Chapter 6 proposes a proxy model for performance prediction of CO_2 injection process using hybrid of experimental design and LSSVM method.

Chapter 7 reports the main conclusions can be drawn from this thesis as well as recommendations for future works.

References

[1] V. Alvarado, E. Manrique, Enhanced oil recovery: an update review, Energies, 3 (2010) 1529-1575.

[2] M. Blunt, F.J. Fayers, F.M. Orr, Carbon dioxide in enhanced oil recovery, Energy Conversion and Management, 34 (1993) 1197-1204.

[3] S. Kumar, A. Mandal, A comprehensive review on chemically enhanced water alternating gas/CO 2 (CEWAG) injection for enhanced oil recovery, Journal of Petroleum Science and Engineering, (2017).

[4] L.W. Lake, Enhanced oil recovery, Society of Petroleum Engineers (SPE), (1989).

[5] S. Thomas, Enhanced oil recovery-an overview, Oil & Gas Science and Technology-Revue de l'IFP, 63 (2008) 9-19.

Chapter Two: Literature Review

Abstract

After primary production stage practically seventy percent of the initial oil in place in a reservoir is not produced. Producing this huge volume of oil requires to apply different Enhanced Oil Recovery (EOR) methods. There are various methods which are employed for EOR as per the compatibility of the reservoirs and the performance of the method. Carbon dioxide injection is one of the interesting EOR methods for improving oil production from the matured and depleted oil reservoirs due to promising microscopic sweep through the fine pores of the reservoir and reducing greenhouse gas, especially carbon dioxide, emission into the atmosphere. These characteristics make CO_2 injection as good EOR option, especially in United States. There are various phenomena involved in oil production under carbon dioxide injection process including CO_2-oil swelling factor, reduction in oil viscosity, and vaporization and condensation drive mechanisms. The paper discusses the process of CO_2 injection in lab scale, pilot scale, and field scale throughout the world. This paper evaluates the contributor mechanisms in the oil production through carbon dioxide injection as well as assessment of the experimental and numerical works, from pore scale to field scale, and case studies. Besides, this paper provides economic and environmental aspects of carbon dioxide injection. Finally, conclusions have been drawn based on the discussed topics.

2.1. Introduction

One of the main concerns of a human being today is increasing the concentration of greenhouse gases, especially carbon dioxide. Increasing this toxic gas concentration in

the atmosphere affects the life style drastically and results in global warming[1, 2]. There are numerous studies regarding the effect of greenhouse gas on global warming. Unfortunately, most of the carbon dioxide emitted from anthropogenic sources. There are different solutions for this problematic issue including replacing fossil fuels with renewable or sustainable energies, i.e., wind, solar, ocean, and capturing carbon dioxide and sequestering in a geological formation[3-6]. Moreover, the number of the depleted oil fields throughout the world is constantly increasing. In most of these oil fields, the oil recovery factor is lower than 30 percent of the oil in place. Producing such significant volume of oil in these oil fields needs applying enhanced oil recovery (EOR) methods. These EOR methods might be water flooding, gas injection, chemical flooding, and so forth [7]. One of the promising and efficient mechanisms for producing the remaining oil is a CO_2 injection. One of the main advantages of this method is a reduction of greenhouse gas emission into the atmosphere; this advantage drives oil companies to apply this method due to worldwide environmental concerns[8-12]. This driving force resulted in running more than 153 CO_2 based EOR projects in worldwide in recent years. The United States employed 139 miscible CO_2 EOR projects which contribute 41% of oil production from EOR methods in this country; this contribution is higher than any other EOR method [13, 14]. However, other countries also motivated to apply CO_2 based EOR techniques to fulfill environmental considerations of governments as well as increasing oil production after primary production stage. For instance, several projects in Brazil, China, Korea, Mexico, Saudi Arabia, United Emirates, and the United Kingdom have planned to start since 5 years ago. It is worth to mention that due to a sharp drop in oil prices since 2014, some of the CO_2 based EOR projects have held on or cancelled. Also, to make such projects affordable and

8

resistive to lower oil prices, technologies of carbon dioxide capturing and transportation should be developed considerably [1-3, 15-21].

CO_2 based EOR method has different pros for improving oil recovery including improvement sweep efficiency, reducing oil viscosity, oil swelling, development of miscibility at lower pressures and high incremental recovery [22]. To evaluate the performance of CO_2 injection in reservoir scale, compositional reservoir simulation studies are necessary; a comprehensive reservoir fluid model is a crucial section in compositional reservoir simulation. The accuracy of results from the reservoir fluid modeling depends on the precision and reliability of rock and fluid properties determination as well capability of reservoir simulation to regenerate the phase behavior during carbon dioxide injection [13]. There are various challenges in numerical reservoir simulation of CO_2 injection process including hysteresis effect on the relative permeability, three phase relative permeability, dynamic change in oil composition, and consideration of reactive flow; reactive solver should be used in a case of carbon dioxide injection in deep saline aquifer or depleted oil reservoir with high water saturation. Numerical reservoir simulation with reactive geotechnical solver helps us to improve the safety and reliability of the CO_2 injection process; however, doing such a work is very time consuming practice because numerous equations have to solve simultaneously for each grid cell; the number of grid cells for modeling of petroleum reservoirs is typically equal to 2-5 million grid cells. As a result, a compromise between budget, time, and safety concerns is needed [23-25].

Besides the advantages of the carbon dioxide injection, there are different technical and operational issues which might be occurred during the process of carbon dioxide flooding. Changing the oil fluid properties after CO_2 injection could affect the process

9

of miscibility because the oil composition continuously changes during the carbon dioxide injection. This means that after a given time from starting CO_2 injection, new samples should be gathered to update the whole process of CO_2 flooding. For instance, Weyburn oil field in Canada is a good example of this issue [26]. Another probable issue in CO_2 injection is changing the rock properties in terms of mineralogy; however, this issue occurs in a case of CO_2 injection in deep saline aquifers. According to Jensen, there is no significant change in rock properties of Weyburn oil field after a long time of carbon dioxide injection[27, 28]. Khather et al. [29] determined experimentally the effect of carbon dioxide injection in petrophysical properties of dolomites including porosity and permeability of the rock samples. They argued that carbon dioxide injection in aquifer section with dolomite medium could damage severely the rock in terms of flow conductivity. In their results, CO_2 injection could reduce the porosity and permeability by 12% and 57% of original values, correspondingly. However, they pointed out that this damage caused by domination of mineral precipitation versus mineral dissolution process[29]. Another concern regarding carbon dioxide injection is the drastic effect of carbon dioxide on the environment, especially plants and microorganisms, due to probable leakage during the injection process. However, there are two different viewpoints regarding this issue; some scholars pointed out further investigations are required to determine side effects of CO_2 contaminants; on the other hand, several researchers discussed CO_2 contaminants have a severe damaging effect on plants and microorganisms if CO_2 leakage occurs [30-32].

The main aim of this paper is to review and discuss the existing and up-to-date research advances in grasping the various mechanisms which are contributed in oil production during CO_2 based EOR methods, particularly simultaneous water alternating gas (SWAG) injection, continuous CO_2 injection, and water alternating gas (WAG)

injection processes. A comprehensive review for carbon dioxide injection from pore scale to field scale is provided in the following sections. In view of the status of the CO_2 based EOR methods, this paper discussed and reviewed some of the recent developments and chances accomplished by the use of the CO_2 based EOR methods in oil recovery and their limitations to execute in both offshore and onshore oil fields. Also, practical issues associated with the process of carbon dioxide injection are explained, and several recommended solutions have provided. Finally, different issues, especially environmental and economic concerns, associated with these EOR methods have been reviewed.

2.2. A review on CO2 injection processes/operations across the world

To specify the performance of CO_2 injection different apparatuses can be employed; these devices determine various mechanisms of oil production from pore scale to core scale. Ning et al. [33] carried out several multiple contact experiment (MCE) to figure out the contribution of oil swelling as well as reduction in oil viscosity on oil production from Alaska North Slope viscous oil. Heidaryan and Moghadasi [34] investigated the effect of swelling and viscosity reduction on the oil production using both experimental and theoretical methods. Based on the results, they concluded that the optimum value of CO_2-oil swelling factor should be 1.7 to reach maximum oil production from the reservoir[34]. Or et al. [35] investigated experimentally the contribution of CO_2-oil swelling and viscosity reduction using CO_2 gas foaming in heavy oil reservoirs. According to the experimental results, they concluded that CO_2 foam swelling increases with increasing the pressure drawdown of the well. Also, higher swelling of foamy oil could mobilize the residual oil to the producer well, especially in the immobilized

zone[35]. Habibi et al. [36] carried out experiments on CO_2-oil system in a tight formation to figure out the interaction between CO_2 and oil in a tight rock samples. They conducted constant composition experiment (CCE) to determine the CO_2-oil swelling factor and other measureable data. Also, they performed CO_2 cyclic injection experiments to determine the amount of oil recovery factor. In their experiments, increasing CO_2 concentration from 48.36% to 71.06% resulted in increasing in CO_2-oil swelling factor from 1.211 to 1.390, respectively. According to the experimental data, they concluded that different mechanisms contributing in oil production including oil swelling and expansion, CO_2 dissolution into the oil, and CO_2 diffusion into core sample[36].
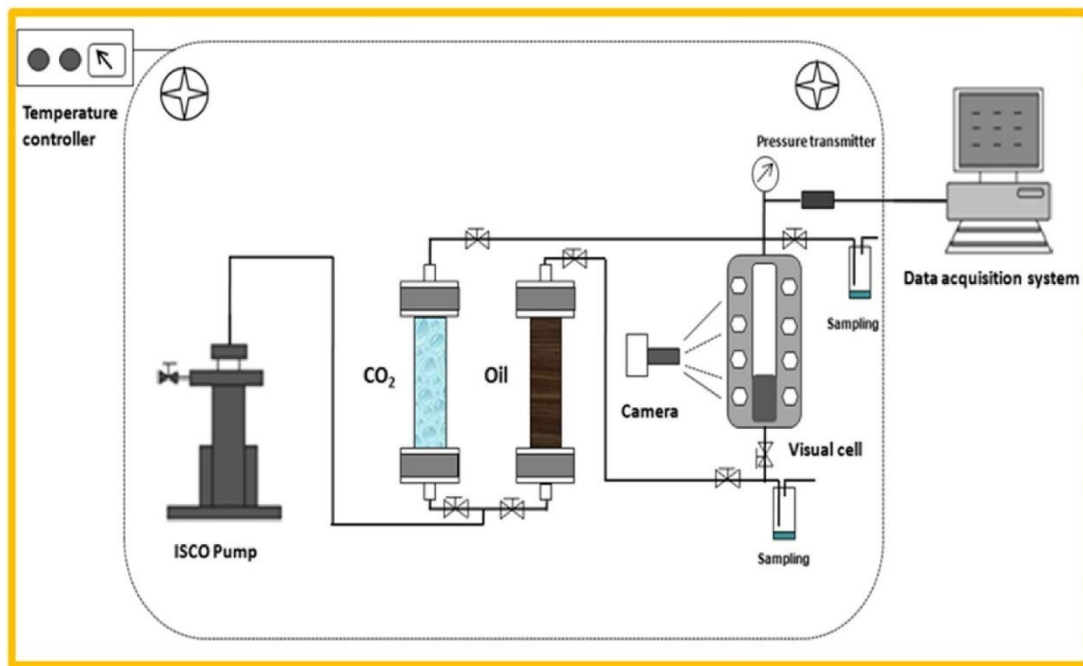
Figure 2-1: Schematic of visual phase behavior experiment[37]

Dehghan et al. [38] employed micro-model visualization method to find the effect of fracture network on the performance of WAG injection. They also studied the effect of

WAG ratio, slug size, and injection rate on the performance of WAG injection process. They provided a correlation for capillary number in a fractured porous media. They used oil wet micro-models in all the experiments[38]. Robin et al. [39] carried out several tests on high pressure-high temperature micromodels to determine the possible mechanisms of production during CO_2 injection process. Experimental data revealed that interaction between carbon dioxide and oil could destabilize asphaltene phase in oil as well as this interaction might results in foam formation[39]. Sugai et al. [40] conducted systematic experimental study on oil swelling factor determination in porous media using two different types of micromodels. They employed two micro models including fine beads and coarse beads micro-models to figure out the effect interfacial area on oil swelling and CO_2-oil swelling factor. They employed glass beads with two different diameters to figure out interfacial area effect on oil swelling factor. To find the amount of oil volume at different time they employed digital camera and taken images was processed using image processing software. They evaluated the steadiness of oil saturation in their micromodels to validate that they can calculate swelling factor from their experiments. Also, they carried out oil-CO_2 simple contact model in a visual cell to determine CO_2-oil swelling factor at different pressure using digital camera and image processing method. They compared CO_2-oil swelling factor from both experiments to determine which extra parameters should be taken into account for further works. According to the experimental results, they concluded that increasing in the interfacial area results in increasing swelling of oil. In other words, the swelling factor in a case of fine beads micro-model was larger than this value in a coarse beads micro-model due to increasing in the interfacial area[40]. Seyyedsar and Sohrabi [41, 42] studied experimentally the microscopic oil displacement mechanisms of immiscible carbon dioxide flooding using high pressure- high temperature micro-model. They

13

concluded that displacement of carbon dioxide rich phase is much easier than those ones in oil rich phases[41, 42]. Also, they discussed the extraction process occurs in a near wellbore, particularly injection wells. Cui et al. [43] carried out various experiments to figure out the mechanism involved in oil production through CO_2 injection in microscopic scale. They employed micro models at reservoir pressure and temperature. They concluded that presence of water could delay the time required for CO_2 dissolution into oil and higher pressure facilitated the process of CO_2 dissolution mechanism. Figure 2-2 depicts the schematic of micro-model setup for EOR purposes.
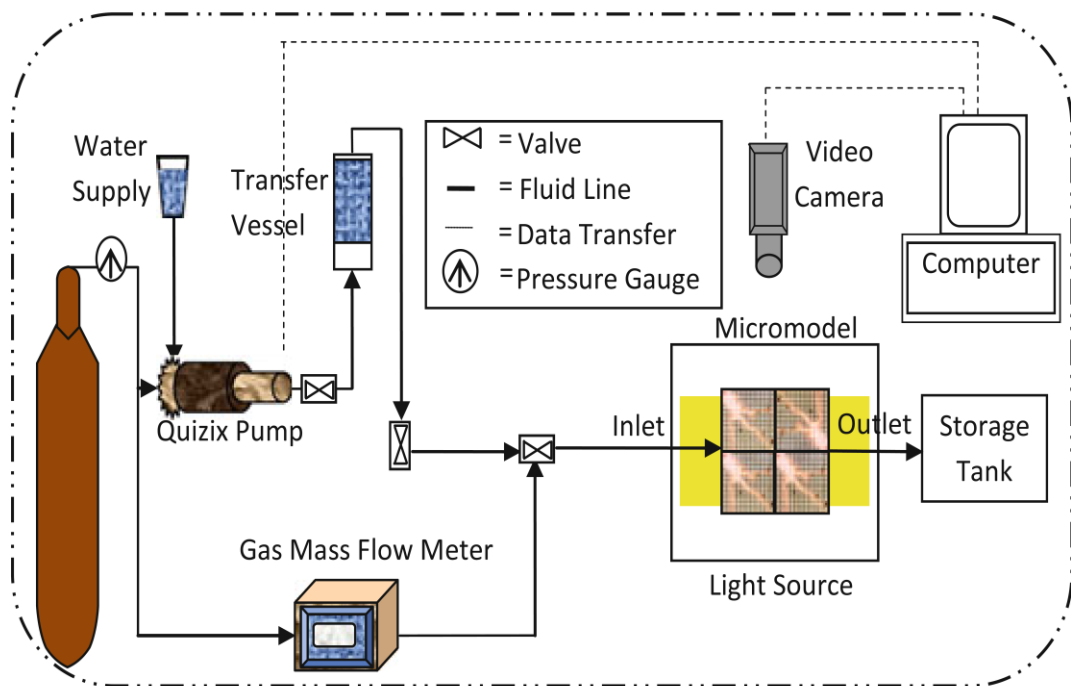
Figure 2-2: Schematic of micromodel visualization apparatus for EOR purposes [38]

One of the most common experiments to figure out the performance of CO_2 injection as well as the value of MMP is slim tube test. Slim tube test provides useful information regarding gas enrichment effect of oil recovery factor and MMP value; however, this

test is too expensive and time-consuming[44-46]. Figure 2-3 shows a graphical demonstration of slim tube apparatus.

1- Pump
2- Oil Accumulator
3- Gas Accumulator
4- Packed Tube
5- Sight Glass
6- Back Pressure Regulator
7- Separator
8- Gas Chromatograph
9- Gas Meter
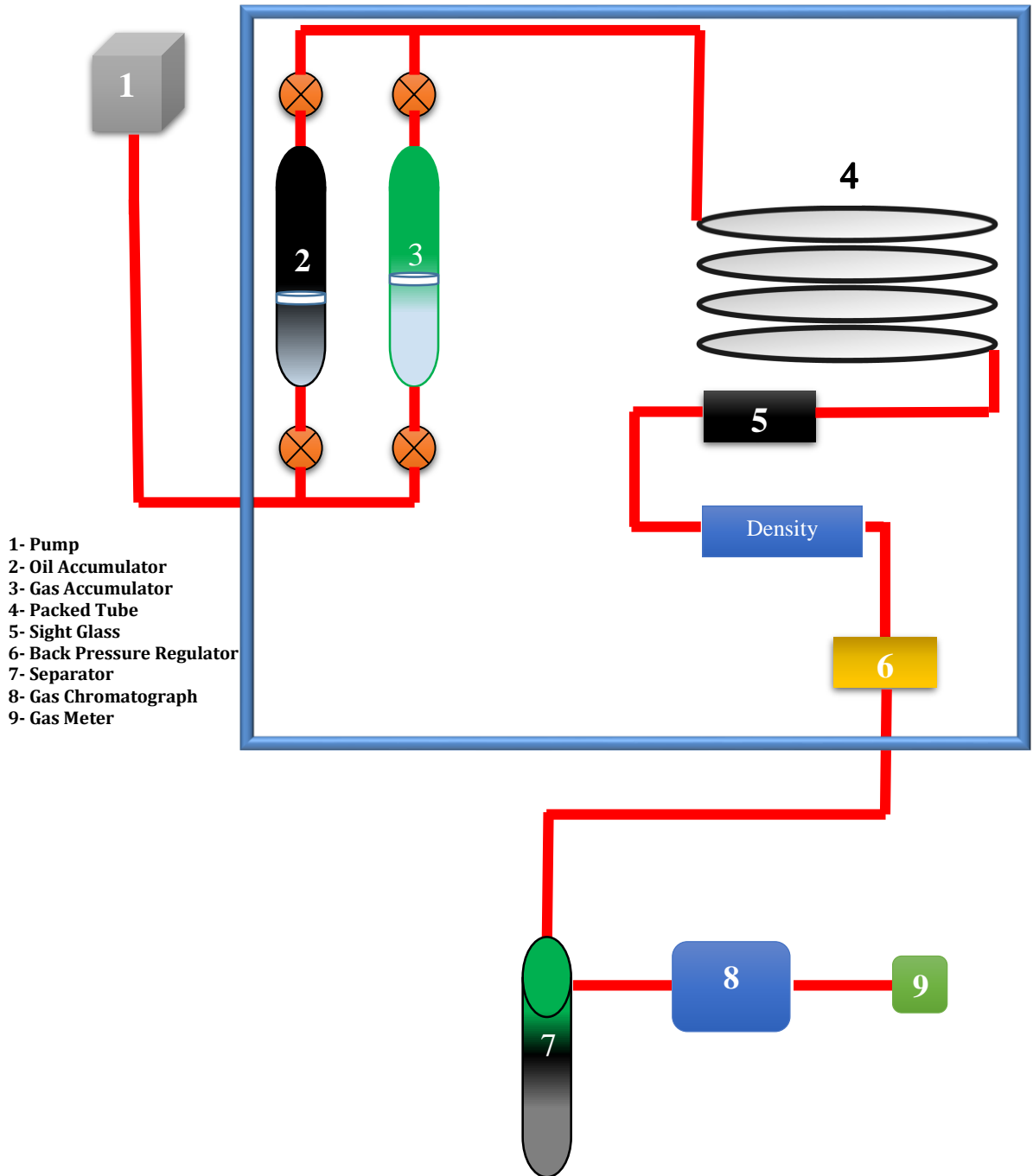
Figure 2-3: Schematic of slim tube experiment [47]

Monger et al. [48] conducted both laboratory and field study of the CO_2 huff 'n' puff process to improve oil recovery from light oil reservoirs. They carried out CO_2 cyclic core flooding experiments with both live and dead oil samples on the Berea Sandstone core. They determined CO_2-oil swelling factor in their experiments. Based on the experimental results, they concluded that the main mechanism contributing in oil production was oil swelling; however, the amount of CO_2-oil swelling factor was not too high. Also, they studied 65 single well CO_2 injection and determined the contribution of oil swelling and solution gas drive mechanisms in oil production. Based on the field observations and experimental data, they concluded that the main oil production mechanism was oil swelling alone[48]. Thomas and Monger [49] studied on the effect of CO_2-oil swelling factor in oil recovery from light-oil reservoirs using core displacement experiment. They correlated the oil incremental value from cyclic CO_2 injection to the CO_2-oil swelling factor. Based on the results, increasing in CO_2-oil swelling factor resulted in increasing in the amount of produced oil[49]. Srivastava et al. [50] carried out an experimental study on CO_2 flooding in Weyburn core samples and they concluded that two main factors contributing in oil production were oil swelling and reduction in oil viscosity. Yongmao et al. [51] investigated systematical experiments to figure out which parameters involved in the oil production of CO_2 flooding. Based on the experimental results, they concluded that the main factor contributing in the incremental oil production was oil swelling and the degree of swelling presented by swelling factor. Swelling factor in their experiments was 1.4 and they pointed out this value means high contribution of oil swelling mechanism in the oil production. Kamali et al. [52] carried out several CO_2 injection experiments on the sandstone core samples at different miscibility condition. Based on the results, they concluded that the oil recovery factor in both near miscible and miscible condition is

almost the same; however, lower oil recovery factor can be gained in immiscible flooding. Also, in immiscible CO_2 injection lower heavy component, especially decane, can be produced. Kamali et al. [53] investigated experimentally both continuous CO_2 injection, WAG, and SWAG injection at different miscibility condition on sandstone core samples. They concluded that based on the experimental results oil recovery factor of WAG injection process was greater than those in SWAG and continuous CO_2 injection[53]. Figure 4 illustrates the schematic of core displacement test for EOR purposes.
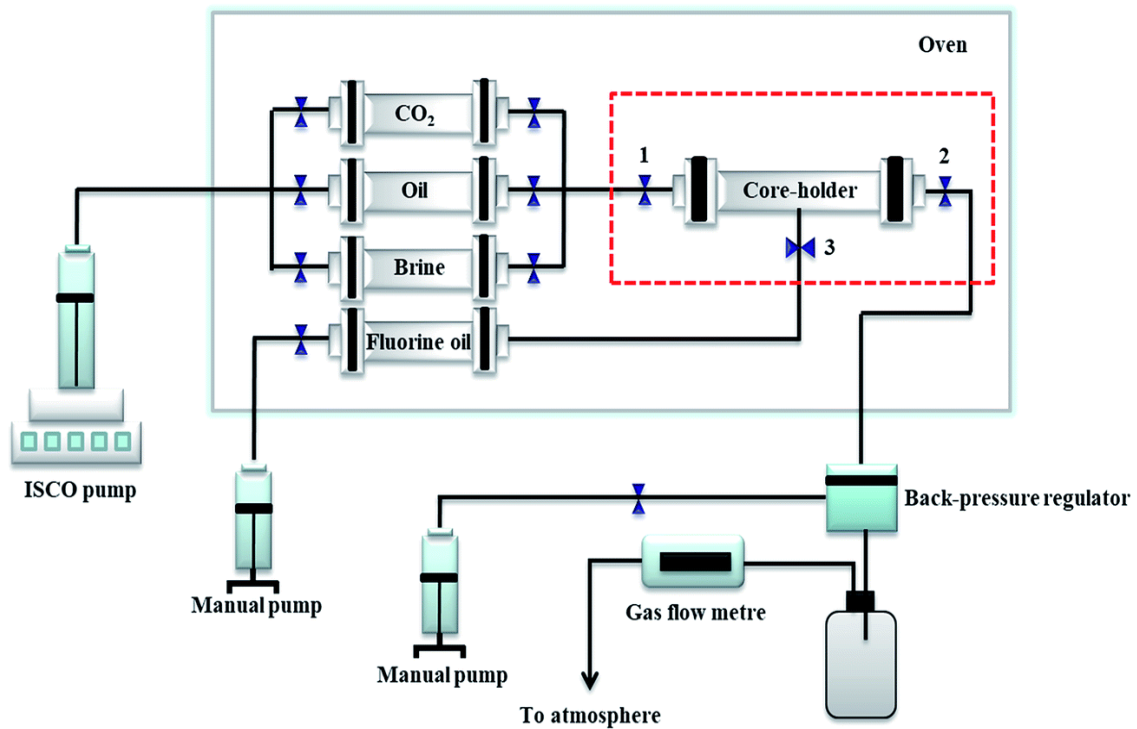
Figure 2-4: Schematic of core displacement test [17]

CO_2 injection can be applied in different ways either as continuous CO_2 flooding, CO_2 foam or WAG/SWAG injection[54]. In a case of WAG/SWAG injection, the amount of water/gas ratio and frequency should be determined prior to field test. Frequency

defines as the number of cycles required for CO_2 and water injection. Moreover, the water/gas ratio is defined as the volume of the injected water to the volume of the injected CO_2 in each cycle[54]. To determine these parameters two main options are available including experimental tests and reservoir simulation which are discussed in the following sections.

Carbon dioxide injection can be executed in different configurations including single well, huff n puff injection, and multi-wells injection. In a case of standard single well CO_2 injection, particularly in immiscible carbon dioxide flooding, carbon dioxide is injected through injection well and oil produces from a production well or wells. In some cases, carbon dioxide is flooded via injection well and produced from four production wells; this configuration is called five spot pattern[44, 55]. In a case of huff-n-puff CO_2 injection, the injection well and production well is the same. In this process, a candidate production well is shut-in and then, carbon dioxide is injected for a given time. In the next step, again the production well maintains zero production; this time is called soaking time. After a specific soaking time, oil production from the producer well is started; the process of huff n puff injection also called cyclic CO_2 flooding. In this case, the amount of required carbon dioxide, and soaking time should be optimized. Cyclic carbon dioxide injection is a good option for heavy oil reservoirs[44, 56-62]. The more frequent CO_2 injection pattern for EOR purposes is multi-wells injection. In this configuration there are different injection wells and different processes including continuous CO_2 flooding, WAG, and SWAG injection can be applied simultaneously. For example, in one injection well CO_2 is injected continuously; however, in other injection well WAG process has been employed. In a case of WAG and SWAG

injection different parameters including WAG ratio, the number of cycles and the amount of required carbon dioxide should be optimized[44, 63].

2.3. Field experience of CO_2 injection processes for underground formations

CO_2 injection process was firstly applied in 1972 in the Sacroc oil field located in Permian basin, Texas[64]. This oil field was discovered in 1948 and crude oils of this field have 42-degree API. In this field five spot pattern was employed as well configuration for this EOR scheme. The estimated oil reserve of this field is 951 million barrels of oil. Since 1972 miscible and near miscible CO_2 injection the oil recovery factor improved by 3% of oil in place up to 1978[13, 44, 65-68].

Another field pilot application of immiscible continuous carbon dioxide injection in two oil fields in Trinidad and Tobago. These oil fields are Forest reserve and Oropouche. Oil gravity of the crude oils from these fields vary between 17 to 29 ^{o} degree API. In these oil fields four different immiscible CO_2 injection projects have been done since 1974. First CO_2 injection in Trinidad and Tobago was initiated in 1974 through upper Forest sands. The estimated volume of oil in this reservoir is equal to 1.874 million barrels of oil. This EOR scheme improved oil recovery performance by 7.6% of original oil in place (OOIP); this pilot is called EOR 33. Upper cruse sands in Forest reserve field contains 36.4 million barrels of oil and CO_2 injection in this reservoir resulted in 4.7 % incremental oil recovery factor. This project is known as EOR 4 in this oil field. Another reservoir under immiscible CO_2 flooding is lower Forest sands which contains 16.194 million barrels of oil. CO_2 flooding in this section improved the oil recovery factor by 9% of oil in place since 1976 and this project is known as EOR 33. Sandstone reservoir of Oropouche oil field is another pilot for immiscible CO_2

injection in Trinidad and Tobago and the process of CO_2 flooding was initiated in 1990. The estimated recoverable oil from this reservoir is equal to 8.728 million barrels of oil and CO_2 flooding yielded 3.9 % additional oil production; this project is known as EOR 44[44, 69, 70].

Little Creek field is a sandstone oil field located in Mississippi, United State; this oil field was explored in 1958 by Shell company. The estimated oil reserve of this oil field is equal to 102 million barrels of oil. The oil samples from this field have 39-degree of API. The process of miscible carbon dioxide injection in this field was initiated in 1985. Miscible CO_2 injection improved the performance of oil recovery factor by 18.4 % of oil in place[69, 71, 72].

Bati Rahman oil field located in southeast Turkey was found in 1961. This oil field contains heavy oils with 11-degree API and the amount of in place oil is approximately 1.85 billion barrels of oil. Immiscible CO_2 injection was selected for enhancing oil production from this oil field and this process was started in 1986 through impure CO_2 injection. It should be noted that this oil field was under water flooding from 1975 to 1985. Since 1986 more than 6 percent of the in place oil was produced[73].

Another field experience was done in East Ford oil field which located in Texas, United States; this oil field comprises sandstone rock. Oil gravity of this field is equal to 40-degree API and the predicted volume of the recoverable oil from this field is equal to 18.4 million barrels of oil. The process of miscible CO_2 injection in this oil field was started in 1995. Miscible carbon dioxide flooding in East Ford oil field enhanced the oil production rate; this EOR scheme increased oil recovery factor by 1% of oil in place[69, 74].

CO_2 injection process was started in Weyburn oilfield located Saskatchewan, Canada, since 2000. This project is one of the largest carbon dioxide sequestration as well as EOR projects in the world. This oil field has 180 square kilometer area which discovered in 1954. This oil field comprises both low permeable chalky dolomite and fractured limestone. API degree of the reservoir oil fluid varies between 25 to 34 degree of API[75]. Source of CO_2 supply is a coal gasification plant in Beulah, North Dakota [76].

Another field application of miscible carbon dioxide flooding in north of America is miscible WAG injection in Cogdell Canyon Reef oil filed which is located in Texas, United States. This oil field is mainly limestone and crude oil of this reservoir has 40-degree API. The recoverable oil reserve from this oil field is equal to 117 million barrels of oil. The process of miscible WAG injection in this field was initiated in 2001. This process improved the oil recovery factor from this field by 11% of original oil in place[69, 77].

Dulang oil field located in Malaysia was selected to apply immiscible WAG injection. The process of immiscible WAG injection in this field was started since 2002 in three reservoirs including E12, E13, and E14. Injecting immiscible WAG resulted in 5 to 7 % additional oil recovery as well as high produced gas with high CO_2 concentration, near 50%. It is worth to mention that this oil field has a waxy oil; to enhance the performance of WAG injection a down-dip scheme along with lateral water injection was used [78-80].

Chihuido-de-la-Sierra-Negra is an under-saturated sandstone oil field located in Argentina. The crude oil of this oil field has 33-degree API. Unfortunately, several operational problems reported during WAG injection process including early

breakthrough of CO_2, problem in CO_2 supply pipelines, as well as failure in the casing of injection well. However, immiscible WAG injection in this reservoir yielded 3 to 8 % of additional oil recovery is reported for this EOR scheme[78, 81].

Lockhart Crossing field is a sandstone oil field located in Louisiana, United states; This oil field was discovered in 1982. Produced oil from this oil field has 42-degree of API and the amount of oil in place in this field is equal to 56 million barrels of oil. Miscible CO_2 injection process in this oil field was initiated in 2007. Miscible carbon dioxide injection in this oil field improved oil recovery factor by 2.7 % of in place oil[69].

Katz Strawn oil field is located in Stonewall County, Texas; this field was found in1951. This field comprises sand stone and reservoir oil fluid has 38-degree API and 2.3 cP viscosity. The estimated oil reserve for this oil field is equal to 206 million barrels of oil. In this oil field both continuous CO_2 flooding and WAG injection were started in 2010. Both injection processes were applied in miscible condition. Miscible CO_2 injection in this oil field resulted in 0.3% improvement in oil recovery factor [69, 82].

Lula oil field in Santos Basin, Brazil, was discovered in 2006. The crude oils from this oil field have 28 to 30 degree of API. The estimated oil in place for this oil field is 5 billion barrels of oil. In 2011 CO_2 injection in a pilot scale was successfully initiated. Due to the promising outcomes from pilot scale tests, Petro Bras started CO_2 injection process in a field scale in 2013. Petro Bras employed both miscible CO_2 flooding and WAG injection in this oil field[83].

CO_2 injection process in Bell Creek oil field located in Fremont County, Wyoming, United States, was started in 2013 using anthropogenic CO_2 source provided by capture plant at ConocoPhillips Lost Cabin in a center of Wyoming. This CO_2 capturing plant delivers near 50 million cubic feet of carbon dioxide per day. The Bell Creek oil field

was found in 1967 and the amount oil in place for this field estimated 350 million barrel of oil. Before starting CO_2 injection process the cumulative oil production was near 133 million barrels of oil. It is expected via CO_2 injection method an additional 35 million barrels of oil can be produced[84, 85].

2.4. CO_2 injection into underground formations: Description and Mechanisms

From a miscibility viewpoint, CO_2 based EOR methods could be applied in miscible and immiscible conditions [15]. Miscibility phenomenon occurs in the miscible CO_2 injection, and solubility phenomenon occurs in the immiscible CO_2 injection [12, 86, 87]. As a rule of thumb for selection which reservoir is appropriate for applying CO_2 injection, a miscible CO_2 injection might be a good candidate for oil reservoirs located at more than 915 m depths and with more than 25° API oil gravity. So, miscibility between CO_2 and oil can only be accomplished under certain temperature and pressure [86]. On the other hand, for immiscible CO_2 injection, there is no requirement for miscibility; immiscible CO_2 injection can be used in heavy oil reservoir or shallow light oil reservoirs [12, 13, 87].

2.4.1. Miscible CO_2 Injection

After a certain injection pressure, there is no significant change in oil recovery value; this certain injection pressure is called "minimum miscibility pressure" which can be predicted using empirical correlations and/or experimental methods [88-90]. So, to reach maximum oil recovery in CO_2 injection in oil reservoirs, the pressure in the injection facilities, as well as reservoir pressure, should be greater than the CO_2-oil minimum miscible pressure [91]. One of the interesting and promising pros of CO_2 in

comparison with the other types of gases, i.e., nitrogen or methane, is low minimum miscibility pressure. This advantage makes CO_2 as an attractive EOR agent which is capable of using in the broad range of the oil reservoirs throughout the world [13, 91]. Two main mechanisms in miscible flooding processes are multiple contact miscibility and first contact miscibility. Jarrell et al. [44] described the process of CO_2 miscibility using the transition zone between the production and injection wells. Jarrell et al. [44] pointed out that there is mass transfer between oil phase and injected CO_2 and this mass transfer produces a transition zone which is miscible with the CO_2 in the back and with oil bank in the front [13].

2.4.1.1. First Contact Miscibility

First contact miscibility defines as a solvent injection process that the solvent and oil become miscible when they first make contact[44]. The mechanism of oil production using liquefied petroleum gas (LPG) and propane injection in light oil reservoir could be first contact miscibility phenomenon. In other words, first contact miscibility occurs at a given pressure and temperature of the reservoir and the solvent and oil make a single phase fluid at any portion of the solvent and oil [44].

2.4.1.2. Multiple Contact Miscibility

Multiple contact miscibility defines as a solvent injection process which miscibility occurs after several different contacts. The oil production mechanism behind most of the miscible gas injection process can be multiple contact miscibility phenomenon [13, 92]. Also, in most oil reservoirs, CO_2 cannot reach first contact miscibility within a practical range of pressures and needs multiple contacts, in which components of the

oil and CO_2 transfer between the phases until the formation of a homogeneous phase using the processes of condensation/ vaporization [13, 91, 93].

2.4.1.2.1.   Vaporizing Gas Drive Mechanism

Based on the oil composition and thermodynamic conditions, i.e., pressure and temperature, carbon dioxide is capable of extracting or vaporizing some intermediate oil components. Vaporizing gas drive mechanism defined as a process in which at contact point of an injected lean gas and reservoir oil rich in intermediate components, some intermediate components vaporize from oil phase into gas phase. During vaporizing gas drive mechanism, a miscible transition zone is created and moves toward the production well and the oil bank behind it. However, several unflavor conditions might affect this process which includes reservoir heterogeneity and limited contact area during injection due to channels and fractures. This vaporization phenomenon facilitates miscibility process at displacement front [44, 89]. The vaporizing gas drive mechanism occurs in a case of a multiple contact miscibility process. It is worth to point out that for occurring this mechanism the pressure at the interface between injected gas and oil phase should be high enough, and oil phase should be enriched with intermediate components C_2-C_6. Carbon dioxide has very low dynamic miscibility pressure in comparison with other gases used as EOR agent. Using carbon dioxide as an injection gas results in vaporization of more intermediate components compared to other gases; this is one of the main pros of CO_2 injection process.

2.4.1.2.2.   Condensing Gas Drive Mechanism

Condensing gas drive mechanism defined as a process in which at contact point of enriched injection gas and intermediate lean reservoir oil, some intermediate

components condensing from injection gas into the reservoir oil. In miscible CO_2 injection, condensing gas drive mechanism occurs after stripping intermediate oil components when the enriched injection gas encounters fresh oil bank toward production well [44, 89]. A miscible transition zone develops owing to condensing some intermediate components from injected gas phase into oil phase. At that point a mechanism like the vaporizing gas drive mechanism will be established, and the reservoir oil behind the injection front becomes gradually lighter. Due to the oil swelling phenomenon the oil bank behind the injection front will occupy a greater pore volume than the fresh reservoir oil. Based on this mechanism the oil bank stripped of intermediate components behind the injection front will create a mobile zone and this process is continuous until the conditions of miscibility encountered. As described previously, carbon dioxide cannot reach first contact miscibility; however, via a vaporizing gas drive mechanism CO_2 enriched with some intermediate component of oil which vaporized from the oil phase. These are consequently re-condensed at the injection front forming an enriched region with satisfactory mobility properties, denoted as a combined condensing and vaporizing drive mechanisms [94].

2.4.2. Immiscible CO_2 Injection

Immiscible CO_2 injection might be a good candidate in some cases in which the reservoir pressure is low compared to MMP value, or oil composition is not appropriate for miscible injection. In these cases, immiscible CO_2 injection could be one of the options as an EOR method. In a case of immiscible CO_2 flooding there is no single phase creation between oil phase and injected carbon dioxide; however, some carbon dioxide dissolved in oil phase. Two concurrent phenomena including reducing oil viscosity and swelling oil with contact CO_2 are the dominate mechanisms which

contribute to the oil production using immiscible CO_2 flooding[44, 90, 94-98]. Dissolving carbon dioxide into oil results in swelling oil and at the same time the oil viscosity reduces. As a result of these mechanisms, clearly the oil production facilitates and improves; however, the amount of oil incremental value highly depends of the amount of viscosity reduction as well as CO_2-oil swelling factor[95].

Comprehensive understanding regarding the phenomena and mechanisms behind the CO_2 based EOR methods is important for effective field application. Besides the reservoir pressure maintenance as a main goal of the gas injection processes, which supports the "artificial drive" for enhancing the oil production, CO_2 based EOR methods employ other mechanisms to improve the oil recovery factor. According to Jarrell et al.[44], Rojas and Ali [99], and Kulkarni [100], different mechanisms contributing in oil production in a reservoir under CO_2-based EOR method; these mechanisms are reduction of oil viscosity, oil swelling, and vaporization and extraction of some intermediate components in oil phase. Oil swelling and reduction in oil viscosity occur at the same time; this means that some carbon dioxide diffuses into oil phase then oil swells and viscosity reduced [12, 13, 44, 89]. However, the significance of the each of these processes depends on the reservoir temperature and pressure, as illustrated in Figure 2-5 [101]. As depicted in Figure 2-5, the area between immiscible and miscible injection process is distinguishable; the immiscible process occurs at lower reservoir pressure and temperature conditions; however, the miscible process taking place at high temperatures and pressures. Comprehensive explanation regarding the effect of the operational and reservoir parameters on the oil production mechanisms in reservoirs under CO_2 injection process can be found in Jarrell et al. [44]. Based on their descriptions, continuous CO_2 injection, slug CO_2 injection, conventional water-

alternating gas (WAG), and simultaneous water-alternating gas (SWAG) are the main CO_2 based EOR methods. Different parameters should be taken into account before considering each of these CO_2 based EOR methods which include fluid and rock properties, the reservoir geology, slug size, schedule after water injection and well-pattern configuration[44, 92].
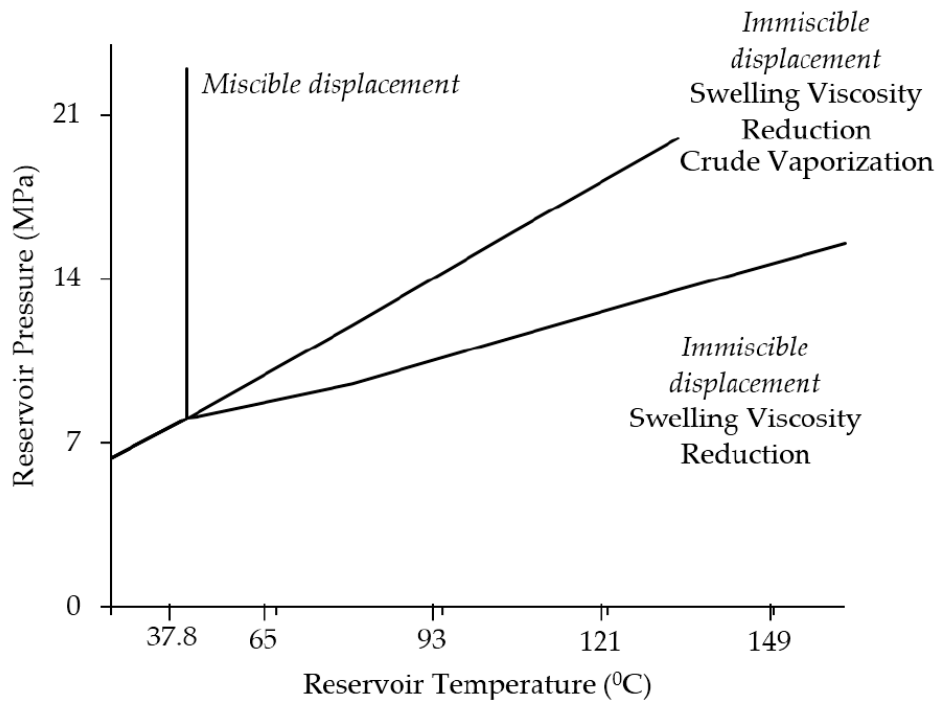
Figure 2-5: Effect of reservoir temperature and pressure on CO2—enhanced oil recovery [101]

2.5. Theoretical and practical Challenges of Experimental works/tests related to CO2 injection

Various theoretical and practical challenges associated with carbon dioxide injection process have been figured out in experimental works. In this section these challenges, which have experimentally investigated, have been discussed. Mohamed and Naser-El-Din [102] carried out several experiments to determine the permeability damage during

28

WAG injection process. They mainly focused on the sulfate based scales. They employed two different carbonate core samples from Austin chalk and Pink Desert limestone; these rock samples mainly comprised by calcite. Based on the experimental results, they concluded that WAG injection in carbonate reservoirs containing sulfur-bearing brines might results in precipitation of sulfur based scales; severity of this type of damage also increases by capillary forces in the low permeability porous media[102]. Wang et al. [17] experimentally studied the effect of asphaltene precipitation during carbon dioxide injection on the efficiency of such a process in low permeability sandstone reservoirs. They employed nuclear magnetic resonance (NMR) core displacement experiment to figure out asphaltene precipitation in pore scale. Experimental results showed that in a case of immiscible CO_2 injection the larger pores have major contribution in oil production; however, in a case miscible injection smaller pores contributed in oil production. Also, asphaltene precipitated in larger pore spaces and this precipitation did not have damage effect on the oil production; however, in few small pores asphaltene precipitation was observed[17]. Another challenge associated with CO_2 injection is fine migration during carbon dioxide injection. Xie et al. [103] experimentally investigated fine migration process during carbon dioxide flooding. They used NMR core displacement experiment to determine permeability impairment owing to fine migration during CO_2 flooding. They concluded that the major portion of permeability reduction during carbon dioxide injection caused by fine migration[103].

Zheng and Yang [104] investigated experimentally two different scenarios for WAG injection to find the suitability of this method in heavy oil recovery. They employed 3D physical model with different configurations of injector and producer wells. Based on the experimental results, they concluded that in a case of horizontal injector and

producer wells, maximum heavy oil recovery could achieve; well configuration has a dominant impact on the ultimate heavy oil recovery[104].

Eide et al. [105] conducted several miscible CO_2 injection experiments in a fractured core samples using both magnetic resonance imaging (MRI) and CT core displacement methods to find out which mechanism contributes in oil production from fractured reservoir in a case of miscible CO_2 injection. Based on the experimental results, they pointed out that diffusion is a main oil production mechanism from core samples with high fracture permeability; however, in a case of low fracture permeability, the dominant oil recovery mechanism is viscos displacement and late time diffusion process. Also, they concluded that tortuosity affects the oil recovery rate in a case of diffusion dominant mechanism; high tortuosity lower oil recovery[105].

Eide et al. [106] employed CT core displacement experiments to find the contribution of diffusion mechanism in CO_2 flooding through fractured reservoir. Based on the experimental data, they concluded that diffusion mechanism could contribute to oil recovery in CO_2 flooding process in fractured reservoir, and diffusion mechanism depends on the fracture distances and carbon dioxide distribution throughout the fracture network.

Liu et al.[107] carried out several CO_2 flooding tests in a synthetic sandstone core samples to figure out the CO_2-oil displacement front quality using MRI method; MRI provides high quality images of the CO_2 flooding process . They employed decane as an oil phase in the core flooding experiments. They analyzed two parameters as indicator of displacement front characteristics; these parameters are the ratio between the length of the front to the front width, and velocity of the displacement front. Based

on the experimental results, they concluded that in case on CO_2 injection at above MMP, the vertical upward CO_2-oil displacement was instable[107].

Wang et al.[108] conducted long-core displacement experiments to evaluate the performance of both miscible CO_2 injection and WAG injection processes as well as permeability reduction owing to asphaltene deposition. They concluded that asphaltene deposition has a waive-like trend and to overcome this obstacle injection of chemical inhibitors is highly recommended.

Al-Ryami et al. [109] studied experimentally the effect of gravity force on the ultimate oil recovery factor and carbon dioxide sequestration performance of miscible and near miscible CO_2 injection on sandstone core samples. The experimental results revealed that in vertical continuous CO_2 injection the ultimate oil recovery factor is much higher those ones in horizontal CO_2 displacement due to considering gravity effect. The most produced components in vertical displacement were light components; however, those ones in horizontal flooding were heavy components, i.e. decane.

Zhang and Gu [110] proposed two quantitative indexes for determining MMP value CO_2 and oil system. These indexes are break-over pressure (BOP), and oil recovery factor (ORF). They conducted five slim tube experiments with the live oil samples as well as five core displacement experiments with dead oil samples. They employed both linear and quadratic interpolation methods for a case of ORF criterion. Also, they used cubic regression method to calculate MMP value based on the measured ORF versus corresponding injection pressure. They concluded that different MMP values can be determined from the plot of ORF against corresponding injection pressure. Mogensen [111] proposed a new protocol for MMP determination using slim-tube experiment. He employed C_1/C_3 ratio as a function of pressure to determine MMP. If the slim-tube

experiment conducts at a pressure lower than MMP, an iterative method can be used to figure out how many steps will be enough to reach MMP. The main drawback of this method is added cost of the produced gas compositional analysis.

Zhang and Gu [112] suggested two quantitative indexes and one qualitative criterion for calculating MMP using the method proposed by Dong et al. [113]; rising bubble apparatus (RBA) technique. These criteria are bubble-rising velocity (BRV), bubble-rising height (BRH), and bubble break-up (BBU), correspondingly. They carried out two rising bubble experiments for both impure and pre CO_2 cases. They concluded that MMP value for the case of light oil sample and pure CO_2 is lower than the value obtained from core displacement experiment. Zhang and Gu [114] proposed two new criteria for MMP determination using vanishing interfacial tension (VIT) method. These criteria are the critical interfacial thickness (CIT), and the linear correlation coefficient (LCC). They carried out six dynamic IFT measurements for both live and dead oil samples under different thermodynamic conditions. They pointed out that the corresponding value of pressure when the LCC is lower than 0.990 or CIT is lower 1.0 nm at the first, is MMP. Based on the experimental results, they concluded that MMP value for live oil samples is slightly higher than MMP value for the dead oil samples; however, the effect of composition in VIT method is minimum but it can be measured for oil samples with high gas-to-oil ratio (GOR).

2.6. Theoretical challenges of modeling works to simulate CO_2 injection into underground formation

Sobers et al. [115] proposed a strategy for CO_2 injection in an field located in the Gulf of Paria using compositional reservoir simulation. Their strategy was based on the both carbon dioxide sequestration and heavy oil recovery. They considered both vertical and

horizontal wells in a simple representative unconsolidated sandstone reservoir. They conducted twelve numerical compositional simulation runs to realize how much carbon dioxide remains in the reservoir as well as the injection performance in oil recovery[115]. The reservoir simulation outputs revealed that in each CO_2 injection strategy at least 50% of the injected carbon dioxide remains in the reservoir; however, the oil production efficiency vary between 17 up to 30%. One of the main reason for occurrence of this process is that heavy oils stripped from intermediate components, i.e., ethane to propane, and absence of these components result in high MMP value in comparison with reservoir pressure[115].

Mohamed and Naser-El-Din [102] conducted different simulation runs to determine the exponents of power law as well as Kozeny-Carman equations using CMG-GEM package and their experimental results. They concluded that calcite precipitation occurred in homogenous rock sample; however, aragonite precipitation took place in a case of low permeability rock sample. Also, they concluded that presence of sulfate scales increased the exponents of both Kozeny-Carman and power-law equations used in simulation studies[102].

Mohebbinia et al. [116] presented a new strategy for flash calculation of occurrence of four phases using reduced flash method proposed by Li and Johns [117]. This strategy for flash calculation noticeably reduced the computational time. They employed this method to figure out the effect of water presence on the phase behavior CO_2 and Texas oil mixture. Outputs of their model revealed that saturation pressure and phase divisions considerably changed in presence of water[116].

Makimura et al. [118] applied molecular dynamic simulation in a case of CO_2 injection into oil resevoirs. They employed Gibbs ensemble Monte Carlo (GEMC) method to determine the equilibrium parameters of CO_2 and oil system. They considered different mixtures including carbon dioxide, nitrogen, n-butane and n-decane; N_2 was used to find the effect of impurity in miscibility behavior of such a system. The outputs of their model were in agreement with the corresponding experimental data samples[118].

Chen et al. [119] studied numerically the impact of reservoir heterogeneity on the performance of CO_2 Huff 'n' puff method for shale oil recovery using UT-COMP compositional reservoir simulator; this simulator developed based on the equation of state. They conducted different scenarios in both homogeneous and heterogeneous shale oil reservoirs. The simulation results showed that both primary and Huff 'n' Puff oil recovery factors mainly depend on the reservoir permeability distribution[119].

Zho et al. [120] investigated numerically the impact of three phase relative permeability model on the ultimate oil recovery under WAG injection process using both compositional and black oil simulation methods. They used two different models including 3D real sector model as well as 2D homogeneous model. They performed several numerical reservoir simulations on both immiscible and miscible WAG injection to consider the effect of miscibility in their investigations. Simulation outputs showed that in a case of immiscible WAG injection using different three phase relative permeability curves resulted in considerable change in oil recovery; the amount of oil recovery mainly depends on the initial conditions and saturation history. In a case of compositional modeling of miscible WAG injection, different three phase relative permeability models might affect the oil recovery; this effect is a function of the size of three phase flow area[120].

Wan et al. [121] developed a compositional numerical reservoir simulation to consider the effect of diffusion phenomenon in CO_2 injection in extensively fractured shale reservoir in United States, Eagle Ford shale-oil reservoir. They employed two diffusion models including matrix/fracture and matrix/matrix to overcome the obstacle caused by single porosity diffusion models. Using single porosity diffusion method requires high resolution grid cell refinement for consideration of fracture system; this refinement results in computation time and makes reservoir simulation time consuming process. Based on the simulation results, they concluded that both matrix/fracture and matrix/matrix diffusion phenomena contribute to the oil production under the process of CO_2 injection.

Beygi et al. [122] proposed two models for three phase hysteresis and three phase relative permeability considering various wettability states and fluid saturations in the reservoir; their model includes both compositional effects and history of fluid saturation. In a case of hysteresis model, they modified the Land trapping model [123] by introducing new coefficient called "Dynamic Land". In a case of three phase relative permeability model, they validated the outputs of the model with the corresponding experimental data of WAG injection process. Also, they conducted different numerical simulations considering the hysteresis effect on the oil recovery and entrapment of gas[122].

Sahverdi and Sohrabi [124] performed numerical simulations to determine three phase relative permeability of WAG injection process using experimental data of two phase WAG injection. They employed in house numerical reservoir simulator to extract three phase relative permeability data using the concept of history matching of production history. According to the results they concluded that there are disagreements between

three and two phase relative permeability curves; relative permeability of all phases are the function of two independent saturations.

Li et al. [125] employed finite volume technique as well as pressure transient analysis to propose a new transient model based on the compositional numerical simulation to develop easy-to-use, cheap and accurate model for estimating miscibility, CO_2 displacement front, and other useful parameters in CO_2 injection. They considered multiple-contact processes, skin factor, and wellbore storage in their model.

Wang et al. [126] conducted reservoir simulation to figure out how preceding cooling effect of water flooding can affect the oil recovery of the CO_2 injection process. Reservoir simulation results revealed that oil recovery factor increases in a case of prior water flooded system due to the cooling effect of the reservoir; lower temperature lower MMP value.

Qiao et al. [127] proposed an approach for modeling to find the dissolution impact on the injectivity of the well under CO_2 injection process using hybrid of reactive solver and in-house compositional reservoir simulator; this in-house reservoir simulator developed based on the finite volume method. They considered WAG, continuous CO_2 injection, and SWAG injection processes to find the effect of dissolution phenomenon on reservoir porosity and permeability. According to the outputs, they pointed that in a case of continuous CO_2 injection there is no considerable change in both reservoir porosity and permeability. In a case of both WAG and SWAG injection processes injectivity increased significantly, especially in SWAG injection. However, different parameters could affect the injectivity including CO_2 slug size, amount of injected water, and number of injection cycles.

Venkatraman et al. [128] presented new model based on the Gibbs free energy to include the impact of geochemical reactions in phase equilibrium and thermodynamic parameter calculations for a real reservoir fluid mixture. This model is able to figure out the effects of geochemical reactions on different parameters including MMP and amount of carbonate scales.

Tran et al. [129] performed different stabilization analyses on both miscible and immiscible CO_2 injections for heavy oil recovery purposes. They included different mass transfer phenomena in their analysis to find the effect of stabilization of CO_2 displacement front on recovery factor. They concluded that, oil viscosity reduction in miscible CO_2 injection results in partial stabilization effect which defeats the adverse mobility ratio impact[129]. CO_2 injection process in the depleted oil reservoirs is a good example of multiphase flow through porous media because the injection process is performed in presence of reservoir oil as well as brine. Clear and reliable measurements of various parameters in this type of multiphase flow is a challenge for oil and gas experts because these measurements in most of the cases are time consuming and challenging[68]. Numerous researches have been done for solving this issue, i.e., numerical and empirical methods for determination the required parameters. Another option is also developing numerical simulators which capable of modeling three phase and multi-components system including complicated porous media, for instance, close bounded reservoirs with sealing faults [8, 13, 44, 68]. However, one of the main issues of the numerical simulation of reservoir models is using thousands and millions of grid blocks which may consume a considerable amount of effort and time, even if high performance processors are employed. This issue is severe and even more time consuming when one needs to perform sensitivity analysis, dynamic control, or multi-

objective optimization because numerical reservoir simulation should be repeated several times to change different reservoir or operational parameters, then objective functions should be evaluated and ranked. Nowadays, proxy models that are based on response surface are employed to reduce the time consumption of the sensitivity analysis and optimization purposes using reservoir simulation. Proxy model is lighter mathematical approach that works much faster and easier instead of using whole reservoir grid model that needs large computation time. However, wide ranges of simulation runs should be performed to provide a reliable data samples for building and validating the proxy model [130].

Olufemi et al. [131] proposed a proxy model for predicting the performance indicator of CO_2 sequestration in Coal seams using artificial neural network (ANN) method. They employed compositional reservoir simulation for creating the response surfaces. Based on the results, they concluded that the ANN proxy model could determine accurately the performance indicator of CO_2 sequestration in Coal seams over different production plan and broad ranges of coal-seams. Also, they pointed out that the ANN proxy model can be employed as a screening and optimization tool for CO_2 sequestration in Coal seams[131].

Shehata et al. [132] developed a proxy model for continuous CO_2 injection, WAG, and simultaneous water alternating gas (SWAG) injection scenarios. They employed D-optimal method for designing simulation runs. Based on the reservoir simulation runs they developed an empirical correlation as a proxy model for CO_2 injection. Also, they investigated sensitivity analysis to find the most important parameters effect the performance of CO_2 injection. They considered well spacing, injection scheme (WAG, SWAG, and continuous CO_2 injection), horizontal injection well, injection rates,

vertical to horizontal permeability, and injection pattern as key parameters for both sensitivity analysis and proxy model development. They concluded that reservoir simulation should be coupled with design of experiment to save time and effort for analyzing different operational and reservoir parameters on the performance of CO_2 injection. Also, they pointed out that D-optimal method could generate a reliable empirical proxy model which is capable to predict the performance of the CO_2 injection process using both operational and reservoir parameters; however, they emphasized that each reservoir should have its own proxy model for performance prediction[132].

Veld et al. [133] conducted an economic analysis for optimization of CO_2 EOR and storage concurrently using Leach et al. [134] method. They coupled Leach et al. [134] method and dynamic reservoir simulation for optimizing CO_2 injection process for both oil recovery and sequestration goals. Parameters they used in their analysis were recycling cost, oil formation volume factor, CO_2 price, CO_2 formation volume factor, and other costs.

Ampomah et al. [135] developed a proxy model aims to optimization of CO_2-EOR and sequestration purposes in a depleted oil reservoir. They employed polynomial response surface method to build a proxy model. Also they conducted a sensitivity analysis on the control parameters to figure out the importance of the control parameters in the proxy model. They implemented genetic algorithm (GA) as an optimization tool to find the optimum development plan to maximize CO_2 sequestration and oil production concurrently. They considered bottom-hole pressure of injectors and producers, oil production rate, water alternating gas cycle and ratio, CO_2 purchase, gas recycle, and infill wells as control variables. They concluded that the reliability and performance of

the proposed proxy model is acceptable and it can be used as a benchmark for further CO_2-EOR pilots in the Anadarko or similar basins.

Jaber et al. [136] developed a proxy model for performance prediction of miscible CO_2-WAG injection in heterogeneous clastic reservoir. They employed Box-Behnken method for designing numerical reservoir simulation runs. They considered four operational parameters including CO_2 slug size, slug ratio, bottom-hole pressure and cyclic length as input parameters of the proxy model. They used polynomial regression to construct a predictive proxy model. Moreover, they performed residual analysis as well as analysis of variance on the results gained from the numerical reservoir simulation. They pointed out several limitations of the developed proxy model including limitation in applying for other oil fields and/or restriction in using for other types of EOR methods[136].

2.7. Practical Challenges for implementation of CO_2 injection into underground formations

As well as the various benefits, the CO_2 based EOR methods are still encountering with several concerns, for instance, handling of produced fluid, flow assurance issue (scale deposition, asphaltene precipitation and deposition), corrosion occurrence in pipeline and production string, injectivity loss, well integrity, leakage occurrence throughout injection well or other inevitable operational concerns, for instance, rapid pressure drop, which cannot be prevented throughout the oil field production window[13, 15, 68, 108, 137, 138]. One of the challenging issues in CO_2 injection method is gravity segregation phenomenon which is a consequence of the density difference between injection fluid and reservoir fluids, i.e., oil and water phases. Owing to very low density of the gas,

this fluid be likely to move upward; however, oil and water phases tend to flow in downward due to their higher density. The occurrence of this process is known as a gravity segregation phenomenon. To defeat this problem several researchers proposed different chemical agents ,i.e., polymer and surfactants, to control such a behavior[139-142]. Another problematic issue is an early breakthrough in producer wells; override or channeling phenomenon results in early breakthrough time in a producer well in a case of gas injection process. To cure such an issue, using WAG injection process is highly recommended[143]. In a case of miscible injection process, maintaining the miscibility is challenging; lower miscibility condition lower incremental oil recovery. This issue caused by reduction in injectivity of carbon dioxide[13, 44, 68].

One of probable issue, especially in injection facilities and pipelines, is corrosion due to the presence of water in WAG and SWAG injection; however, there is no such a problem in a continuous CO_2 injection process. To defeat corrosion issue in an injection wells adding corrosion inhibitor chemicals or using corrosion resistive pipes is frequently recommended [68, 144]. Asphaltene precipitation and deposition in both reservoir and production string could considerably affect the oil production efficiency. Asphaltene deposition in reservoir could results in severe permeability reduction and in some cases permanent near wellbore damage; however, asphaltene deposition on to the tubing or production string surface is not a permanent damage[108, 145]. Any reduction in permeability of the reservoir might results in disturb oil production rate and consequently, it could reduce the possible revenue from CO_2 injection project. There are different methods available for solving such a complex issue due to CO_2 injection. These methods could be using chemical inhibitor agents, injecting asphaltene solvents, redesigning production facilities to change the final state of the fluid, and changing

41

chock size in some cases[146]. In a case of CO_2 injection in offshore oil reservoir temperature fluctuation during the nights and cold days could results in wax precipitation or deposition in wellhead or pipelines [147-149]. To cure such a problem using chemical inhibitors or wellhead insulators are the main suggestions [148, 149]. Moreover, temperature difference between the injection fluids, especially in a case of WAG injection, may facilitates failures in production string or tubing. Increasing injection pressure for maintaining miscibility condition in both miscible CO_2 injection results in increasing the risk of leakage in both formation and injection wells. Maffeis et al. [68, 150] reported several activities required for monitoring, evaluating, and controlling operational issues which might be occurred during the carbon dioxide or WAG injection processes to enhance the performance of the injection scheme. Besides to the practical issues associated by CO_2 based EOR process discussed above several operational concerns have been observed including foam formation during oil production, corrosion of downhole facilities, especially pumps and compressors, malfunctioning of production string, paritucarly tubing, gas deliverability and storage, pump issues in a case of oil with high GOR, and early breakthrough of the injection carbon dioxide [13, 15, 68, 108, 137, 138].

2.8. Economic prospects of CO_2 injection into underground formations

The most important question in execution of any EOR methods is satisfaction from an economic viewpoint. In other words, after technical considerations, feasibility study based on the economic considerations should be conducted. Also, from a reservoir management point of view, risk analysis and economic optimization should be performed[68]. Gozalpour et al. [151] presented an economic investigation the feasibility of miscible CO_2 flooding and WAG injection considering the costs of CO_2

42

injection, transportation and oil separation. Advances in CO_2 capturing and transportation technologies could considerably reduce the final cost of CO_2 based EOR methods. According to the reported data in previous works, WAG injection process has higher efficiency than CO_2 flooding alone; 80% of WAG injection if US oil fields are economic [13, 68, 152, 153]. Ravagnani et al. [154] investigated economically and technically the feasibility of carbon dioxide storage through CO_2 based EOR method. They considered different scenarios to determine the applicability of CO_2 injection as an efficient CO_2 storage process. They concluded that feasibility of CO_2 sequestration through CO_2 injection depends on oil production rate, oil price, and capital costs.

Salem et al. [155] studied the feasibility of different CO_2 injection scenarios in a prior water flooded reservoir. They considered payback period, cash flow, net present value (NPV), and CO_2 utilization factor as economic parameters in their analysis. In their study, oil price was 60$/barrel, discount rate 10%, and CO_2 price 2.38 $/MMSCF (Million Standard Cubic Feet). Based on these values, applying CO_2 injection was feasible with 409 million $ NPV[155].

Merschmann et al. [156] performed technical and economic analysis on CO_2 injection for EOR purposes to find abatement cost of CO_2. They concluded that in a case of oil company investment the abatement cost of CO_2 is 200$/ton; on the other hand, 350$/ton is a abatement cost of CO_2 in a case of distillatory company investment. Skaugen et al. [157] investigated economically and technically the impact of impurities on the transportation of carbon dioxide for sequestration purposes. They found out that presence of impurities affected the cost of transportation pipelines in carbon dioxide storage process.

Noureldin et al. [138] performed Monte Carlo simulation to figure out the effects of uncertainties associated with CO_2 injection process on the economic status of the project. Kwak and Kim [15] conducted economic study on CO_2 injection process for EOR goals to optimize carbon dioxide supply resulting maximum NPV value. Also, they applied sensitivity analysis of the design parameters to find the importance each variables in CO_2 based EOR method. Lindeberg et al. [137] conducted both technical and economic analysis of CO_2 injection in 23 Norwegian oil fields as EOR candidates. They considered NPV as an index of economic analysis. Based on the outputs of the economic analysis, if CO_2 price is zero, CO_2 injection scenario might be profitable even if in low oil price conditions[137].

Welkenhuysen et al. [158] studied economically the feasibility of concurrent CO_2 injection for both carbon dioxide sequestration and oil recovery on North Sea oil fields. Considering the oil price between 10€ up to 70€/ barrel, they concluded that in a scenario of CO_2 injection for oil recovery and CO_2 sequestration could be profitable. Fukai et al. [159] determined CO_2 break-even price for profitable CO_2 injection in East Canton oil field in Ohio. According to their outputs, CO_2 break-even price is equal to 4-6 /ton/barrel for oil fields in north of America, particularly United States and Canada[159].

2.9. Environmental aspects of CO_2 injection into underground formations

One of the interesting advantages of CO_2 injection process is preventing CO_2 emission into atmosphere. However, the big question is how much carbon dioxide required for EOR goals and the amount of CO_2 emissions from different industries [160]. Also, several environmental concerns associated with CO_2 injection process might be exist.

These environmental issues are as consequences of CO_2 leakage in any section of CO_2 injection process including capture, transportation and injection systems as well as depleted oil and reservoir formation. The possibility of any leakage in surface facilities, i.e., transportation, capturing and injection, is very low due to periodical inspections of facilities under health, safety, and environmental regulations[161]. On the other hand, the possibility of leakage through reservoir formation is significant. So, the main issues regarding CO_2 leakage are contamination both soil and ground drinking water with carbon dioxide. In a case of offshore CO_2 injection, the effect of water contamination with CO_2 on micro-organism communities and sea creatures should be evaluated. Smith et al. [162] investigated experimentally the effect of the contaminated soil with different CO_2 concentrations on plants growing. According to their experimental results, they concluded that CO_2 could severely damaging effect on plant growing; however, the severity of such an issue mainly depends on the type of soil and herb[162]. Xiao et al. [163] investigated numerically the risks associated with CO_2 injection process on underground drinking water sources. They considered different ranges for CO_2 leakage from underground reservoirs which vary between 10^{-14} to 10^{-10} kg / (m^2. Year) for 200 years in different elevations. They pointed out that these values of leakage rate could not affect considerably the water quality. Ko et al. reviewed most of the experimental works regarding the responses of plant and micro-organisms to CO_2 leakage. Based on their report, very limited field experiments are available to determine the effect of CO_2 leakage on micro-organisms community. They pointed out that plants are sensitive to soil contamination with high concentration of carbon dioxide; however, micro-organisms are much harder and diverse than plants. As a result, more experimental investigations are needed to evaluate this effect and figure out the mechanisms behind any damaging effect. Chen et al. [164] studied experimentally the negative impact of

CO_2 leakage into upper formations on soil microbial communities. According the experimental results, they condemn that micro-organisms could have different detrimental results from low damage to high damage in a same condition. This means that different groups of micro-organisms have different hardness respect to CO_2 contamination [164].

2.10. Conclusions

CO_2 based EOR methods provide good options to improve the efficiency of oil production scheme effectively in a case of less accessible oil zones. Different mechanisms contribute in the oil production efficiency through CO_2 injection; these mechanisms are vaporization/condensation, oil swelling, and reduction in oil viscosity, especially in heavy oil recovery. Besides other advantages, CO_2 injection process also gives a chance to reduce greenhouse gas emissions, particularly carbon dioxide, into atmosphere though sequestration in depleted or mature oil fields; however, risk assessment and the costs associated with such a process should be evaluated and dynamic monitoring leakage sites should be constructed in field scale. Also, effective optimization approaches should be employed to optimize the process of CO_2 injection in depleted oil and gas reservoirs in terms of both technical and economic points of view. Several advances in numerical modeling of CO_2 based EOR processes have been described, i.e., three-phase relative permeability models, hysteresis models, finite element and finite volume approaches, consideration of geochemical reactions in fluid flow modeling, stabilization analysis of the CO_2-oil interface, and development of proxy models. Economic considerations including NPV, effect of impurities, discount

rate, CO_2 break-even price have been discussed. This review reported various field experience in a case of CO_2 flooding, immiscible and miscible, and WAG injection throughout different countries. This paper covers almost all the subjects associated with CO_2 based EOR methods as well as the challenges and future plans. The main economic parameters affect the feasibility of CO_2 based EOR methods are oil price and costs associated with CO_2 capture and transportation. As a result, developing technologies particularly in CO_2 capture and transportation might make CO_2 injection process economical. Moreover, formulating of different chemicals including both polymer and surfactants could improve the performance of CO_2 injection as well as providing more opportunities in different oil fields from an application view. To provide better understanding regarding the mechanisms behind the CO_2 injection process, establishment of different protocols for experiment works and using measured parameters in a modeling phase of development plan. Consequently, development such approaches for improving the performance and reliability of numerical based methods which are responsible for EOR screening, feasibility study and risk analysis for applying the cost effective CO_2 based EOR methods play a crucial role in improvement of the efficiency of CO_2 injection methods.

References

[1] N.A. Azzolina, W.D. Peck, J.A. Hamling, C.D. Gorecki, S.C. Ayash, T.E. Doll, D.V. Nakles, L.S. Melzer, How green is my oil? A detailed look at greenhouse gas accounting for CO 2-enhanced oil recovery (CO 2-EOR) sites, International Journal of Greenhouse Gas Control, 51 (2016) 369-379.

[2] Q. Li, Z. Chen, J.-T. Zhang, L.-C. Liu, X. Li, L. Jia, Positioning and revision of CCUS technology development in China, International Journal of Greenhouse Gas Control, 46 (2016) 282-293.

[3] W. Yang, B. Peng, Q. Liu, S. Wang, Y. Dong, Y. Lai, Evaluation of CO_2 enhanced oil recovery and CO_2 storage potential in oil reservoirs of Bohai Bay Basin, China, International Journal of Greenhouse Gas Control, 65 (2017) 86-98.

[4] J.-Q. Shi, Z. Xue, S. Durucan, Supercritical CO_2 core flooding and imbibition in Tako sandstone—Influence of sub-core scale heterogeneity, International Journal of Greenhouse Gas Control, 5 (2011) 75-87.

[5] J.L. Shelton, J.C. McIntosh, A.G. Hunt, T.L. Beebe, A.D. Parker, P.D. Warwick, R.M. Drake, J.E. McCray, Determining CO_2 storage potential during miscible CO_2 enhanced oil recovery: noble gas and stable isotope tracers, International Journal of Greenhouse Gas Control, 51 (2016) 239-253.

[6] Y. Sun, Q. Li, C. Fan, Laboratory core flooding experiments in reservoir sandstone under different sequestration pressures using multichannel fiber Bragg grating sensor arrays, International Journal of Greenhouse Gas Control, 60 (2017) 186-198.

[7] P. Schenewerk, EOR can extend the promise of unconventional oil and gas, Oil & Gas Journal, 110 (2012) 48-48.

[8] M.A. Ahmadi, B. Pouladi, T. Barghi, Numerical modeling of CO_2 injection scenarios in petroleum reservoirs: application to CO_2 sequestration and EOR, Journal of Natural Gas Science and Engineering, 30 (2016) 38-49.

[9] D.P. Schrag, Preparing to capture carbon, science, 315 (2007) 812-813.

[10] M. Perera, P. Ranjith, D. Airey, S.-K. Choi, Sub-and super-critical carbon dioxide flow behavior in naturally fractured black coal: An experimental study, Fuel, 90 (2011) 3390-3397.

[11] M. Perera, P. Ranjith, Carbon dioxide sequestration effects on coal's hydro-mechanical properties: a review, International Journal of Energy Research, 36 (2012) 1015-1031.

[12] L.H. Bui, Near miscible CO2 application to improve oil recovery, in, University of Kansas, 2010.

[13] M.S.A. Perera, R.P. Gamage, T.D. Rathnaweera, A.S. Ranathunga, A. Koay, X. Choi, A Review of CO2-Enhanced Oil Recovery with a Simulated Sensitivity Analysis, Energies, 9 (2016) 481.

[14] A. Wilson, Experimental and Numerical Studies of CO 2 EOR in Unconventional Reservoirs, Journal of Petroleum Technology, 69 (2017) 45-47.

[15] D.-H. Kwak, J.-K. Kim, Techno-economic evaluation of CO 2 enhanced oil recovery (EOR) with the optimization of CO 2 supply, International Journal of Greenhouse Gas Control, 58 (2017) 169-184.

[16] A. González-Díaz, M.O. González-Díaz, A.M. Alcaráz-Calderón, J. Gibbins, M. Lucquiaud, Priority projects for the implementation of CCS power generation with enhanced oil recovery in Mexico, International Journal of Greenhouse Gas Control, 64 (2017) 119-125.

[17] C. Wang, T. Li, H. Gao, J. Zhao, H.A. Li, Effect of asphaltene precipitation on CO 2-flooding performance in low-permeability sandstones: a nuclear magnetic resonance study, RSC Advances, 7 (2017) 38367-38376.

[18] L. Zhang, X. Li, B. Ren, G. Cui, Y. Zhang, S. Ren, G. Chen, H. Zhang, CO 2 storage potential and trapping mechanisms in the H-59 block of Jilin oilfield China, International Journal of Greenhouse Gas Control, 49 (2016) 267-280.

[19] F. Karimi, R. Khalilpour, Evolution of carbon capture and storage research: Trends of international collaborations and knowledge maps, International Journal of Greenhouse Gas Control, 37 (2015) 362-376.

[20] S. Sgouridis, S. Griffiths, S. Kennedy, A. Khalid, N. Zurita, A sustainable energy transition strategy for the United Arab Emirates: Evaluation of options using an Integrated Energy Model, Energy Strategy Reviews, 2 (2013) 8-18.

[21] S. Caserini, G. Dolci, A. Azzellino, C. Lanfredi, L. Rigamonti, B. Barreto, M. Grosso, Evaluation of a new technology for carbon dioxide submarine storage in glass capsules, International Journal of Greenhouse Gas Control, 60 (2017) 140-155.

[22] K. Bybee, Challenges for offshore heavy-oil field development, Journal of petroleum technology, 55 (2003) 66-67.

[23] A.G. Cahill, R. Jakobsen, Geochemical modeling of a sustained shallow aquifer CO_2 leakage field study and implications for leakage and site monitoring, International Journal of Greenhouse Gas Control, 37 (2015) 127-141.

[24] B.N. Nguyen, Z. Hou, D.H. Bacon, C.J. Murray, M.D. White, Three-dimensional modeling of the reactive transport of CO_2 and its impact on geomechanical properties of reservoir rocks and seals, International Journal of Greenhouse Gas Control, 46 (2016) 100-115.

[25] N. Ahmad, A. Wörman, X. Sanchez-Vila, J. Jarsjö, A. Bottacin-Busolin, H. Hellevang, Injection of CO_2-saturated brine in geological reservoir: A way to enhanced storage safety, International Journal of Greenhouse Gas Control, 54 (2016) 129-144.

[26] P. Luo, V. Er, N. Freitag, S. Huang, Recharacterizing evolving fluid and PVT properties of Weyburn oil–CO_2 system, International Journal of Greenhouse Gas Control, 16 (2013) S226-S235.

[27] G.K. Jensen, Weyburn oilfield core assessment investigating cores from pre and post CO_2 injection: Determining the impact of CO_2 on the reservoir, International Journal of Greenhouse Gas Control, 54 (2016) 490-498.

[28] I. Hutcheon, M. Shevalier, K. Durocher, J. Bloch, G. Johnson, M. Nightingale, B. Mayer, Interactions of CO_2 with formation waters, oil and minerals and CO_2 storage at the Weyburn IEA EOR site, Saskatchewan, Canada, International Journal of Greenhouse Gas Control, 53 (2016) 354-370.

[29] M. Khather, A. Saeedi, R. Rezaee, R.R. Noble, D. Gray, Experimental investigation of changes in petrophysical properties during CO_2 injection into dolomite-rich rocks, International Journal of Greenhouse Gas Control, 59 (2017) 74-90.

[30] J. West, D. Jones, A. Annunziatellis, T. Barlow, S. Beaubien, A. Bond, N. Breward, P. Coombs, D. de Angelis, A. Gardner, Comparison of the impacts of elevated CO_2 soil gas concentrations on selected European terrestrial environments, International Journal of Greenhouse Gas Control, 42 (2015) 357-371.

[31] M. Krüger, D. Jones, J. Frerichs, B.I. Oppermann, J. West, P. Coombs, K. Green, T. Barlow, R. Lister, R. Shaw, Effects of elevated CO_2 concentrations on the vegetation and microbial populations at a terrestrial CO_2 vent at Laacher See, Germany, International Journal of Greenhouse Gas Control, 5 (2011) 1093-1098.

[32] F. Gal, K. Michel, Z. Pokryszka, S. Lafortune, B. Garcia, V. Rouchon, P. De Donato, J. Pironon, O. Barres, N. Taquet, Study of the environmental variability of gaseous emanations over a CO_2 injection pilot—Application to the French Pyrenean foreland, international journal of Greenhouse Gas Control, 21 (2014) 177-190.

[33] S.X. Ning, B.S. Jhaveri, N. Jia, B. Chambers, J. Gao, Viscosity reduction EOR with CO2 & enriched CO2 to improve recovery of Alaska North Slope viscous oils, in: SPE Western North American Region Meeting, Society of Petroleum Engineers, 2011.

[34] E. Heidaryan, J. Moghadasi, A laboratory investigation into carbon dioxide flooding by focusing on the viscosity and swelling factor changes, Petroleum Science and Technology, 30 (2012) 1441-1452.

[35] C. Or, K. Sasaki, Y. Sugai, M. Nakano, M. Imai, Swelling and Viscosity Reduction of Heavy Oil by CO 2-Gas Foaming in Immiscible Condition, SPE Reservoir Evaluation & Engineering, 19 (2016) 294-304.

[36] A. Habibi, M.R. Yassin, H. Dehghanpour, D. Bryan, CO2-Oil Interactions in Tight Rocks: An Experimental Study, in: SPE Unconventional Resources Conference, Society of Petroleum Engineers, 2017.

[37] B. Wei, H. Gao, W. Pu, F. Zhao, Y. Li, F. Jin, L. Sun, K. Li, Interactions and phase behaviors between oleic phase and CO 2 from swelling to miscibility in CO 2-based enhanced oil recovery (EOR) process: A comprehensive visualization study, Journal of Molecular Liquids, 232 (2017) 277-284.

[38] A. Dehghan, S. Ghorbanizadeh, S. Ayatollahi, Investigating the fracture network effects on sweep efficiency during WAG injection process, Transport in porous media, 93 (2012) 577-595.

[39] M. Robin, J. Behot, V. Sygouni, CO2 Injection in Porous Media: Observations un Glass Micromodels Under Reservoir Conditions, in: SPE Improved Oil Recovery Symposium, Society of Petroleum Engineers, 2012.

[40] Y. Sugai, T. Babadagli, K. Sasaki, Consideration of an effect of interfacial area between oil and CO2 on oil swelling, Journal of Petroleum Exploration and Production Technology, 4 (2014) 105-112.

[41] S.M. Seyyedsar, M. Sohrabi, Visualization observation of formation of a new oil phase during immiscible dense CO 2 injection in porous media, Journal of Molecular Liquids, (2017).

[42] M. Sohrabi, A. Emadi, Novel Insights into the Pore-Scale Mechanisms of Enhanced Oil Recovery by CO2 Injection, in: SPE Europec/EAGE Annual Conference, Society of Petroleum Engineers, 2012.

[43] M. Cui, R. Wang, C. Lv, Y. Tang, Research on microscopic oil displacement mechanism of CO 2 EOR in extra-high water cut reservoirs, Journal of Petroleum Science and Engineering, 154 (2017) 315-321.

[44] P.M. Jarrel, C. Fox, M. Stein, S. Webb, Practical Aspects of CO2 flooding, SPE Monograph, Society of Petroleum Engineers, Richardson, TX, (2002).

[45] S. Zendehboudi, M.A. Ahmadi, A. Bahadori, A. Shafiei, T. Babadagli, A developed smart technique to predict minimum miscible pressure—EOR implications, The Canadian Journal of Chemical Engineering, 91 (2013) 1325-1337.

[46] D.N. Rao, J.I. Lee, Determination of gas–oil miscibility conditions by interfacial tension measurements, Journal of colloid and interface science, 262 (2003) 474-482.

[47] M.-A. Ahmadi, M. Ebadi, Fuzzy modeling and experimental investigation of minimum miscible pressure in gas injection process, Fluid Phase Equilibria, 378 (2014) 1-12.

[48] T. Monger, J. Ramos, J. Thomas, Light oil recovery from cyclic CO2 injection: influence of low pressures impure CO2, and reservoir gas, SPE Reservoir Engineering, 6 (1991) 25-32.

[49] G. Thomas, T. Monger-McClure, Feasibility of cyclic CO2 injection for light-oil recovery, SPE Reservoir Engineering, 6 (1991) 179-184.

[50] R. Srivastava, S. Huang, Laboratory investigation of Weyburn CO_2 miscible flooding, in: Technical Meeting/Petroleum Conference of the South Saskatchewan Section, Petroleum Society of Canada, 1997.

[51] H. Yongmao, W. Zenggui, J. Binshan, C. Yueming, L. Xiangjie, Laboratory investigation of CO_2 flooding, in: Nigeria Annual International Conference and Exhibition, Society of Petroleum Engineers, 2004.

[52] F. Kamali, F. Hussain, Y. Cinar, A Laboratory and Numerical-Simulation Study of Co-Optimizing CO_2 Storage and CO_2 Enhanced Oil Recovery, SPE Journal, 20 (2015) 1,227-221,237.

[53] F. Kamali, F. Hussain, Y. Cinar, An experimental and numerical analysis of water-alternating-gas and simultaneous-water-and-gas displacements for carbon dioxide enhanced oil recovery and storage, SPE Journal, 22 (2017) 521-538.

[54] J. Sheng, Enhanced oil recovery field case studies, Gulf Professional Publishing, 2013.

[55] Y. Zhang, B. Freifeld, S. Finsterle, M. Leahy, J. Ennis-King, L. Paterson, T. Dance, Single-well experimental design for studying residual trapping of supercritical carbon dioxide, International Journal of Greenhouse Gas Control, 5 (2011) 88-98.

[56] P. Zuloaga, W. Yu, J. Miao, K. Sepehrnoori, Performance evaluation of CO_2 Huff-n-Puff and continuous CO_2 injection in tight oil reservoirs, Energy, 134 (2017) 181-192.

[57] C. Song, D. Yang, Experimental and numerical evaluation of CO_2 huff-n-puff processes in Bakken formation, Fuel, 190 (2017) 145-162.

[58] M. Tang, H. Zhao, H. Ma, S. Lu, Y. Chen, Study on CO_2 huff-n-puff of horizontal wells in continental tight oil reservoirs, Fuel, 188 (2017) 140-154.

[59] J. Ma, X. Wang, R. Gao, F. Zeng, C. Huang, P. Tontiwachwuthikul, Z. Liang, Enhanced light oil recovery from tight formations through CO_2 huff 'n'puff processes, Fuel, 154 (2015) 35-44.

[60] D. Sanchez-Rivera, K. Mohanty, M. Balhoff, Reservoir simulation and optimization of Huff-and-Puff operations in the Bakken Shale, Fuel, 147 (2015) 82-94.

[61] B. Iraji, S.R. Shadizadeh, M. Riazi, Experimental investigation of CO_2 huff and puff in a matrix-fracture system, Fuel, 158 (2015) 105-112.

[62] J. Ma, X. Wang, R. Gao, F. Zeng, C. Huang, P. Tontiwachwuthikul, Z. Liang, Study of cyclic CO_2 injection for low-pressure light oil recovery under reservoir conditions, Fuel, 174 (2016) 296-306.

[63] Y. Zhang, R. Lu, F. Forouzanfar, A.C. Reynolds, Well placement and control optimization for WAG/SAG processes using ensemble-based method, Computers & Chemical Engineering, 101 (2017) 193-209.

[64] D. Merchant, Enhanced Oil Recovery–the History of CO_2 Conventional Wag Injection Techniques Developed from Lab in the 1950's to 2017, in: Carbon Management Technology Conference, Carbon Management Technology Conference, 2017.

[65] J.D. Henry, Status and outlook for oil recovery using carbon dioxide injection operations, in: Annual Meeting Papers, Division of Production, American Petroleum Institute, 1981.

[66] D. Graue, T. Blevins, SACROC tertiary CO2 pilot project, in: SPE Symposium on Improved Methods of Oil Recovery, Society of Petroleum Engineers, 1978.

[67] G. Yuncong, Z. Mifu, W. Jianbo, Z. Chang, Performance and gas breakthrough during CO2 immiscible flooding in ultra-low permeability reservoirs, Petroleum Exploration and Development, 41 (2014) 88-95.

[68] S. Kumar, A. Mandal, A comprehensive review on chemically enhanced water alternating gas/CO 2 (CEWAG) injection for enhanced oil recovery, Journal of Petroleum Science and Engineering, (2017).

[69] R.A. Olea, Carbon Dioxide Enhanced Oil Recovery Performance According to the Literature, in, US Geological Survey, 2017.

[70] L. Singh, A. Singhal, Lessons from trinidad's CO2 immiscible pilot projects, SPE Res Eval & Eng, 8 (2005) 397-403.

[71] D. Senocak, S.P. Pennell, C.E. Gibson, R.G. Hughes, Effective use of heterogeneity measures in the evaluation of a mature CO2 flood, in: SPE Symposium on Improved Oil Recovery, Society of Petroleum Engineers, 2008.

[72] D. Senocak, Evaluation of Sweep Efficiency of a Mature CO2 Flood in Little Creek Field, Mississippi, (2008).

[73] S. Sahin, U. Kalfa, D. Celebioglu, Bati Raman Field Immiscible CO2 Application--Status Quo and Future Plans, SPE Reservoir Evaluation & Engineering, 11 (2008) 778-791.

[74] S.P. Dutton, W.A. Flanders, M.D. Barton, Reservoir characterization of a Permian deep-water sandstone, East Ford field, Delaware basin, Texas, AAPG bulletin, 87 (2003) 609-627.

[75] G. Protti, Win-Win: Enhanced Oil Recovery and CO2 Storage at EnCana's Weyburn Oilfield, in: 18th World Petroleum Congress, World Petroleum Congress, 2005.

[76] A.D. Boyd, Connections between community and emerging technology: Support for enhanced oil recovery in the Weyburn, Saskatchewan area, International Journal of Greenhouse Gas Control, 32 (2015) 81-89.

[77] J.P. Meyer, Summary of carbon dioxide enhanced oil recovery (CO2EOR) injection well technology, American Petroleum Institute, 54 (2007).

[78] M.H. Holtz, Immiscible Water Alternating Gas (IWAG) EOR: Current State of the Art, in: SPE Improved Oil Recovery Conference, Society of Petroleum Engineers, 2016.

[79] G. Nadeson, S.G. Sayegh, M. Girard, Assessment of Dulang Field Immiscible Water-Alternating-Gas (WAG) Injection Through Composite Core Displacement Studies, in: SPE Asia Pacific Improved Oil Recovery Conference, Society of Petroleum Engineers, 2001.

[80] G. Nadeson, N.A.B. Anua, A. Singhal, R.B. Ibrahim, Water-alternating-gas (WAG) pilot implementation, a first EOR development project in Dulang field, offshore Peninsular Malaysia, in: SPE Asia Pacific Oil and Gas Conference and Exhibition, Society of Petroleum Engineers, 2004.

[81] E. Fernandez Righi, M.R. Pascual, Water-Alternating-Gas Pilot in the Largest Oil Field in Argentina: Chihuido de la Sierra Negra, Neuquen Basin, in: Latin American & Caribbean Petroleum Engineering Conference, Society of Petroleum Engineers, 2007.

[82] D.J. Smith, T.R. Kelly, D.L. Schmidt, C.E. Bowden, Katz (Strawn) Unit Miscible CO2 Project: Design, Implementation, and Early Performance, in: SPE Improved Oil Recovery Symposium, Society of Petroleum Engineers, 2012.

[83] R.O. de Moraes Cruz, M.B. Rosa, C.C.M. Branco, J.O. de Sant'Anna Pizarro, C.T. de Souza Silva, Lula NE Pilot Project-An Ultra-Deep Success in the Brazilian Pre-Salt, in: Offshore Technology Conference, Offshore Technology Conference, 2016.

[84] C.D. Gorecki, J.A. Hamling, J. Ensrud, E.N. Steadman, J.A. Harju, Integrating CO2 EOR and CO2 storage in the Bell Creek oil field, in: Carbon Management Technology Conference, Carbon Management Technology Conference, 2012.

[85] https://sequestration.mit.edu/tools/projects/bell_creek.html, in.

[86] P. Ozan, Advanced resources international, basin oriented strategies for CO2 enchanced oil recovery, Onshore Gulf Coast, 34 (2003) 117-118.

[87] G.C. Bank, D.E. Riestenberg, G.J. Koperna, CO2-enhanced oil recovery potential of the appalachian Basin, in: Eastern Regional Meeting, Society of Petroleum Engineers, 2007.

[88] F. Poettmann, Improved oil recovery, Interstate Oil Compact Commission: Oklahoma City, OK, USA, (1983).

[89] L. Holm, V. Josendal, Mechanisms of oil displacement by carbon dioxide, Journal of petroleum Technology, 26 (1974) 1,427-421,438.

[90] M.A. Ahmadi, M. zeinali Hasanvand, S. Shokrolahzadeh, Technical and economic feasibility study of flue gas injection in an Iranian oil field, Petroleum, 1 (2015) 217-222.

[91] S.F. Ali, S. Thomas, A Realistic Look at Enhanced () il Recovery, Scientia Iranica, 1 (1994).

[92] V.A. Tabrizy, Investigated miscible CO2 flooding for enhancing oil recovery in wettability altered chalk and sandstone rocks, (2012).

[93] M.H. Holtz, E.K. NANCE, R.J. Finley, Reduction of greenhouse gas emissions through CO2 EOR in Texas, Environmental Geosciences, 8 (2001) 187-199.

[94] M. zeinali Hasanvand, M.A. Ahmadi, S.R. Shadizadeh, R. Behbahani, F. Feyzi, Geological storage of carbon dioxide by injection of carbonated water in an Iranian oil

reservoir: a case study, Journal of Petroleum Science and Engineering, 111 (2013) 170-177.

[95] R. Simon, D. Graue, Generalized correlations for predicting solubility, swelling and viscosity behavior of CO2-crude oil systems, Journal of Petroleum Technology, 17 (1965) 102-106.

[96] F. Martin, J. Taber, Carbon Dioxide Flooding. JPT 44 (4): 396–400, in, SPE-23564-PA. DOI: 10.2118/23564-PA, 1992.

[97] J. Welker, Physical properties of carbonated oils, Journal of Petroleum Technology, 15 (1963) 873-876.

[98] M.A. Ahmadi, M. zeinali Hasanvand, S.S. Behbahani, A. Nourmohammad, A. Vahidi, M. Amiri, G. Ahmadi, Effect of operational parameters on the performance of carbonated water injection: Experimental and numerical modeling study, The Journal of Supercritical Fluids, 107 (2016) 542-548.

[99] G. Rojas, S. Ali, Scaled model studies of carbon dioxide/brine injection strategies for heavy oil recovery from thin formations, Journal of Canadian Petroleum Technology, 25 (1986).

[100] M.M. Kulkarni, Immiscible and miscible gas-oil displacements in porous media, (2003).

[101] M.A. Klins, Carbon dioxide flooding: Basic mechanisms and project design, (1984).

[102] I. Mohamed, H.A. Nasr-El-Din, Fluid/rock interactions during CO2 sequestration in deep saline carbonate aquifers: laboratory and modeling studies, SPE Journal, 18 (2013) 468-485.

[103] Q. Xie, A. Saeedi, C. Delle Piane, L. Esteban, P.V. Brady, Fines migration during CO_2 injection: Experimental results interpreted using surface forces, International Journal of Greenhouse Gas Control, 65 (2017) 32-39.

[104] S. Zheng, D.T. Yang, Pressure maintenance and improving oil recovery by means of immiscible water-alternating-$CO2$ processes in thin heavy-oil reservoirs, SPE Reservoir Evaluation & Engineering, 16 (2013) 60-71.

[105] O. Eide, G. Ersland, B. Brattekas, A. Haugen, A. Graue, M. Ferno, $CO2$ EOR by Diffusive Mixing in Fractured Reservoirs, Petrophysics, 56 (2015) 23-31.

[106] Ø. Eide, M.A. Fernø, Z. Alcorn, A. Graue, Visualization of carbon dioxide enhanced oil recovery by diffusion in fractured chalk, SPE Journal, 21 (2016) 112-120.

[107] Y. Liu, Y. Teng, L. Jiang, J. Zhao, Y. Zhang, D. Wang, Y. Song, Displacement front behavior of near miscible CO_2 flooding in decane saturated synthetic sandstone cores revealed by magnetic resonance imaging, Magnetic resonance imaging, 37 (2017) 171-178.

[108] Z. Wang, S. Yang, H. Lei, M. Yang, L. Li, S. Yang, Oil recovery performance and permeability reduction mechanisms in miscible CO_2 water-alternative-gas (WAG) injection after continuous CO_2 injection: An experimental investigation and modeling approach, Journal of Petroleum Science and Engineering, 150 (2017) 376-385.

[109] H.F. Al-Riyami, F. Kamali, F. Hussain, Effect of Gravity on Near-Miscible $CO2$ Flooding, in: SPE Kingdom of Saudi Arabia Annual Technical Symposium and Exhibition, Society of Petroleum Engineers, 2017.

[110] K. Zhang, Y. Gu, Two different technical criteria for determining the minimum miscibility pressures (MMPs) from the slim-tube and coreflood tests, Fuel, 161 (2015) 146-156.

[111] K. Mogensen, A novel protocol for estimation of minimum miscibility pressure from slimtube experiments, Journal of Petroleum Science and Engineering, 146 (2016) 545-551.

[112] K. Zhang, Y. Gu, New qualitative and quantitative technical criteria for determining the minimum miscibility pressures (MMPs) with the rising-bubble apparatus (RBA), Fuel, 175 (2016) 172-181.

[113] M. Dong, S. Huang, S.B. Dyer, F.M. Mourits, A comparison of CO 2 minimum miscibility pressure determinations for Weyburn crude oil, Journal of Petroleum Science and Engineering, 31 (2001) 13-22.

[114] K. Zhang, Y. Gu, Two new quantitative technical criteria for determining the minimum miscibility pressures (MMPs) from the vanishing interfacial tension (VIT) technique, Fuel, 184 (2016) 136-144.

[115] L.E. Sobers, M.J. Blunt, T.C. LaForce, Design of simultaneous enhanced oil recovery and carbon dioxide storage with potential application to offshore trinidad, Spe Journal, 18 (2013) 345-354.

[116] S. Mohebbinia, K. Sepehrnoori, R.T. Johns, Four-phase equilibrium calculations of carbon dioxide/hydrocarbon/water systems with a reduced method, SPE Journal, 18 (2013) 943-951.

[117] Y. Li, R.T. Johns, Rapid flash calculations for compositional simulation, SPE Reservoir Evaluation & Engineering, 9 (2006) 521-529.

[118] D. Makimura, M. Kunieda, Y. Liang, T. Matsuoka, S. Takahashi, H. Okabe, Application of molecular simulations to CO2-enhanced oil recovery: phase equilibria and interfacial phenomena, SPE Journal, 18 (2013) 319-330.

[119] C. Chen, M.T. Balhoff, K.K. Mohanty, Effect of reservoir heterogeneity on primary recovery and CO2 Huff'n'Puff recovery in shale-oil reservoirs, SPE Reservoir Evaluation & Engineering, 17 (2014) 404-413.

[120] L. Zuo, Y. Chen, Z. Dengen, J. Kamath, Three-Phase Relative Permeability Modeling in the Simulation of WAG Injection, SPE Reservoir Evaluation & Engineering, 17 (2014) 326-339.

[121] T. Wan*, J.J. Sheng, M. Watson, Compositional modeling of the diffusion effect on EOR process in fractured shale oil reservoirs by gas flooding, in: Unconventional Resources Technology Conference, Denver, Colorado, 25-27 August 2014, Society of Exploration Geophysicists, American Association of Petroleum Geologists, Society of Petroleum Engineers, 2014, pp. 2248-2264.

[122] M.R. Beygi, M. Delshad, V.S. Pudugramam, G.A. Pope, M.F. Wheeler, Novel three-phase compositional relative permeability and three-phase hysteresis models, SPE Journal, 20 (2015) 21-34.

[123] C.S. Land, Calculation of imbibition relative permeability for two-and three-phase flow from rock properties, Society of Petroleum Engineers Journal, 8 (1968) 149-156.

[124] H. Shahverdi, M. Sohrabi, Relative permeability characterization for water-alternating-gas injection in oil reservoirs, SPE Journal, 21 (2016) 799-808.

[125] L. Li, J. Yao, Y. Li, M. Wu, L. Zhang, Pressure-transient analysis of CO 2 flooding based on a compositional method, Journal of Natural Gas Science and Engineering, 33 (2016) 30-36.

[126] Z. Wang, A. Khanzode, R.T. Johns, A Parametric Study of Reservoir Cooling for Enhanced Recovery by Carbon Dioxide Flooding, SPE Journal, 21 (2016) 839-852.

[127] C. Qiao, L. Li, R.T. Johns, J. Xu, Compositional modeling of dissolution-induced injectivity alteration during CO 2 flooding in carbonate reservoirs, SPE journal, 21 (2016) 809-826.

[128] A. Venkatraman, B. Dindoruk, H. Elshahawi, L.W. Lake, R.T. Johns, Modeling Effect of Geochemical Reactions on Real-Reservoir-Fluid Mixture During Carbon Dioxide Enhanced Oil Recovery, SPE Journal, (2017).

[129] T.Q.M.D. Tran, P. Neogi, B. Bai, Stability of CO 2 Displacement of an Immiscible Heavy Oil in a Reservoir, SPE Journal, (2017).

[130] B.M. Negash, L.D. Tufa, M. Ramasamy, M.B. Awang, System Identification Based Proxy Model of a Reservoir under Water Injection, Modelling and Simulation in Engineering, 2017 (2017).

[131] O. Olufemi, T. Ertekin, D.H. Smith, G. Bromhal, W.N. Sams, S. Jikich, Carbon Dioxide Sequestration in Coal Seams: A Parametric Study and Development of a Practical Prediction/Screening Tool Using Neuro-Simulation, in: SPE Annual Technical Conference and Exhibition, Society of Petroleum Engineers, 2004.

[132] A.M. Shehata, A.H. El-banbi, H. Sayyouh, Guidelines to optimize CO2 EOR in heterogeneous reservoirs, in: North Africa Technical Conference and Exhibition, Society of Petroleum Engineers, 2012.

[133] K. van't Veld, X. Wang, V. Alvarado, Economic Co-optimization of Oil Recovery and CO2 Sequestration, in: SPE Annual Technical Conference and Exhibition, Society of Petroleum Engineers, 2014.

[134] A. Leach, C.F. Mason, K. van't Veld, Co-optimization of enhanced oil recovery and carbon sequestration, Resource and Energy Economics, 33 (2011) 893-912.

[135] W. Ampomah, R.S. Balch, R.B. Grigg, B. McPherson, R.A. Will, S.Y. Lee, Z. Dai, F. Pan, Co-optimization of CO2-EOR and storage processes in mature oil reservoirs, Greenhouse Gases: Science and Technology, 7 (2017) 128-142.

[136] A.K. Jaber, M.B. Awang, C.P. Lenn, Box-Behnken design for assessment proxy model of miscible CO 2-WAG in heterogeneous clastic reservoir, Journal of Natural Gas Science and Engineering, 40 (2017) 236-248.

[137] E. Lindeberg, A.-A. Grimstad, P. Bergmo, D. Wessel-Berg, M. Torsæter, T. Holt, Large Scale Tertiary CO 2 EOR in Mature Water Flooded Norwegian Oil Fields, Energy Procedia, 114 (2017) 7096-7106.

[138] M. Noureldin, W. Allinson, Y. Cinar, H. Baz, Coupling risk of storage and economic metrics for CCS projects, International Journal of Greenhouse Gas Control, 60 (2017) 59-73.

[139] M.M. Salehi, M.A. Safarzadeh, E. Sahraei, S.A.T. Nejad, Experimental study of surfactant alternating gas injection versus water alternating gas and water flooding enhanced oil recovery methods, Journal of Petroleum and Gas Engineering, 4 (2013) 160-172.

[140] W. Li, D.S. Schechter, Using Polymer Alternating Gas to Maximize CO2 Flooding Performance for light oils, SPE 169942-MS, (2014).

[141] Y. Zhang, S.S. Huang, P. Luo, Coupling immiscible CO2 technology and polymer injection to maximize EOR performance for heavy oils, Journal of Canadian Petroleum Technology, 49 (2010) 25-33.

[142] R.H. Lane, A.H. Al-Ali, D.S. Schechter, Application of Polymer Gels as Conformance Control Agents for Carbon Dioxide EOR WAG Floods, in: SPE International Symposium on Oilfield Chemistry, Society of Petroleum Engineers, 2013.

[143] Y. Wu, J.J. Carroll, Z. Du, Carbon dioxide sequestration and related technologies, John Wiley & Sons, 2011.

[144] W. Feng, Z. Deping, Y. Guojun, P. Ruosheng, X. Shuai, CO Flooding WAG Safety Control Technology, in: SPE Asia Pacific Oil and Gas Conference and Exhibition, Society of Petroleum Engineers, 2013.

[145] M. Ali, N.U. Dahraj, S.A. Haider, Study of Asphaltene Precipitation during CO2 Injection in Light Oil Reservoirs, in: SPE/PAPG Pakistan section Annual Technical Conference, Society of Petroleum Engineers, 2015.

[146] M.Z. Hasanvand, M.A. Ahmadi, R.M. Behbahani, Solving asphaltene precipitation issue in vertical wells via redesigning of production facilities, Petroleum, 1 (2015) 139-145.

[147] S. Zheng, H.S. Fogler, A. Haji-Akbari, A fundamental wax deposition model for water-in-oil dispersed flows in subsea pipelines, AIChE Journal, (2017).

[148] S. Anisuzzaman, S. Abang, A. Bono, D. Krishnaiah, R. Karali, M. Safuan, Wax inhibitor based on ethylene vinyl acetate with methyl methacrylate and diethanolamine for crude oil pipeline, in: Materials Science and Engineering Conference Series, 2017, pp. 012074.

[149] N. Ridzuan, F. Adam, Z. Yaacob, Evaluation of the inhibitor selection on wax deposition for Malaysian crude oil, Petroleum Science and Technology, 34 (2016) 366-371.

[150] I. Maffeis, K. Mogensen, M. Rinaudo, M. De Simoni, F. Scarfato, G. Galli, G. Tripaldi, F. Belaid, H. Hachelaf, On the Road to 60% Oil Recovery by Implementing Miscible Hydrocarbon WAG in a North-African Field, in: SPE Asia Pacific Enhanced Oil Recovery Conference, Society of Petroleum Engineers, 2015.

[151] F. Gozalpour, S. Ren, B. Tohidi, CO2 EOR and storage in oil reservoir, Oil & gas science and technology, 60 (2005) 537-546.

[152] W. Li, Z. Dong, J. Sun, D.S. Schechter, Polymer-alternating-gas simulation: A Case Study, in: SPE EOR Conference at Oil and Gas West Asia, Society of Petroleum Engineers, 2014.

[153] J.R. Christensen, E.H. Stenby, A. Skauge, Review of WAG field experience, in: International Petroleum Conference and Exhibition of Mexico, Society of Petroleum Engineers, 1998.

[154] A.G. Ravagnani, E. Ligero, S. Suslick, CO 2 sequestration through enhanced oil recovery in a mature oil field, Journal of Petroleum Science and Engineering, 65 (2009) 129-138.

[155] S. Salem, T. Moawad, Economic study of miscible CO2 flooding in a mature waterflooded oil reservoir, in: SPE Saudi Arabia Section Technical Symposium and Exhibition, Society of Petroleum Engineers, 2013.

[156] P.R.d.C. Merschmann, A.S. Szklo, R. Schaeffer, Technical potential and abatement costs associated with the use of process emissions from sugarcane ethanol distilleries for EOR in offshore fields in Brazil, International Journal of Greenhouse Gas Control, 52 (2016) 270-292.

[157] G. Skaugen, S. Roussanaly, J. Jakobsen, A. Brunsvold, Techno-economic evaluation of the effects of impurities on conditioning and transport of CO 2 by pipeline, International Journal of Greenhouse Gas Control, 54 (2016) 627-639.

[158] K.M. Welkenhuysen, Bruno; Piessensa, Kris A profitability study of CO2-EOR and subsequent CO2 storage in the North Sea under low oil market prices, Energy Procedia, 114 (2017) 7060-7069.

[159] I.M. Fukai, Srikanta; Pasumarti, Ashwin, Technical and economic performance metrics for CCUS projects: Example from the East Canton Consolidated Oil Field, Ohio, USA, Energy Procedia, 114 (2017) 6968 – 6979.

[160] B. Harrison, G. Falcone, Carbon capture and sequestration versus carbon capture utilisation and storage for enhanced oil recovery, Acta Geotechnica, 9 (2014) 29-38.

[161] J.J. Heinrich, H.J. Herzog, D.M. Reiner, Environmental assessment of geologic storage of CO2, in: Second National Conference on Carbon Sequestration, 2003, pp. 5-8.

[162] K.L.S. Smith, M.D., Jones, D.G., West, J.M., Coombs, P., Green, K.A., Barlow, T.S., Breward, N., Gwosdz, S., Krüger, M., Beaubien, S.E., Annunziatellis, A.; Graziani, S.; Lombardi, L., Environmental impacts of CO2 leakage: recent results from the ASGARD facility, UK, Energy Procedia, 37 (2013) 791 – 799.

[163] T. Xiao, B. McPherson, F. Pan, R. Esser, W. Jia, A. Bordelon, D. Bacon, Potential chemical impacts of CO 2 leakage on underground source of drinking water assessed by quantitative risk analysis, International Journal of Greenhouse Gas Control, 50 (2016) 305-316.

[164] F. Chen, W. Zhang, J. Ma, Y. Yang, S. Zhang, R. Chen, Experimental study on the effects of underground CO 2 leakage on soil microbial consortia, International Journal of Greenhouse Gas Control, 63 (2017) 241-248.

Chapter Three: Equilibrium Ratio of Hydrocarbons and Non-Hydrocarbons at Reservoir Conditions

Abstract

Determination of equilibrium composition for various multi-phase systems is important in the context of thermodynamics. Three methods are generally employed to calculate the gas/liquid equilibrium compositions; namely, empirical graphs, correlations, and equations of state (EOSs). Empirical graphs and correlations are simple and fast in terms of calculation procedure. Furthermore, using an EOS requires an initial guess, which is usually obtained via empirical correlations. In this study, the gas-oil composition of 10 different crude oils (20 to 40 °API) are experimentally determined by a gas chromatography (GC) apparatus within a temperature range of 600 to 1212 °R and a pressure range of 14.7 psi to 7000 psi. A robust predictive model is then proposed to estimate the equilibrium ratios (K_i) of hydrocarbons and non-hydrocarbons. This model is generated by utilizing the least squares support vector machine (LSSVM), while genetic algorithm (GA) is used for selection and optimization of hyper parameters (γ and σ^2) that are embedded in the LSSVM model. The coefficient of determination (R^2) for the introduced model is 0.9991 and 0.9979 and the mean squared error (MSE) is 0.00074 and 0.044 for the hydrocarbons and non-hydrocarbons, respectively. The proposed model is simple to use and exhibits high accuracy and reliability, which can have various applications in chemical and petroleum industries where the thermodynamic equilibrium is maintained.

3.1. Introduction

Accurate knowledge of phase equilibria is vital in several engineering processes. The empirical graphs, correlations, and equations of state (EOSs) are three common techniques to obtain mixture characteristics at equilibrium conditions [1-3]. An important parameter in gas-oil equilibrium predictions is the equilibrium ratio. The equilibrium ratio of ith component in a mixture (K_i) is defined as the ratio of the fraction of ith component in the gas phase to that in the liquid phase, at vapor-liquid equilibrium, as shown below.

$$K_i = \frac{y_i}{x_i} \tag{3-1}$$

where y_i and x_i stand for the mole fraction of component i in the vapor phase and the liquid phase, respectively. Equilibrium ratios may reach unity at high pressures for some multi-component mixtures, meaning that the concentration of ith component is equal in both liquid and vapor phases[4].

The most common empirical graphs used in the phase equilibrium calculations are Katz and Cox charts. In both charts, the K_i values of each component are independent of the composition mixture. These charts, which were presented by Gas Processors Society in 1957, are available for paraffins (C_1-C_{10}), ethylene, propylene, nitrogen, and carbon dioxide[4, 5].

According to the Raoult's law for hydrocarbons, a plot of K_i values versus pressure yields a straight line with a slope of unity at low pressures (10-500 psi). The intercept of the line is dependent on the molecular weight of the constituent. Katz et al. [5] presented a series of revised graphs for various hydrocarbons for a convergence pressure of 5000 psi. They also showed that K_i value of CO_2 can be estimated as the square root of the product of K_i values of methane and ethane [5].

Empirical correlations are the mathematical forms of the empirical graphs. These correlations generally include convergence pressure and a parameter representing the component as the variables [6]. For example, standing et al. proposed an equation for estimating K_i value of Oklahoma oil/gas mixtures [7]. The K-value in Standing et al.'s Equation is assumed independent of the mixture composition. The correlation is only accurate at low pressures (below 1000 psi) [7]. There is another empirical correlation which is called the Wilson correlation. This equation is commonly used for calculating K_i values of paraffins. The correlation is applicable over the pressure range of 14.7-500 psi. This relationship results in accurate estimations where the target pressure is below the critical pressures of components. The modified Wilson equation is an extension of Wilson equation which can be utilized at higher pressures up to sub-critical condition [8].

Support vector machine (SVM), which was first introduced by Vapnik in 1998, is a type of machine learning approach [9]. SVM is an efficient method that has been widely employed for solving different complex cases in various engineering disciplines[10]. The main aim of SVM is to convert the nonlinear input space into a high-dimensional characteristic space and to obtain a hyper-plane through nonlinear mapping[11]. This new methodology is based on the different statistical concepts[12]. Quadratic programming (QP) is rather than returning many local solutions like other regression methodologies, the solution returned by SVM is global or even unique. This is because the QP puzzle is a convex function[13]. This method might be time-consuming and difficult to be used as it should find a solution for a set of nonlinear equations. Suykens and Vandewalle proposed the least square support vector machine (LSSVM) method as an alternative form of the SVM method [14-16]. LSSVM's advantage over SVM is

that it only requires a group of linear calculations. This makes LSVVM computationally straightforward and easier.

This study uses the LSSVM model, as a generalization of traditional SVM, to estimate the equilibrium ratios (K_i) of hydrocarbons and non-hydrocarbons. Genetic algorithm (GA) is implemented as an optimizer scheme for adjustment of LSSVM variables. This work contains the novelty of using the SVM approach to forecast the equilibrium ratios (K_i) of hydrocarbons and non-hydrocarbons. No records of such a mathematical approach are found in the literature.

3.2. Experimental Methodology

10 different oil samples from different Iranian oil reservoirs were employed in our experiments. As a result, the values of gas to oil ratio (GOR), bubble point pressure, and reservoir temperature were different. To analyze the components of each live oil sample, 100 cm^3 of each oil sample were flashed from the reservoir condition to the atmospheric condition. The number of flashing steps strongly depends on the bubble point pressure and GOR. As each oil sample has an unique GOR and bubble point pressure, the starting pressure in the flash tests is different for various oil samples. Hence, the flash steps are different for various samples. After the flash process of the live oil sample, the compositional analysis of produced gas phase and residual hydrocarbon liquid was carried out via Agilent 7890A gas chromatograph (GC). The range of temperature of the stationary phase at operating conditions was 600 to 1212 ^{o}R. Using the flame ionization detector (FID), the relative concentration of each component can be determined. In this work, the thermal conductivity detector (TCD) was used to analyze the components up to C_4 and the FID detector was employed to measure the concentrations of heavier components, particularly C_{5+} .

71

3.3. Theory

3.3.1. Least Square Support Vector Machine (LSSVM)

The methodology of LSSVM for nonlinear function approximation is as below. A training data set is defined for generating the model. The data set is defined as: $\{x_k, y_k\}$, $k = 1, 2, \ldots, N$, where $x_k \in \mathbb{R}^n$ is the kth input data in the input space, $y_k \in \mathbb{R}$ is the output value for a specified input variable (e.g., x_k) and N represents the number of the training data points. We consider the given inputs x_k such as critical pressure (P$_c$, psia), critical temperature (T$_c$, ºR), acentric factor, gas oil ratio (GOR, SCF/STB), temperature, and pressure. The output y is the equilibrium ratio. Using the nonlinear function, $\varphi(\cdot)$, that maps the training set in the input space to the high dimensional space, the regression paradigm of Equation (3-2) is created [17, 18] :

$$y = w^T \varphi(x) + b \quad with \quad w \in \mathbb{R}^n, \quad b \in \mathbb{R}, \quad \varphi(\cdot) \in \mathbb{R}^n \to \mathbb{R}^{n_h}, \quad n_h \to \infty \quad (3\text{-}2)$$

where w is the vector of weight and b represents a term of bias. The superscript "n" stands for the data space's dimension, and "n_h" denotes the unidentified characteristic space's dimension [13]. When the LSSVM modeling is performed, a new optimization problem is obtained. The developed model deals with the optimization problem as presented by Equation (3-3) [17, 18].

$$\underset{w,b,e}{min} \quad \mathcal{J}(w,e) = \frac{1}{2} w^T w + \frac{1}{2}\gamma \sum_{k=1}^{N} e_k^2 \quad (3\text{-}3)$$

Equation (3-3) is subject to the equality constraint shown by the following expression:

$$y_k = w^T \phi(x_k) + b + e_k \quad k = 1, 2, \ldots, N \quad (3\text{-}4)$$

in which, γ is the regularization parameter, which balances the complexity of the model and the training error, and e_k represents the regression error [12].

To specify the solution to the restricted optimization puzzle, the Lagrangian is constructed as illustrated below.

$$\mathcal{L}(w, b, e, \alpha) = \mathcal{J}(w, e) - \sum_{k=1}^{N} \alpha_k \{w^T \phi(x_k) + b + e_k - y_k\} \tag{3-5}$$

where α_k are the Lagrange multipliers or support values. Solving this equation requires differentiating Equation (3-5).

Equations (3-6) to (3-9) show the differentiated forms of Equation (3-5) with respect to w, b, e_k, and α_k, respectively [17, 18].

$$\frac{\partial \mathcal{L}(w, b, e, \alpha)}{\partial w} = 0 \rightarrow w = \sum_{k=1}^{N} \alpha_k \varphi(x_k) \tag{3-6}$$

$$\frac{\partial \mathcal{L}(w, b, e, \alpha)}{\partial b} = 0 \rightarrow \sum_{k=1}^{N} \alpha_k = 0 \tag{3-7}$$

$$\frac{\partial \mathcal{L}(w, b, e, \alpha)}{\partial e_k} = 0 \rightarrow \alpha_k = \gamma e_k, \quad k = 1, \dots, N \tag{3-8}$$

$$\frac{\partial \mathcal{L}(w, b, e, \alpha)}{\partial \alpha_k} = 0 \rightarrow y_k = \varphi(x_k) w^T + b + e_k, \quad k = 1, \dots, N \tag{3-9}$$

After substituting the variables w and e with their equivalents as found by the previous formulas, the Karush-Kuhn-Trucker system is achieved as shown by Equation (3-10) [17, 18].

$$\begin{bmatrix} 0 & 1_v^T \\ 1_v & \Omega + \gamma^{-1}I \end{bmatrix} \begin{bmatrix} b \\ \alpha \end{bmatrix} = \begin{bmatrix} 0 \\ y \end{bmatrix} \tag{3-10}$$

where $y = [y_1 \dots y_N]^T, 1_N = [1 \dots 1]^T, \alpha = [\alpha_1 \dots \alpha_N]^T$ and I is an identity matrix. The symbol $\Omega_{kl} = \varphi(x_k)^T . \varphi(x_l) = K(x_k, x_l) \forall\ k\ l = 1, \dots, N. K(x_k, x_l)$ represents the kernel function and should meet the Mercer's circumstance[19]. The kernel functions are well-known and widely used in engineering problems. They are listed below [17, 18].

- $K(x, x_k) = x_k^T x$ (3-11)

- $K(x, x_k) = (\tau + x_k^T x)^d$ (3-12)

- $K(x, x_k) = exp(-\|x - x_k\|^2 / \sigma^2)$ (3-13)

Finally, the yielding expression of LSSVM method for the function approximation is obtained as displayed by the following relationship [17, 18].

$$y(x) = \sum_{k=1}^{N} \alpha_k K(x, x_k) + b \tag{3-14}$$

in which, (b, α) stands for the solution of the linear system in Equation (3-14).

In the literature, an extensive introduction to SVM is presented [9, 14-16, 20-22]. The theory of LSSVM has been also thoroughly reviewed [14, 15, 20]. Ahmadi et al. also described the detailed concepts and procedure of the LSSVM strategy [17, 22, 23].

3.3.2. Genetic Algorithm (GA)

Genetic algorithm (GA) is a stochastic method for solving optimization problems. It is based on the Darwinian evolution theorem and various genetic operators [17-20]. These genetic operators include mutation and crossover [23]. A favorable feature of GAs is that they do not require the differentiating of complex functions. The stochastic nature of the GA with dynamic evaluation of the fitness function makes it an efficient random search engine. This algorithm is a superior alternative to derivative-based algorithms, since the fitness function can be non-differentiable, stochastic, and potentially highly nonlinear[17, 24, 25].

3.4. Modeling Methodology

Equilibrium ratio (K_i) for hydrocarbons and non-hydrocarbons, as output, was estimated using the proposed method. The model consists of six inputs including critical pressure (P_c, psia), critical temperature (T_c, ^{o}R), acentric factor, gas oil ratio (GOR, SCF/STB), temperature (^{o}R), and absolute pressure (psia).

The experimental data was divided into two subsets. This grouping is conducted so that a portion of the data is used for model development and the rest is utilized for evaluation of the generated model (testing data set). The training data set contains 80% of the total data: 158 data points for evaluation of non-hydrocarbon K_i values and 634 data points for K_i of hydrocarbons. The remaining 20% of the data is used for examining the prediction capability of the proposed model.

The RBF kernel was chosen as the kernel function due to its simplicity (fewer parameters involved) and better overall performance [15, 17-19, 23, 26, 27]. According to Equations (3-10) to (3-14), the regularization factor (γ) and kernel sample variance (σ^2) influence the accuracy and generalization of the obtained LSVVM model, while utilizing the RBF kernel function[13].

The GA algorithm is applied to specify the optimum values of γ and σ^2. The fitness function in the GA was the average absolute relative deviation (AARD) of testing data. The flow chart in Figure 3-1 shows the procedure for hyper parameters using GA. The following procedure provides an explanation of a GA for adjusting hyper parameters of the LSSVM model step by step.
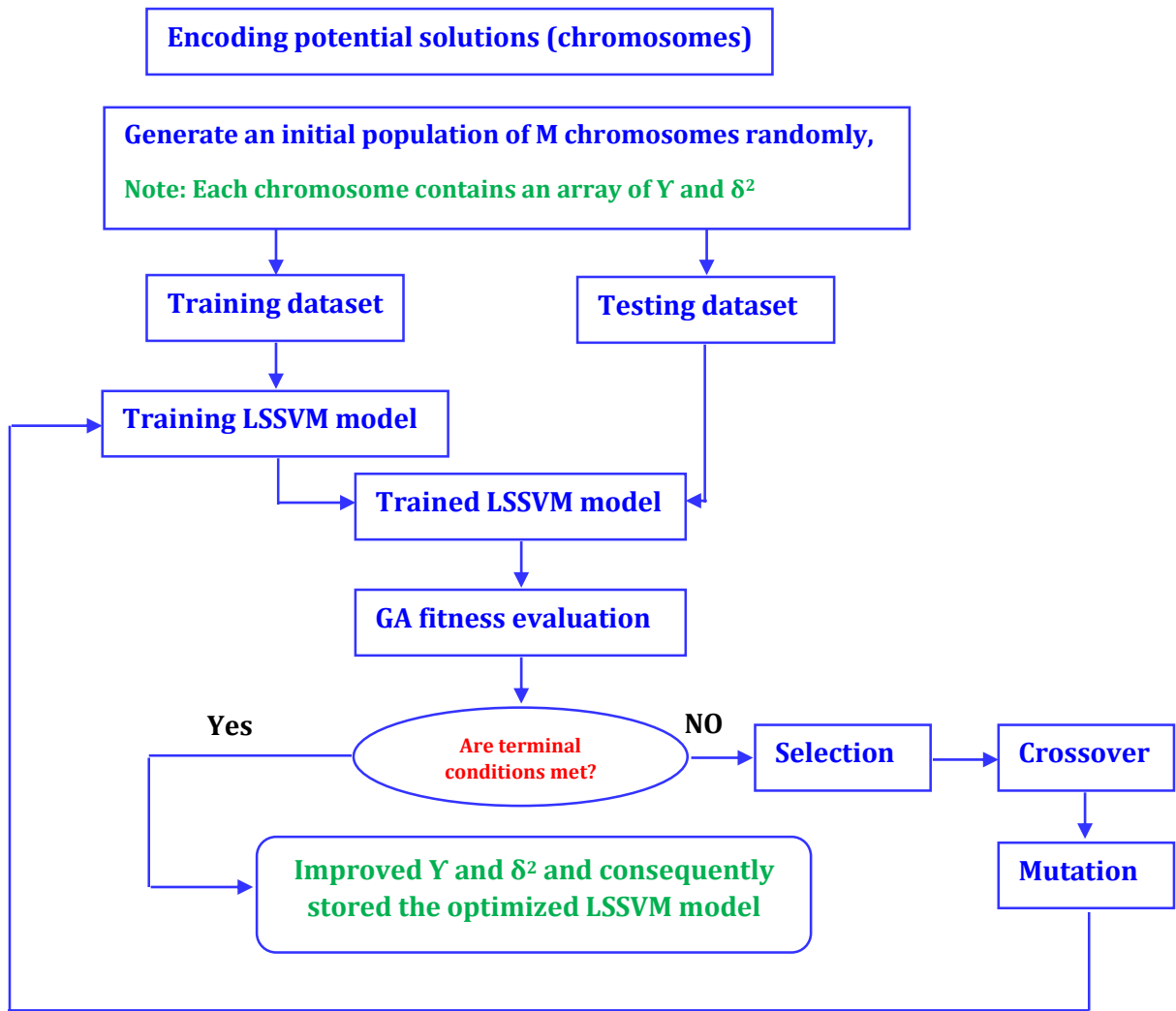
Figure 3-1: Flowchart of hyper parameters selection based on GA

i.   GA begins with an initial population (a set of randomly candidate solutions) represented by chromosomes. Each chromosome comprises an array of the hyper parameters (γ and σ^2).

ii.   The AARD (as the fitness) of each chromosome in the population is determined.

iii. On the basis of their calculated fitness magnitudes, some chromosomes in the present population are chosen to be a part of the population examined throughout further creation. Chromosomes with greater

fitness values have a higher opportunity of stand chosen than those having lower fitness. The selected chromosomes are implemented to make fresh offspring through genetic operators (mutation and crossover) to engender the population for further creation.

iv.   Crossover is defined as the progress of taking two parent outcomes and creating offspring from them. Using this procedure, the population with better chromosomes will be generated.

v.   Mutation is defined as the progress of randomly altering the extent of genes throughout a chromosome. The primary goal of mutation is to involve fresh genetic matters in the population, leading to the diversity of genetics. Moreover, the mutation avoids the GA to entrapment in local optima.

vi.   The fresh population (new combination of hyper parameters) is employed for next execution of the algorithm.

vii.   This process is repeated until meeting the termination criteria (e.g., when an acceptable outcome or the minimum value of the AARD is attained).

The optimization procedure was repeated several times for obtaining the most possible global optimal of the fitness function. The final values of σ^2 and γ were found to be 4.48527337 and 19067.1487 for the hydrocarbons and 0.39915 and 3.8272 for the non-hydrocarbons, respectively.

3.5. Results and Discussion

3.5.1. Experimental Results

This section provides the main results and discussion on the deterministic model development of equilibrium ratio for hydrocarbon and non-hydrocarbon systems where a systematic parametric sensitivity analysis and comparison strategies are performed to examine the effectiveness of the developed tool.

Figure 3-2 depicts the variation of equilibrium ratio versus corresponding pressure for hydrocarbon gases for an oil sample. It should be noted that the temperature of the experiments was 663 ^{o}R and the gas oil ratio (GOR) was 293 SCF/STB. As seen in Figure 3-2, the equilibrium ratio is decreased by increasing the pressure. The rate of decreasing for light components (C_1, and C_2) was greater than heavier ones (C_7, C_8, and C_9). Figure 3-3 illustrates the variation of equilibrium ratio with pressure for hydrocarbon gases when T = 672 ^{o}R and GOR = 321 SCF/STB. The equilibrium ratio versus corresponding pressure for hydrocarbon gases is demonstrated in Figure 3-4 where GOR = 1217 SCF/STB and T = 735 ^{o}R. The same trend as observed in Figure 3-2 is noticed in Figure 3-4.
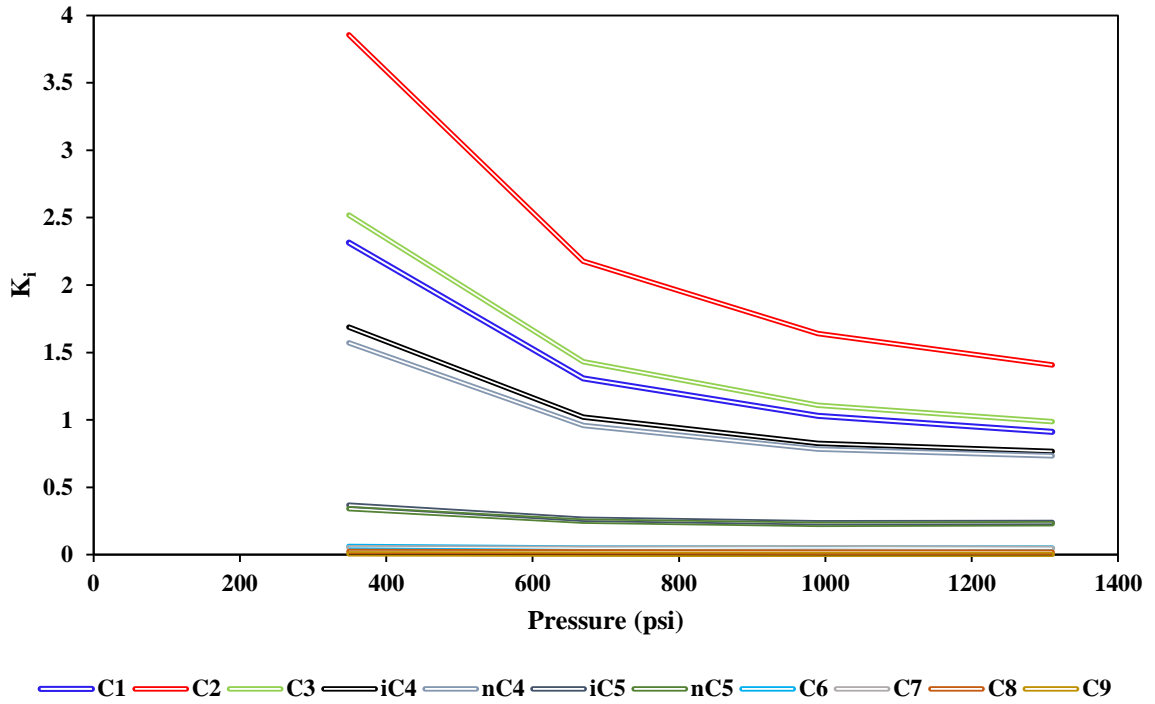
Figure 3-2: Measured equilibrium ratio (K_i) for hydrocarbon gases versus pressure at T= 663 °R and GOR = 293 SCF/STB
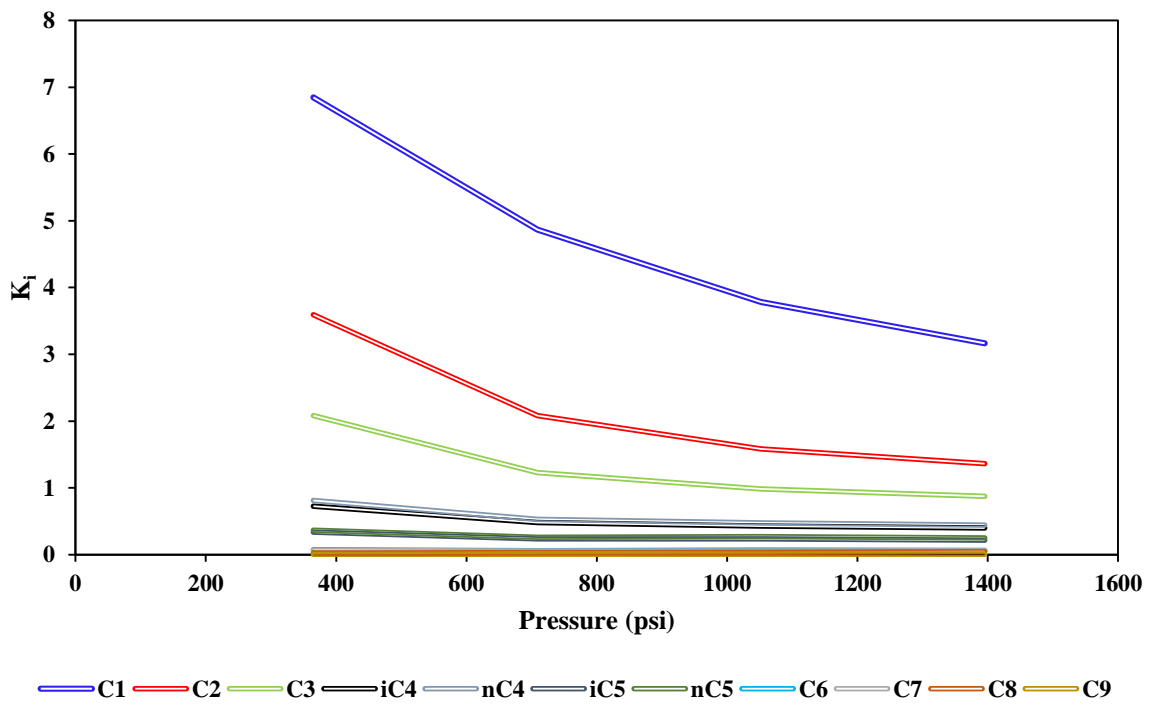
Figure 3-3: Measured equilibrium ratio (K_i) for hydrocarbon gases versus pressure at T= 672 °R and GOR = 321 SCF/STB
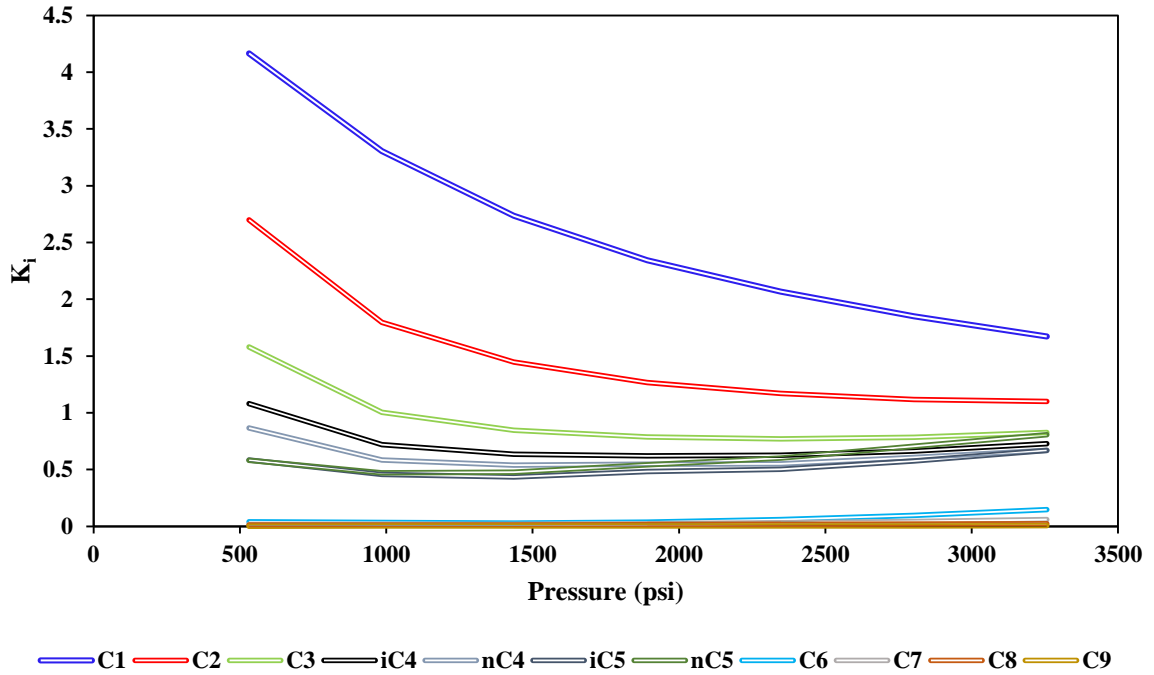
Figure 3-4: Measured equilibrium ratio (K_i) for hydrocarbon gases versus pressure at T= 735 °R and GOR = 1217 SCF/STB

Figure 3-5 illustrates the variation of equilibrium ratio against pressure for H_2S gas at various gas oil ratios and T = 663 °R. As depicted in Figure 3-5, at a constant temperature by increasing the pressure the equilibrium ratio of H_2S is decreased. According to Figure 3-5, at constant pressure and temperature, the equilibrium ratio of H_2S lowers as the gas oil ratio increases.
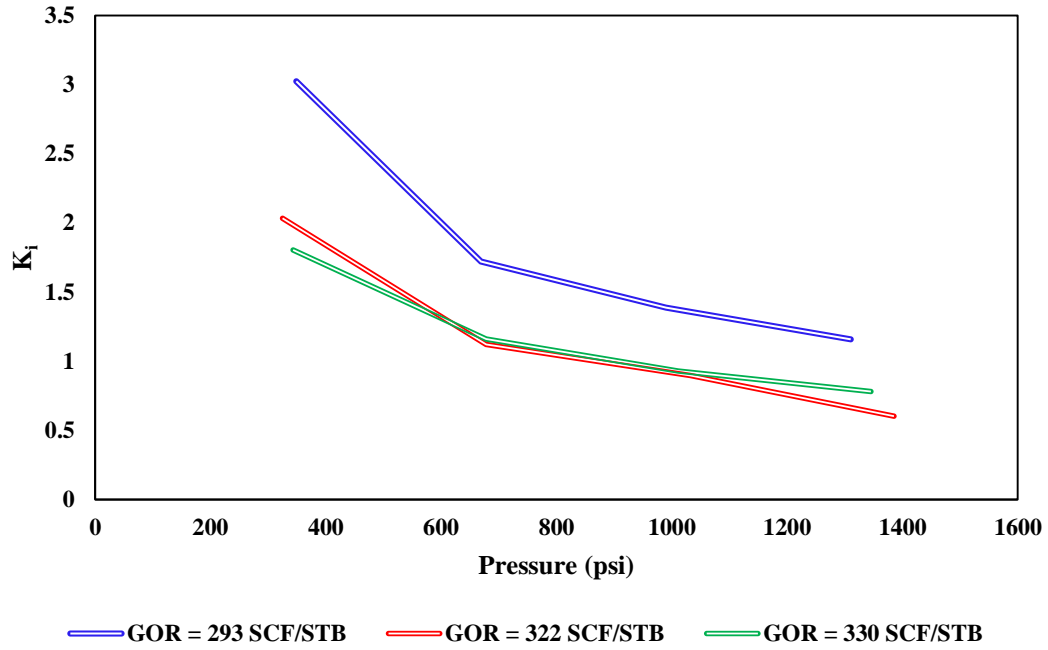
Figure 3-5: Measured equilibrium ratio (K_i) for H_2S versus pressure at different GORs

Figure 3-6 presents the equilibrium ratio versus pressure for N_2 gas at various gas oil ratios and T = 663 °R. As illustrated in Figure 3-6, at a constant temperature by increasing the pressure the equilibrium ratio of N_2 is first increased and then is reduced. As clear from Figure 3-6, at constant pressure and temperature, the gas oil ratio affects the equilibrium ratio of N_2.

Figure 3-6: Measured equilibrium ratio (K_i) for N_2 versus pressure at different GORs

The equilibrium ratio versus pressure for CO_2 gas at various gas oil ratios and T = 663 ᵒR is presented in Figure 3-7. At a constant temperature, the equilibrium ratio of CO_2 decreases as the pressure increases.
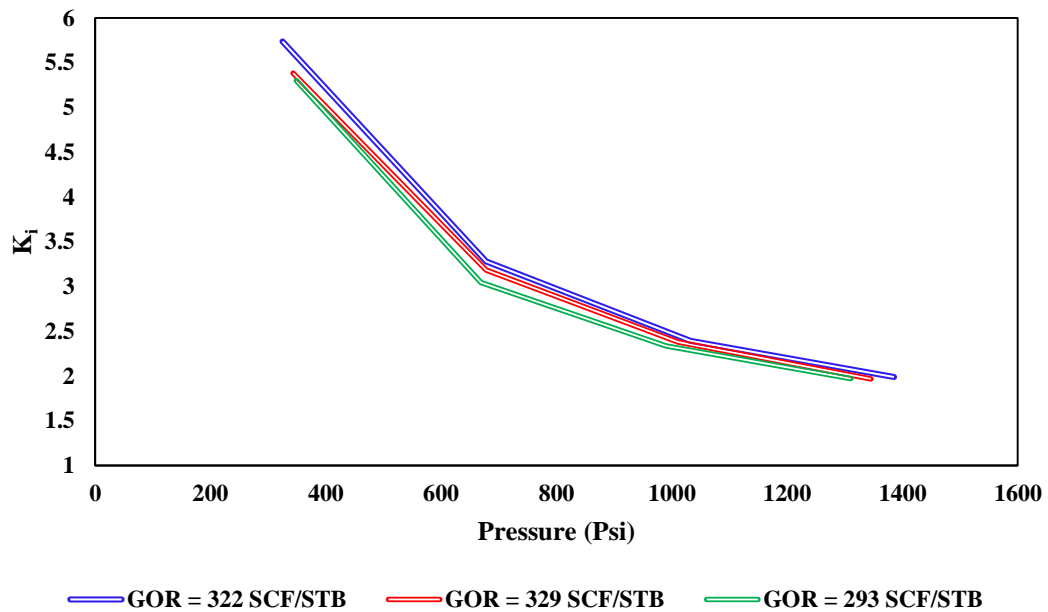
Figure 3-7: Measured equilibrium ratio (K_i) for CO_2 versus pressure at different GORs

3.5.2. Modeling Results

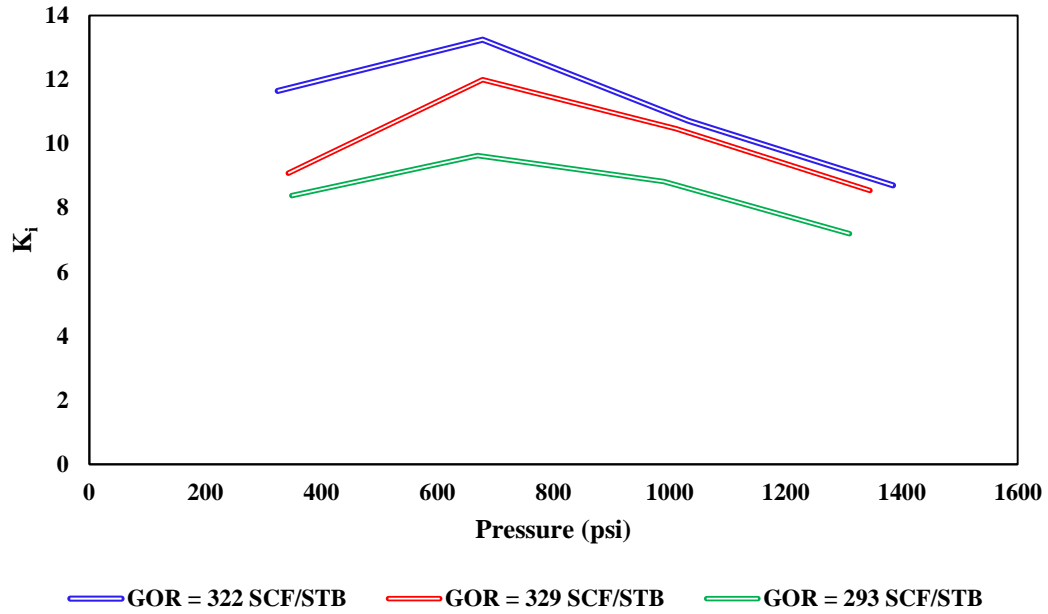The main criteria for evaluating the proposed model's performance are the mean squared error (MSE), and correlation coefficient (R^2). The value of MSE reaches zero and R^2 reaches unity in an ideal model. Equations (3-15) and (3-16) show the expressions used to calculate MSE and R^2, respectively.

$$MSE = \frac{1}{N} \sum_{i=1}^{N} (y^{actual}_i - y^{predicted}_i)^2 \tag{3-15}$$

$$R^2 = 1 - \frac{\sum_{i=1}^{N} (y^{actual}_i - y^{predicted}_i)^2}{\sum_{i=1}^{N} (y^{actual}_i - \overline{y^{actual}})^2} \tag{3-16}$$

where N denotes the number of data points, y^{actual}_i is the ith target, $y^{predicted}_i$ is the ith output of the model and $\overline{y^{actual}}$ stands for the average of the measured real values. Table 3-1 lists the calculated values of MSE and R^2 for all groups of data. According to this table, the R^2 values are close to one and the MSE is very low (close to zero) for both hydrocarbon and non-hydrocarbon cases. This implies that the model exhibits a satisfactory performance.

Table 3-1: Performance of GA-LSSVM method with optimized parameters for prediction of equilibrium ratio (K_i) of hydrocarbons and non-hydrocarbons in terms of statistical parameters

	Equilibrium Ratio (K_i) of Hydrocarbon		
	Training data	**Testing data**	**Overall data**
MSE	0.0003	0.0023	0.0007
R^2	0.9986	0.9980	0.9991
	Equilibrium Ratio (K_i) of non-hydrocarbons		
MSE	0.0524	0.0144	0.0440
R^2	0.9979	0.9986	0.9979

Figure 3-8 depicts the experimental K_i value of methane versus pressure at two different temperatures for a GOR of 322 SCF/STB. Figure 3-9 includes the similar curve (experimental hydrocarbon K_i values as a function of pressure), but at different GOR and a temperature of 663 °R.
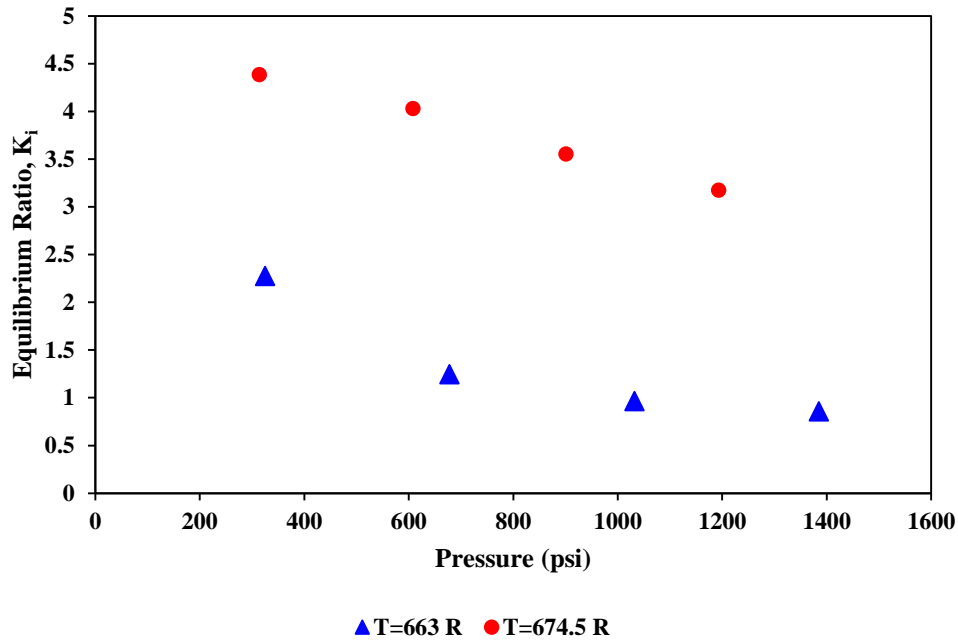
Figure 3-8: Measured equilibrium ratio (K_i) for methane versus pressure at GOR=322 SCF/STB
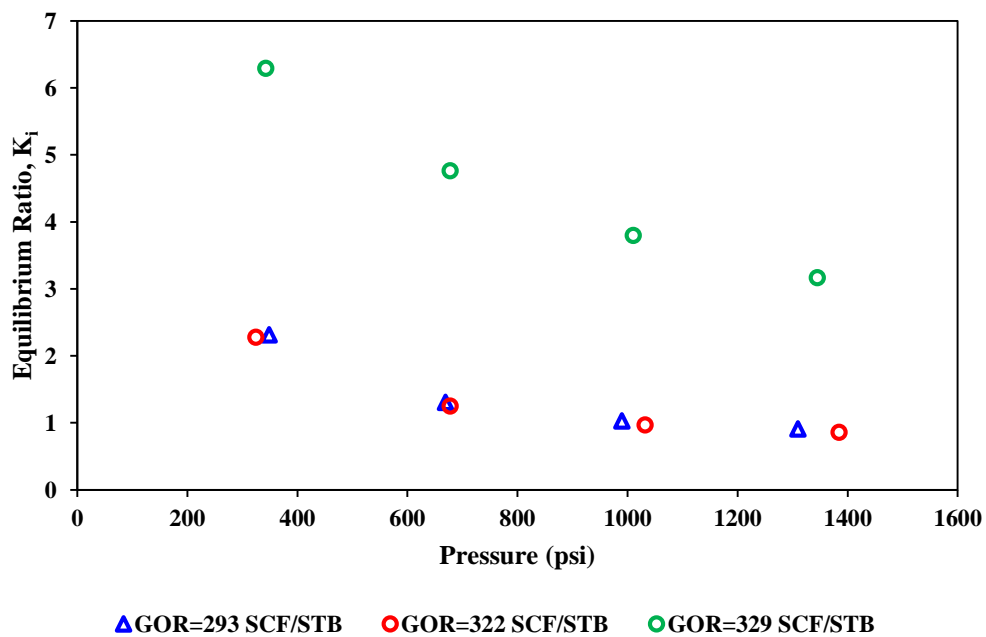
Figure 3-9: Measured equilibrium ratio (K_i) for methane versus pressure at T=663 °R

Figures 3-10 through 3-13 evaluate the model's performance on determining K_i values of hydrocarbons based on various parameters. Figures 3-14 through 3-17 investigate the same matter for non-hydrocarbons.

Figure 3-10 is a plot that describes the variation of hydrocarbon K_i values with pressure. This graph consists of both real data and the GA-LSSVM predictions. This figure shows that the model's output is almost a replicate of the experimental data. The excellent performance of the model is better seen in Figure 3-11. As it is clear, the plot of experimental K_i values of hydrocarbons versus the model's predictions fall on a straight line with a slope of unity and there is a low number of actual data points in the vicinity of the line.

Figure 3-10: Comparison between estimated and measured equilibrium ratio (K_i) for hydrocarbons versus data index

Figure 3-11: Scatter plot of estimated and measured equilibrium ratio (K_i) for hydrocarbons

In addition, the plot of actual K_i data and predicted K_i values versus pressure shows high accuracy in forecasting K_i at both tested temperatures (Figure 3-12). The model's precision can also be evaluated according to the distribution of relative deviation of the estimated K_i values versus the experimental K_i data of hydrocarbons (Figure 3-13). According to Figure 3-13, the relative errors lie in the range of -9.766% to 9.982%, the absolute value of the minimum relative error is 0.00179%, and the average absolute error is 2.093%.
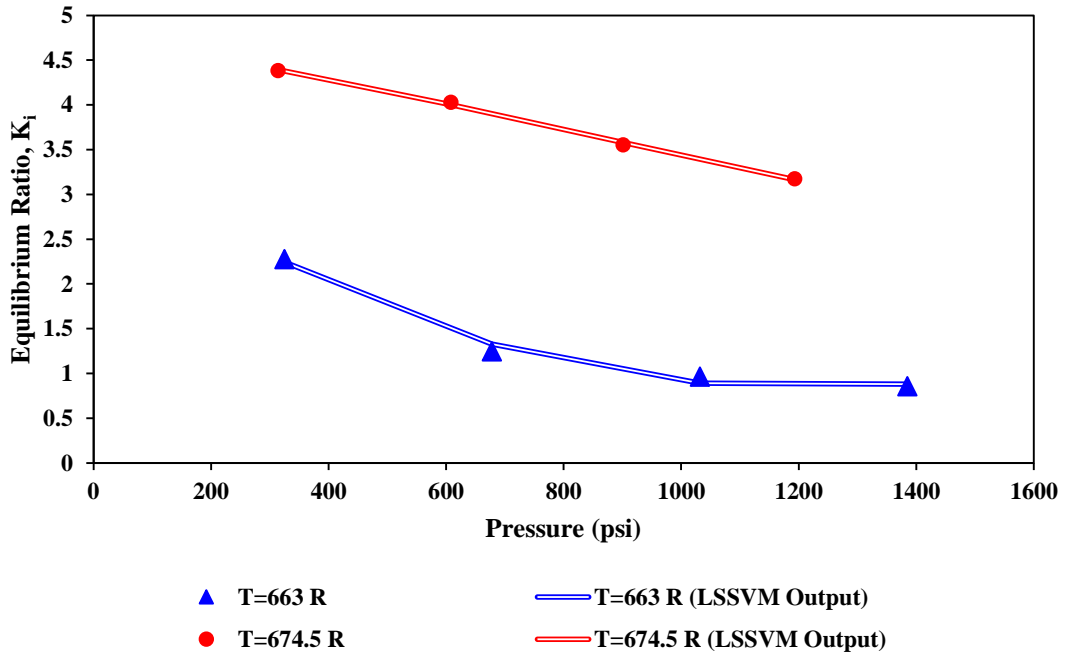
Figure 3-12: Comparison between predicted and measured equilibrium ratio (K$_i$) for methane versus pressure at GOR=322 SCF/STB

Figure 3-13: Relative error distribution of the estimated target versus equilibrium ratio (K$_i$) for hydrocarbons

Figure 3-14 shows the actual and predicted K_i values of non-hydrocarbons. According to Figure 3-14, there is a very good match between the GA-LSSVM model's predictions and the experimental data. Figure 3-15 compares the K_i values with model's predictions for two data groups: training and testing data sets. According to Figure 3-15, the fitted line tracks the actual data points entirely. This further confirms the model's exceptional performance.
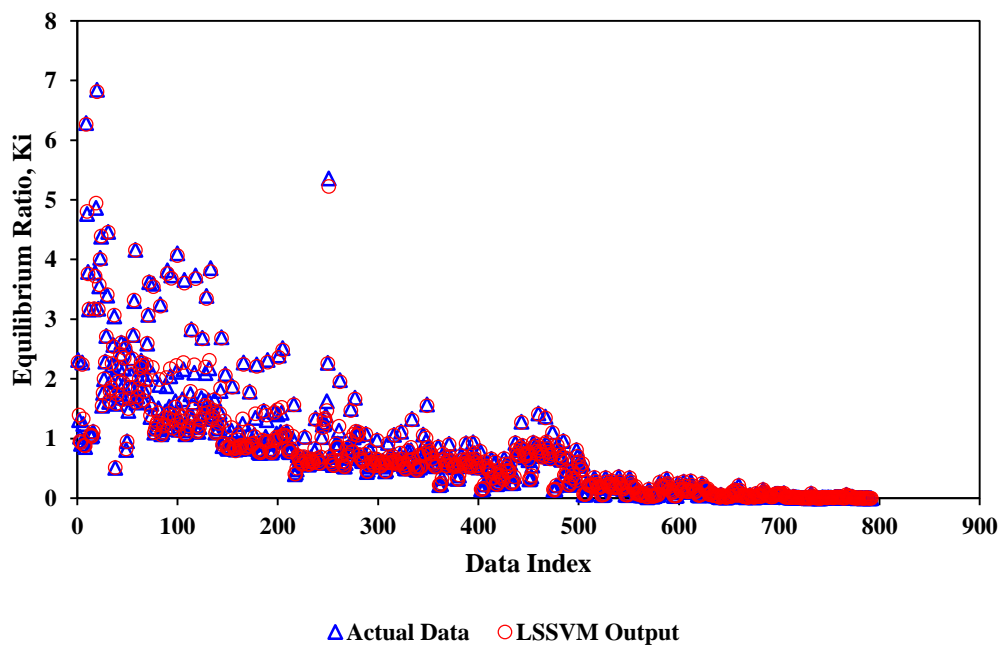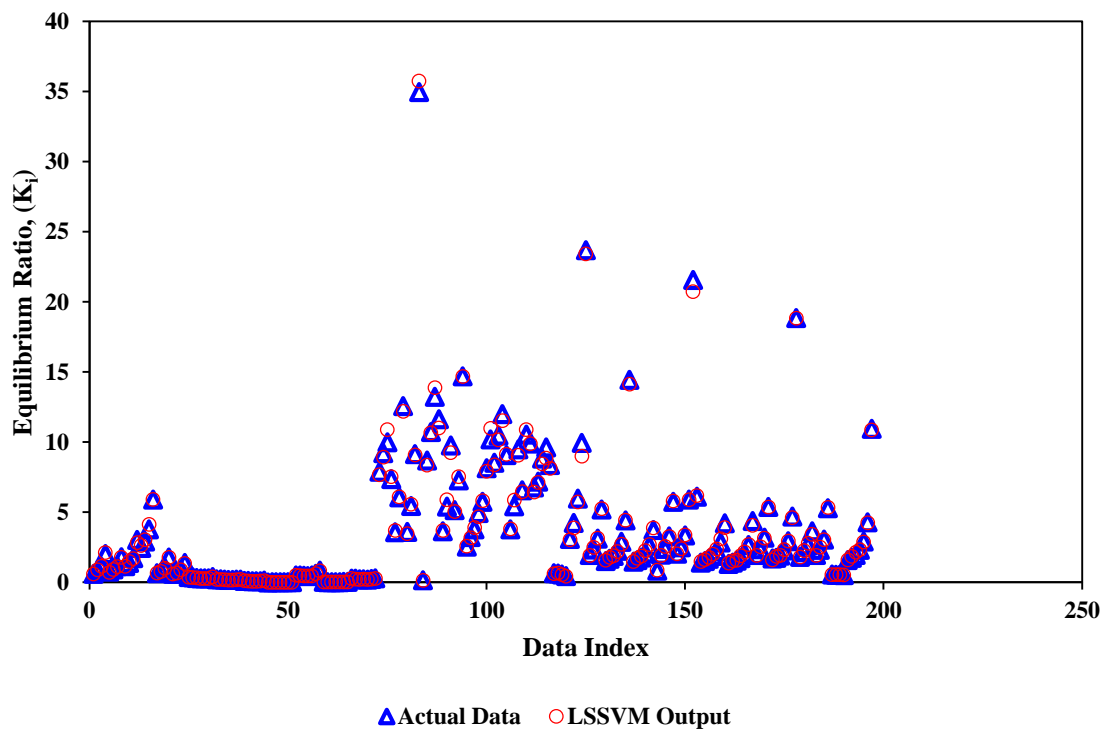

Figure 3-14: Comparison between estimated and measured equilibrium ratio (K_i) for non-hydrocarbons versus data index
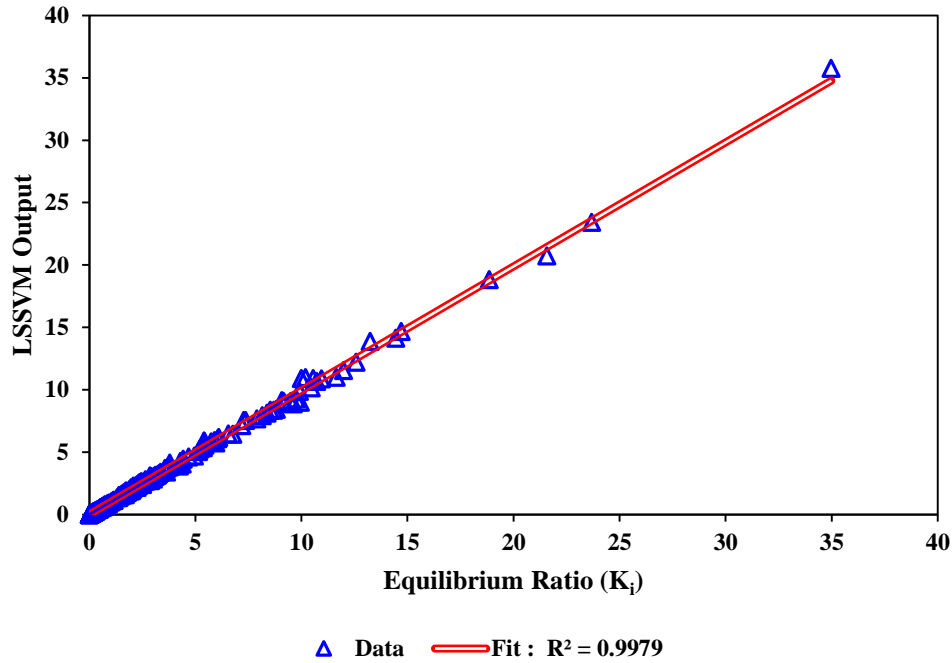
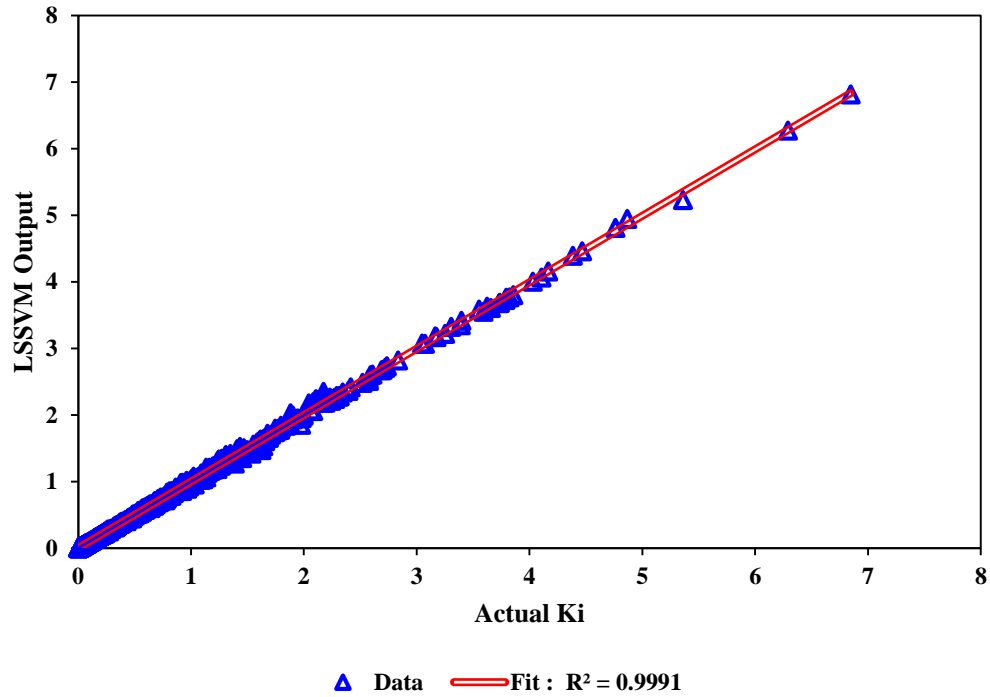Figure 3-15**:** Scatter plot of estimated and measured equilibrium ratio (K_i) for non-hydrocarbons

A broader evaluation can be made based on Figure 3-16, which describes hydrogen sulphide K value against pressure at two tested temperatures and a GOR of 332 SCF/STB. Figure 3-16 again approves the exactness of the model's results. According to Figure 3-17 that presents the relative deviation of model's output from real K_i values versus pressure, the relative errors lie in the range of -10.06% to 9.88%, the absolute value of the minimum relative error is 0.0162 %, and the average absolute error is 3.17%. The values of error percent clearly imply a very good agreement between the estimated values and measured data.

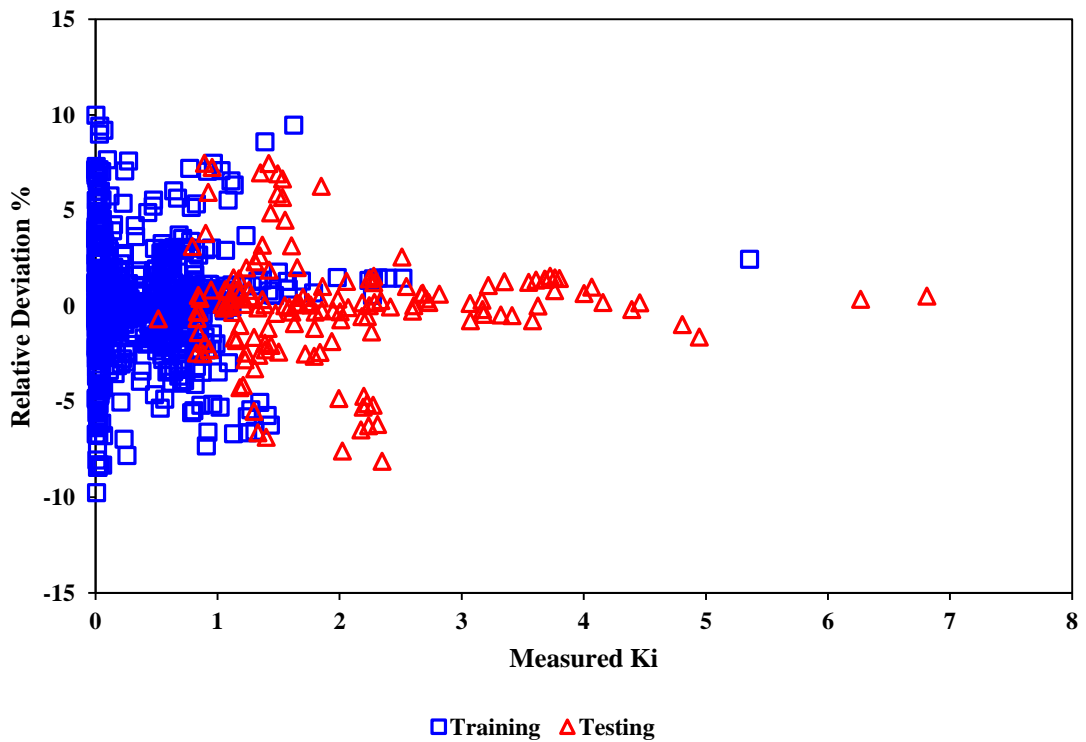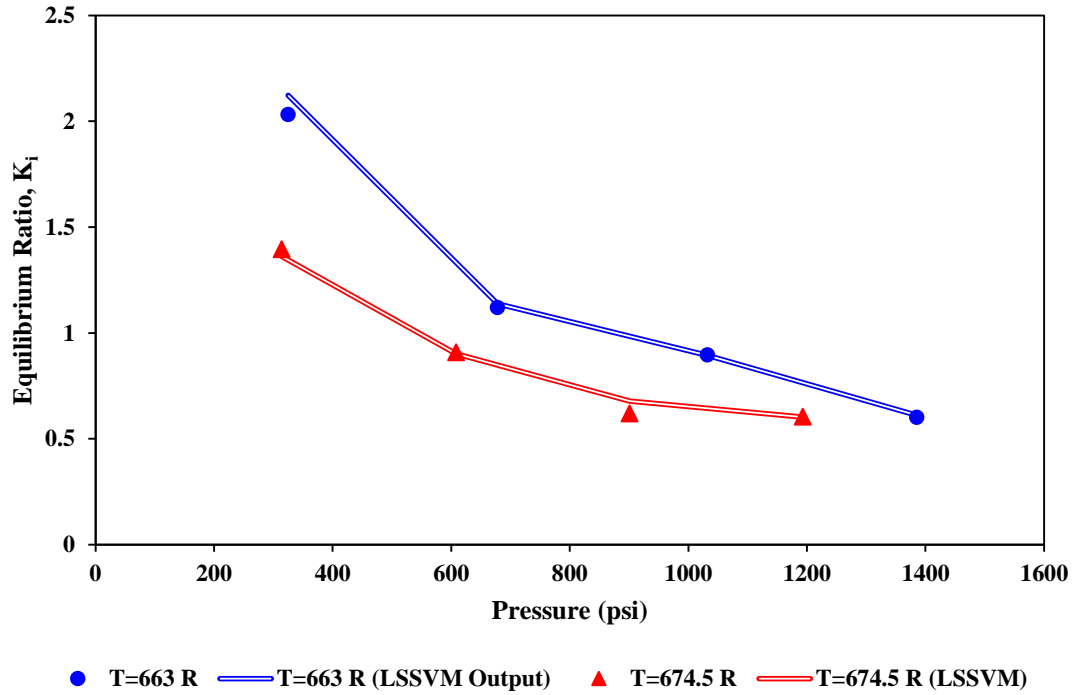Figure 3-16: Comparison between estimated and measured equilibrium ratio (K_i) for hydrogen sulfide (H_2S) versus pressure
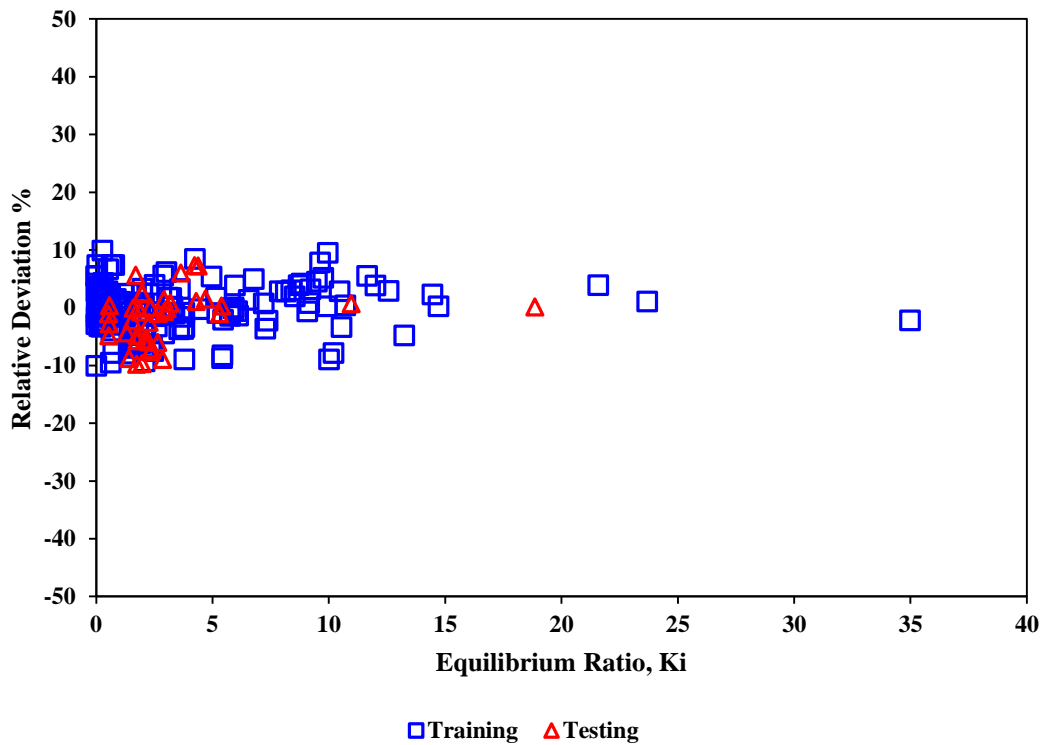
Figure 3-17: Relative error distribution of the estimated target versus equilibrium ratio (K_i) for non-hydrocarbons

To further examine the model, Wilson and Standing's correlations are applied to the experimental data. Computer Group Modeling (CMG) reservoir simulation software uses Wilson correlation for determination of equilibrium ratio for hydrocarbons. A scatter plot of Wilson K_i values of both hydrocarbons and non-hydrocarbon is shown in Figure 3-18. As seen in the figure, the Wilson correlation has a very low R^2 for non-hydrocarbons. This means that the Wilson correlation is a weak estimator of non-hydrocarbon K_i values. Figure 3-19 illustrates the similar scatter plot based on Standing correlation. Like the Wilson correlation, the Standing correlation yields high errors in predicting non-hydrocarbon K_i values. The R^2 of these two well-known correlations is equal while estimating hydrocarbon K_i values. Figures 3-20 and 3-21 also show the MSE and mean absolute error for these two correlations along with the MSE of the proposed model for both fluid systems, respectively. The maximum, minimum, and average values of absolute error in predicting non-hydrocarbons' equilibrium ratio using the LSSVM model are [94.83; 0.0024; 11.38], using the standing correlation are [1808; 9.444; 280.4], and using the Wilson correlation are [5672.2; 4.2; 492.8]. The maximum, minimum and average values of absolute error in predicting hydrocarbons' equilibrium ratio using the LSSVM model are [17.6; 3.34×10^{-5}; 1.3], using the Standing correlation are [2448.472; 2.1199; 226.2], and using the Wilson correlation are [2807.1; 0.006; 98.2].
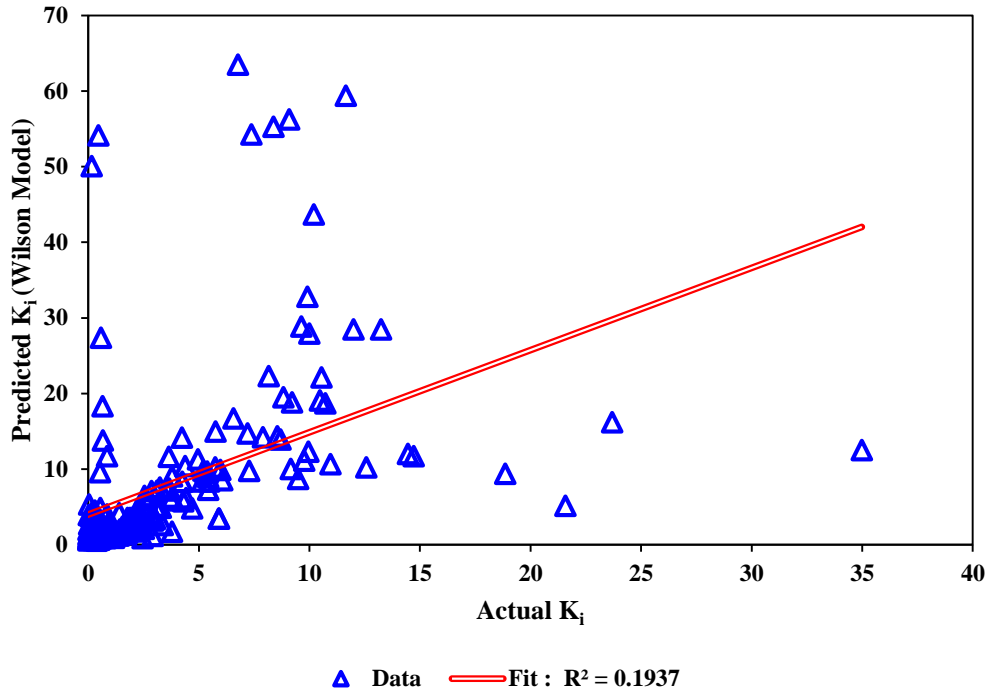
(a)
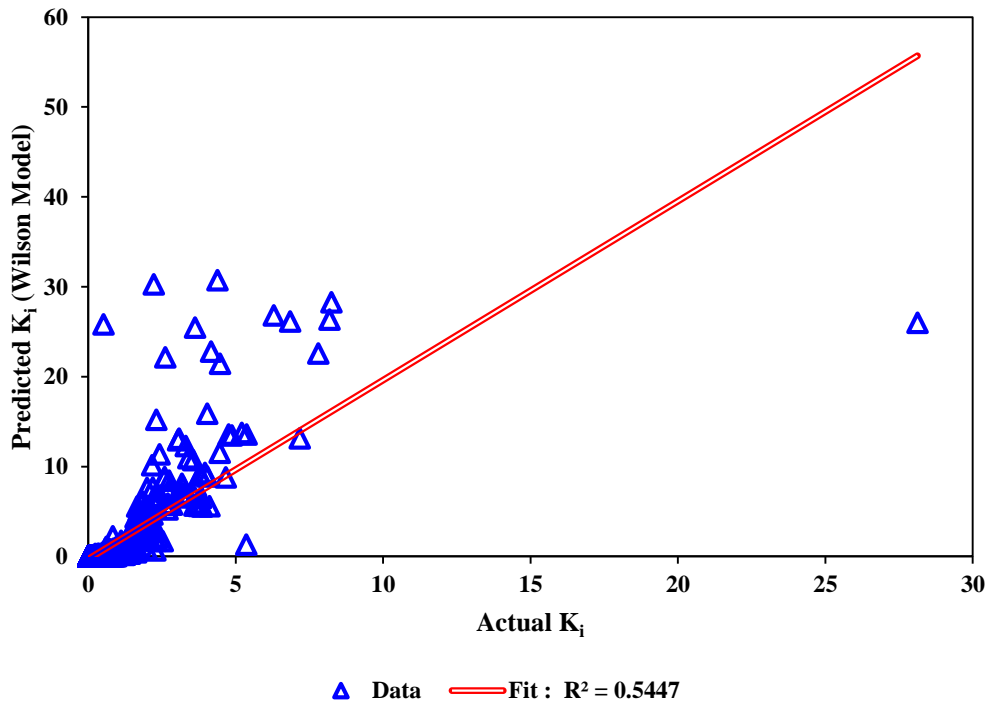
(b)

Figure 3-18: Scatter plot of estimated and measured equilibrium ratio (K_i) via Wilson model for a) non-hydrocarbons and b) hydrocarbons
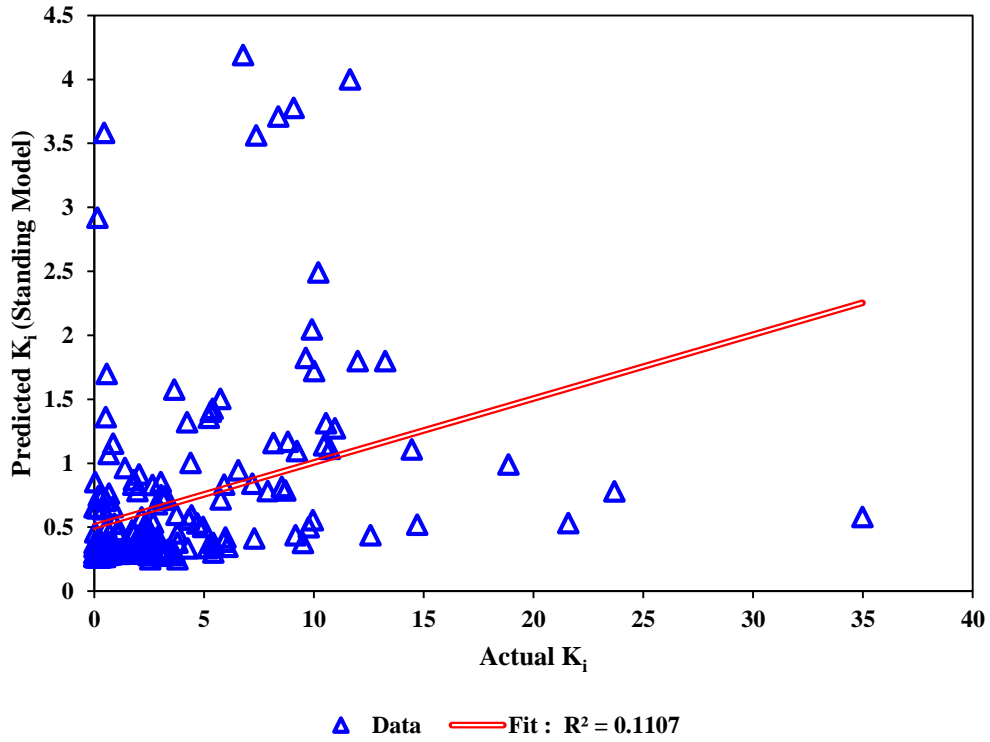
(a)
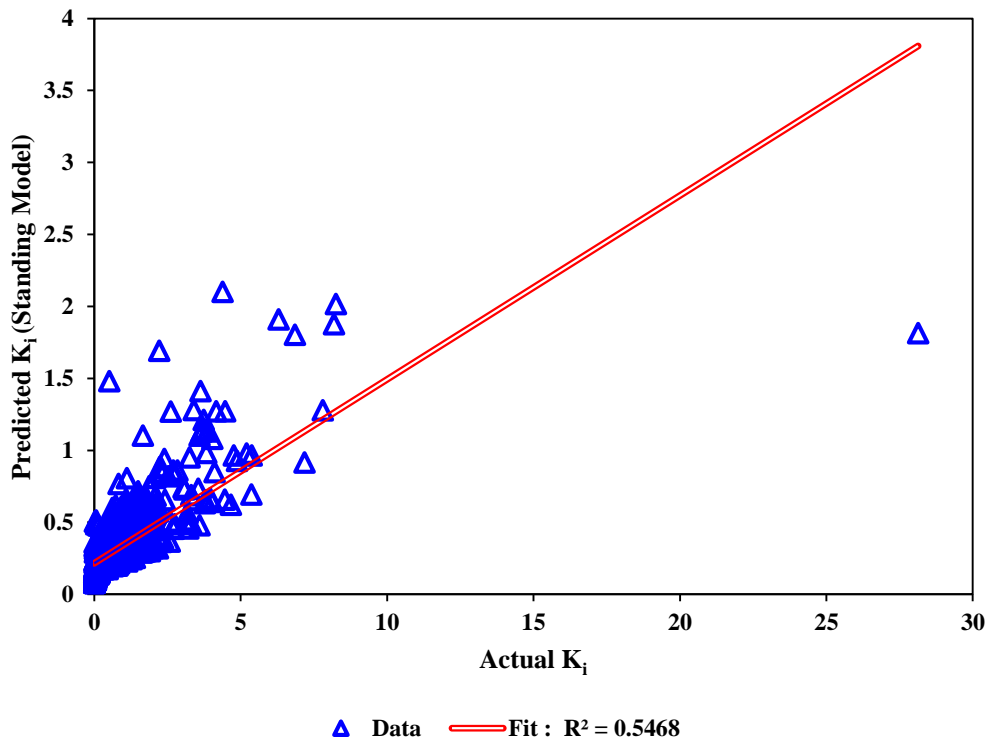
(b)

Figure 3-19: Scatter plot of estimated and measured equilibrium ratio (K_i) while using standing model for a) non-hydrocarbons and b) hydrocarbons
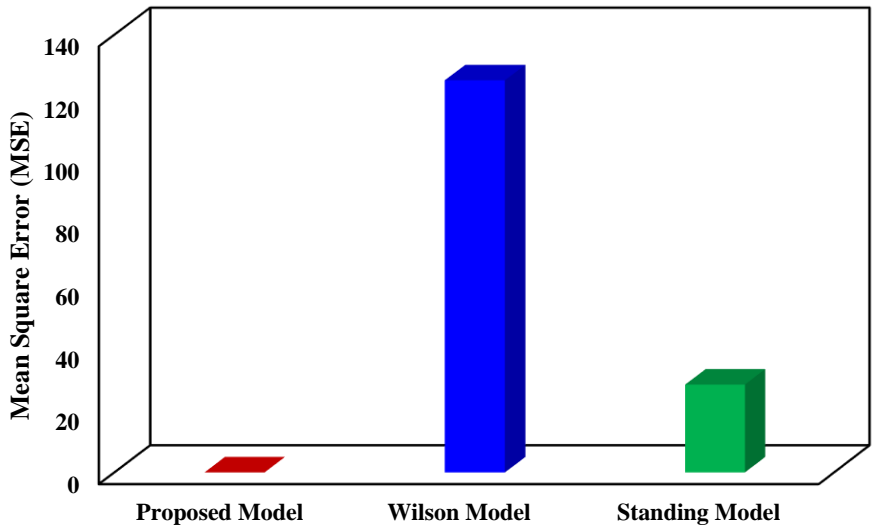
(a)
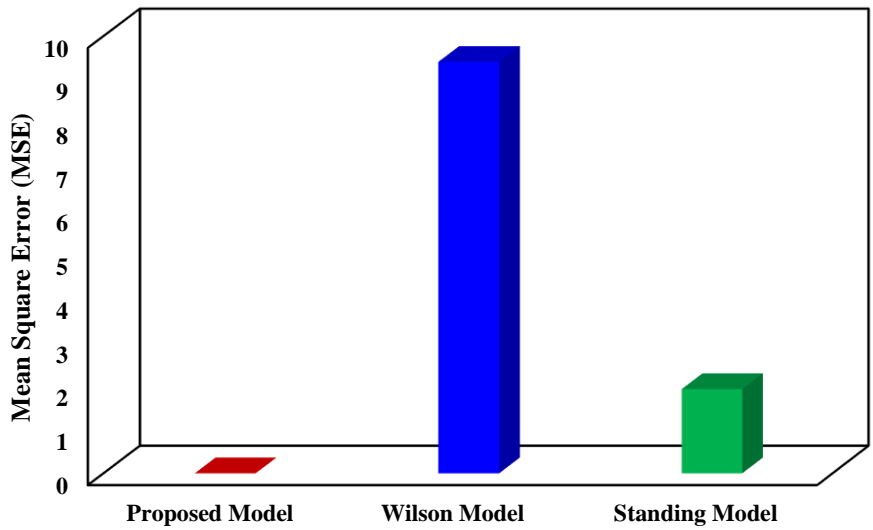
(b)

Figure 3-20: Comparison between the mean squared errors of used models for prediction of equilibrium ratio (K_i) for a) non-hydrocarbons and b) hydrocarbons
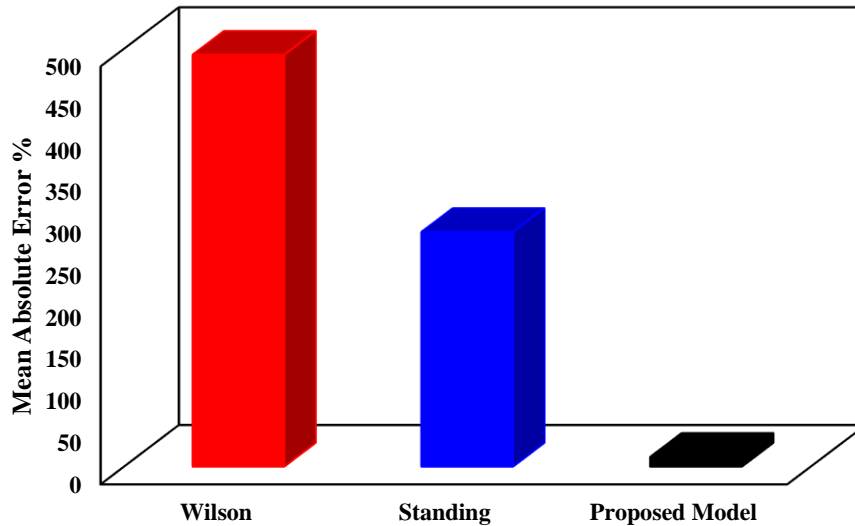
(a)
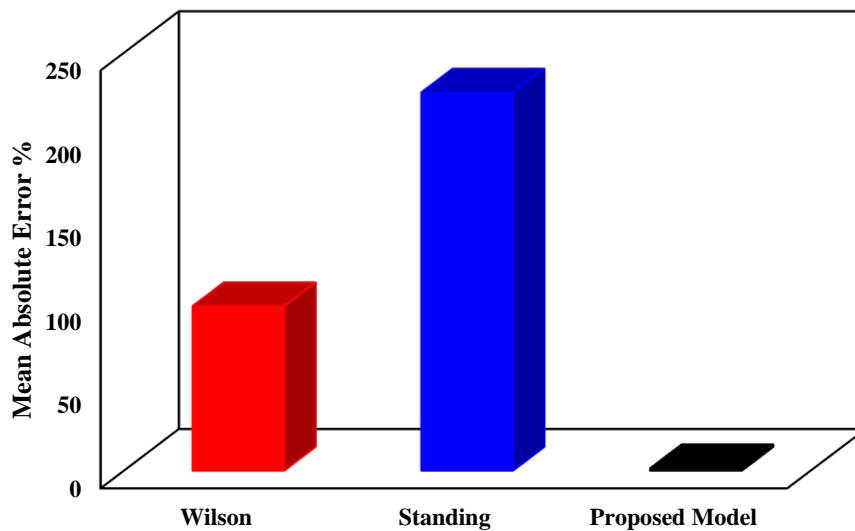
(b)

Figure 3-21: Comparison between the mean absolute errors of used models for prediction of equilibrium ratio (K_i) for a) non-hydrocarbons and b) hydrocarbons

As demonstrated in the calculation, the proposed model is much more accurate in forecasting the thermodynamic equilibrium ratio of both hydrocarbons and non-hydrocarbons. Figure 3-22 depicts the relative importance of the input parameters on the equilibrium ratio using the analysis of variance (ANOVA) method. As illustrated in Figure 3-22, the most important parameters are the critical temperature, acentric factor, and critical pressure of the hydrocarbons and non-hydrocarbons.

95
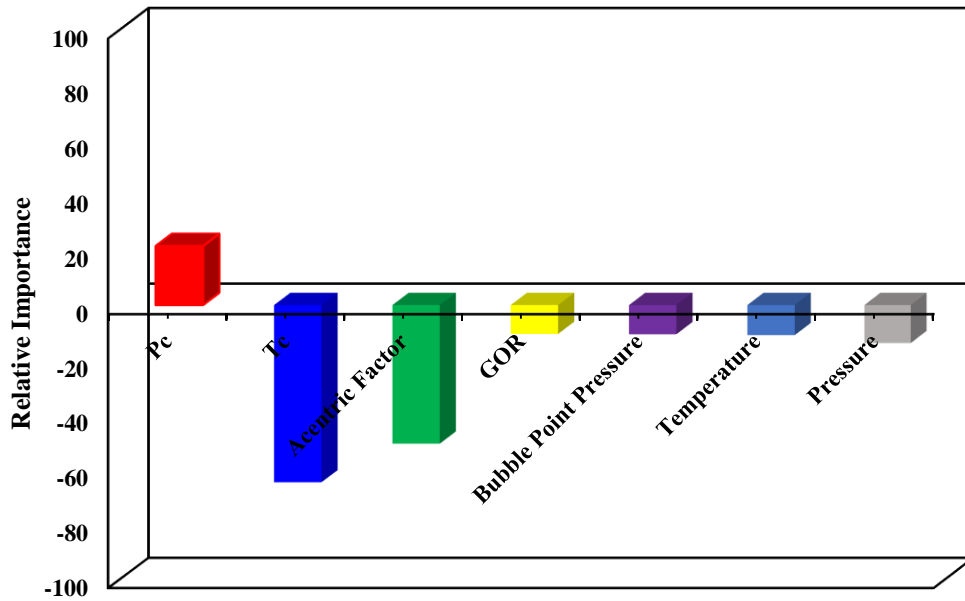
Figure 3-22: Comparison between the relative importance of the parameters on the equilibrium ratio (K_i) of both hydrocarbon and non-hydrocarbons

It is important to note that utilization of an equation or/and correlation is a much easier task for engineers, researchers, and managers to determine thermodynamic parameters such as K-value, compared to conducting simulation runs through employing simulation packages such as Aspen Plus and CMG WinProp (e.g., it generally uses Wilson equation for calculating the equilibrium ratio) that might need adequate training. In addition, it normally takes less time to obtain a parameter using a correlation (or a developed model), compared to a simulator.

The present study provides an accurate and simple-to-use model to estimate equilibrium ratio for both hydrocarbons and non-hydrocarbons. The precise prediction of equilibrium ratio for both hydrocarbons and non-hydrocarbons improves the reliability of the phase behavior analysis. The accurate magnitude of this parameter also assists engineers/researchers in precisely determining the compositional evolution of

hydrocarbon mixtures from the reservoir to the surface facilities while operating conditions such as temperature and pressure vary in terms of time and elevation.

References

[1] M.L. Michelsen, Calculation of phase envelopes and critical points for multicomponent mixtures, Fluid Phase Equilibria, 4 (1980) 1-10.

[2] C. Whitson, S. Torp, Evaluating Constant-Volume Depletion Data. JPT 35 (3): 610–620, in, SPE-10067-PA. DOI: 10.2118/10067-PA, 1983.

[3] N. Varotsis, A robust prediction method for rapid phase-behavior calculations, SPE Reservoir Engineering, 4 (1989) 237-243.

[4] A. Danesh, PVT and phase behaviour of petroleum reservoir fluids, Elsevier, 1998.

[5] G. GPSA, Engineering data book, Gas Processors Suppliers Association, 2 (2004) 16-24.

[6] A. Lawal, I. Silberberg, A New Correlation of Vapor-Liquid Equilibrium Ratios Internally Consistent With Critical Behavior, in: SPE Annual Technical Conference and Exhibition, Society of Petroleum Engineers, 1981.

[7] M. Standing, A set of equations for computing equilibrium ratios of a crude oil/natural gas system at pressures below 1,000 psia, Journal of Petroleum Technology, 31 (1979) 1,193-191,195.

[8] M.L. Michelsen, Phase equilibrium calculations. What is easy and what is difficult?, Computers & chemical engineering, 16 (1992) S19-S29.

[9] V.N. Vapnik, V. Vapnik, Statistical learning theory, Wiley New York, 1998.

[10] C. Cortes, V. Vapnik, Support-vector networks, Machine learning, 20 (1995) 273-297.

[11] A. Baylar, D. Hanbay, M. Batan, Application of least square support vector machines in the prediction of aeration performance of plunging overfall jets from weirs, Expert Systems with Applications, 36 (2009) 8368-8374.

[12] B. Mehdizadeh, K. Movagharnejad, A comparative study between LS-SVM method and semi empirical equations for modeling the solubility of different solutes in supercritical carbon dioxide, Chemical Engineering Research and Design, 89 (2011) 2420-2427.

[13] C.-M. Vong, P.-K. Wong, Y.-P. Li, Prediction of automotive engine power and torque using least squares support vector machines and Bayesian inference, Engineering Applications of Artificial Intelligence, 19 (2006) 277-287.

[14] J.A. Suykens, J. Vandewalle, Least squares support vector machine classifiers, Neural processing letters, 9 (1999) 293-300.

[15] J.A. Suykens, J. Vandewalle, Training multilayer perceptron classifiers based on a modified support vector method, IEEE Transactions on Neural Networks, 10 (1999) 907-911.

[16] J.A. Suykens, J. Vandewalle, Recurrent least squares support vector machines, IEEE Transactions on Circuits and Systems I: Fundamental Theory and Applications, 47 (2000) 1109-1114.

[17] M.-A. Ahmadi, A. Bahadori, S.R. Shadizadeh, A rigorous model to predict the amount of Dissolved Calcium Carbonate Concentration throughout oil field brines: Side effect of pressure and temperature, Fuel, 139 (2015) 154-159.

[18] T. Van Gestel, J.A. Suykens, B. Baesens, S. Viaene, J. Vanthienen, G. Dedene, B. De Moor, J. Vandewalle, Benchmarking least squares support vector machine classifiers, Machine Learning, 54 (2004) 5-32.

[19] K. Pelckmans, J.A. Suykens, T. Van Gestel, J. De Brabanter, L. Lukas, B. Hamers, B. De Moor, J. Vandewalle, LS-SVMlab: a matlab/c toolbox for least squares support vector machines, Tutorial. KULeuven-ESAT. Leuven, Belgium, 142 (2002) 1-2.

[20] J.A. Suykens, T. Van Gestel, J. De Brabanter, Least squares support vector machines, World Scientific, 2002.

[21] J.A. Suykens, J. De Brabanter, L. Lukas, J. Vandewalle, Weighted least squares support vector machines: robustness and sparse approximation, Neurocomputing, 48 (2002) 85-105.

[22] M.-A. Ahmadi, A. Bahadori, A LSSVM approach for determining well placement and conning phenomena in horizontal wells, Fuel, 153 (2015) 276-283.

[23] M.A. Ahmadi, M. Ebadi, P.S. Marghmaleki, M.M. Fouladi, Evolving predictive model to determine condensate-to-gas ratio in retrograded condensate gas reservoirs, Fuel, 124 (2014) 241-257.

[24] M.A. Ahmadi, M. Ebadi, Evolving smart approach for determination dew point pressure through condensate gas reservoirs, Fuel, 117 (2014) 1074-1084.

[25] M.A. Ahmadi, M. Ebadi, S.M. Hosseini, Prediction breakthrough time of water coning in the fractured reservoirs by implementing low parameter support vector machine approach, Fuel, 117 (2014) 579-589.

[26] S.S. Keerthi, C.-J. Lin, Asymptotic behaviors of support vector machines with Gaussian kernel, Neural computation, 15 (2003) 1667-1689.

[27] J.A. Suykens, J. Vandewalle, Multiclass least squares support vector machines, in: Neural Networks, 1999. IJCNN'99. International Joint Conference on, IEEE, 1999, pp. 900-903.

Chapter Four: Minimum Miscibility Pressure of CO₂-Oil System in Miscible Gas Flooding Processes

Abstract

Minimum miscibility pressure (MMP) is one of the key parameters that affects the microscopic and macroscopic effectiveness (displacement performance) of gas injection for enhanced oil recovery. Numerous research efforts have been made to measure and predict the MMP, including experimental, analytical, numerical, and empirical methodologies. Despite these efforts, a comprehensive, user-friendly, and accurate model does not exist yet. In this study, we introduce "Gene Expression Programming (GEP)" as a novel connectionist tool to determine the MMP parameter. This new model is developed and tested using a large databank available in the literature for the MMP measurements. The accuracy of the proposed model is validated and compared with the outcomes from the commercial simulators. The performance of the proposed model is also examined through a systematic parametric sensitivity analysis where various input variables such as temperature and volatile-to-intermediate ratio are considered. The new GEP model outperforms all the published correlations in term of accuracy and reliability.

4.1. Introduction

Gas injection is being considered as an important enhanced oil recovery method [1]. Ultimate oil recovery by gas flooding, especially CO_2 injection, into oil reservoirs can reach up to 25% of the Original Oil in Place (OOIP). The storage of CO_2 in mature and

depleted oil reservoirs is one of the efficient possible methods to mitigate CO_2 emissions which favors the new regulations imposed by several governments across the world. There are a number of extensive research works in the literature that evaluate the feasibility of CO_2–EOR methods in mature oil reservoirs [2-8]. The researchers proposed different frameworks for CO_2 injection, discussed the technical and non-technical uncertainties of CO_2 injection strategies, conducted optimal CO_2 storage and EOR simultaneously, and performed risk analysis on various CO_2 injection operations. Systematic studies in the form of parametric sensitivity analysis have been conducted to investigate the effects of important variables such as the amount of injected CO2, phase behaviour of CO_2/brine/oil systems, reservoir characteristics, and minimum miscible pressure (MMP) on the fluids displacement, production mechanisms, and operation performance over CO_2 injection processes [2-8]. Several experiences in EOR projects show that oil recovery performance is strongly dependent on operational and capital costs, equipment/facility availability, and oil price. To have a better evaluation of injection operations prior to implementation, the uncertainties with the rock and fluids properties should be considerably lowered. Hence, determination of these important parameters with the minimum uncertainty and high accuracy can guarantee the success of the CO_2 injection processes in terms of performance, economic, and environmental prospects [2-8].

The minimum miscibility pressure (MMP) is a critical parameter in the design of gas injection facilities in which local displacement performance by CO_2 is a function of the minimum miscible pressure. The MMP in the gas-oil systems is the lowest pressure at which the crude oil will become completely miscible with the gas [9-13]. In one-dimensional displacement of two-phase flow systems such as gas and oil with a

negligible dispersion, a piston-like displacement occurs when the pressure approaches MMP. In this case, the oil recovery will be nearly 100% after one pore volume gas injection [9-11].

The miscibility between injected gas and reservoir oil is a complicated process which is strongly affected by transfer phenomena, specifically by mass, and consequently pore-scale mixing and local temperature profiles. For economic reasons, the choice of gas in the flooding operation for a given oil reservoir is based on the reservoir pressure and MMP.

Given the importance of MMP in oil production mechanisms and performance, for screening an oil reservoir for possible gas injection, an accurate mathematical model to predict the MMP will be an asset as it reduces the engineering, research, and development costs in the field of enhanced oil recovery. The aim of this paper is to develop a reliable and accurate model to easily predict the MMP parameter. To achieve this objective, we use the application of "Gene Expression Programming (GEP)" to obtain MMP. The new GEP model is developed and tested using an extensive MMP databank [14-24]. The strength of the proposed predictive model in estimating gas–oil MMP from literature data is first illustrated. Then, the GEP model is used to simulate thermodynamic data/behavior for one of the northern Persian Gulf oilfields in Iran.

4.2. Methodology

4.2.1. Genetic Programming

Genetic Programming (GP) is a part of the genetic algorithms (GAs) with a countless aptitude to develop computer programs [50] automatically. The theory of GP was first proposed by Koza [51]. The primary difference between the GP and original genetic algorithm is the demonstration/form of the final solution. The target outcomes from the

GP are computer-based programs that are demonstrated as tree topologies which are formulated in a functional programming language, representing the solution as a combination of the functions [51] while the original genetic algorithm generates a string of numbers as a potential solution. The GP gives the basic topology of the potential tools together with the values of its parameters [50-53]. Owing to the fitness value calculated using the introduced fitness function in GP, Genetic Programming (GP) optimizes a population of the computer program [50, 53-54].

The original GP method is referred to a tree-based GP. Each member of the GP is a ranked topology tree containing functions and required terminals. The implemented functions and terminals are collected from an assortment of the proposed function groups and a group of terminals. The proposed function (in the addressed tree) may comprise the basic math operations and any mathematical functions such as $+$, $-$, $\times$, $/$, AND, OR, NOT. In addition, the considered terminal category T includes functions, numerical constants, logical constants, and variables. To generate computer approach in a tree-like topology with an origin point containing branches (expanding from each function and closing in a terminal), the functions and terminals are randomly selected and constructed together [50]. A simple tree demonstration of genetic programming (GP) is depicted in Figure 4-1 [53].

It should be noted that Gene Expression Programming (GEP) is a linear branch of the addressed GP. The linear branch of GP assembles an explicit difference between the phenotype and the genotype of an individual. Therefore, the individuals are explicated in linear strings [50, 55-57].
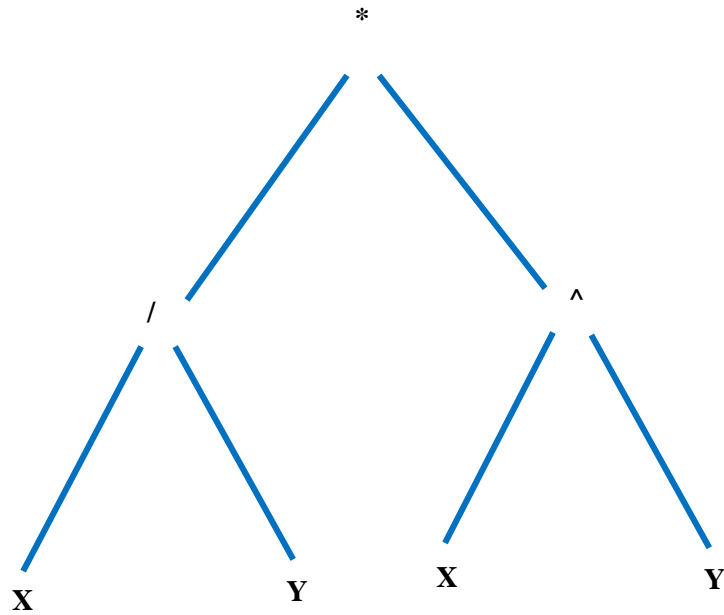
Figure 4-1**:** A typical parse tree that demonstrates an algebraic expression formed by a two-gene chromosome $[(X/Y)*(X^Y)]$.

4.2.2. Gene Expression Programming (GEP)

GEP was first developed by Ferreira on the basis of Genetic Programming (GP) [50,56]. Most of the implemented GEP operators are similar to those in genetic algorithms (GAs) with minor corrections. The structure of the GEP consists of a function set, a terminal set, fitness functions, control parameters, and stop criteria [57-59]. The GEP implements a fixed string length (of characters) to demonstrate routs to the targets which will be presented as parse trees with different sizes and shapes. These trees are called GEP expression trees (ETs). The GEP ability in presenting an algebraic relationship between output and input variables is an important characteristic of the GEP which considerably increases the strength and accuracy of the tool in the prediction cases [50]. The unique multigenic nature of the GEP is that which permits the evolution of more complex programs comprising various subprograms [57]. Any

GEP gene includes a list of symbols with a fixed length which can be a function set such as $\{+,-,\times, /,\sqrt{\ }\}$ and a terminal set such as $\{X,Y, 8\}$ [50,55-59].

The following set denotes a sample GEP gene with the given function and terminal sets [50, 56-59]:

$$+.-.^\wedge./.X.Y.X.Y \qquad\qquad\qquad\qquad (4\text{-}1)$$

Where X and Y are the variables; it is noted that ''.'' is element separator to simplify its readability. This expression is called Karva notation or a K-expression [56,58-59]. A K-expression can be illustrated as a diagram which is known as an ET in GEP (see Figure 4-2) [50]. The above GEP statement can also be represented in a mathematical formulation form as [50]:

$$(X - Y) + (X^Y) \qquad\qquad\qquad\qquad (4\text{-}2)$$

As discussed previously, GEP genes contain a fixed length which is defined initially. Thus, the size of the relevant ETs assorts in the GEP, not the length of the genes [50, 57-59]. There is a specific number of suspended components which are not appropriate for genome mapping. Therefore, the length of the GEP gene may be same or longer than the valid length of a K-expression. The GEP utilizes a head–tail approach to assure the correctness of a randomly collected genome. Hence, each GEP gene is comprised of a head and a tail; the head may consist of both function and terminal symbols, while the tail may have only terminal symbols [50, 56-59]. To summarize the previous description on GEP, a graphical illustration of the addressed approach is described in Figure 4-3 [56, 57-59]. Selection of the fitness function on the basis of the statistical error indicators is the first step. In this paper, the mean squared error (MSE) was used as the fitness function. Creating the chromosomes through employing the functions and terminals is the second stage. The set of terminals appears in the form of various

combinations including the input parameters (e.g., T_{cm}, MW_{c5+}, T, and Vol./Int.). Also, the set of functions is the primary mathematics operators $\{+,-,\times,\div\}$ and arithmetical functions $\{x^2, x^3, x, \ln x, e^x\}$. The head size and number of genes as the chromosomes' architectures are selected through a systematic procedure (see Figures 3-1 to 3-3). As an important stage, the addition function is employed to make a link between the expression trees. Finally, the genetic operators for instance mutation, inversion, transposition, and recombination are chosen. In fact, the mentioned parameters are borderlines of the GEP which considerably affect the performance of the GEP.
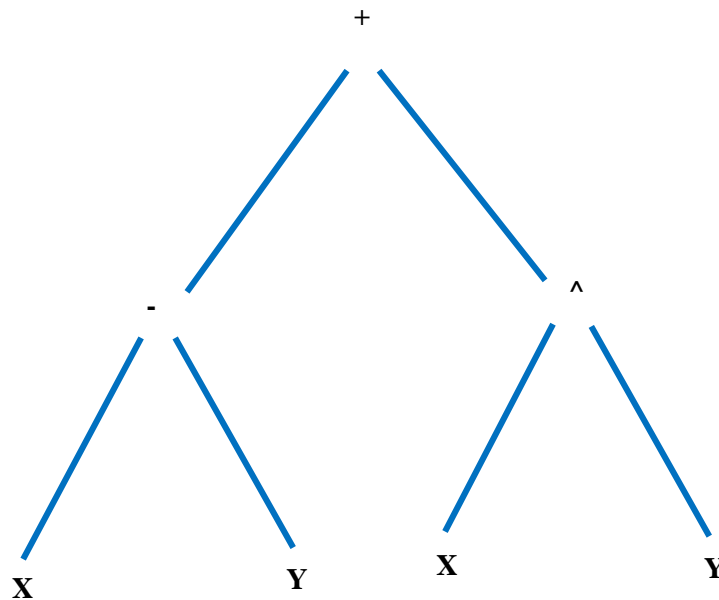
Figure 4-2: A typical algebraic equation $[(X-Y)+(X^Y)]$ represented in a Karva Language program. This operation conducted through a two-gene chromosome demonstrates the GEP strategy.
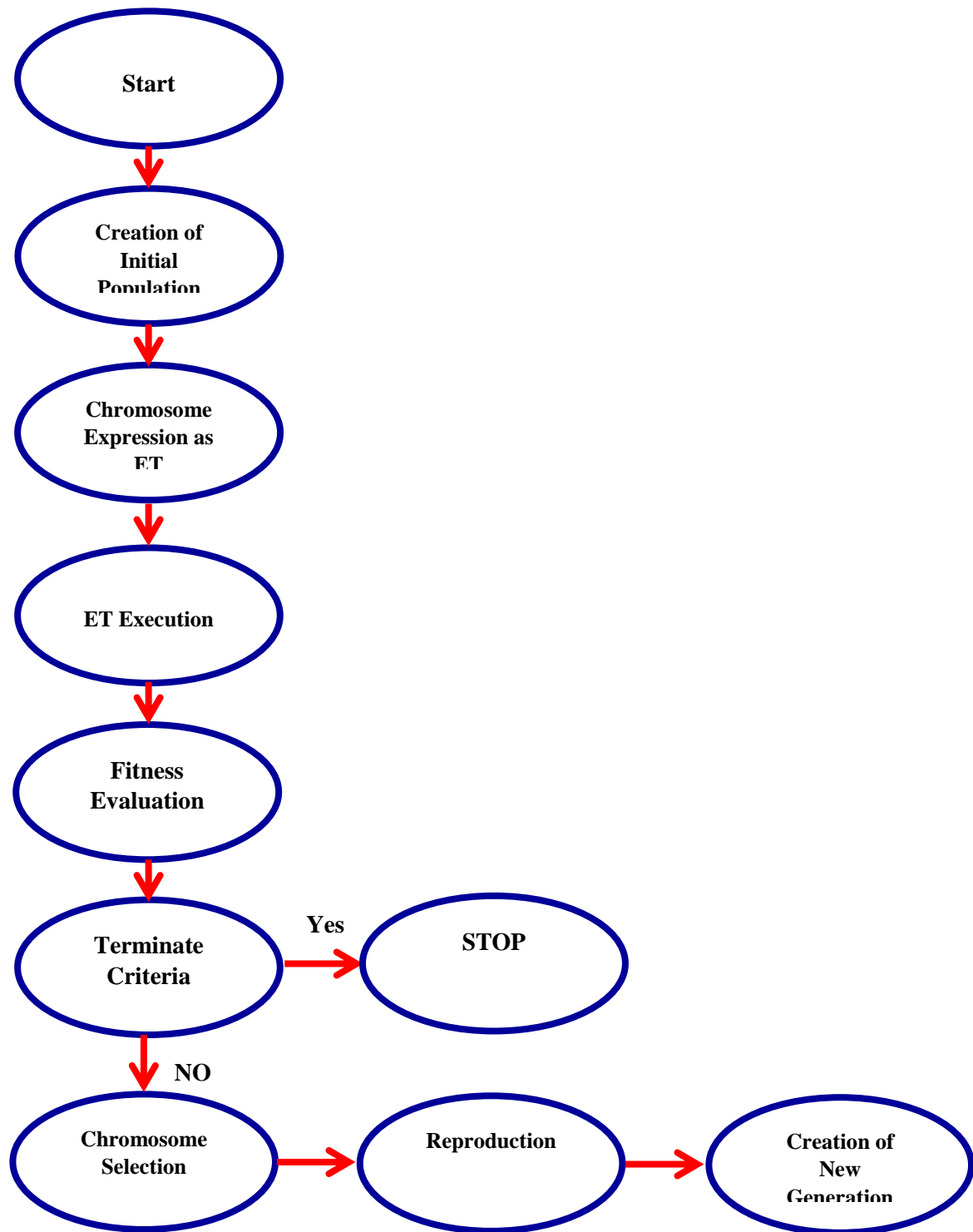
Figure 4-3: Graphical demonstration of GEP method

4.3. Results and Discussion

This study presents a new strategy for accurate determination of minimum miscible pressure (MMP) which is required for design and operation of various gas injection processes including CO_2 flooding. A summary of the crude oil compositions, temperature range, and measured minimum miscibility pressures is presented in Table 4-1. A schematic of the input parameters through gene expression programming (GEP) method for obtaining MMP is also depicted in Figure 4-4.

Table 4-1: Statistical parameters of the utilized minimum miscible pressure (MMP) data

	Mean	Std. Deviation	Maximum	Minimum
MMP	14.86	5.42	34.474	6.536
T_{cm}	302.22	10.26	338.77	281.44
$T_{reservoir}$	341.92	22.34	391.45	305.35
MW_{C5+}	188.98	34.05	302.50	136.47
volatile-to-intermediate	1.7912	2.24	13.60	0.14
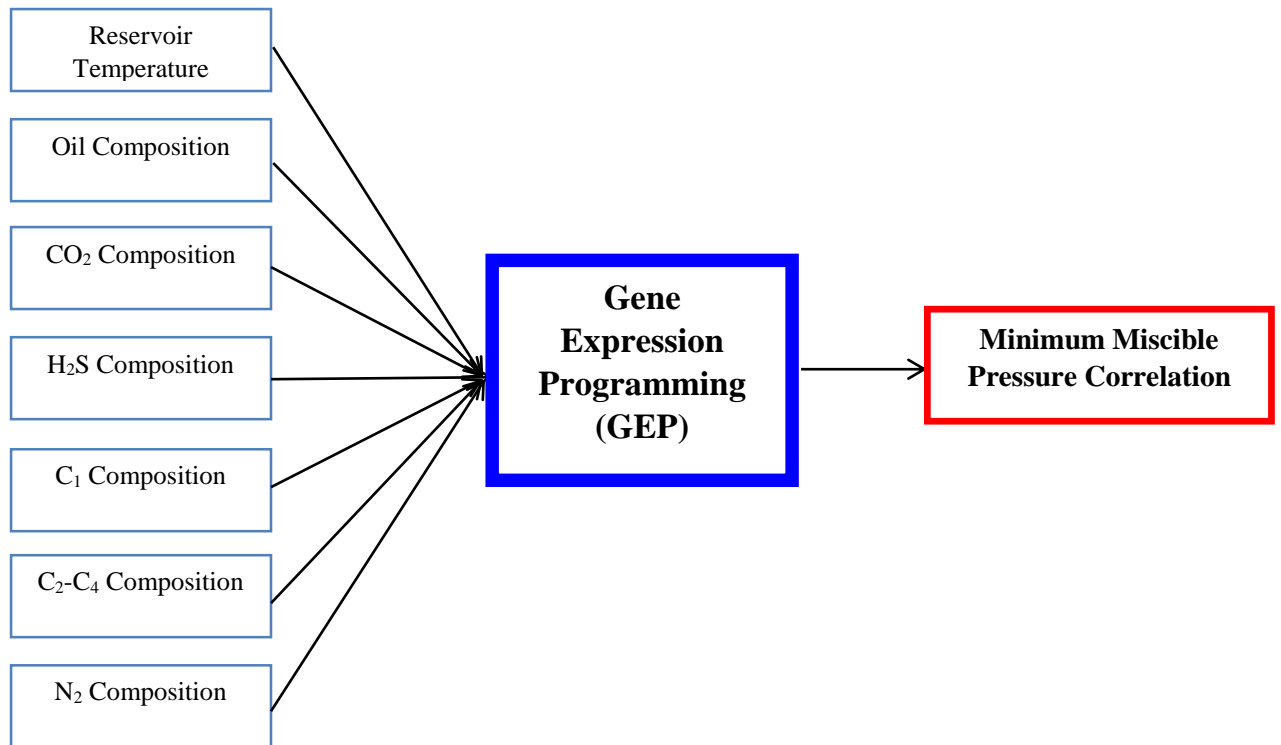
Figure 4-4: Input variables used for development of a new MMP correlation through implementation of the GEP

To compare the accuracy of the evolved GEP-MMP correlation and other conventional approaches, the predicted values versus the experimental MMP are plotted. Figure 4-5(a) demonstrates the experimental data versus MMP predicted by Lee's model [25]. This figure exhibits a large scatter in the MMP data around the straight line y=x with a low correlation coefficient (R^2=0.3582). This clearly indicates that Lee's model fails to forecast the correct MMP for most of the data used in this study. It is also found that nearly 85% deviation occurs in the pressure range of 10MPa to 15MPa. Comparison between the measured MMP and the corresponding values obtained by Yelling and Metcalfe model [21] is shown in Figure 4-5(b). This figure also shows a noticeable scatter in the data around the straight line y=x, indicating a poor fit and a large error while predicting the MMP so that a low correlation coefficient (R^2=0.3698) was achieved. The large deviation between the measured and predicted MMP comes from

the fact that the Yelling and Metcalfe model correlates MMP to the reservoir temperature and ignores the compositional effect. The performance of Orr and Jensen correlation is shown in Figure 4-5(c). A poor performance for Orr and Jensen correlation was also noticed based on Figure 4-5(c), leading to a low correlation coefficient (R^2=0.3573). The reasons for this poor predictive capability are that the composition of the crude oil is not considered in this model and the data is restricted to low temperatures. A high relative error percentage (about 140%) was observed for a part of the MMP data considered in this study while employing the Orr and Jensen model. Figures 5(d) and 5(e) display the predictive performance of Glasø's [30] and Alston et al. [14] models, respectively. Very low coefficient of correlations; R^2=0.2731 for Glasø's model, and R^2= 0.4927 for Alston et.al model are seen in Figures 3-5(d) and 3-5(e). Surprisingly, both models exhibit a poor fit, although the Glaso's model takes into account the impact of intermediates (C_2–C_6) only when F_R (C_2–C_6)<18 mol.% and the Alston model considers the effect of intermediate-to-volatile ratio.

(a)
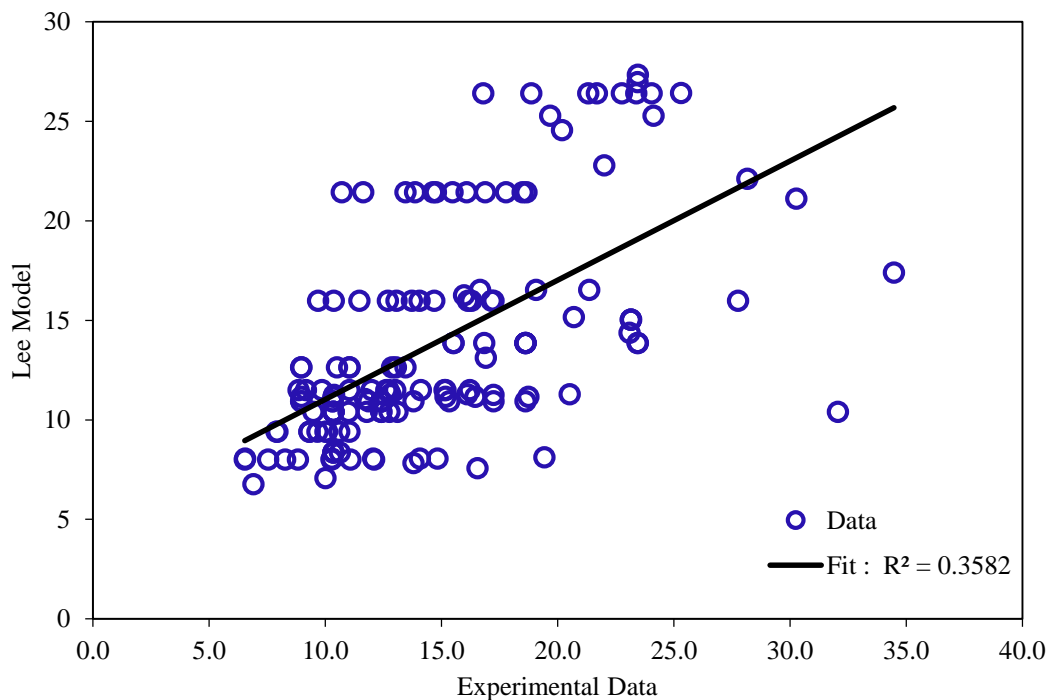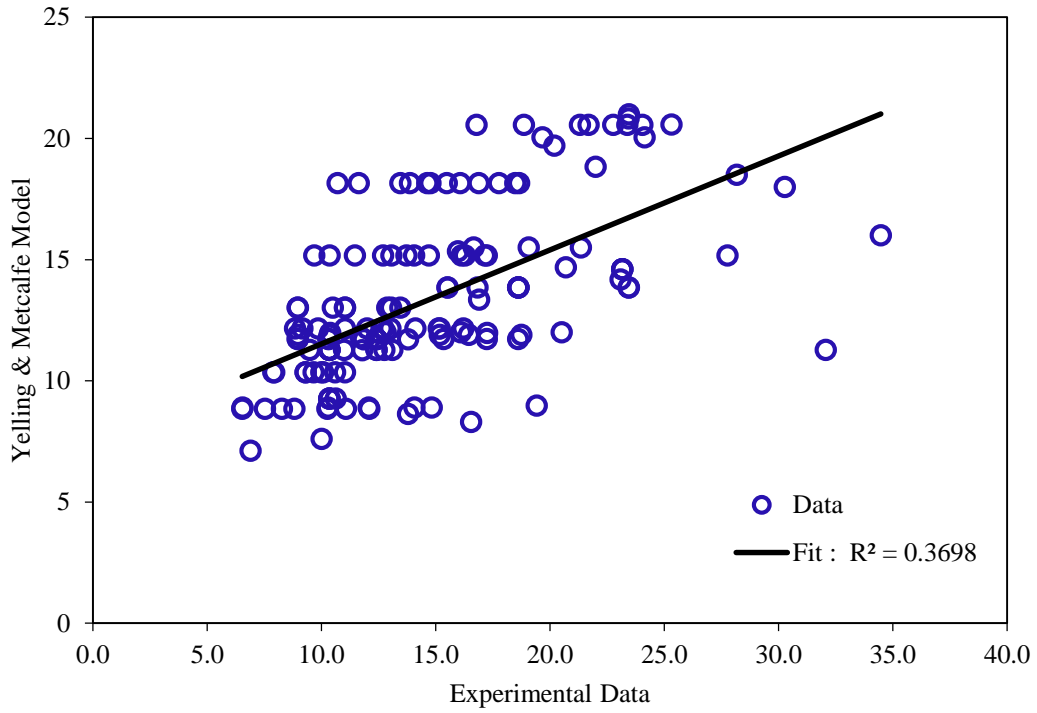
(b)
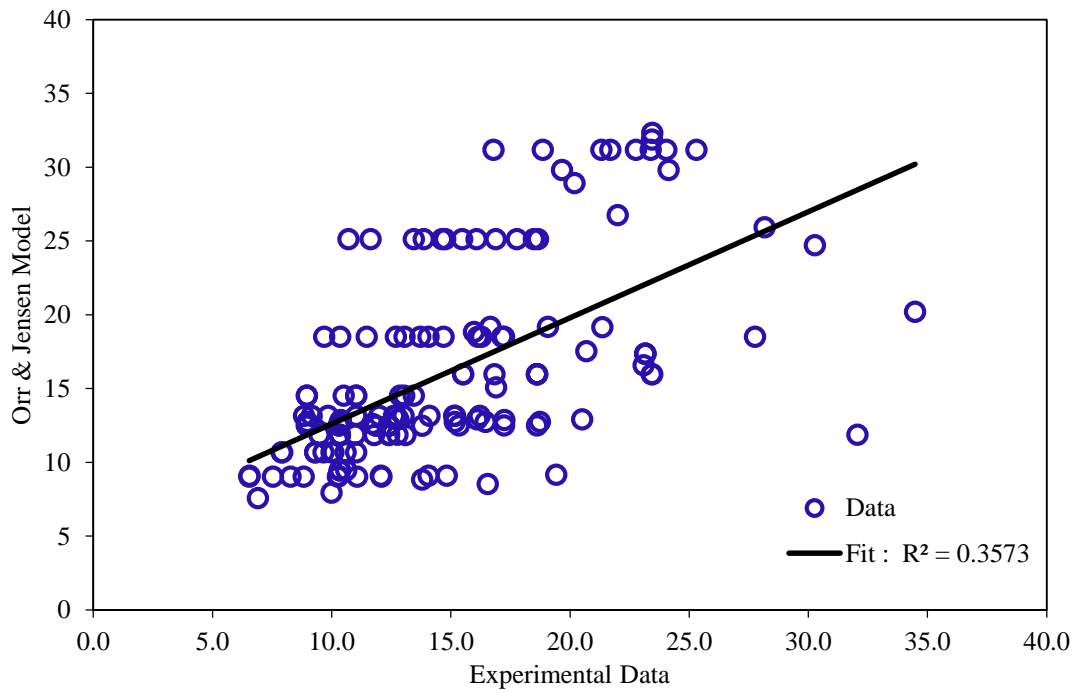
(c)
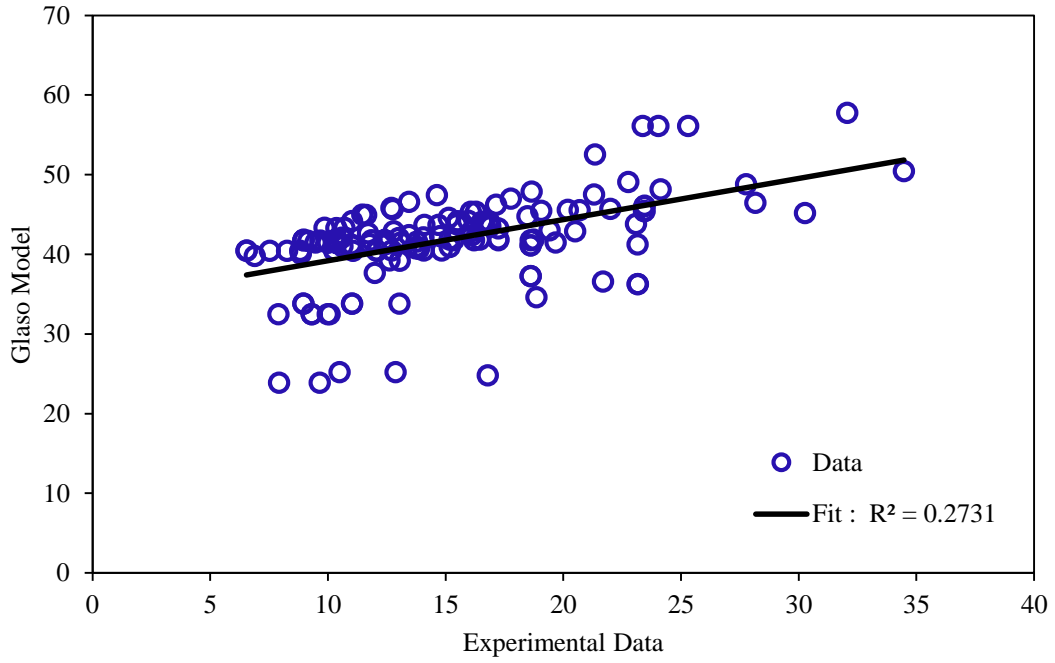
(d)
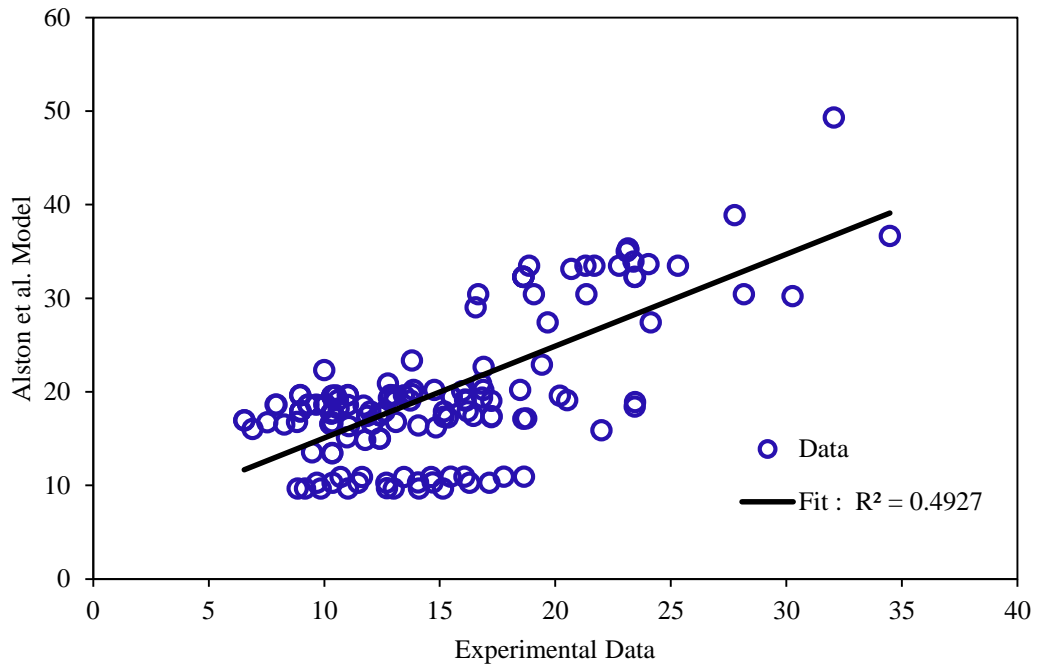
(e)

Figure 4-5: Comparison of experimental and predicted MMP by a) Lee's model b) Yelling & Metcalfe model c) Orr & Jensen model d) Glaso's model e) Alston et al. model

Due to the limitations of the previous models (e.g., temperature range, compositions, and intermediate-to-volatile ratio), a new model MMP is introduced in this paper, based on GEP strategy.

The GEP tool estimates the optimal set of parameters that results in a minimal error with the proposed input variables (T_{cm}, Vol. /Int., T, MW_{C5+}). The developed MMP model has the following from:

$$MMP = -500.366 + T \times 3.20265 - T \times Mw \times 0.00209858 + T \times Vol \times 0.00678601 + T \times A \times 0.0402589 - (T^2) \times 0.00511536 + Mw \times 0.674393 - Vol. \times A \times 0.161501 - A \times 12.2039 + A^2 \times 0.0156023 \tag{4-3}$$

where the coefficient is expressed as follows:

$$A = 684.089 - T_{cm} \times 3.35383 + T_{cm} \times T \times 0.00531718 - T_{cm} \times Mw \times 0.0025835 + T_{cm} \times Vol. \times 0.0382678 + (T_{cm}^2) \times 0.00312355 - T \times 1.40996 - T \times Mw \times 0.000472001 + T \times Vol. \times 0.0154773 + Mw \times 0.794565 + Mw \times Vol. \times 0.0123257 + (Mw^2) \times 0.000507237 - Vol. \times 18.7077 \tag{4-4}$$

In the above equations, the minimum miscible pressure, MMP, is calculated in MPa, T is the reservoir temperature in ^{o}F, T_{cm} represents the pseudo-critical temperature, and M_w stands for the molecular weight of C_{5+} fraction. Several attempts were made to design the network structure that gives the best match through optimization of the GEP algorithm. The functions and terminals selected for the developed MMP correlation are listed in Table 4-2, which reports important parameters, containing the genes, chromosomes, implemented operators, and mutation and inversion coefficients.

Table 4-2**:** The Gene Expression Programming (GEP) parameters utilized in computational steps

GEP algorithm parameters	Value
Number of chromosomes	40
Head Size	8
Number of Genes	8
Linking function	Plus (+)
Generations without change	2000
Fitness function	Mean Square Error (MSE)
Mutation	0.044
Inversion	0.1
IS transposition	0.1
RIS transposition	0.1
One-point recombination	0.3
Two-point recombination	0.3
Gene recombination	0.1
Gene transposition	0.1
Constant per gene	2
Operators used	+, -, /, ×, Power

A comparison between the GEP predictions and measured values of MMP is illustrated in Figure 4-6. This figure reveals that most of the calculated MMP are in a very good agreement with the measured MMP data. In addition, the performance of the proposed GEP model for prediction of MMP in terms of R^2 is exhibited in Figure 4-7 where the real data is included. One important feature of the GEP model shown in Figure 4-7 is that most of the data fall around the straight line y=x, indicating a satisfactory match to the measured data. The high magnitude of the correlation coefficient (R^2=0.9199) also confirms the capability and effectiveness of this correlation in predicting MMP. The validity of the proposed model to demonstrate the effects of the input variables such as temperature and volatile-to-intermediate ratio on MMP is investigated as depicted in Figures 3-8 and 3-9. The variations of the MMP with temperature are shown in Figure 8, implying the rightness of the developed GEP correlation in terms of physical interpretation. It should be noted that other models considered in this study fail to

capture the changes in MMP with respect to temperature. Figure 4-9 also shows MMP versus the volatile-to-intermediate ratio. It is obvious that the proposed GEP model is able to accurately capture the variations of MMP with the volatile -to-intermediate ratio based on a very good match between the calculated and real MMP values. Finally, the statistical analysis is conducted to examine the precision and reliability of the GEP equation, compared to other predictive models discussed in this study. This comparison in terms of mean squared error (MSE) is illustrated in Figure 4-10. It is concluded from Figure 4-10 that the proposed MMP model using the GEP tool exhibits higher accuracy and captures the physics and variations of MMP much better, in comparison with the previous models including Orr and Jensen, Yelling & Metcalfe, Lee, Glasø, and Alston et al. .
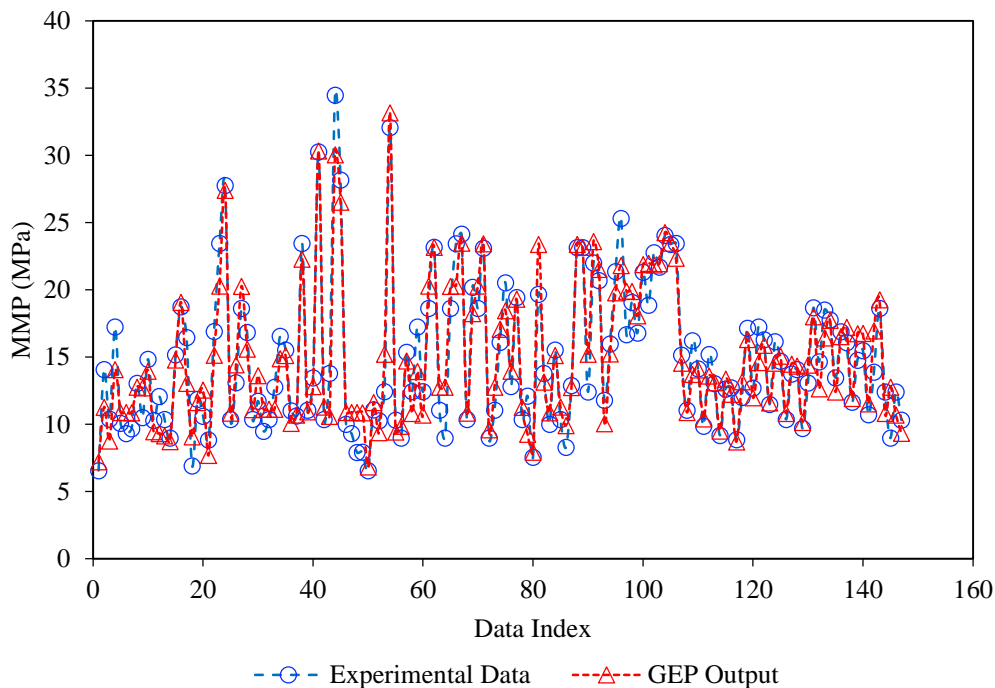
Figure 4-6: Comparison between modeling results obtained from the proposed tool and actual MMP
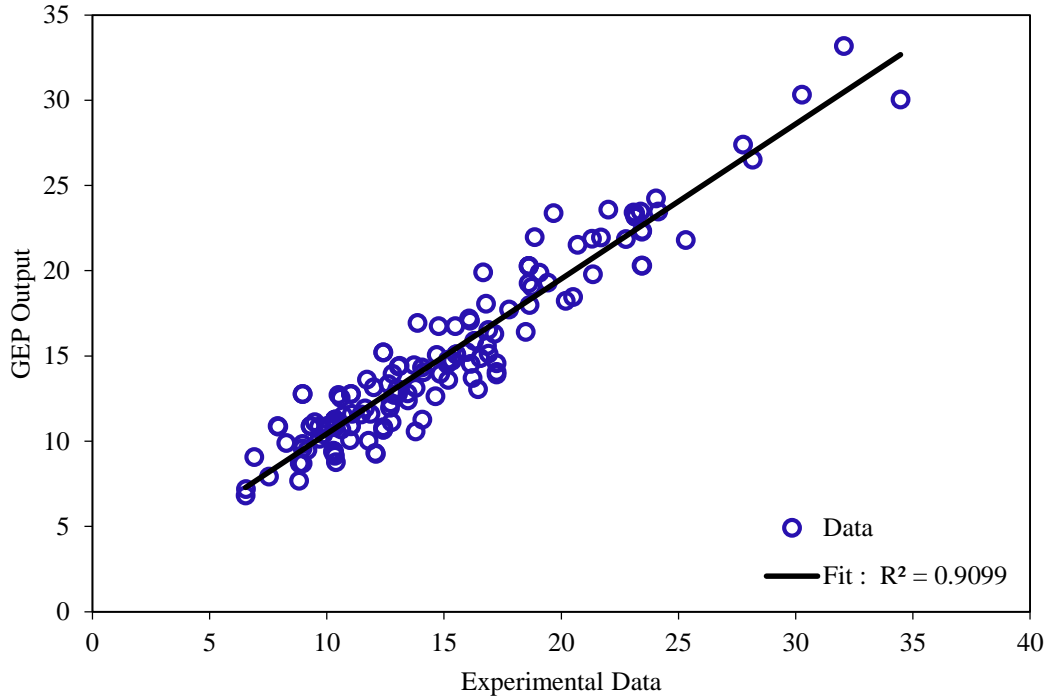
Figure 4-7: Effectiveness of the GEP strategy in determining MMP in terms of R^2
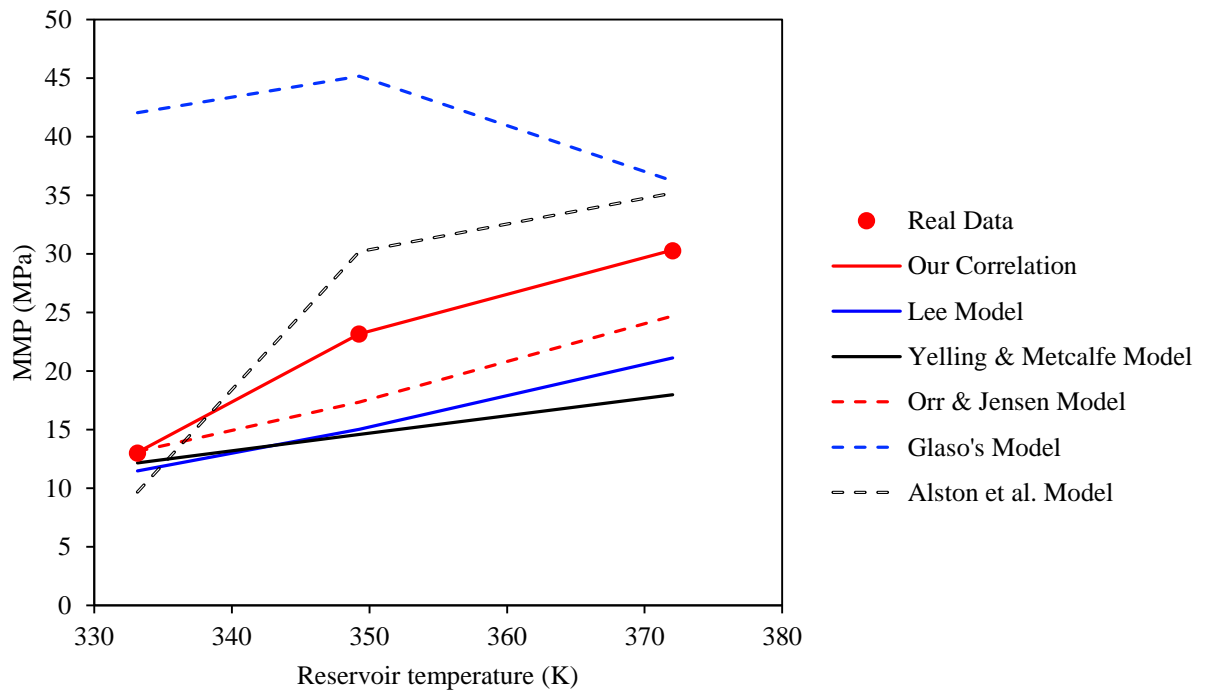
Figure 4-8: Models' performance: Effect of temperature on MMP
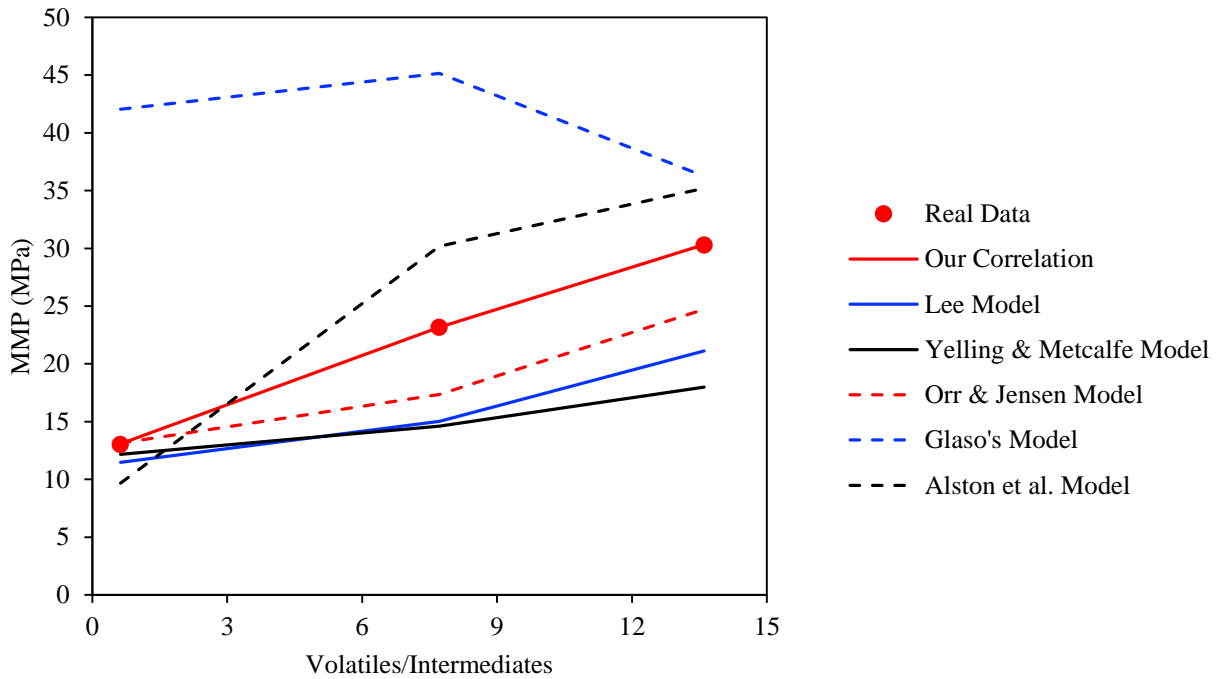
Figure 4-9: Models' performance: Effect of volatile-to-intermediate ratio on MMP
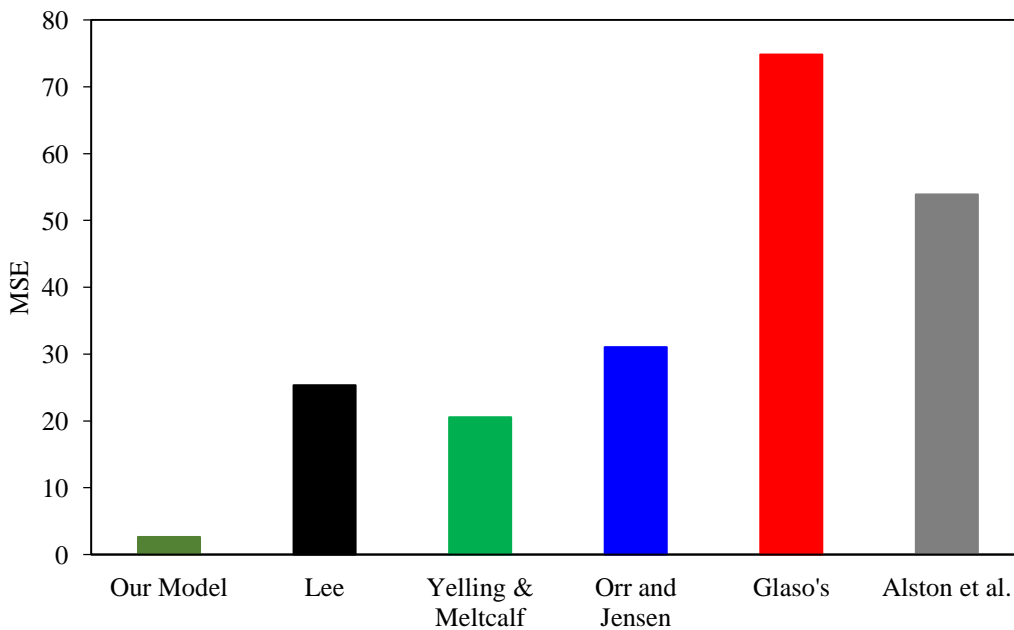
Figure 4-10: Mean squared error while estimating MMP by all models

MMP is a vital factor in screening, design, and operation of gas (particularly CO_2)

injection processes in various petroleum reservoirs. Since the experimental

measurement of this parameter is laborious, costly, and time-consuming, this research study was conducted to develop a cheap, quick, and easy-to-use correlation for precise estimation of MMP.

References

[1].   R.B. Grigg, D.S. Schechter, State of the industry in CO2 floods*, SPE Annual Technical Conference and Exhibition*, San Antonio, Texas, U.S.A, 5–8 October **1997**. https://doi.org/10.2118/38849-MS

[2].   W. Ampomah, R. Balch, M. Cather, D. Rose-Coss, Z. Dai, J. Heath, T. Dewers, P. Mozley, Evaluation of CO2 Storage Mechanisms in CO2 Enhanced Oil Recovery Sites: Application to Morrow Sandstone Reservoir. Energy and Fuels, **2010**, 30 (10), pp 8545-8555. https://doi.org/ 10.1021/acs.energyfuels.6b01888

[3].   W. Ampomah, R. S. Balch, D. Rose-Coss, R. Will, M. Cather, Z. Dai, M.R. Soltanian, Optimal Design of CO2 Storage and Oil Recovery under Geological Uncertainty,   Applied   Energy,   **2017**,   195,   80-92. https://doi.org/10.1016/j.apenergy.2017.03.017

[4].   W. Ampomah, R.S. Balch, R.B. Grigg, R. Will, S.Y., Lee, Z. Dai, F. Pan, Co-optimization of CO2 -EOR and storage processes in mature oil reservoirs: Original Research Article: Co-optimization of CO2 -EOR and storage processes in mature oil reservoirs, Greenhouse Gases: Science and Technology, **2017**, 7(1), 128-142. https://doi.org/10.1002/ghg.1618

[5].   Z. Dai, H. Viswanathan, R. Middleton, F. Pan, W. Ampomah, C. Yang, W. Jia, T. Xiao, S. Lee, B. McPherson, R. Balch, R. Grigg, and M. White, CO2 Accounting and Risk Analysis for CO2 Sequestration at Enhanced Oil Recovery Sites,

Environmental Science & Technology, **2016**, 50, 7546-7554. https://doi.org/10.1021/acs.est.6b01744

[6]. Z. Dai, R. Middleton, H. Viswanathan, J. Fessenden-Rahn, J. Bauman, R. Pawar, S. Lee and B. McPherson, An integrated framework for optimizing CO2 sequestration and enhanced oil recovery, Environmental Science & Technology Letters, **2014**, 1, 49-54. https://doi.org/10.1021/ez4001033

[7]. F. Pan, B. J. McPherson, Z. Dai, W. Jia, S. Lee, W. Ampomah, H. Viswanathan, R. Esser, Uncertainty Analysis of Carbon Sequestration in an Active CO2-EOR Field, Int. J. of Greenh. Gas Control, **2016**, 51, 18-28. https://doi.org/10.1016/j.ijggc.2016.04.010

[8]. J.N. Jaubert , L. Avaullee , C. Pierre, Is It Still Necessary to Measure the Minimum Miscibility Pressure?, Ind. Eng. Chem. Res., **2002**, 41 (2), 303–310. https://doi.org/10.1021/ie010485f

[9]. F. Stalkup, Miscible Displacement. *SPE Monograph Series*, **1983**, 137-158. https://doi.org/10.2118/9992-PA

[10]. M.A. Ahmadi, B. Pouladi, T. Barghi, Numerical modeling of CO2 injection scenarios in petroleum reservoirs: Application to CO2 sequestration and EOR, *Journal of Natural Gas Science and Engineering*, **2016**, 30, 38-49. https://doi.org/10.1016/j.jngse.2016.01.038

[11]. M.A. Ahmadi, M. Ebadi, Fuzzy Modeling and Experimental Investigation of Minimum Miscible Pressure in Gas Injection Process, *Fluid Phase Equilibria*, **2014**, 378, 1-12. https://doi.org/10.1016/j.fluid.2014.06.022

[12]. J.N. Jaubert, L. Wolff, L. Avaulle´e, E. Neau, A very simple multiple mixing cell calculation to compute the minimum miscibility pressure whatever the

displacement mechanism. *Industrial Engineering Chemistry Res*earch, **1998**, 37 (12), 4854-4859. https://doi.org/10.1021/ie980348r

[13]. Y. Wang, F.M. Orr, Calculation of minimum miscibility pressure. *Journal of Petroleum Science and Engineering,* **2000**, 27, 151-164. https://doi.org/10.1016/S0920-4105(00)00059-0

[14]. R.B. Alston, G.P. Kokolis, C.F. James, CO2 Minimum Miscibility Pressure: a Correlation for Impure CO2 Streams and Live Oil Systems, *SPE Journal*, **1985**, 25(2), 268-274. https://doi.org/10.2118/11959-PA

[15]. M.K. Emera, H.k. Sarma, Use of genetic algorithm to estimate Co_2-oil minimum miscibility pressure- a key parameter in design of CO_2 miscible flood, *Journal of Petroleum Science and Engineering*, **2004**, 46 , 37-52. https://doi.org/10.1016/j.petrol.2004.10.001

[16]. M.K. Emera, H.K. Sarma, Use of genetic algorithm to predict minimum miscibility pressure between flue gases and oil in design of flue gas injection project, *Middle East Oil & gas show and conference*, Bahrain, 12-15 March **2005**. https://doi.org/10.2118/93478-MS

[17]. M. Dong, Task 3-minimum miscibility pressure (MMP) studies, in the technical report: potential of greenhouse storage and utilization through Enhanced Oil Recovery. Petroleum research center, saskatchewan research council, **1999** (SRC publication No. P-10-468-C-99).

[18]. M. Dong, S. Huang, S.B. Dyer, F.M. Mourits, A comparison of Co_2 minimum miscibility pressure determination for weyburn crude oil, *Journal of petroleum science and engineering*, **2001**, 31, 13-22. https://doi.org/10.1016/S0920-4105(01)00135-8

[19].   M. Dong, S. Huang, R. Srivastava, Effect of solution gas in oil on CO_2-oil minimum miscibility pressure, *J. Can. Pet. Technol.* **2000**, 39 (11),   53-61. https://doi.org/10.2118/00-11-05

[20].   J.J. Rathmell, F.J. Stalkup, R.C. Hassinger, A laboratory investigation of miscible displacement by carbon dioxide, *Annual Fall Meeting of the Society of Petroleum Engineering of AIME*, New Orleans, **1971**. https://doi.org/10.2118/3483-MS

[21].   W.F. Yelling, R.S. Metcalfe, Determination and prediction of CO_2 minimum miscibility pressure, *Journal of Petroleum Technology*, **1980**, 32(01),160-168. https://doi.org/10.2118/7477-PA

[22].   R.S. Metcalfe, Effects of impurities on minimum miscibility pressure and minimum enrichment levels for CO_2 and rich-gas displacement, *SPE Journal*, **1982**, (4), 219-225. https://doi.org/10.2118/9230-PA

[23].   B.E. Eakin, F.J. Mitch, Measurement and correlation of miscibility pressures of reservoir oils, *Annual Technical Conference and Exhibition*, Houston, Texas, **1988**. https://doi.org/10.2118/18065-MS

[24].   M.A. Ahmadi, Z. Zahedzadeh, S.R. Shadizadeh, R. Abbassi, Connectionist model for predicting minimum gas miscibility pressure: Application to gas injection process, *Fuel*, **2015**, 148, 202-211. https://doi.org/10.1016/j.fuel.2015.01.044

[25].   J. I. Lee, Effectiveness of Carbon Dioxide Displacement under Miscible and Immiscible Conditions, Petroleum Recovery Institute, **1979**.

[26].   P. Johnson James, S. Pollin James, Measurement and Correlation of CO2 Miscibility Pressure, *SPE/DOE Enhanced Oil Recovery Symposium*, Oklahoma, Tulsa, 5-8 April **1981**. https://doi.org/10.2118/9790-MS

[27].   C. Cronquist, Carbon Dioxide Dynamic Displacement with Light Reservoir Oils, *U. S. DOE Annual Symposium*, Oklahoma, Tulsa, 28-30 August **1978**.

[28]. M.A. Klins, Carbon Dioxide Flooding, Basic Mechanisms and Project Design, *International Human Resources Development Corporation*, **1984**.

[29]. Jr. F.M. Orr, C.M. Jensen, Interpretation of Pressure Composition Phase Diagrams for CO2/Crude–Oil Systems, *SPE Journal*, **1984**, 24 (5), 485-497. https://doi.org/10.2118/11125-PA

[30]. O. Glaso, Generalized Minimum Miscibility Pressure Correlation, *SPE Journal*, **1985**, 25 (6), 927-934. https://doi.org/10.2118/12893-PA

[31]. H.M. Sebastian, R.S. Wenger, T.A. Renner, Correction of Minimum Miscibility Pressure for Impure CO2 Streams, *Journal of Petroleum Technology*, **1985**, 37(11), 2076-2082. https://doi.org/10.2118/12648-PA

[32]. Jr. F.M. Orr, M.K. Silva, Effect of Oil Composition on Minimum Miscibility Pressure: Part 2. Correlation, *SPE Journal*, **1987**, 2(4), 479-491. https://doi.org/10.2118/14150-PA

[33]. M. El-M. Shokir Eissa, CO2–oil Minimum Miscibility Pressure Model for Impure and Pure CO2 Streams, *Journal of Petroleum Science and Engineering*, **2007**, 58(1-2), 173-185. https://doi.org/10.1016/j.petrol.2006.12.001

[34]. D. Zhou, Jr., F.M. Orr, An Analysis of Rising Bubble Experiments to Determine Minimum Miscibility Pressures , *SPE Journal*, **1998**, 3(01), 19–25. https://doi.org/10.2118/30786-PA

[35]. D.N. Rao, A New Technique of Vanishing Interfacial Tension for Miscibility Determination, *Fluid Phase Equilibria*, **1997**, 139(1-2), 311-324. https://doi.org/10.1016/S0378-3812(97)00180-5

[36]. D. N. Rao, F. J. Mcintyre, D. K. Fong, Application of a New Technique to Optimize Injection Gas Composition For the Rainbow Keg River F Pool Miscible

Flood, *Journal of Canadian Petroleum Technology*, **1999**, 38(13), 96-100. https://doi.org/10.2118/99-13-22

[37]. D.N. Rao, J.I. Lee, Application of the New Vanishing Interfacial Tension Technique to Evaluate Miscibility Conditions for the Terra Nova Offshore Project, *Journal of Petroleum Science and Engineering*, **2002**, 35(3-4), 247-262. https://doi.org/10.1016/S0920-4105(02)00246-2

[38]. D.N. Rao, J.I. Lee, Determination of Gas–Oil Miscibility Conditions by Interfacial Tension Measurements, *Journal of Colloid and Interface Science*, **2003**, 262(2), 474-482. https://doi.org/10.1016/S0021-9797(03)00175-9

[39]. D.N. Rao, J. Casteel, Comparison of Minimum Miscibility Pressures Determined from Gas-Oil Interfacial Tension Measurements with Equation of State Calculations, *SPE Annual Technical Conference and Exhibition*, Colorado, Denver, 5-8 October **2003**. https://doi.org/10.2118/84187-MS

[40]. S.C. Ayirala, D.N. Rao, Comparative Evaluation of a New MMP Determination Technique, *Journal of Canadian Petroleum Technology*, **2011**, 50(9) , 71-81. https://doi.org/10.2118/99606-PA

[41]. Jr. F. M. Orr, J. Kristian, An Analysis of the Vanishing Interfacial Tension Technique for Determination of Minimum Miscibility Pressure, *Fluid Phase Equilibria,* **2007**, 255(2) , 99-109. https://doi.org/10.1016/j.fluid.2007.04.002

[42]. L.W. Holm, V.A. Josendal, Mechanisms of Oil Displacement by Carbon Dioxide, *Journal of Petroleum Technology*, **1974**, 26 (12), 1427-1436. https://doi.org/10.2118/4736-PA

[43]. L.W. Holm, V.A. Josendal, Effect of Oil Composition on Miscible-Type Displacement by Carbon Dioxide, *Journal of Petroleum Technology*, **1982**, 22(1), 87-98. https://doi.org/10.2118/8814-PA

[44]. R.M. Enick, G.D. Holder, B.I. Morsi, A Thermodynamic Correlation for the Minimum Miscibility Pressure in CO2 Flooding of Petroleum Reservoirs, *SPE Reservoir Engineering*, **1988**, 3(1), 81-92. https://doi.org/10.2118/14518-PA

[45]. Kh. Nasrifar, M. Moshfeghian, Application of an Improved Equation of State to Reservoir Fluids: Computation of Minimum Miscibility Pressure, *Journal of Petroleum Science and Engineering*, **2004**, 42(2-4), 223-234. https://doi.org/10.1016/j.petrol.2003.12.013

[46]. Kh. Nasrifar, M. Moshfeghian, A New Cubic Equation of State for Simple Fluids: Pure and Mixture: Pure and Mixture, *Fluid Phase Equilibria*, **2001**, 190(1-2), 73-88. https://doi.org/10.1016/S0378-3812(01)00592-1

[47]. Kh. Nasrifar, M. Moshfeghian, Liquid–Liquid Equilibria of Water–Hydrocarbon Systems from Cubic Equations of State, *Fluid Phase Equilibria*, **2002**, 193(1-2), 261-275. https://doi.org/10.1016/S0378-3812(01)00743-9

[48]. Kh. Nasrifar, M. Moshfeghian, Vapor–Liquid Equilibria of LNG and Gas Condensate Mixtures by the Nasrifar – Moshfeghian Equation of State, *Fluid Phase Equilibria*, **2002**, 200(1), 203-216. https://doi.org/10.1016/S0378-3812(02)00028-6

[49]. Y.F. Huang, G.H. Huang, M.Z. Dong, Development of an Artificial Neural Network Model for Predicting Minimum Miscibility Pressure in CO2 Flooding, *Journal of Petroleum Science and Engineering*, **2003**, 37(1-2), 83-95. https://doi.org/10.1016/S0920-4105(02)00312-1

[50]. A.H. Gandomi, S.M. Tabatabaei, M.H. Moradian, A. Radfar, A.H. Alavi, A new prediction model for the load capacity of castellated steel beams, *Journal of Constructional Steel Research,* **2011**, 67, 1096–1105. https://doi.org/10.1016/j.jcsr.2011.01.014

[51].   JR. Koza, Genetic programming: on the programming of computers by means of natural selection. Cambridge (MA): MIT Press; **1992**.

[52].   A.A. Javadi, M. Rezania, Applications of artificial intelligence and data mining techniques in soil modeling. *Geomechanics and Engineering*, **2009**, 1, 53–74. https://doi.org/10.12989/gae.2009.1.1.053

[53].   A.H. Alavi, M. Ameri, A.H. Gandomi, M.R. Mirzahosseini, Formulation of flow number of asphalt mixes using a hybrid computational method. *Construction and Building Materials*, **2011**, 25, 1338–1355. https://doi.org/10.1016/j.conbuildmat.2010.09.010

[54].   R.S. Torres, A.X. Falcão, M.A. Gonçalves, J.P. Papa, B. Zhang, W. Fan, et al. A genetic programming framework for content-based image retrieval, *Pattern Recognition*, **2009**, 42, 283–92. https://doi.org/10.1016/j.patcog.2008.04.010

[55].   M.A. Ahmadi, S. Zendehboudi, L. James, A. Elkamel, M. Dusseault, I. Chatzis, A. Lohi, New tools to determine bubble point pressure of crude oils: Experimental and modeling study, *Journal of Petroleum Science and Engineering*, **2014**, 123 , 207-216. https://doi.org/10.1016/j.petrol.2014.08.018

[56].   C. Ferreira, Gene expression programming: a new adaptive algorithm for solving problems. *Complex Systems*, **2001**, 13(2) , 87–129. https://arxiv.org/abs/cs/0102027

[57].   A.H. Gandomi, A.H. Alavi, M.R. Mirzahosseini, F. Moghadas Nejad, Nonlinear genetic-based models for prediction of flow number of asphalt mixtures. *Journal of Materials in Civil Engineering*, **2011**, 23(3), 1–18. http://dx.doi.org/ 10.1061/(ASCE)MT.1943-5533.0000154

[58].   C. Ferreira, Gene expression programming: mathematical modeling by an artificial intelligence. 2nd ed. Germany: Springer-Verlag; **2006**.

[59]. M.A. Ahmadi, R. Haghbakhsh, R. Soleimani, M. Bazrgar Bajestani, Estimation of H$_2$S Solubility in Ionic Liquids Using a Rigorous Method, *The Journal of Supercritical Fluids*, **2014**, 92, 60-69. https://doi.org/10.1016/j.supflu.2014.05.003

Chapter Five: Hybrid Connectionist Model Determines CO₂-Oil Swelling Factor

Abstract

In depth understanding of the interactions between crude oil and CO_2 provides insight into the CO_2-based enhanced oil recovery (EOR) process design and simulation. When CO_2 contacts the crude oil, the dissolution process takes place. This phenomenon results in oil swelling which depends on the temperature, pressure, and composition of the oil. The residual oil saturation in a CO_2 based EOR process is inversely proportional to the oil swelling factor. Hence, it is important to estimate this influential parameter with high precision. The current study suggests the predictive model based on the least square support vector machine (LSSVM) to calculate the CO_2-oil swelling factor. A Genetic algorithm (GA) is employed to optimize hyperparameters (γ and σ^2) of the LSSVM model. This model showed the high coefficient of determination ($R^2=0.9953$), and a low value for the mean squared error (MSE=0.0003) based on the available experimental data while estimating the CO_2-oil swelling factor. It was found that LSSVM is a straightforward and accurate method to determine the CO_2-oil swelling factor with negligible uncertainty. This method can be incorporated in the commercial reservoir simulators to include the effect of a CO_2-oil swelling factor when the experimental data are not adequately available.

5.1. Introduction

Due to the growing concern about global warming and the ongoing demand for energy resources, CO_2 based enhanced oil recovery (EOR) methods have been attracting both the scientific and industrial interests [1-4]. When CO_2 is injected into depleted oil

reservoirs, different mechanisms contribute to the oil production. These mechanisms depend on the operational conditions and oil composition. The most common oil production mechanisms in CO_2 based EOR methods are oil viscosity reduction, oil swelling, condensation, vaporization and interfacial tension (IFT) reduction [1, 5-12]. Reducing the level of CO_2 emissions in the atmosphere for the use of geological CO_2 storage in depleted oil reservoirs as well as its role in the oil recovery processes highlight the importance of further studies on CO_2 injection operations and the corresponding PVT behaviors [5, 10-24].

According to [25] and [26], there are four effective mechanisms contributing to oil production using CO_2-enhanced oil recovery strategies; including, (1) oil viscosity reduction, (2) oil swelling, (3) oil and water density reduction, and (4) vaporization and extraction of portions of oil. It is clear that when CO_2 is dissolved in the oil phase, the oil swells and its viscosity reduces. Hence, the variation in swelling factor allows the CO_2 to substantially expand oil, which eventually improves the oil displacement and recovery [27]. The immiscible CO_2-EOR technique is dominated by the oil swelling phenomenon and oil viscosity reduction. The degree of oil swelling and oil viscosity are dependent on different parameters including CO_2 solubility in oil, pressure, temperature, and API degree of oil samples. CO_2 solubility is generally considered as the most significant factor that influences the efficiency of CO_2-based EOR, particularly at low pressure conditions. For instance, this mechanism was confirmed through implementation of pilot-scale tests in Turkey [27-29].

Experimental investigations and numerical reservoir simulations on binary systems including hydrocarbon and CO_2 were conducted to study methods to improve the hydrocarbon recovery [10-16, 30-40]. Most of these studies investigated the oil

swelling effect primarily as a result of CO_2 dissolution in the light fractions of oil. Bessieres et al. [32] and Kiran et al.[33] examined the variation in the volume of several CO_2–alkane systems. They concluded that the excess volume follows a sigmoidal change with the composition/concentration of CO_2. The oil swelling effect was measured by the volume swelling coefficient defined by Yang et al.[5, 34-38]. These investigations reveal that with an increase in pressure (and consequently the solubility of CO_2 in oil), the volume swelling coefficient of the oil increases. Yang et al.[5] studied the behavior of oil swelling by qualitatively studying the dispersion of CO_2 in oil. Experiments at reservoir conditions (high temperature and high pressure, and live oil conditions) are however challenging.

There are a few studies to develop a reliable correlation, or a deterministic model for predicting CO_2-oil swelling factor. Welker and Dunlop [41] proposed a very simple correlation for calculation of the CO_2-oil swelling factor. Their correlation suffers from the lack of applicability, especially for light and intermediate crude oil samples. Simon and Graue[42] developed a graphical method to determine the oil swelling factor. Their method was developed based on limited data samples from heavy crudes. Chung et al.[43] proposed a simple correlation to estimate the oil swelling factor for CO_2 /heavy crude oil systems. Emera and Sarma [44] developed a correlation for predicting the oil swelling factor for both light and heavy crude oils. However, they utilized a limited number of data points while developing their correlation. Table 5-1 demonstrates a summary of correlations and models to calculate the CO_2-oil swelling factor.

Table 5-1: Correlations and models for calculating CO_2-oil swelling factor

	Correlation	Considerations/ Limitations
Welker and Dunlop [41]	$SF = 1.0 + \dfrac{0.35(solubility\ (scf/bbl))}{1000}$	Developed for oils at T=80ºF and 20º API<oil gravity<40º API
Simon and Graue [42]	Graphical correlation. The function of CO_2 solubility, oil MW and oil density at 60ºF. Not recommended for high-pressure ranges	P<2300 psi 110ºF <T<250ºF 12º API<oil gravity<33º API
Chung et al. [43]	$SF = \dfrac{\rho_l}{\rho - S}$ S = CO_2 solubility (g/cm^3) ρ = oil density without CO_2 at the same temperature and 1atm pressure (g/cm^3) ρ$_l$ = solution density (g/cm^3)	API=16.89 75ºF <T<200ºF 14.7<P<5014.7 psi
Emera and Sarma [44]	For MW>300 $$SF = 1 + 0.3302Y - 0.8417Y^2 + 1.5804Y^3 \\ - 1.074Y^4 - 0.0318Y^5 \\ + 0.21755Y^6$$ For MW<300 $$SF = 1 + 0.48411Y - 0.9928Y^2 + 1.6019Y^3 \\ - 1.2773Y^4 + 0.48267Y^5 \\ - 0.06671Y^6$$ $$Y = 1000 \times \left(\left(\left(\frac{\gamma}{MW}\right) \times sol(mole\ fraction)^2\right)^{\exp\left(\frac{\gamma}{MW}\right)}\right)$$ MW = oil molecular weight γ = oil specific gravity	23 ºC <T<121.1 ºC 0.1<P<27.4 MPa 12º API<oil gravity<37º API

Vapnik [45] proposed support vector machine (SVM) as an application of artificial intelligence. SVM is a practical method which has been widely used for classification, regression, and pattern recognition[46]. The principle idea of SVM is to transform the nonlinear input space to a higher-dimension feature space to find a hyperplane via nonlinear mapping [46, 47]. It is based on the statistical learning theory (SLT) and

structural risk minimization (SRM) concepts [48]. SVM tools obtain the solution via solving the quadratic programming (QP); the SVM always results in a global optimum solution, unlike other regression techniques such as neural networks, as QP problem is a convex function [49]. However, it suffers from computational burden.

The LSSVM has not been used to model the CO_2-oil swelling factor in the literature, to the best of our knowledge. This study uses the applicability of the least square support vector machine (LSSVM) paradigm, as a hybridized version of the original SVM method, to calculate the CO_2-oil swelling factor. Genetic algorithm (GA) is utilized as an optimization technique to optimize the hyperparameters of the LSSVM model. Thorough the comprehensive literature review, extensive experiemtnal data were used for model development and validation.

5.2. Theory

5.2.1. Least-squares support vector machine (LSSVM)

Suykens and Vandewalle [50] proposed least squares-support vector machine (LSSVM) models as an alternate formulation of SVM regression. LSSVM enjoys similar advantages as SVM. Also, it requires solving a set of only linear equations instead of a quadratic programming (QP) problem, which is computationally less demanding.

Given the training set $\{x_k, y_k\}$, $k = 1, 2, \ldots, N$, where $x_k \in \mathbb{R}^n$ is the kth input data in input space and $y_k \in \mathbb{R}$ is output variable for the given input variable (i.e. x_k) and N refers to the number of the training samples. Using nonlinear function $\varphi(\cdot)$, which

131

maps the training set in input space to the high (and possibly infinite) dimensional space, the following regression model is constructed:

$$y = w^T \varphi(x) + b \quad with \quad w \in \mathbb{R}^n, \quad b \in \mathbb{R}, \quad \varphi(\cdot) \in \mathbb{R}^n \to \mathbb{R}^{n_h}, \quad n_h \to \infty \quad (5\text{-}1)$$

in which, w denotes the weight vector and b is a bias term. Note that, the superscript "n" refers to the dimension of data space, and "n_h" is the higher dimension feature space [49]. When the LSSVM is applied, a new optimization case will be generated. The applied method deals with the following optimization problem:

$$\underset{w,b,e}{min} \quad J(w,e) = \frac{1}{2} w^T w + \frac{1}{2} \gamma \sum_{k=1}^{N} e_k^2 \tag{5-2}$$

subject to the following equality constraint:

$$y_k = w^T \phi(x_k) + b + e_k \qquad k = 1, 2, \dots, N \tag{5-3}$$

where γ represents the regularization parameter which compromises between the model's complexity and the training error [48], and e_k is the regression error. The Lagrangian is constructed as follow in order to find the solution of the un-constrained optimization problem:

$$\mathcal{L}(w, b, e, \alpha) = J(w, e) - \sum_{k=1}^{N} \alpha_k \{ w^T \phi(x_k) + b + e_k - y_k \} \tag{5-4}$$

where α_k stands for the Lagrange multiplier or support value. In order to acquire the solution of above equation, differentiating the above equation with respect to w, b, e_k, α_k gives:

$$\frac{\partial \mathcal{L}(w,b,e,\alpha)}{\partial w} = 0 \rightarrow w = \sum_{k=1}^{N} \alpha_k \varphi(x_k) \tag{5-5}$$

$$\frac{\partial \mathcal{L}(w,b,e,\alpha)}{\partial b} = 0 \rightarrow \sum_{k=1}^{N} \alpha_k = 0 \tag{5-6}$$

132

$$\frac{\partial \mathcal{L}(w,b,e,\alpha)}{\partial e_k} = 0 \rightarrow \alpha_k = \gamma e_k, \quad k = 1, \dots, N \tag{5-7}$$

$$\frac{\partial \mathcal{L}(w,b,e,\alpha)}{\partial \alpha_k} = 0 \rightarrow y_k = \varphi(x_k)w^T + b + e_k, \quad k = 1, \dots, N \tag{5-8}$$

After removing of the variables w and e one acquires the Karush-Kuhn-Trucker system as follow:

$$\begin{bmatrix} 0 & 1_v^T \\ 1_v & \Omega + \gamma^{-1}I \end{bmatrix} \begin{bmatrix} b \\ \alpha \end{bmatrix} = \begin{bmatrix} 0 \\ y \end{bmatrix} \tag{5-9}$$

In Equation (5-9), $y = [y_1 \dots y_N]^T, 1_N = [1 \dots 1]^T$, $\alpha = [\alpha_1 \dots \alpha_N]^T$, I is an identity matrix and $\Omega_{kl} = \varphi(x_k)^T.\varphi(x_l) = K(x_k, x_l) \forall k, l = 1, \dots, N.K(x_k, x_l)$ is the kernel function and must meet Mercer's condition [51].

The resulting formulation of LSSVM model for function estimation becomes:

$$y(x) = \sum_{k=1}^N \alpha_k K(x, x_k) + b \tag{5-10}$$

where (b, α) is the solution to the linear system of equations shown by Equation(5-9).

In the literature, some comprehensive descriptions of the SVM are available [45, 50, 52]. The theory of LSSVM is explained clearly in [50, 53]. Also, Liu et al.[54-56] provide a detailed comparison of the SVM and LSSVM methods.

5.2.2. Genetic Algorithm

Genetic algorithm (GA) is a stochastic method to solve optimization problems defined a fitness criterion, survival of the fittest, and different genetic operators, including crossover and mutation to satisfy a pre-defined fitness quantity, resembling the Darwinian evolution by natural selection [57]. The significant feature of the GAs and

the other similar evolutionary algorithms is that they are derivative-free. The stochastic nature of the algorithm with dynamic evaluation of the fitness function brings a powerful systematic random search engine. This approach is an alternative to derivative-based methods to deal with problems in which the fitness function is: non-differentiable, discontinuous, highly nonlinear, with multiple local optima, or stochastic [58].

5.2.3. Data Gathering

Extensive data points for the CO_2-oil swelling factor have been extracted from literature [43, 59-62]. The statistical parameters for these data samples are reported in Table 5-2. As reported in this table, the data samples contain a broad range of crude oils from heavy oils to extra-light oil samples. Also, these data points comprise a wide range of temperature, pressure, and CO_2 solubility.

Table 5-2: Statistical parameters of the data points [43, 59-62] used for developing LSSVM model

Parameter	Minimum	Maximum	Average
API	16.8	46.11	32.8
Temperature (F)	68	200	109.5
Pressure (Psia)	14.7	4100	1187.6
CO_2 Solubility (mole fraction)	0	0.86	0.525

5.2.4. Methodology

In this chapter, four parameters are considered as input variables to the LSSVM model. These parameters are 1) CO_2 solubility in oil (mole fraction of CO_2), 2) pressure, 3) temperature, and 4) the oil API degree. The output variable from the LSSVM model is the CO_2-oil swelling factor.

A total number of 225 data samples were extracted from the literature to develop our LSSVM model to estimate the CO_2-oil swelling factor. These data samples were divided into two data sets. The first set (also called training data set) contains 80% of the total data points, and is used to construct the LSSVM model. The second set of data contains 20% of data points, and is employed to validate the LSSVM model.

We have employed radial basis kernel function (RBF) because of its promising performance and simplicity as it only contains one adjustable parameter and has been proven successful in the literature [58, 63, 64]. In the model development using LSSVM with RBF kernel function, according to Eqs. (5-9) and (5-10), the optimization of γ and σ^2 are crucial tasks, where γ is the regularization factor, and σ^2 represents the kernel sample variance. These two parameters play important roles in the design of LSSVM model, with high prediction accuracy and generalization capabilities [49].

According to Ahmadi et al. [65-68], the application of non-population based optimization methods (such as Simulated Annealing, and Levenberg–Marquardt) are not recommended due to their inability to deal with the nonlinearity in the SVM methods. GA, is used here to optimize the parameters of LSSVM (γ and σ^2), and the average absolute relative deviation (AARD). The flow chart for the hyperparameter optimization using GA algorithm is depicted in Figure 5-1. The optimization procedure was repeated several times as an attempt to reach the most plausible solution corresponding to global optimum of the fitness function. As a result, values of σ^2 and γ were obtained: 0.268829 and 33.4091, respectively.
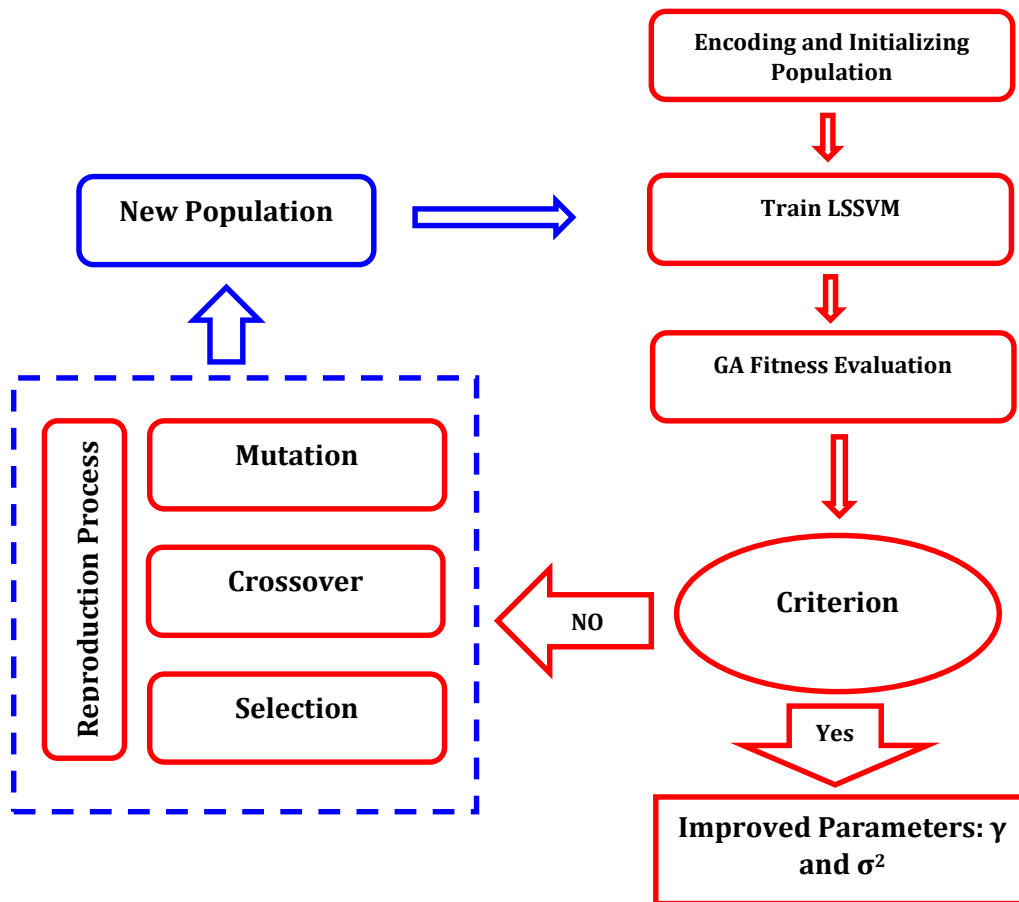
Figure 5-1**:** The flowchart of hyperparameters selection based on GA

5.3. Results and Discussion

This study presents a new deterministic approach to obtain the swelling factor with higher accuracy. The oil swelling factor for the system of CO_2 and light oil versus pressure at different temperatures is demonstrated in Figure 5-2. The trends in the oil swelling factor versus pressure at different temperatures are shown in Figures 5-3 and 5-4 for intermediate and heavy oil samples, respectively.
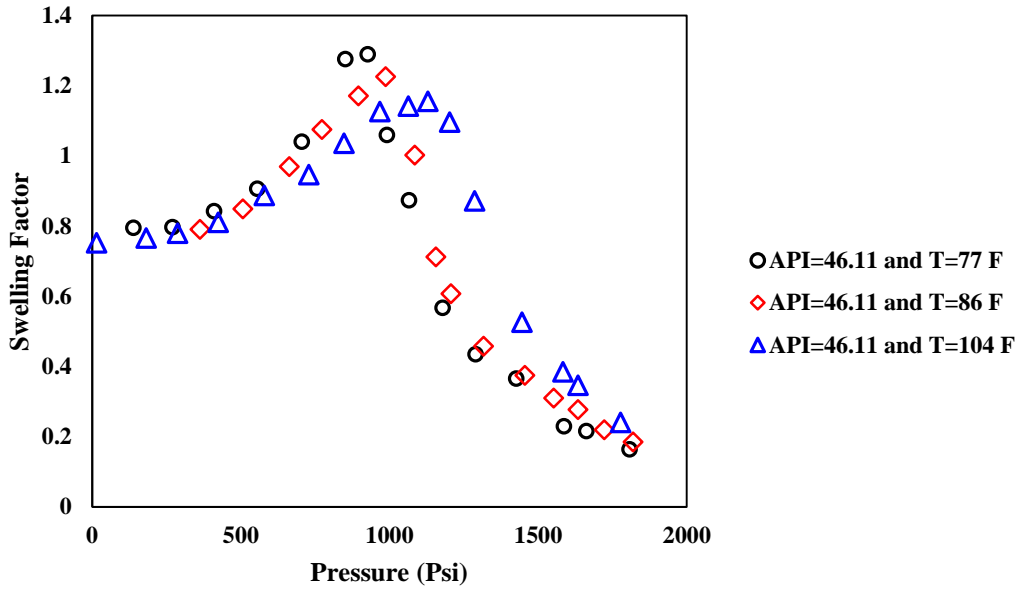
Figure 5-2: Swelling factor of CO_2-light oil system versus corresponding pressure at different temperatures [43, 59-62]
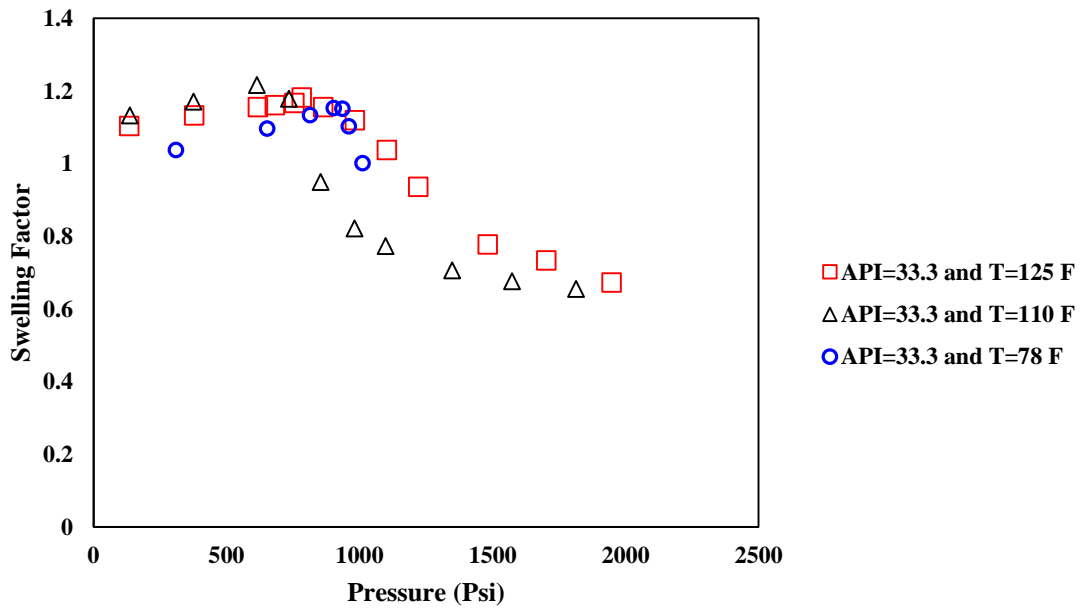
(a)
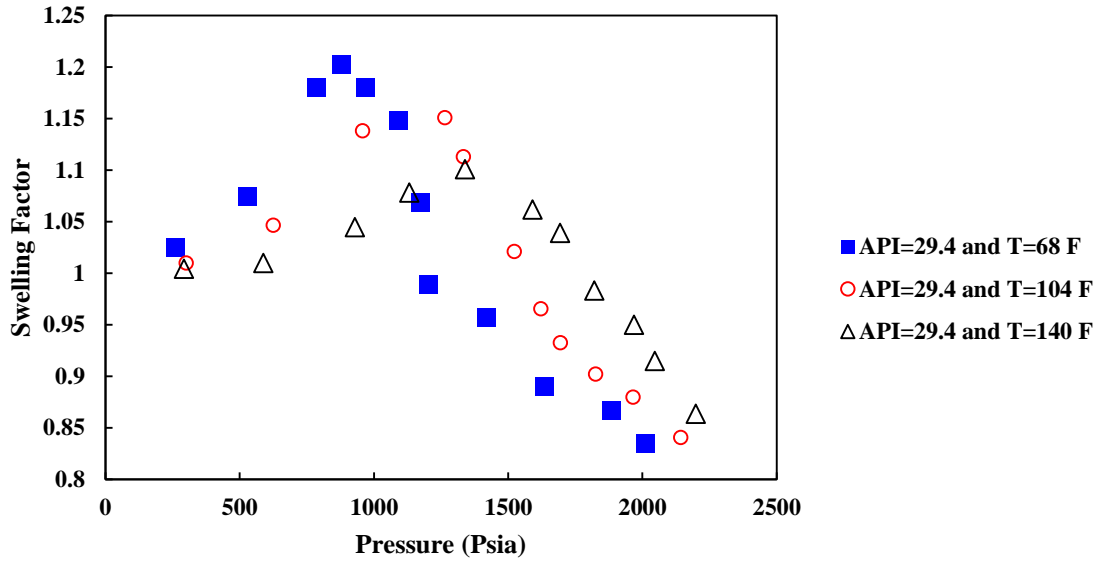
(b)

Figure 5-3: Swelling factor of CO_2-intermediate oil system versus corresponding pressure at different temperatures [43, 59-62] a) API=33.3 b) API=29.4
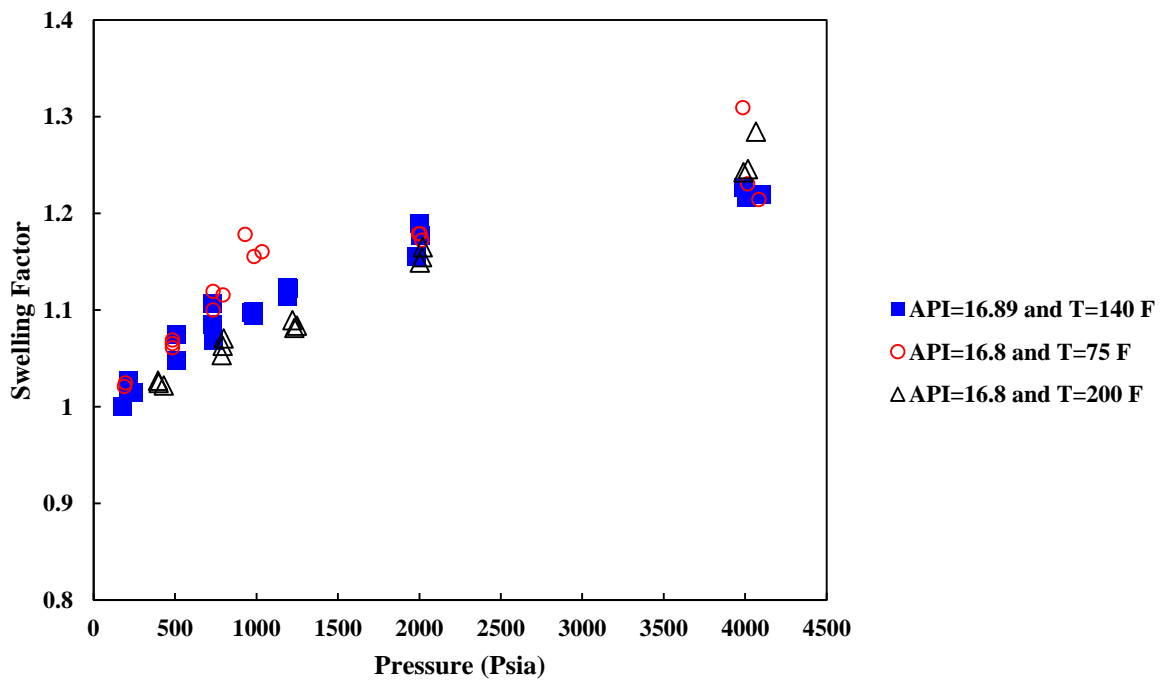
Figure 5-4: Swelling factor of CO_2-heavy oil system versus corresponding pressure at different temperatures [43, 59-62]

Mean squared error (MSE) and coefficient of determination (R^2) are employed here as the performance evaluation criteria for the LSSVM model in estimating the CO_2-oil swelling factor. The expressions to evaluate MSE and R^2 are given below:

$$MSE = \frac{1}{N}\sum_{i=1}^{N}(y^{actual}{}_i - y^{predicted}{}_i)^2 \qquad (5\text{-}11)$$

$$R^2 = 1 - \frac{\sum_{i=1}^{N}(y^{actual}{}_i - y^{predicted}{}_i)^2}{\sum_{i=1}^{N}(y^{actual}{}_i - \overline{y^{actual}})^2} \qquad (5\text{-}12)$$

where, N represents the number of data points, $y^{actual}{}_i$ is the ith observation (real data), $y^{predicted}{}_i$ is the ith output from the model and $\overline{y^{actual}}$ is the average of observations. The values of MSE and R^2 are reported in Table 5-3 for training, testing and also overall data stages. The GA-LSSVM predictions are satisfactory if R^2 and MSE are close to 1 and 0 respectively. As can be seen these criteria were fulfilled.

Table 5-3**:** Performance of GA-LSSVM method with optimized parameters for prediction swelling factor in terms of statistical parameters.

Statistical Parameters			
	Training data	**Testing data**	**Overall data**
MSE	0.00016	0.0009	0.0003
R²	0.9944	0.9931	0.9953
Average Absolute Relative Deviation (AARD)	0.7918	4.549	1.5433
Maximum Absolute Error	5.3403	5.4205	5.4205

Figure 5-5 depicts the comparison between the experimental data for CO_2-oil swelling factor and the values estimated by the LSSVM. Figure 5-5 (a) shows a comparison between estimated and experimental data in the training phase. Figure 5-5 (b) demonstrates the comparison between actual and predicted CO_2-oilswelling factor

behavior against data index. As illustrated in Figure 5-5, there is an excellent match between the oil swelling factor estimated from LSSVM and those from experiments.
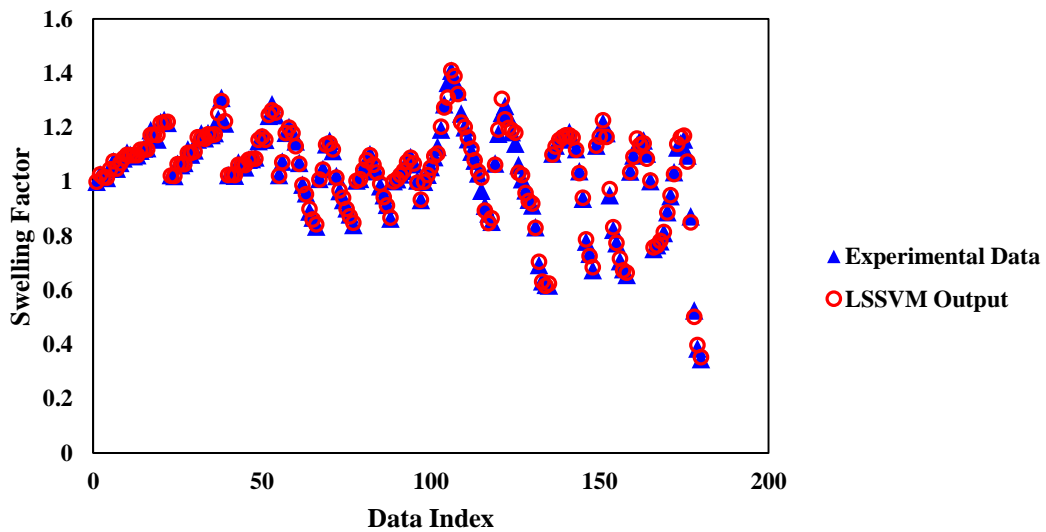
(a)
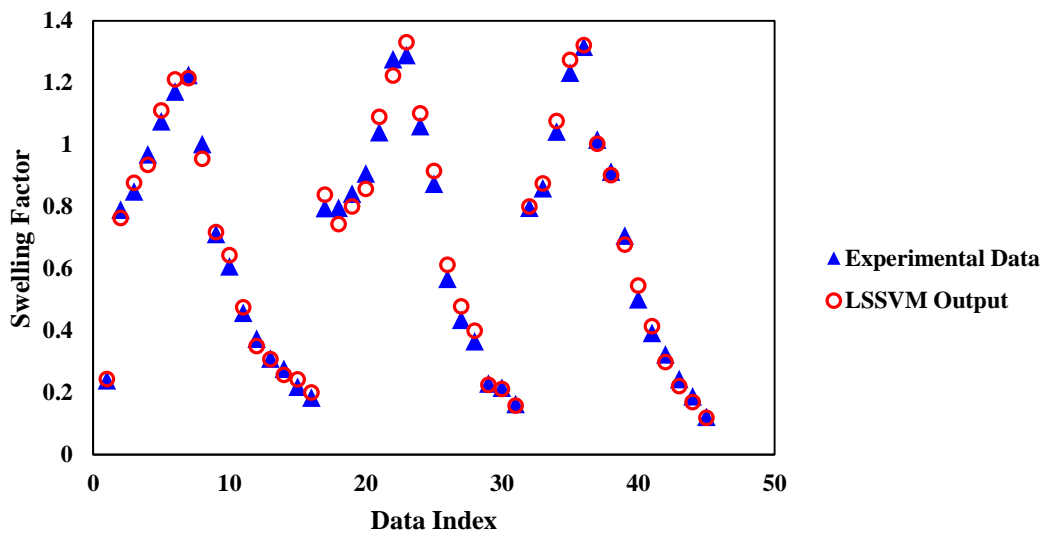
(b)

Figure 5-5: Comparison between estimated and measured Swelling factor versus data index a) Training data b) Testing data

Figure 5-6 demonstrates the regression plot between the CO_2-oil swelling factor determined by LSSVM model and the experimental ones. Figure 5-6 (a) depicts the

scatter plot for results obtained in the training phase of the LSSVM model. As shown in Figure 5-6 (a), the linear fit to data $y = 0.9892x + 0.0103$ has a high correlation of coefficient ($R^2 = 0.9944$), meaning that the training phase of the LSSVM model is performed very well. Figure 5-6 (b) shows the scatter plot for the results from the testing (validating) phase of the LSSVM model. As depicted in Figure 5-6 (b), the high value of the correlation coefficient ($R^2 = 0.9931$) between the predicted and experimental oil swelling factor shows the superior performance of the LSSVM model. Figure 5-6 (c) illustrates the regression plot for the whole data set. The predicted swelling factor values are found to be scattered approximately around the y=x line, indicating that the LSSVM model that is optimized by GA predicts the swelling factor very well.

$$y = 0.9892x + 0.0103$$
$$R^2 = 0.9944$$

○ Data

— Best Fit : $R^2 = 0.9944$
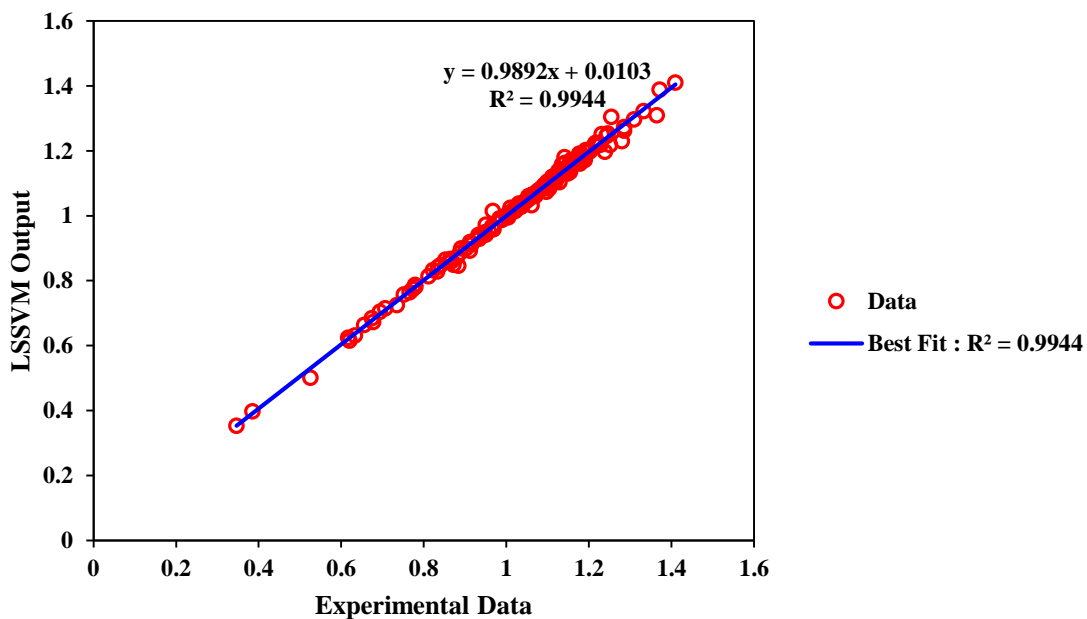
(a)
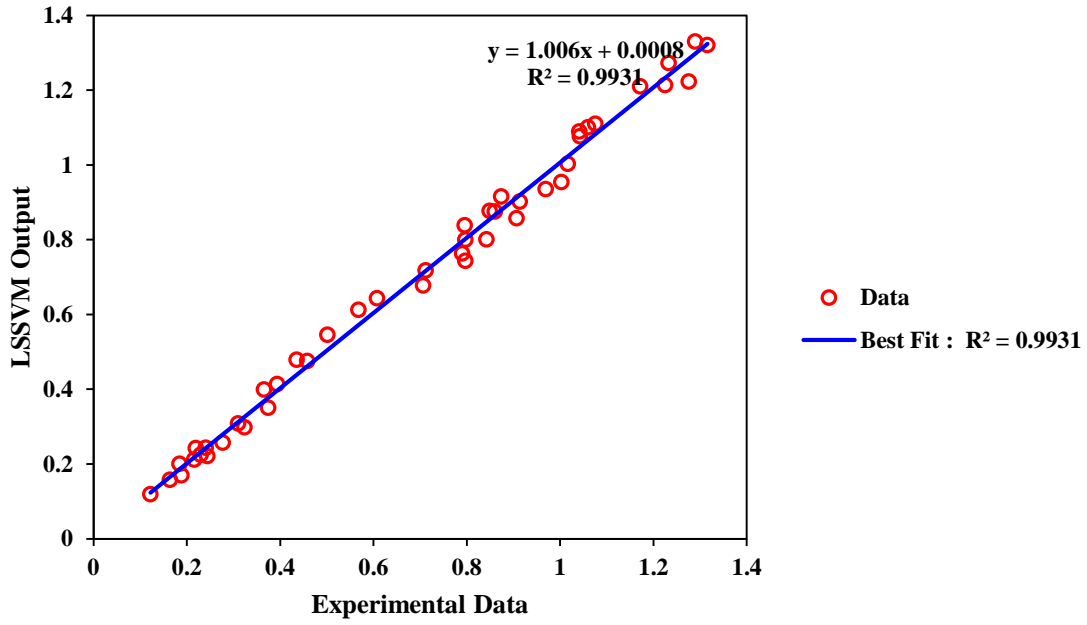
(b)
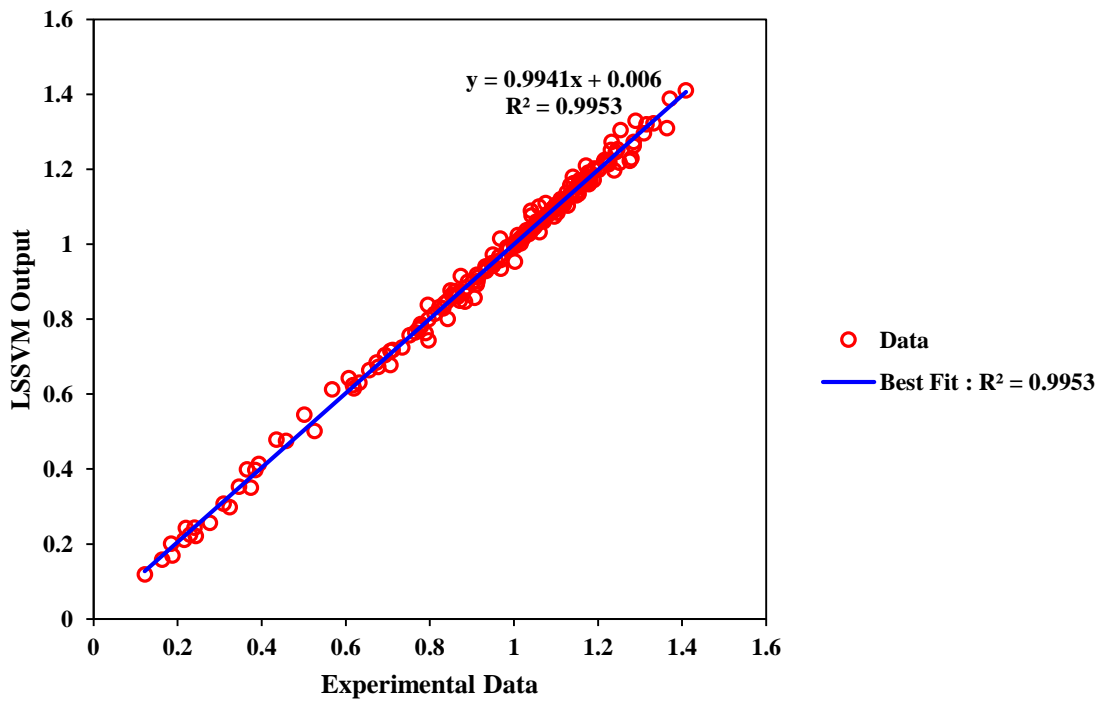
(c)

Figure 5-6: Scatter plot of estimated and measured Swelling factor a) training data b) testing data c) whole data

Figure 5-7 illustrates a comparison between the CO_2-oil swelling factor from LSSVM model and the experimental ones versus the corresponding pressure at different temperatures. As shown in Figure 5-7, the LSSVM model follows the trend of experimental data points for an oil sample with API=29.4. As the experimental data points show, the swelling factor predicted lowers by increasing the temperature. This behaviour was confirmed by LSSVM model. This imlpies that the proposed LSSVM model for determination of CO_2-oil swelling factor is valid/acceptable in terms of technical and conceptual prospects.
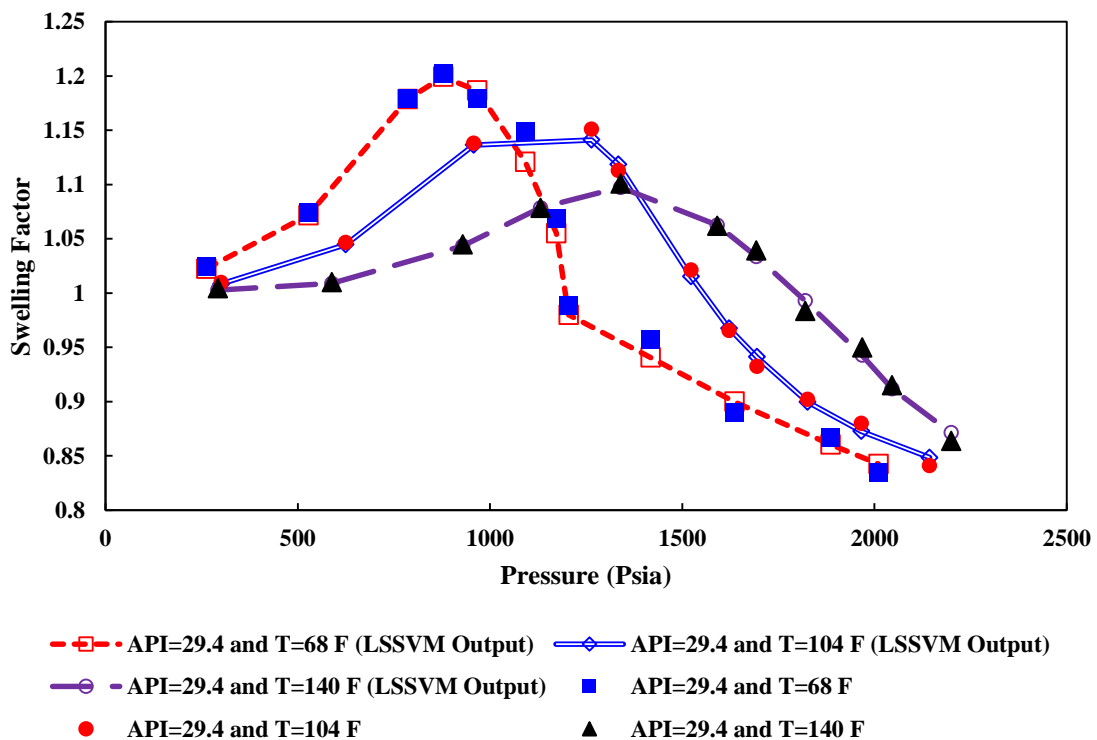
Figure 5-7: Comparison between calculated and measured Swelling factor versus corresponding pressure at different temperatures

Figure 5-8 shows the relative error distribution for both the training and testing phases in developing the LSSVM model. As shown in Figure 5-8, the maximum relative deviation between the outputs of the LSSVM model and the experimental CO_2-oil

swelling factor is within ±5% for the training phase. Also, the maximum relative deviation between the CO_2-oil swelling factor calculated by the LSSVM model and experimental ones is within ±15% for the testing phase.
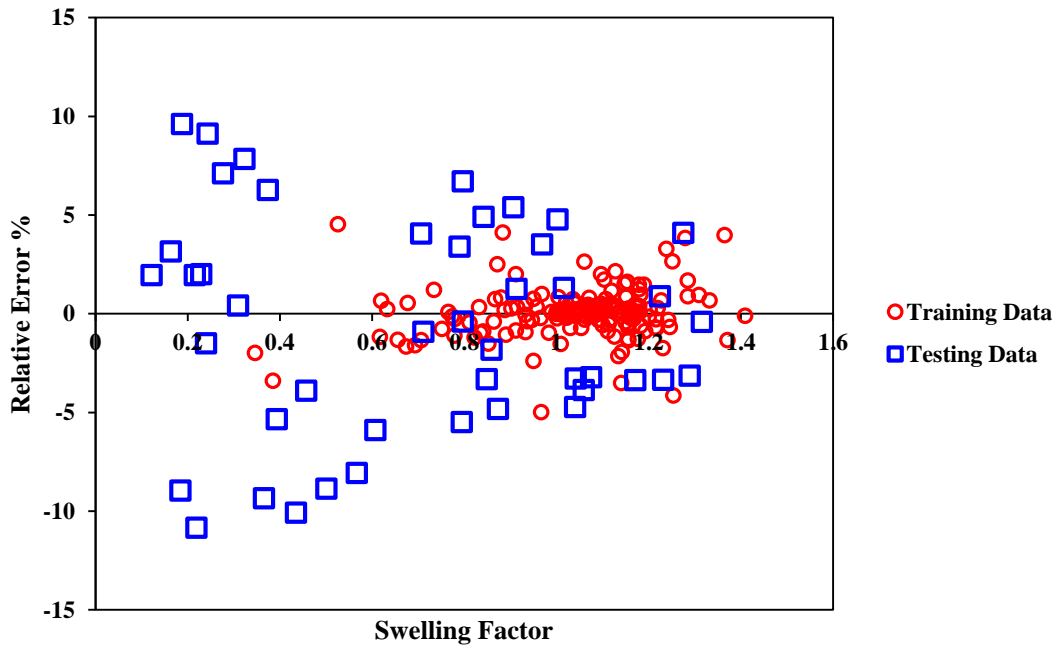
Figure 5-8: Relative error distribution of the estimated target versus Swelling factor

Figure 5-9 demonstrates the scatter plot of the results by the graphical method proposed by Simon and Graue [42] versus the experimental values of the CO_2-oil swelling factor. As depicted in Figure 5-9, the linear fit has a low correlation coefficient (R^2). Also, the linear fit has a negative slope, meaning that the value of oil swelling factor at the lower boundary is overestimated. In other words, Simon and Graue [42] proposed a graphical method for determination of CO_2-oil swelling factor. In this method, the minimum value of the CO_2-oil swelling factor is equal to 1 and the maximum value is equal to 1.38. Also, the Simon and Graue technique offers acceptable values for swelling factor within the limited ranges of API, temperature, and CO_2 solubility. Hence, this graphical method is not able to provide reliable outputs over wide ranges of the input parameters.
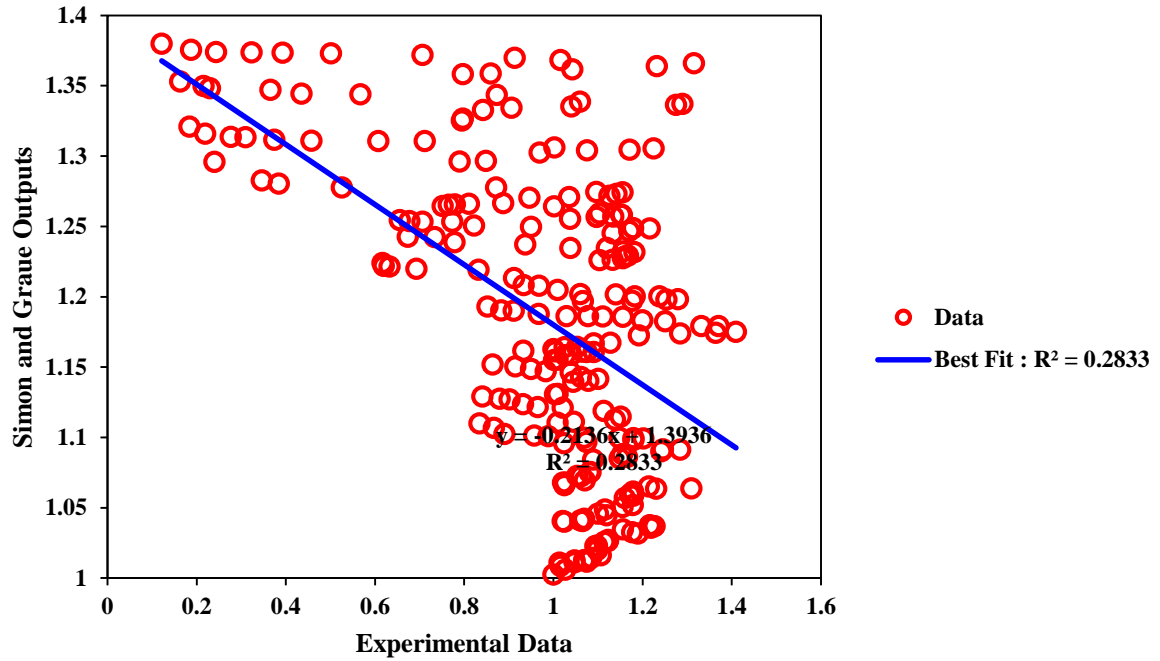
Figure 5-9**:** Scatter plot of estimated data using Simon-Graue [42] method and measured Swelling factor

Figure 5-10 illustrates the scatter plot of the results by Emera and Sarma [44] correlation versus the experimental values of the CO_2-oil swelling factor. As shown in Figure 5-10, the linear fit has a higher value of correlation of coefficient in comparison with the method proposed by Simon and Graue [42]. It is because the correlation proposed by Emera and Sarma [44] is developed using a wider range of data points. However, this correlation still suffers from the common drawback for the most emprical correlations so that it just works for the limited ranges of API, temperature, and CO_2 solubility. As illustrated in Figure 5-10, the swelling factor results from Emera and Sarma [44] correlation are underestimated the magnitudes of the swelling factor in the middle range.
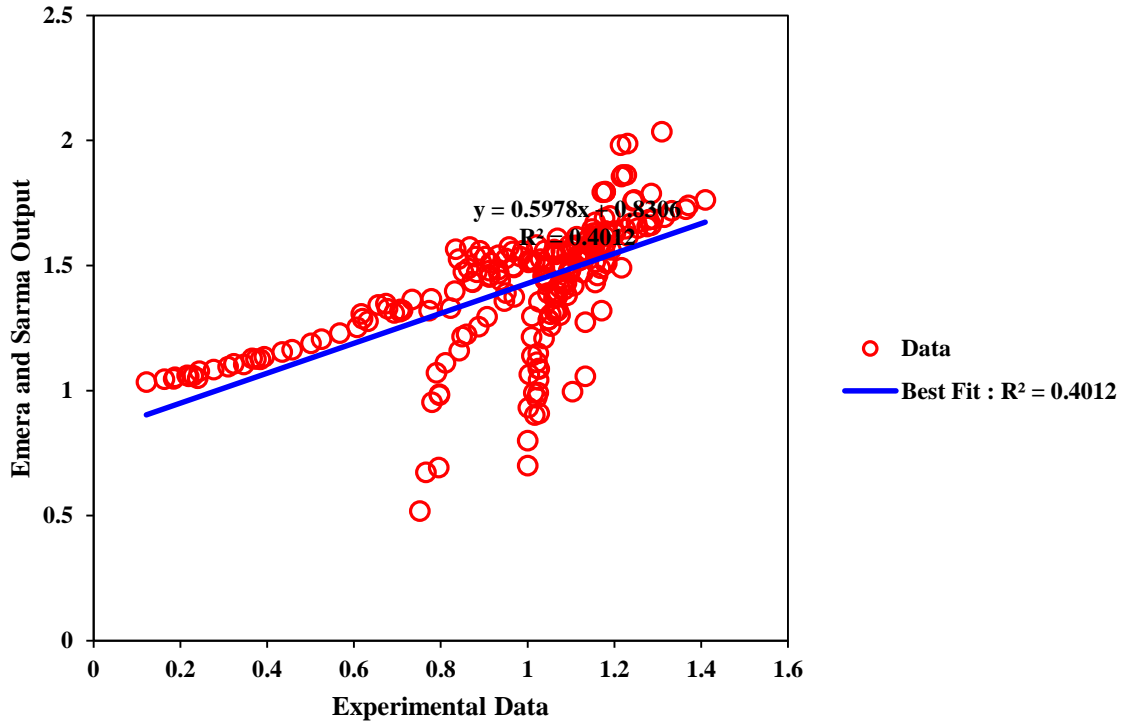
Figure 5-10: Scatter plot of estimated data using Emera and Sarma [44] correlation and measured Swelling factor

Figure 5-11 shows a comparison between the maximum absolute error (MAE) between different models and the experimental values of the CO_2-oil swelling factor. As depicted in Figure 5-11, the value of the MAE for the LSSVM model is lower than those obtained for the Emera and Sarma [44], and Simon and Graue [42] methods. This superior performance comes from the proper procedure for the training phase and careful selection of the data samples. Using a broader range of data samples enables us to develop a more precise and accurate model to calculate the CO_2-oil swelling factor.
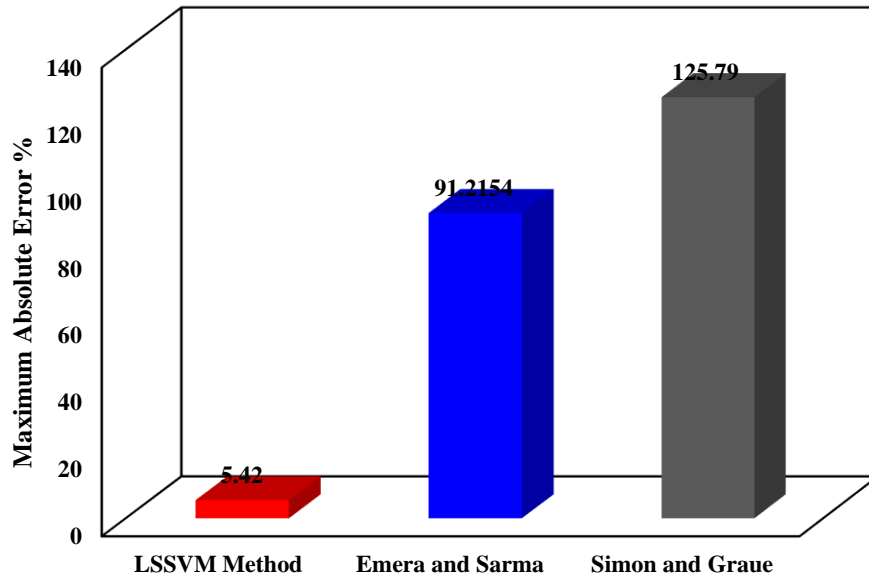
Figure 5-11: Comparison between maximum absolute error between the predicted values and experimental ones

Figure 5-12 depicts a comparison between the average absolute relative deviation (ARD) from different models and the experimental data on CO_2-oil swelling factor. It should be noted the correlation proposed by Emera and Sarma [44] is used in the computer group modeling (CMG) reservoir simulator package. Our proposed LSSVM model can be included in the commercial reservoir simulators for applications such as the simulation of gas injection processes.
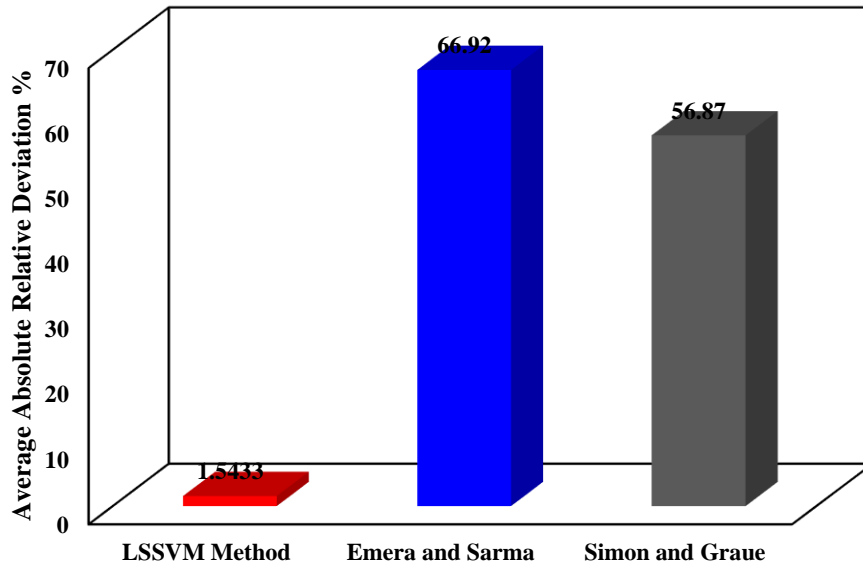
Figure 5-12: Comparison between average absolute relative deviation between the predicted values and experimental ones

One of the statistical methods for identifying the applicability of the model is implementing a technique for the outlier detection. Detection of an outlier is to determine which data points may differ from the bulk of the data present in the data bank under study [69, 70]. For examining the capability of the LSSVM model, the approach of Leverage Value Statistics has been carried out [70, 71]. A graphical method (William plot) is used for outlier determination here. William plot depicts the standardized residual of the outputs versus corresponding hat (H) values. An explanation with details for mathematical backgrounds and computational procedure of the William method can be found in the references [69-71]. Figure 5-13 shows the Williams plot for the results gained from the LSSVM model in estimating the CO_2-oil swelling factor. Having the majority of data points in the ranges of $0 \leq H \leq 0.055$ and $-3 \leq R \leq 3$ reveals that the LSSVM model is convincing and reliable in terms of statistical criteria. In addition, it conveys the message that the entire data are located

148

within the acceptable domains, again confirming the LSSVM model offers accurate and satisfactory results.
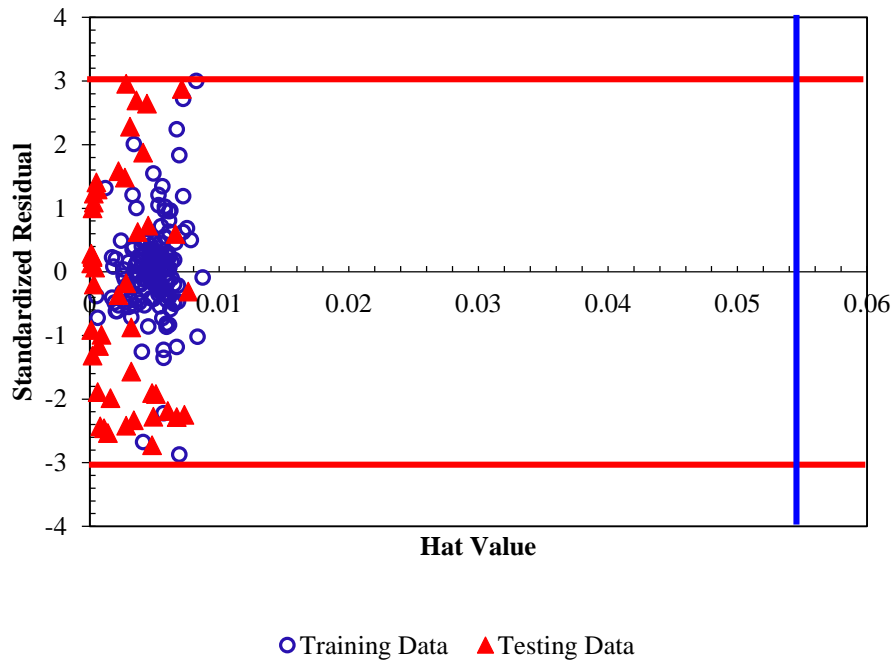
Figure 5-13: Detection of the possible doubtful measured Swelling factor and the applicability domain of the suggested approach for the CO_2-oil swelling factor. The H* value is 0.0555

Analysis of variance was employed in this study to determine the relative importance of all input parameters which are incorporated in this modeling strategy to develop the connectionist tool for estimation of CO_2-oil swelling factor. The relative importance of independent variables including API, temperature, pressure, and CO_2 solubility (mole fraction) on the swelling factor is demonstrated in Figure 5-14. As it is clear from the results, the most significant independent parameter is API degree of the oil samples, temperature holds the second rank, and the concentration has the least impact on the target parameter.
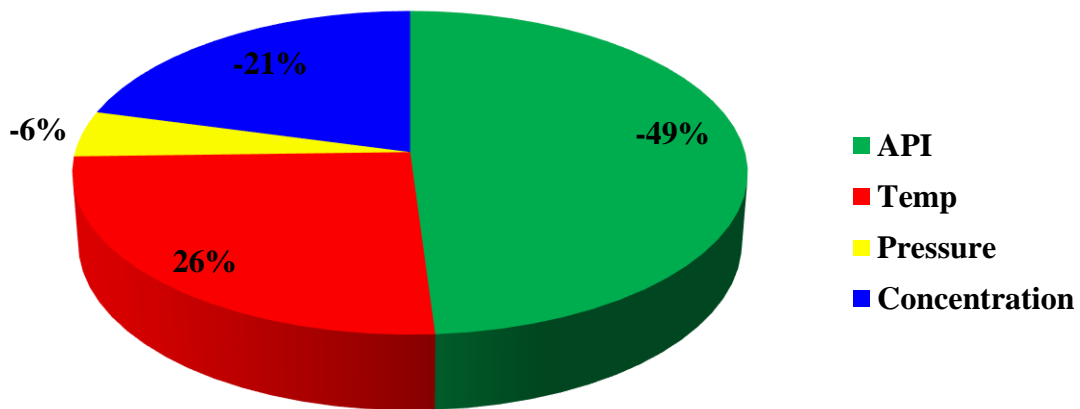
Figure 5-14: Relative importance of the independent variables affecting swelling factor

The residual oil saturation which directly corrsponds to the oil recovery factor is inversely proportional to the swelling factor in CO_2 based EOR processes. Hence, an accurate magnitude of the CO_2-oil swelling factor increases the precision and reliability of the modeling and simulation studies which are conducted to capture the main recovery mechanisms and determine production performance of CO_2-EOR strategies for both heavy oil and conventional oil reserves. The present study introduces an accurate and simple-to-use approach to calculate the CO_2-oil swelling factor which is an influential parameter throughout CO_2 injection operations. The precise value of this parameter helps engineers/researchers obtain the residual oil saturation and oil and water relative permeability curves with greater reliability for various oil reservoir development stages (e.g., optimization of operational conditions and economical analysis).

References

[1] R. Farajzadeh, A. Andrianov, H. Bruining, P.L. Zitha, Comparative study of CO2 and N2 foams in porous media at low and high pressure− temperatures, Industrial & Engineering Chemistry Research, 48 (2009) 4542-4552.

[2] T. Kuznetsova, B. Kvamme, Thermodynamic properties and interfacial tension of a model water–carbon dioxide system, Physical chemistry chemical physics, 4 (2002) 937-941.

[3] J. Ma, X. Wang, R. Gao, F. Zeng, C. Huang, P. Tontiwachwuthikul, Z. Liang, Study of cyclic CO 2 injection for low-pressure light oil recovery under reservoir conditions, Fuel, 174 (2016) 296-306.

[4] M.L. Godec, V.A. Kuuskraa, P. Dipietro, Opportunities for using anthropogenic CO2 for enhanced oil recovery and CO2 storage, Energy & Fuels, 27 (2013) 4183-4189.

[5] Z. Yang, M. Li, B. Peng, M. Lin, Z. Dong, Dispersion Property of CO2 in Oil. 1. Volume Expansion of CO2+ Alkane at near Critical and Supercritical Condition of CO2, Journal of Chemical & Engineering Data, 57 (2012) 882-889.

[6] R. Czarnota, D. Janiga, J. Stopa, P. Wojnarowski, Determination of minimum miscibility pressure for CO 2 and oil system using acoustically monitored separator, Journal of CO2 Utilization, 17 (2017) 32-36.

[7] A. Abedini, F. Torabi, On the CO 2 storage potential of cyclic CO 2 injection process for enhanced oil recovery, Fuel, 124 (2014) 14-27.

[8] X. Li, D.A. Ross, J.M. Trusler, G.C. Maitland, E.S. Boek, Molecular dynamics simulations of CO2 and brine interfacial tension at high temperatures and pressures, The Journal of Physical Chemistry B, 117 (2013) 5647-5652.

[9] M.A. Ahmadi, M. zeinali Hasanvand, S. Shokrolahzadeh, Technical and economic feasibility study of flue gas injection in an Iranian oil field, Petroleum, 1 (2015) 217-222.

[10] J.L. Shelton, J.C. McIntosh, A.G. Hunt, T.L. Beebe, A.D. Parker, P.D. Warwick, R.M. Drake, J.E. McCray, Determining CO_2 storage potential during miscible CO_2 enhanced oil recovery: Noble gas and stable isotope tracers, International Journal of Greenhouse Gas Control, 51 (2016) 239-253.

[11] S. Bachu, Identification of oil reservoirs suitable for CO_2-EOR and CO_2 storage (CCUS) using reserves databases, with application to Alberta, Canada, International Journal of Greenhouse Gas Control, 44 (2016) 152-165.

[12] L. Li, S. Khorsandi, R.T. Johns, R.M. Dilmore, CO_2 enhanced oil recovery and storage using a gravity-enhanced process, International Journal of Greenhouse Gas Control, 42 (2015) 502-515.

[13] S. Kim, J.C. Santamarina, Engineered CO_2 injection: The use of surfactants for enhanced sweep efficiency, International Journal of Greenhouse Gas Control, 20 (2014) 324-332.

[14] P. Luo, V. Er, N. Freitag, S. Huang, Recharacterizing evolving fluid and PVT properties of Weyburn oil–CO_2 system, International Journal of Greenhouse Gas Control, 16 (2013) S226-S235.

[15] A. Jamali, A. Ettehadtavakkol, CO_2 storage in Residual Oil Zones: Field-scale modeling and assessment, International Journal of Greenhouse Gas Control, 56 (2017) 102-115.

[16] X. Li, X. Fan, Effect of CO_2 phase on contact angle in oil-wet and water-wet pores, International Journal of Greenhouse Gas Control, 36 (2015) 106-113.

[17] W. Yu, H.R. Lashgari, K. Wu, K. Sepehrnoori, CO 2 injection for enhanced oil recovery in Bakken tight oil reservoirs, Fuel, 159 (2015) 354-363.

[18] M. zeinali Hasanvand, M.A. Ahmadi, S.R. Shadizadeh, R. Behbahani, F. Feyzi, Geological storage of carbon dioxide by injection of carbonated water in an Iranian oil reservoir: a case study, Journal of Petroleum Science and Engineering, 111 (2013) 170-177.

[19] Y. Liu, J. Wilcox, Molecular simulation studies of CO2 adsorption by carbon model compounds for carbon capture and sequestration applications, Environmental science & technology, 47 (2012) 95-101.

[20] K. Sell, F. Enzmann, M. Kersten, E. Spangenberg, Microtomographic quantification of hydraulic clay mineral displacement effects during a CO2 sequestration experiment with saline aquifer sandstone, Environmental science & technology, 47 (2012) 198-204.

[21] M.A. Ahmadi, M. zeinali Hasanvand, S.S. Behbahani, A. Nourmohammad, A. Vahidi, M. Amiri, G. Ahmadi, Effect of operational parameters on the performance of carbonated water injection: Experimental and numerical modeling study, The Journal of Supercritical Fluids, 107 (2016) 542-548.

[22] S.J. Davis, K. Caldeira, H.D. Matthews, Future CO2 emissions and climate change from existing energy infrastructure, Science, 329 (2010) 1330-1333.

[23] M.A. Ahmadi, B. Pouladi, T. Barghi, Numerical modeling of CO 2 injection scenarios in petroleum reservoirs: Application to CO 2 sequestration and EOR, Journal of Natural Gas Science and Engineering, 30 (2016) 38-49.

[24] F.M. Orr, J.P. Heller, J.J. Taber, Carbon dioxide flooding for enhanced oil recovery: Promise and problems, Journal of the American Oil Chemists' Society, 59 (1982) 810A-817A.

[25] G. Rojas, S. Ali, Scaled model studies of carbon dioxide/brine injection strategies for heavy oil recovery from thin formations, Journal of Canadian Petroleum Technology, 25 (1986).

[26] S.Q. Tunio, A.H. Tunio, N.A. Ghirano, Z.M. El Adawy, Comparison of different enhanced oil recovery techniques for better oil productivity, International Journal of Applied Science and Technology, 1 (2011).

[27] M.S.A. Perera, R.P. Gamage, T.D. Rathnaweera, A.S. Ranathunga, A. Koay, X. Choi, A Review of CO2-Enhanced Oil Recovery with a Simulated Sensitivity Analysis, Energies, 9 (2016) 481.

[28] A. Bagci, Immiscible CO2 flooding through horizontal wells, Energy Sources, Part A, 29 (2007) 85-95.

[29] K. Issever, I. Topkaya, Use of carbon dioxide to enhanced heavy oil recovery, in: 7th Unitar International Conference on Heavy Crude and Tar Sands, Beijing China, 1998, pp. 27-30.

[30] G. Lv, Q. Li, S. Wang, X. Li, Key techniques of reservoir engineering and injection–production process for CO 2 flooding in China's SINOPEC Shengli Oilfield, Journal of CO2 Utilization, 11 (2015) 31-40.

[31] P. Diep, K.D. Jordan, J.K. Johnson, E.J. Beckman, CO2− Fluorocarbon and CO2− hydrocarbon interactions from first-principles calculations, The Journal of Physical Chemistry A, 102 (1998) 2231-2236.

[32] D. Bessières, H. Saint-Guirons, J.-L. Daridon, Volumetric behavior of decane+ carbon dioxide at high pressures. Measurement and calculation, Journal of Chemical & Engineering Data, 46 (2001) 1136-1139.

[33] E. Kiran, H. Pöhler, Y. Xiong, Volumetric properties of pentane+ carbon dioxide at high pressures, Journal of Chemical & Engineering Data, 41 (1996) 158-165.

[34] X. Li, H. Li, D. Yang, Determination of Multiphase Boundaries and Swelling Factors of Solvent (s)–CO2–Heavy Oil Systems at High Pressures and Elevated Temperatures, Energy & Fuels, 27 (2013) 1293-1306.

[35] C.A. Mulliken, S.I. Sandler, The prediction of CO2 solubility and swelling factors for enhanced oil recovery, Industrial & Engineering Chemistry Process Design and Development, 19 (1980) 709-711.

[36] P. Luo, C. Yang, Y. Gu, Enhanced solvent dissolution into in-situ upgraded heavy oil under different pressures, Fluid Phase Equilibria, 252 (2007) 143-151.

[37] C. Yang, Y. Gu, A novel experimental technique for studying solvent mass transfer and oil swelling effect in the vapour extraction (VAPEX) process, in: Canadian international petroleum conference, Petroleum Society of Canada, 2005.

[38] H. Do, W. Pinczewski, Diffusion controlled swelling of reservoir oil by direct contact with injection gas, Chemical engineering science, 46 (1991) 1259-1270.

[39] I. Fukai, S. Mishra, M.A. Moody, Economic analysis of CO 2-enhanced oil recovery in Ohio: Implications for carbon capture, utilization, and storage in the Appalachian Basin region, International Journal of Greenhouse Gas Control, 52 (2016) 357-377.

[40] D.-H. Kwak, J.-K. Kim, Techno-economic evaluation of CO 2 enhanced oil recovery (EOR) with the optimization of CO 2 supply, International Journal of Greenhouse Gas Control, 58 (2017) 169-184.

[41] J. Welker, Physical properties of carbonated oils, Journal of Petroleum Technology, 15 (1963) 873-876.

[42] R. Simon, D. Graue, Generalized correlations for predicting solubility, swelling and viscosity behavior of CO2-crude oil systems, Journal of Petroleum Technology, 17 (1965) 102-106.

[43] F.T. Chung, R.A. Jones, H.T. Nguyen, Measurements and correlations of the physical properties of CO2-heavy crude oil mixtures, SPE reservoir engineering, 3 (1988) 822-828.

[44] M. Emera, H. Sarma, A genetic algorithm-based model to predict co-oil physical properties for dead and live oil, in: Canadian International Petroleum Conference, Petroleum Society of Canada, 2006.

[45] V. Vapnik, Statistical learning theory. 1998, in, Wiley, New York, 1998.

[46] C. Cortes, V. Vapnik, Support-vector networks, Machine learning, 20 (1995) 273-297.

[47] A. Baylar, D. Hanbay, M. Batan, Application of least square support vector machines in the prediction of aeration performance of plunging overfall jets from weirs, Expert Systems with Applications, 36 (2009) 8368-8374.

[48] B. Mehdizadeh, K. Movagharnejad, A comparative study between LS-SVM method and semi empirical equations for modeling the solubility of different solutes in supercritical carbon dioxide, Chemical Engineering Research and Design, 89 (2011) 2420-2427.

[49] C.-M. Vong, P.-K. Wong, Y.-P. Li, Prediction of automotive engine power and torque using least squares support vector machines and Bayesian inference, Engineering Applications of Artificial Intelligence, 19 (2006) 277-287.

[50] J.A. Suykens, J. Vandewalle, Least squares support vector machine classifiers, Neural processing letters, 9 (1999) 293-300.

[51] C.-H. Li, X.-J. Zhu, G.-Y. Cao, S. Sui, M.-R. Hu, Identification of the Hammerstein model of a PEMFC stack based on least squares support vector machines, Journal of Power Sources, 175 (2008) 303-316.

[52] C.J. Burges, A tutorial on support vector machines for pattern recognition, Data mining and knowledge discovery, 2 (1998) 121-167.

[53] J.A. Suykens, T. Van Gestel, J. De Brabanter, Least squares support vector machines, World Scientific, 2002.

[54] H. Liu, X. Yao, R. Zhang, M. Liu, Z. Hu, B. Fan, Accurate quantitative structure−property relationship model to predict the solubility of C60 in various solvents based on a novel approach using a least-squares support vector machine, The Journal of Physical Chemistry B, 109 (2005) 20565-20571.

[55] H. Liu, X. Yao, R. Zhang, M. Liu, Z. Hu, B.T. Fan, Prediction of the tissue/blood partition coefficients of organic compounds based on the molecular structure using least-squares support vector machines, Journal of computer-aided molecular design, 19 (2005) 499-508.

[56] J. Li, H. Liu, X. Yao, M. Liu, Z. Hu, B. Fan, Quantitative structure–activity relationship study of acyl ureas as inhibitors of human liver glycogen phosphorylase using least squares support vector machines, Chemometrics and intelligent laboratory systems, 87 (2007) 139-146.

[57] A. Niazi, S. Jameh-Bozorghi, D. Nori-Shargh, Prediction of toxicity of nitrobenzenes using ab initio and least squares support vector machines, Journal of hazardous materials, 151 (2008) 603-609.

[58] M. Reihanian, S. Asadullahpour, S. Hajarpour, K. Gheisari, Application of neural network and genetic algorithm to powder metallurgy of pure iron, Materials & Design, 32 (2011) 3183-3188.

[59] B. Wei, H. Gao, W. Pu, F. Zhao, Y. Li, F. Jin, L. Sun, K. Li, Interactions and phase behaviors between oleic phase and CO 2 from swelling to miscibility in CO 2-based

enhanced oil recovery (EOR) process: A comprehensive visualization study, Journal of Molecular Liquids, 232 (2017) 277-284.

[60] N. Mosavat, A. Abedini, F. Torabi, Phase Behaviour of CO2–Brine and CO2–Oil Systems for CO2 Storage and Enhanced Oil Recovery: Experimental Studies, Energy Procedia, 63 (2014) 5631-5645.

[61] A. Abedini, N. Mosavat, F. Torabi, Determination of Minimum Miscibility Pressure of Crude Oil–CO2 System by Oil Swelling/Extraction Test, Energy Technology, 2 (2014) 431-439.

[62] J.-S. Tsau, L.H. Bui, G.P. Willhite, Swelling/extraction test of a small sample size for phase behavior study, in: SPE Improved Oil Recovery Symposium, Society of Petroleum Engineers, 2010.

[63] M.A. Ahmadi, Connectionist approach estimates gas–oil relative permeability in petroleum reservoirs: application to reservoir simulation, Fuel, 140 (2015) 429-439.

[64] S.S. Keerthi, C.-J. Lin, Asymptotic behaviors of support vector machines with Gaussian kernel, Neural computation, 15 (2003) 1667-1689.

[65] H. Fazeli, R. Soleimani, M.-A. Ahmadi, R. Badrnezhad, A.H. Mohammadi, Experimental study and modeling of ultrafiltration of refinery effluents using a hybrid intelligent approach, Energy & Fuels, 27 (2013) 3523-3537.

[66] M.A. Ahmadi, M. Ebadi, P.S. Marghmaleki, M.M. Fouladi, Evolving predictive model to determine condensate-to-gas ratio in retrograded condensate gas reservoirs, Fuel, 124 (2014) 241-257.

[67] M.A. Ahmadi, M. Ebadi, Evolving smart approach for determination dew point pressure through condensate gas reservoirs, Fuel, 117 (2014) 1074-1084.

[68] M.A. Ahmadi, M. Ebadi, S.M. Hosseini, Prediction breakthrough time of water coning in the fractured reservoirs by implementing low parameter support vector machine approach, Fuel, 117 (2014) 579-589.

[69] P.J. Rousseeuw, A.M. Leroy, Robust regression and outlier detection, John wiley & sons, 2005.

[70] P. Gramatica, Principles of QSAR models validation: internal and external, Molecular Informatics, 26 (2007) 694-701.

[71] C.R. Goodall, 13 Computation using the QR decomposition, Handbook of statistics, 9 (1993) 467-508.

Chapter Six: Developing a Robust Proxy Model of CO$_2$ Injection

Abstract

The CO$_2$ based enhanced oil recovery methods (EORs) in the petroleum industry are considered as one of the efficient technologies for further production where the natural driving forces become weak. To determine which EOR method is more appropriate for the understudied reservoir, there is a need to develop a reliable and fast tool to predict the performance of the EOR methods due to assumptions and central processing unit (CPU) time of reservoir simulation. We develop a promising approach for predicting the ultimate oil recovery factor of the miscible CO$_2$ injection process. To attain this goal, the least square support vector machine (LSSVM) was used to build the proxy model. The Box-Behnken design as a branch of response surface method is employed to design simulation runs for miscible CO$_2$ injection processes, and the leverage method is applied to validate the proxy model in terms of statistical perspective. An artificial heterogeneous reservoir is used to perform compositional reservoir simulations. Five operational parameters of the miscible CO$_2$ injection process are considered, including bottom-hole flowing pressure (BHP) of injection well (psi), CO$_2$ injection rate (MMSCF/D), injected CO$_2$ concentration (mole fraction), bottom-hole flowing pressure (BHP) of production well (psi), and oil production rate (STB/D). The developed proxy model can be employed to forecast the ultimate oil recovery factor of the miscible CO$_2$ injection operations at the different rock, fluids, and process conditions. The proposed method appears to be an efficient simulation strategy that offers guidelines and screening criteria for the application of miscible CO$_2$ injection.

6.1. Introduction

Nowadays, the main source of energy is fossil fuels which are deposited in the oil and gas reservoirs. Most of the oil reservoirs are approaching the end of their primary production lives. However, around 70% of the original oil in place (OOIP) remain in the geological formation after primary production stage. To produce the remaining oil from the depleted reservoirs, enhanced oil recovery (EOR) techniques should be implemented to produce more oil from reservoirs [1-5].

To dynamically evaluate the performance of any EOR scenario (e.g. water flooding, CO_2 injection, chemical flooding, etc.) and to understand the contributions of oil production mechanisms (e.g. interfacial tension (IFT) reduction, oil swelling, oil viscosity reduction, etc.) to fluids displacement, the reservoir simulation studies should be conducted [5-13]. One of the promising EOR methods is gas injection where the injection fluid is a gas, such as N_2, CO_2, associated gas, flue gas, and air. Among the gas injection methods, CO_2 injection is not only an efficient EOR method, but it also provides a solution for reducing emissions of greenhouse gases by injecting CO_2 in depleted oil reservoirs and aquifers [10, 14-15].

Various parameters are contributing to the oil production and oil sweep efficiency during CO_2 injection [14,16-17]. There is no robust, fast, and easy-to-use method to determine the performance of miscible CO_2 injection into a given oil reservoir. In addition, it is challenging to categorize/screen the candidate reservoirs for miscible CO_2 injection.

Several scholars made attempts to introduce dimensionless numbers to consider different oil production mechanisms. For instance, Wood et al. [18] proposed some dimensionless numbers such as the dip angle group, effective aspect ratio, buoyancy number, and CO_2-oil mobility ratio to select appropriate candidates for CO_2 injection.

161

They neglected the impact of reservoir heterogeneity in their research work, while the performance of CO_2 injection (both miscible immiscible) is considerably affected by reservoir heterogeneity. Hence, developing a straightforward and robust strategy such as a proxy model for predicting and evaluating the performance of the miscible CO_2 injection is of great interest to the petroleum industry.

Helaleh and Alizadeh [19] developed a proxy model for predicting the performance of miscible surfactant- CO_2 flooding. Their proposed model was built on hybridization of ant colony and support vector regression (SVR) method. They concluded that the SVR model is able to forecast the performance of surfactant- CO_2 flooding with a high degree of reliability and precision.

Jaber et al. [20] proposed a proxy model to determine the performance of the CO_2-WAG (water alternative gas) injection for a heterogeneous clastic reservoir. They employed a Box-Behnken design method to build their proxy model. They considered four parameters (e.g., controllable variables) including the ratio of CO_2 slug size to water slug size, CO_2 slug size, bottom hole pressure, and cyclic length. According to their results, their developed model can be used at different levels of operational parameters to reasonably estimate the incremental oil recovery over the miscible CO_2-WAG flooding processes.

The main objective of this research work is to avoid performing reservoir simulation runs which are costly and time-consuming by introducing a simpler and valid approach. This paper is planned to develop a promising proxy model for prediction of the ultimate oil recovery achievable through miscible CO_2 injection. To design reservoir simulations versus the operational parameters, the response surface method (RSM) was employed. Least square support vector machine (LSSVM) as a subset of connectionist models was

used to develop the proxy model for obtaining the target function. To statistically evaluate the applicability of the proxy model, the leverage method was implemented.

6.2. Methodology

6.2.1. Characterization of the Reservoir Model

A synthetic oil reservoir [4] has been used to simulate the miscible CO_2 injection process; for this goal, GEM package (as compositional reservoir simulator engine) of the computer modeling group (CMG) reservoir simulator 2016.1$^{©}$ was used. The reservoir properties including initial oil saturation, porosity, permeability, and pressure are depicted in Figure 6-1. The initial oil saturation distribution of the reservoir is shown in Figure6-1(a). Figures 6-1(b) and 6-1(c) illustrate the distribution of porosity and permeability of the reservoir. Permeability is assumed to be similar in x, y and z directions (isotropic system). Figure 6-1(d) shows the reservoir pressure variation versus depth and reservoir layers. Grid depth ranges from 6072.83 to 6258.87 ft. and the reference pressure is considered to be 3932.3 psi at a depth of 6165 ft. The water-oil-contact (WOC) is set at 6200.87 ft. Initially, the reservoir is above the bubble point since initial gas saturation in the reservoir is zero. An infinite acting bottom aquifer supports the reservoir [5]. This aquifer has a thickness of 60 ft., the porosity of 0.25, the permeability of 1.65 mD and radius of 518.22 ft. Two wells are drilled for the production and injection. Both wells start operation from Jan 1st, 1901. Our control parameters in simulating miscible CO_2 injection are bottom-hole flowing pressure (BHP) of the injection well (psi), CO_2 injection rate (MMSCF/D), injected CO_2 concentration (mole fraction), bottom-hole flowing pressure (BHP) of the production well (psi), and the oil production rate (STB/D). The oil reservoir under CO_2 injection has been simulated for 35 years (1901-1935).

(a)

(b)

(c)

164
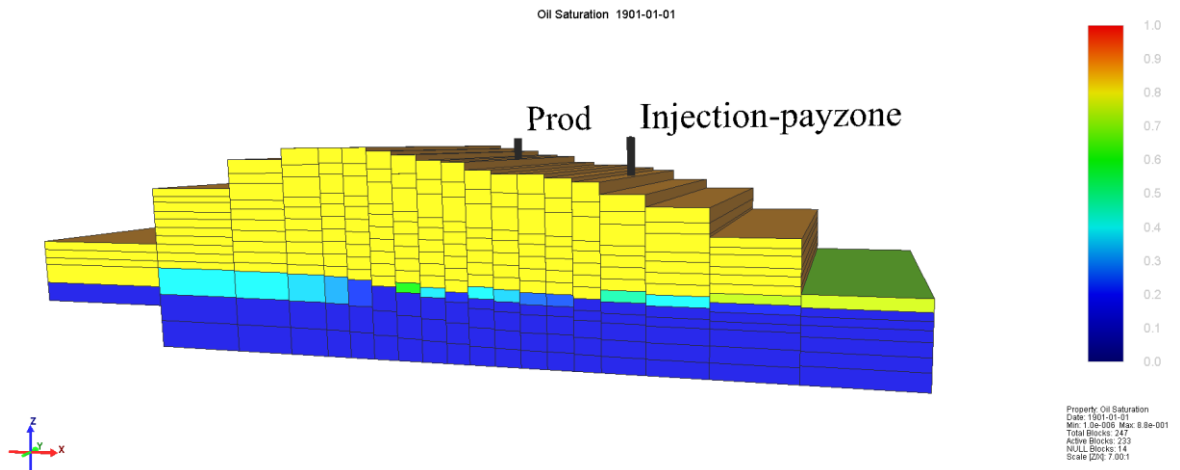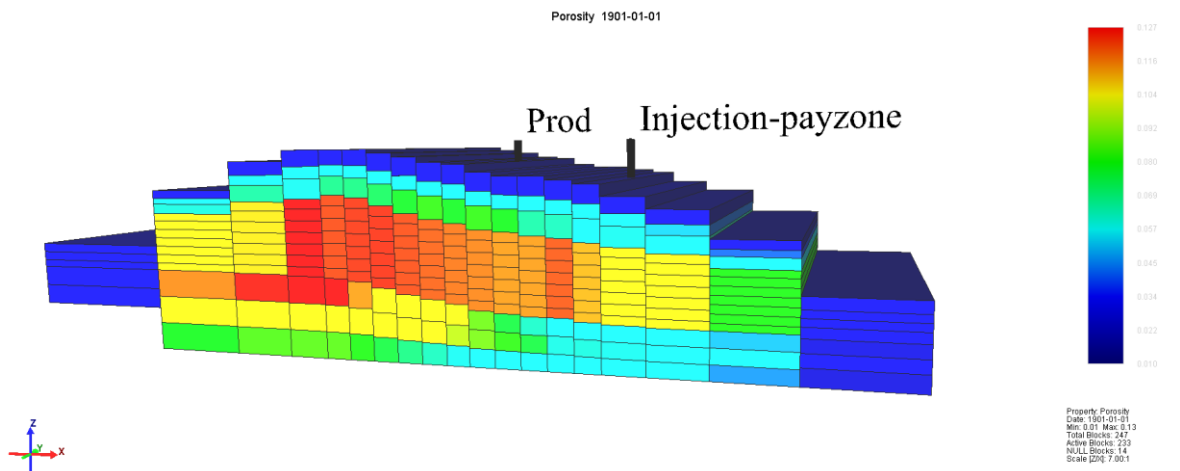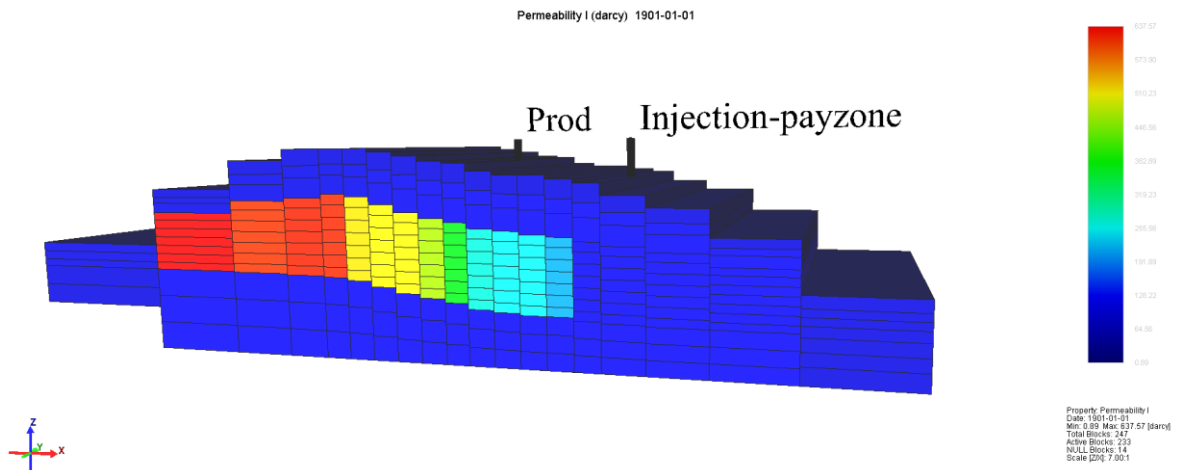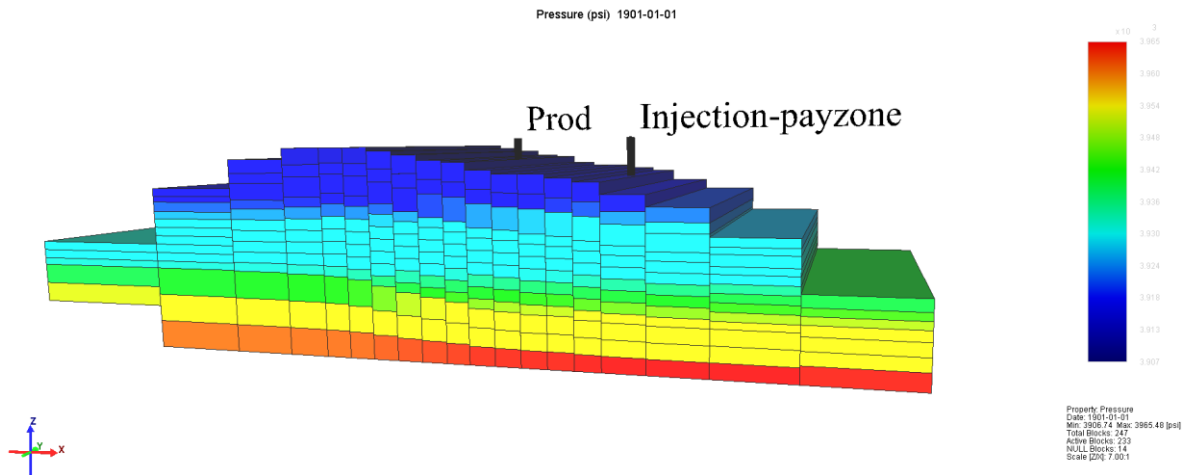
(d)

Figure 6-1: 3D view of distribution for the a) oil saturation b) porosity c) permeability d) reservoir pressure for the synthetic reservoir used in this study

6.2.2. Least Square Support Vector Machine (LSSVM)

The least square SVM theorem was proposed and developed by Suykens and Vandewalle (1999), based on the idea that the data samples S={(x$_1$,y$_1$),…,(x$_n$,y$_n$)} with a nonlinear trend can be formulated as in equation (1). In equation (1), *w* stands for the weight factor, φ denotes the nonlinear function which correlates the input space to a high-dimension characterization area and conducts linear regression, b represents the bias term [21-25]. Following expression was implemented as a cost function of the LSSVM in calculation steps [26-34].

$$y = w^T . \varphi(x) + b \quad with \quad w \in \mathbb{R}^n, \quad b \in \mathbb{R}, \quad \varphi(\cdot) \in \mathbb{R}^n \to \mathbb{R}^{n_h}, \quad n_h \to \infty \quad (6\text{-}1)$$

Which is constrained as [30-38]:

$$y_k = w^T \varphi(x_k) + b + e_k \quad k=1, 2,…, N \quad\quad (6\text{-}2)$$

For the function estimation, the structural risk minimization (SRM) is suggested; the optimization objective function is shown with J below in which γ is the regularization constant, and e_k is the regression error [26-35].

$$J(w, e) = \frac{1}{2} w^T w + \frac{1}{2} \gamma \sum_{k=1}^{N} e_k^2 \qquad (6\text{-}3)$$

To obtain w and e, the Lagrange multiplier optimum programming approach is performed to solve Eq. (6-3); the employed approach considers impartial and restriction parameters simultaneously. The mentioned Lagrange function L is formulated as the following equation [26-38]:

$$L(w,b,e,\alpha)=J(w,e)\text{-}\sum_{k=1}^{m} \alpha_i \{w^T \emptyset(x_k) + b + e_k - Y_k\} \qquad (6\text{-}4)$$

Through above equation, α_i denotes the Lagrange multipliers that may be either positive or negative as the LSSVM has equality restrictions. Using Karush Kuhn–Tucher's (KKT) conditions, for optimum solution in Eq. (6-4) [30-38].

$$\begin{cases} \partial_\omega L = w - \sum_{i=1}^{n} \alpha_i \varphi(x_i) = 0 \\ \partial_b L = \sum_{i=1}^{n} \alpha_i = 0 \\ \partial_{e_i} L = C e_i - \alpha_i = 0 \\ \partial_{\alpha_i} L = (w^T \emptyset(x_k) + b + e_k - y_k = 0 \end{cases} \qquad (6\text{-}5)$$

The linear set of equations can be demonstrated as [30-38]:

$$\begin{bmatrix} 0 & -1^T \\ 1 & \Omega + \frac{1}{\gamma} I_N \end{bmatrix} \begin{bmatrix} b \\ \alpha \end{bmatrix} = \begin{bmatrix} 0 \\ y \end{bmatrix} \qquad (6\text{-}6)$$

where, $y = (y_1, ..., y_n)^T$, $I_n = (1, ..., 1)^T$, $\alpha = (\alpha_1; ...; \alpha_n)^T$ and $\Omega_{il} = \varphi(x_i)^T \varphi(x_l)$ for $i, l = 1, ..., n$. Using Mercer's theorem, the resulting LSSVM model for function approximation is [30-38]:

$$f(x) = \sum_{k=1}^{N} \alpha_k K(x, x_k) + b \qquad (6\text{-}7)$$

where α and b are [30-38]:

$$b = \frac{1_n^T (\Omega + \frac{1}{\gamma} I_n)^{-1} y}{1_n^T (\Omega + \frac{1}{\gamma} I_n)^{-1} 1_n} \qquad (6\text{-}8)$$

$$\alpha = \left(\Omega + \frac{1}{\gamma} I_n \right)^{-1} (y - 1_n b) \qquad (6\text{-}9)$$

Eq. (6-10) uses nonlinear regression with Kernel function K [30-38]:

$$f(x) = \sum_{k=1}^{N} \alpha_k K(x, x_k) + b \qquad (6\text{-}10)$$

while $K(x,x_k)$ is Kernel function relating to the transfer functions (to feature space) $\Phi(x)$ and $\Phi(x_i)$ as below [30-38]:

$$K(x, x_k) = \Phi(x)^T \Phi(x_k)$$

(6-11)

We use radial basis function (RBF) Kernel [30-34]:

$$K(x, x_k) = \exp(-\|x_k - x\|^2 / \sigma^2)$$

(6-12)

where σ^2 is the variance of the distribution and it is the only parameter to be tuned by GA. To obtain optimal parameter of LSSVM, we use mean square error (MSE) as the objective function to be minimized [25, 38]:

$$MSE = \frac{\sum_{i=1}^{n}(RF_{est i} - RF_{exp \cdot i})^2}{ns}$$

(6-13)

where, RF represents the recovery factor, subscripts *est.* and *exp.* represents the predicted and actual recovery factor, respectively, and *ns* stands for the number of data from the initially assigned population.

6.2.3. Genetic Algorithm (GA)

Genetic Algorithm (GA) as one of the best optimization methods which is attributed to its unique features which are searching quickly and optimizing efficiently; the two essential characteristics which have been derived from the principle of "survival of the fittest" element of natural evolution with the genetic propagation of properties. In more details, GA operates through clarifying a variety of zones in the target area determined by experts and defining simultaneously and randomly a large number of possible paths [25, 28]. The GA has this capability of being replaced with classic optimization techniques thanks to its origination which is based on the idea of Darwinian natural selection and genetics in biological systems. Based on the supporting concept of 'survival of the fittest', the GA could converge towards the best point in the prepared

space soon after a series of repetitive calculations. Foundations of this searching process are based on technical operations such as artificial mutation, crossover, and selection [25, 28,31,38]. To run the above algorithm, it is preliminarily required to prepare an initial population containing a particular number of so-called individuals which are representing the possible paths toward the ideal goal. The next step which is supposed to be taken is turning each chromosome, already introduced under the title of an individual, into an encoded string. After that, each string must show its suitability with nature of the problem through becoming introduced into the fitness function. Subsequently, the output of fitness function related to each chromosome is taken as a criterion to make a decision if the related string can provide a satisfying performance. After removing some the weakest individuals which is determined by the designer, it is the turn to operate crossover and mutation rates to produce new individuals with higher performance. Then, implementation of the crossover operation on the couple of chosen strings (chromosomes) to recombine them has to be followed. It has been suggested by the previous studies that the best performance of the GA becomes possible when the crossover point of any two chromosomes is randomly set. The process is followed by switching some randomly selected position to 1 if they are 0, and vice versa. The last described step is named mutation which is run to prevent the procedure to trap in any local maxima. The final step is defining as returning the generated off-springs into the first step during the next population to be evaluated again [25, 28,31,38]. Figure 6-2 depicts the schematic of the hyper-parameters optimization using genetic algorithm
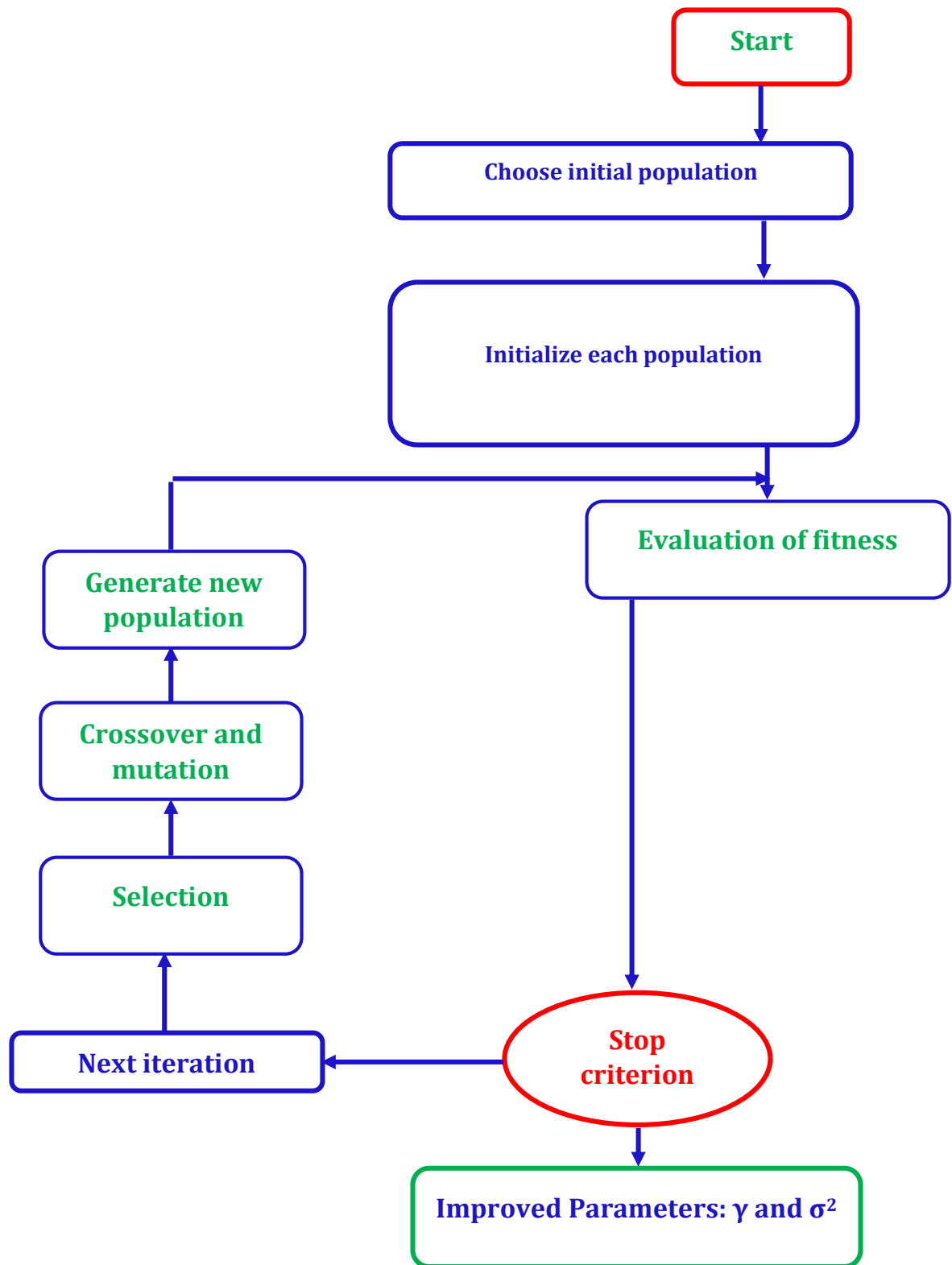
Figure 6-2: Schematic of the hyper-parameters optimization using genetic algorithm

6.3. Proxy Model Development

Proxy methods are popular techniques for CPU-time reduction in population-based optimizers, in which the cost function (CF) is replaced by a function, called proxy [39], and the proxy is employed to assess all or some of the individuals in the optimization process. A proxy is trained by a set of samples taken from the original fitness function landscape. Usually, a large number of training data is needed to build an accurate proxy model that gives an acceptable approximation of the global optimum point of the CF [40-44]. Although imperfect proxy models might not have the capabilities to approximate the global optimum, they can provide an overview of the entire fitness function landscape and a good estimation of sampled regions. Based on this fact, a new-generation of proxy models is proposed in which the CF is carried out in conjunction with the proxy for the fitness evaluation of the individuals. This method is effectively implemented in different disciplines [40,44-45]. Several techniques were proposed to enhance proxy-modeling, by applying different sampling strategies and various types of proxy [44-46]. For instance, Silva et al. [47], Cullick et al. [39] and Sampaio et al. [48] employed an artificial neural network, as the proxy model, and gained acceptable outcomes. In this study, LSSVM method as a promising connectionist approach has been used to develop a new generation of the proxy model. Figure 6-3 illustrates the schematic of the proxy model development strategy. As noted previously, our control variables for simulating CO_2 injection into the reservoir are BHP of the injection well (psi), CO_2 injection rate (MMSCF/D), injected CO_2 concentration (mole fraction), BHP of production well (psi), and oil production rate (STB/D). So, it is required to define an acceptable and reasonable range for the parameters above. Table 6-1 reports the Ranges of the proxy model input parameters. There are various methods for designing the simulation runs such as 2-level full factorial, 2-level partial factorial, and response

surface methodology (RSM). RSM includes two main categories Box–Behnken design (BBD) and central composite design (CCD). In this paper, Box–Behnken method has been employed to design our CO_2 injection scenarios. Table 6-2 reports the different scenarios designed for CO_2 injection using Box–Behnken method along with their proxy roles. As shown in Table 6-2, to build the proxy model, 37 simulation runs have used, and for validating the proposed proxy model, 9 simulation runs have employed.

Table 6-1: Ranges of the proxy model input parameters

Parameter	Unit	Min	Max
CO_2 Injection Rate	MMSCF/D	1000000	10000000
Maximum Bottom-hole pressure of Injection well	psi	1500	7500
Minimum Bottom-hole pressure of Production well	Psi	200	2000
Oil Production Rate	STB/D	1000	10000
CO_2 concentration	Mole fraction	0.8	1
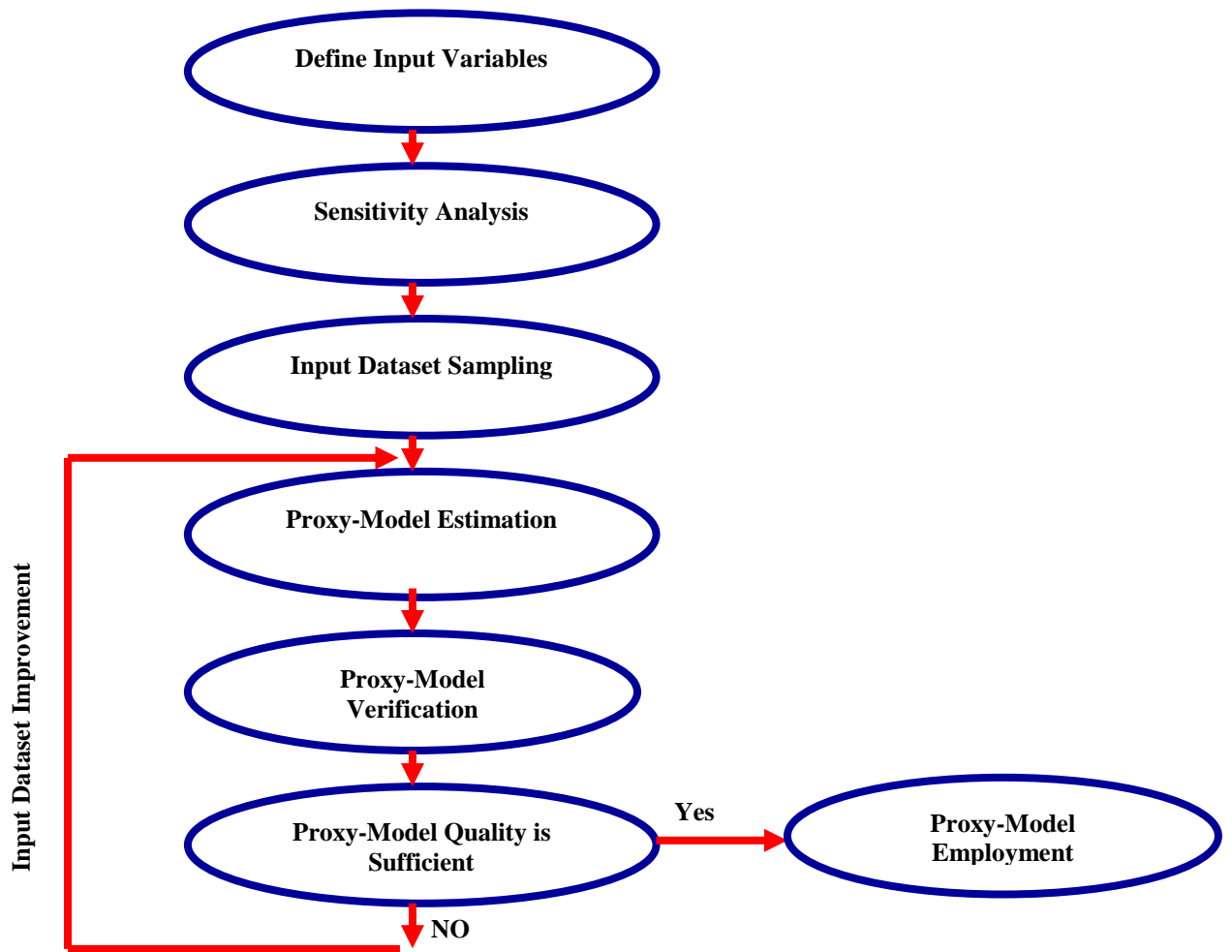
Figure 6-3: Schematic of the proxy model development strategy

Table 6-2: Box–Behnken designs for CO_2 injection

ID	Proxy Role	Maximum Injector BHP (psi)	CO_2 Mole Fraction	CO_2 Injection Rate (MMSCF/D)	Minimum Producer BHP (psi)	Oil Production Rate (STB/D)	RF (%OOIP)
1	Training	3900	0.895	3700000	1640	7300	41.787663
2	Training	5700	0.88	2800000	740	6400	55.878799
3	Training	2100	0.97	7300000	2000	2800	40.404835
4	Training	1500	1	1000000	1820	7300	38.104408
5	Training	5700	0.925	7300000	1640	8200	43.034195
6	Training	2700	0.925	3700000	920	1000	53.062904
7	Training	7500	0.91	1900000	920	6400	54.576023
8	Training	2700	1	3700000	740	1900	55.891567
9	Training	7500	0.85	8200000	1100	2800	47.592541
10	Training	5100	0.97	5500000	1820	4600	42.57518
11	Training	3900	0.85	1000000	1820	3700	40.414654

12	Training	5100	0.955	9100000	1280	8200	45.362228
13	Training	1500	0.85	9100000	1100	6400	47.569981
14	Training	6300	0.88	6400000	1460	5500	43.288555
15	Training	5700	0.925	9100000	1460	1000	43.350037
16	Training	4500	0.985	10000000	200	7300	61.073956
17	Training	2100	0.865	4600000	560	8200	63.530128
18	Training	6900	0.91	1000000	740	10000	53.268475
19	Training	5100	0.91	7300000	2000	3700	42.159241
20	Training	3900	0.88	10000000	1100	9100	47.142193
21	Training	6900	0.985	8200000	2000	4600	43.338001
22	Training	2700	0.895	2800000	1460	1900	42.260117
23	Training	3300	0.94	6400000	1280	10000	45.047085
24	Training	1500	0.895	10000000	560	5500	59.897743
25	Training	2100	1	1900000	920	9100	50.524914
26	Training	1500	0.94	6400000	1820	3700	38.096645
27	Training	2700	0.91	3700000	1100	7300	47.234138
28	Training	3300	0.91	6400000	740	3700	56.332222
29	Training	3900	0.88	8200000	380	10000	60.53804
30	Training	6900	0.955	7300000	920	7300	52.912228
31	Training	5100	0.925	9100000	1280	2800	45.21104
32	Training	6900	0.85	4600000	560	9100	64.277306
33	Training	6300	0.895	5500000	1820	5500	42.303593
34	Training	3900	0.865	7300000	560	6400	63.738056
35	Training	2100	0.88	3700000	1100	3700	47.920063
36	Training	3900	0.925	6400000	1100	3700	46.46006
37	Training	3300	1	2800000	560	7300	60.874733
38	Verification	6300	0.925	7300000	560	8200	65.921333
39	Verification	3300	0.85	4600000	920	5500	53.176949
40	Verification	2100	0.97	9100000	1280	5500	46.097
41	Verification	6300	1	4600000	1640	5500	42.837906
42	Verification	3300	0.88	3700000	740	9100	60.084507
43	Verification	3678.7058	0.98058705	3944118.5	503.8387	7745.4823	63.805046
44	Verification	6241.9439	0.91739496	2720340	1950.3223	9582.3154	41.126812
45	Verification	4902.9465	0.97855853	6192838.4	1617.1389	7192.1755	42.910915
46	Verification	5408.7404	0.89545431	6916595.7	943.61662	2932.1513	51.572277

6.4. Results and Discussion

6.4.1. Proxy Model

Figure 6-4 depicts the recovery factor determined by CMG software for miscible CO_2 injection versus the corresponding BHP of the injection well. As depicted in Figure 6-4, recovery factor significantly changes from near 66% as a maximum recovery factor

173

to 38% as a minimum recovery factor. Figure 6-4 shows that recovery factor highly changes with the flowing bottom-hole pressure of injection well; however, there is no linear relation between recovery factor and flowing bottom-hole pressure of injection well.
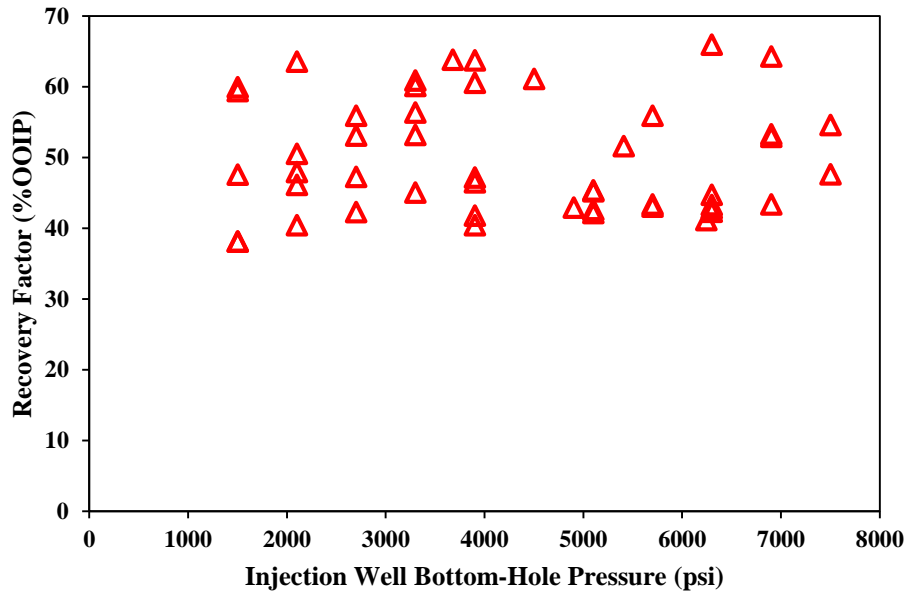
Figure 6-4: Recovery factor of miscible CO_2 injection versus the corresponding BHP of injection well

Figure 6-5 illustrates the recovery factor determined by CMG software for miscible CO_2 injection versus the corresponding BHP of the production well. As shown in Figure 6-5, recovery factor considerably decreases from near 65% in case of BHP = 500 psi to near 45% when BHP is equal to 2000 psi. Figure 6-5 reveals that recovery factor extremely depends on the flowing bottom-hole pressure of production well.
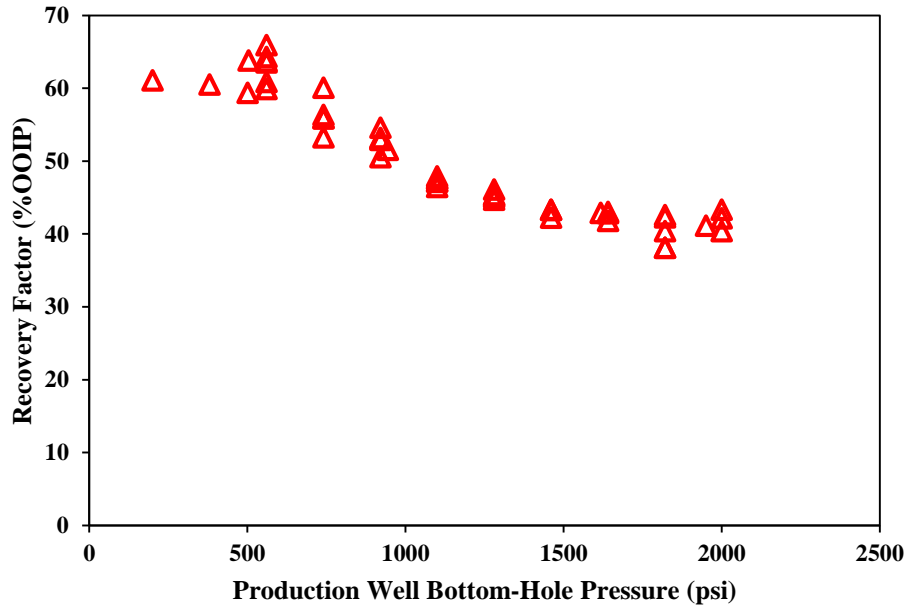
Figure 6-5: Recovery factor of miscible CO_2 injection versus the corresponding BHP of production well

Figure 6-6 demonstrates the simulation results that have done using CMG software for miscible CO_2 injection versus the corresponding oil production rate. As illustrated in Figure 6-6, there is no recognizable relation between recovery factor and the related oil production rate. This is primarily because different parameters contributed in oil. For example, when oil production rate is equal to 10000 STB/D (standard barrel per day), the ultimate recovery factor might be near 42% or 62%. It means that for developing a proxy model to predict ultimate oil recovery factor of miscible CO_2 injection linear regression methods do not work properly.

175
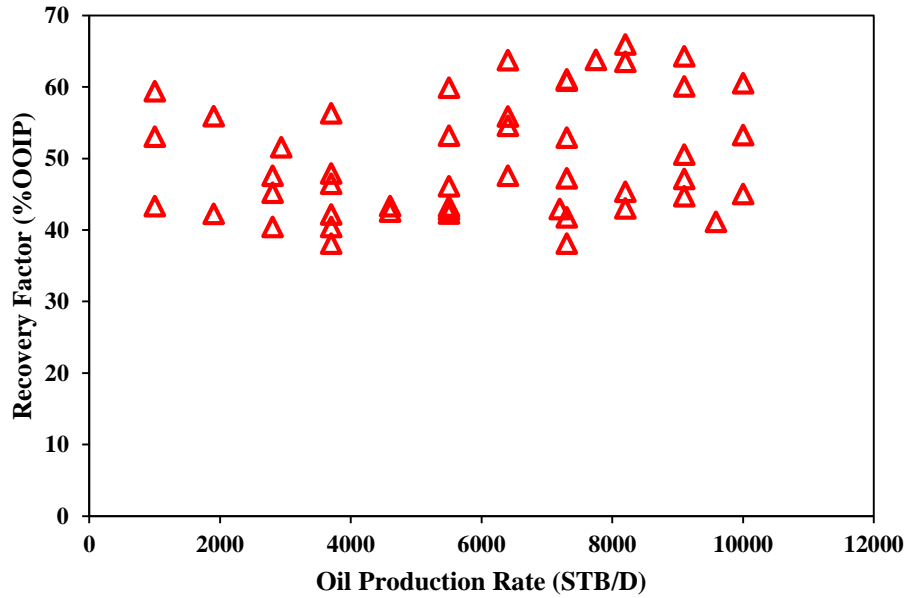
Figure 6-6: Recovery factor of miscible CO_2 injection versus the corresponding oil production rate

Figure 6-7 shows the variation of the ultimate oil recovery factor of miscible CO_2 injection versus the related CO_2 injection rate. As depicted in Figure 6-7, the ultimate oil recovery factor varies with changing in CO_2 injection rate; however, there is no doubt the ultimate oil recovery factor does not change linearly with CO_2 injection rate.
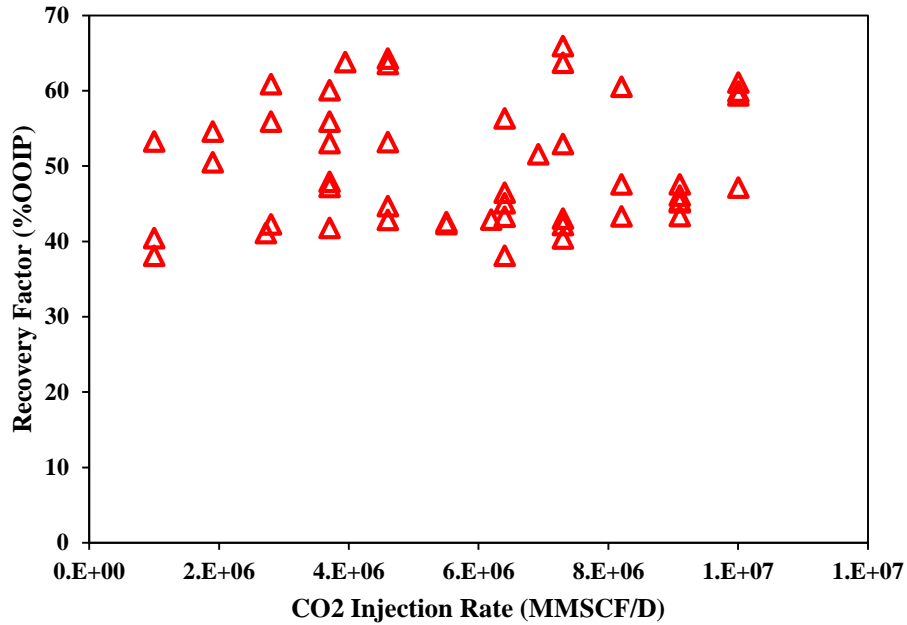
Figure 6-7: Recovery factor of miscible CO_2 injection versus the corresponding CO_2 injection rate

The values of the global optimum for hyper-parameters of the proxy model including σ^2 and γ were determined for predicting recovery factor (RF) of miscible CO_2 injection as 1.687654 and 27.578421, correspondingly.

Figure 6-8 depicts the scatter plot of the outputs of the proxy model versus the corresponding recovery factor gained from CMG software. As shown in Figure 6-8 (a), the recovery factor predicted by the proposed proxy model versus the simulation results of CMG software falls into the straight line very close to Y=X line. One of the statistical index for evaluating the performance of the proposed proxy model in this study is correlation coefficient of the regression plot. As illustrated in this figure, the best fitted straight line has high correlation coefficient which is equal to 0.9816. It means that the proxy model trained adequately for predicting the ultimate oil recovery of the miscible CO_2 injection process. Figure 6-8 (b) illustrates the regression plot between the simulation results and the predicted ones by the developed proxy model. As clear be

seen from this figure, ultimate recovery factors calculated by the proxy model are much closer to ones using CMG simulator. Figure 6-8 (c) demonstrates the scatter plot of the estimated recovery factor using proxy model and commercial simulator for whole data samples. The high correlation coefficient of the linear best fit line reveals the promising effectiveness of the developed proxy model.

(a)

y = 0.9301x + 2.7581
R² = 0.9934

◆ Testing Data   ——— Best Fit Testing Data : R² = 0.9934

(b)

y = 0.9592x + 1.9446
R² = 0.9816

○ Data   ——— Best Fit Overal Data : R² = 0.9816
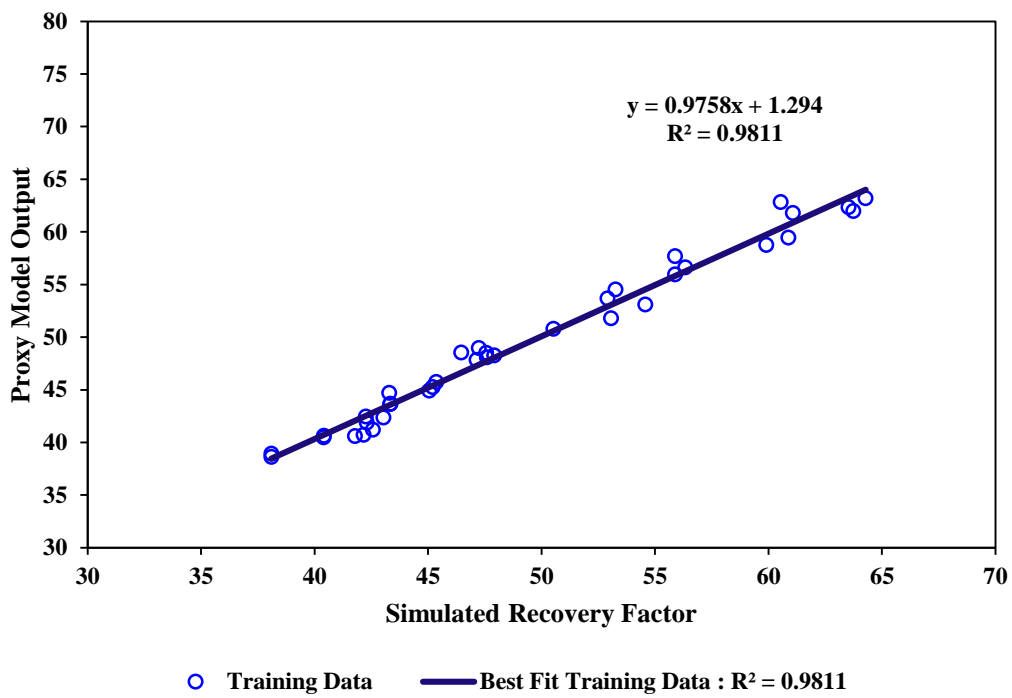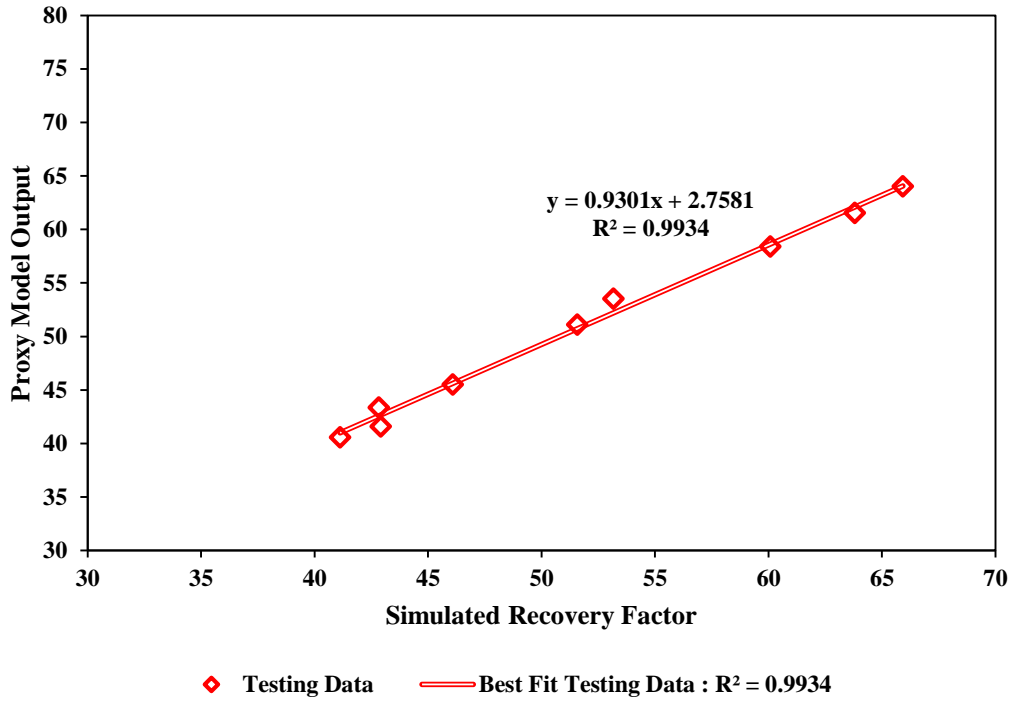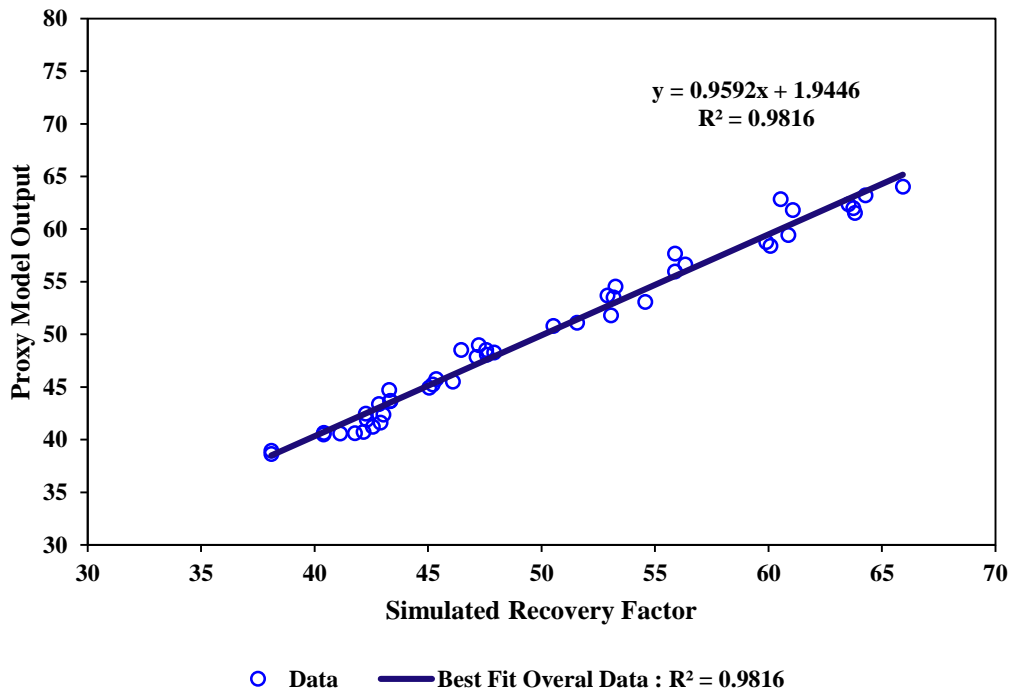
(c)

Figure 6-8: Scatter plot of the outputs of the proxy model versus the corresponding recovery factor gained from CMG software for a) training data points b) testing data points c) overall data points

Figure 6-9 shows the relative deviation of the outputs of the proxy model from recovery factor of miscible CO_2 injection gained from CMG software versus corresponding values of the CO_2 injection rate for both testing and training data samples. As depicted in Figure 6-9, the maximum relative error for training data samples belongs to the medium CO_2 injection rate from 4×10^6 to 6×10^6 MMSCF/D (million standard cubic feet per day). And the maximum relative error for testing data points is +3.54% which occurred at an injection rate of 4×10^6 MMSCF/D. As shown in Figure 6-9, the relative error for both training and testing data samples falls between ±5% lines.

Figure 6-9: Relative deviation of the outputs of the proxy model from recovery factor of miscible CO_2 injection gained from CMG software versus corresponding values of the CO_2 injection rate

Figure 6-10 shows the relative deviation of the outputs of the proxy model from recovery factor of miscible CO_2 injection gained from CMG software versus corresponding values of the oil production rate. As depicted in Figure 6-10, the maximum relative error for testing phase belongs to oil production rate of 7745 STB/D

(standard barrel per day), and the maximum relative error for training phase occurred when oil production rate is 9100 STB/D.

Figure 6-10: Relative deviation of the outputs of the proxy model from recovery factor of miscible CO_2 injection gained from CMG software versus corresponding values of the oil production rate

Figure 6-11 depicts the relative deviation of the outputs of the proxy model from recovery factor of miscible CO_2 injection gained from CMG software versus corresponding values of the BHP of the injection well. As shown in Figure 6-11, the maximum relative deviation for testing data points occurred when BHP of the injection well is near 3700 psi. Also, the maximum relative error for training data samples happened when BHP of the injection well is equal to 3900 psi. Figure 6-12 demonstrates the relative deviation of the outputs of the proxy model from recovery factor of miscible CO_2 injection gained from CMG software versus corresponding values of the BHP of production well. As demonstrated in Figure 6-12, the maximum relative error for

training and testing stages occurred when the well-flowing pressure of the production well is equal to 1100 psi and 503 psi, respectively.

Figure 6-11: Relative deviation of the outputs of the proxy model from recovery factor of miscible CO_2 injection gained from CMG software versus corresponding values of the BHP of injection well
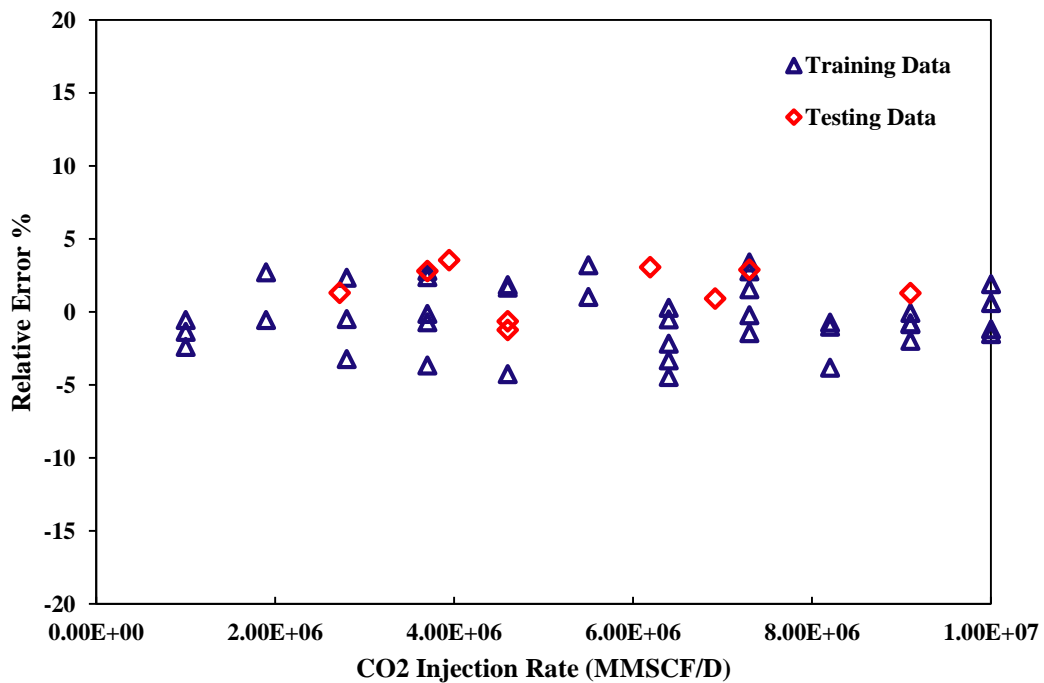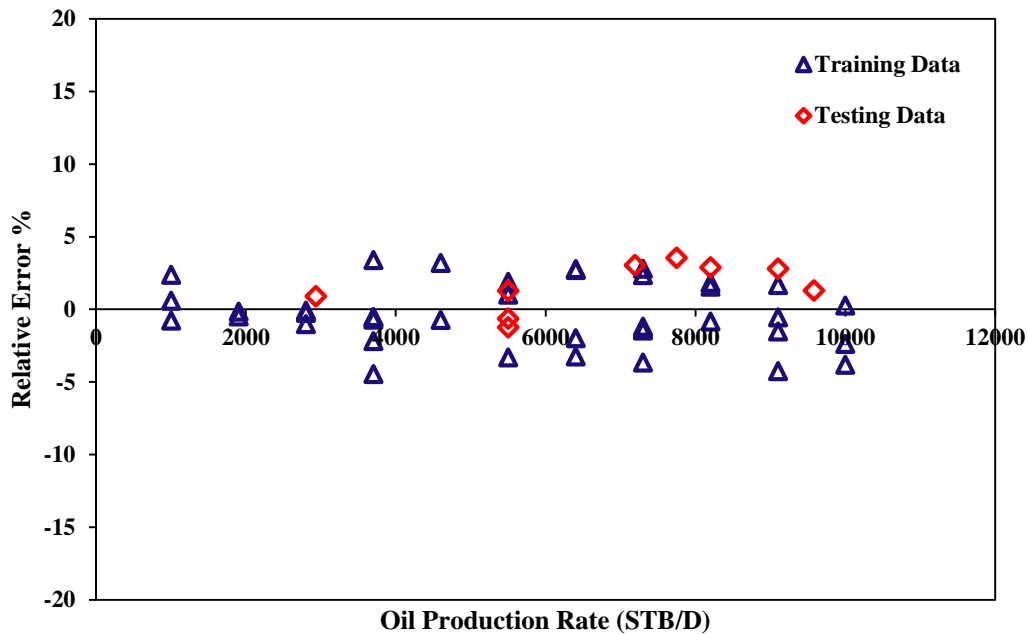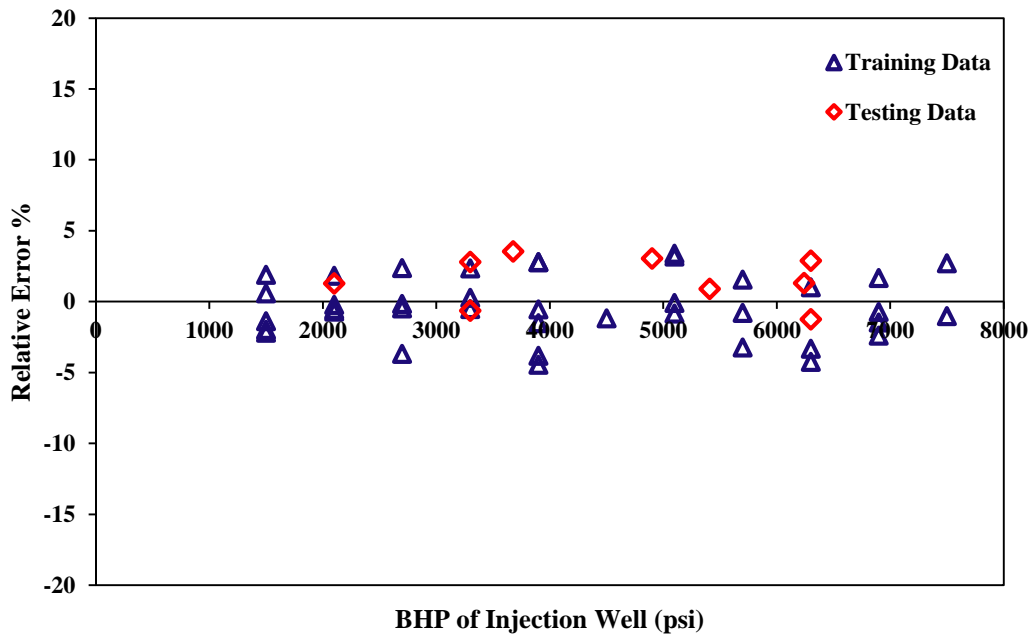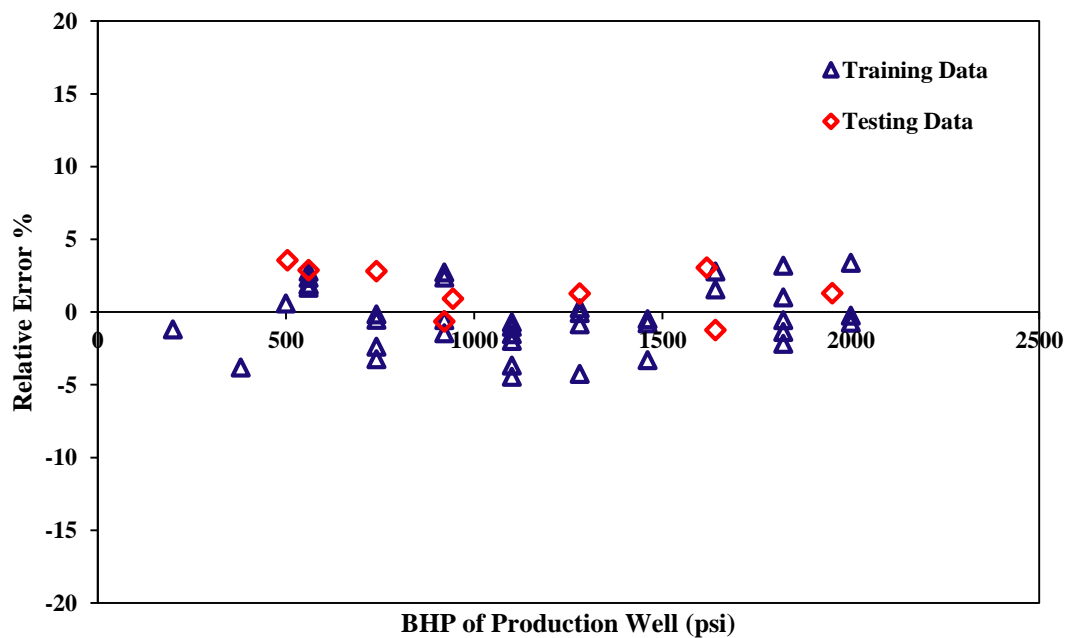

Figure 6-12: Relative deviation of the outputs of the proxy model from recovery factor of miscible CO_2 injection gained from CMG software versus corresponding values of the BHP of production well

182

Table 6-3 reports the simulation results gained from GEM package of CMG software and the ultimate recovery factor predicted by the developed proxy model along with residual, mean squared error (MSE), and average relative deviation (ARD). As reported in Table 6-3, the minimum residual value is -2.31396 and the maximum residual value is +2.2643. Also, the maximum MSE value is equal to 5.3544, and the minimum one is 0.001373. It means that the developed proxy model provides a promising approach for determining ultimate recovery factor of the miscible CO_2 injection process.

Table 6-4 reports the indexes for performance evaluation of the proxy model proposed in this study. These indexes are correlation coefficient (R^2), mean square error (MSE), and average absolute relative deviation (AARD). As reported in Table 6-4, the proxy model proposed in this paper provides promising results from a statistical viewpoint. High correlation coefficient value besides very low MSE and AARD values confirm the outstanding efficiency of the developed proxy model for the miscible CO_2 injection process.

Table 6-3: Simulation results, proxy model outputs, and errors of the predicted RF

ID	RF- CMG	RF-LSSVM	MSE	ARD	Residual
1	41.787663	40.6199	1.36367	2.794516	1.167763
2	55.878799	57.6858	3.265253	-3.23379	-1.807
3	40.404835	40.5007	0.00919	-0.23726	-0.09587
4	38.104408	38.6277	0.273835	-1.37331	-0.52329
5	43.034195	42.3646	0.448357	1.55596	0.669595
6	53.062904	51.804	1.584839	2.372475	1.258904
7	54.576023	53.0936	2.197578	2.716253	1.482423
8	55.891567	55.9757	0.007078	-0.15053	-0.08413
9	47.592541	48.0771	0.234797	-1.01814	-0.48456
10	42.57518	41.2198	1.837055	3.183498	1.35538
11	40.414654	40.6365	0.049216	-0.54892	-0.22185
12	45.362228	45.7412	0.14362	-0.83544	-0.37897
13	47.569981	48.5135	0.890228	-1.98343	-0.94352
14	43.288555	44.7213	2.052758	-3.30975	-1.43275
15	43.350037	43.6891	0.114964	-0.78215	-0.33906
16	61.073956	61.7984	0.524819	-1.18618	-0.72444
17	63.530128	62.3648	1.357989	1.834292	1.165328
18	53.268475	54.5412	1.619829	-2.38926	-1.27273
19	42.159241	40.7305	2.041301	3.388915	1.428741
20	47.142193	47.8575	0.511664	-1.51734	-0.71531

21	43.338001	43.6543	0.100045	-0.72984	-0.3163
22	42.260117	42.464	0.041568	-0.48245	-0.20388
23	45.047085	44.9271	0.014396	0.266355	0.119985
24	59.897743	58.7616	1.290821	1.896804	1.136143
25	50.524914	50.8064	0.079234	-0.55712	-0.28149
26	38.096645	38.9281	0.691317	-2.18249	-0.83145
27	47.234138	48.9685	3.008012	-3.67184	-1.73436
28	56.332222	56.6274	0.08713	-0.52399	-0.29518
29	60.53804	62.852	5.354411	-3.82232	-2.31396
30	52.912228	53.6868	0.599962	-1.46388	-0.77457
31	45.21104	45.2481	0.001373	-0.08197	-0.03706
32	64.277306	63.2059	1.147911	1.66685	1.071406
33	42.303593	41.876	0.182836	1.010772	0.427593
34	63.738056	61.9744	3.110482	2.767038	1.763656
35	47.920063	48.261	0.116238	-0.71147	-0.34094
36	46.46006	48.5317	4.291692	-4.45897	-2.07164
37	60.874733	59.4471	2.038136	2.345198	1.427633
38	65.921333	64.0203	3.613926	2.88379	1.901033
39	53.176949	53.5167	0.115431	-0.63891	-0.33975
40	46.097	45.5089	0.345862	1.275788	0.5881
41	42.837906	43.3724	0.285684	-1.24771	-0.53449
42	60.084507	58.4017	2.831839	2.800734	1.682807
43	63.805046	61.5407	5.127263	3.548851	2.264346
44	41.126812	40.5923	0.285703	1.299668	0.534512
45	42.910915	41.6025	1.71195	3.049143	1.308415
46	51.572277	51.1041	0.21919	0.907808	0.468177

Table 6-4: Statistical parameters of the outputs gained from the proxy model developed in this study for miscible CO_2 injection

	Training	Testing	Overall
Correlation Coefficient (R^2)	0.9811	0.9934	0.9811
Mean Square Error (MSE)	1.153	1.615	1.243
Average Absolute Relative Deviation (AARD)	1.758	1.9613	1.797

6.4.2. Validity of the Proxy Model

The Leverage method was employed to verify the applicability range of the proposed proxy model for miscible CO_2 injection process and to assess the quality of the simulation results for miscible CO_2 injection [49-51]. For this purpose, hat value and standardized residuals were determined for both data samples including training and testing. Figure 6-13 demonstrates William plot containing hat value and standardized residuals for the whole data samples. As graphically shown in Figure 6-13, all the data

samples fall in the range ±3 standardized residuals. The red horizontal lines indicate the doubtful index i.e. data points have greater standardized residual (SR) value than +3 or lower than -3 are doubtful. The blue vertical line represents the value of the warning Leverage for the data samples [49-51]. As depicted in Figure 6-13, all the outputs of the proposed proxy model are located within the limitations mentioned above. As a result, it can be concluded that the presented model based on the LSSVM method and Box–Behnken design (BBD) approach for estimation of the recovery factor of miscible CO_2 injection is statistically correct.
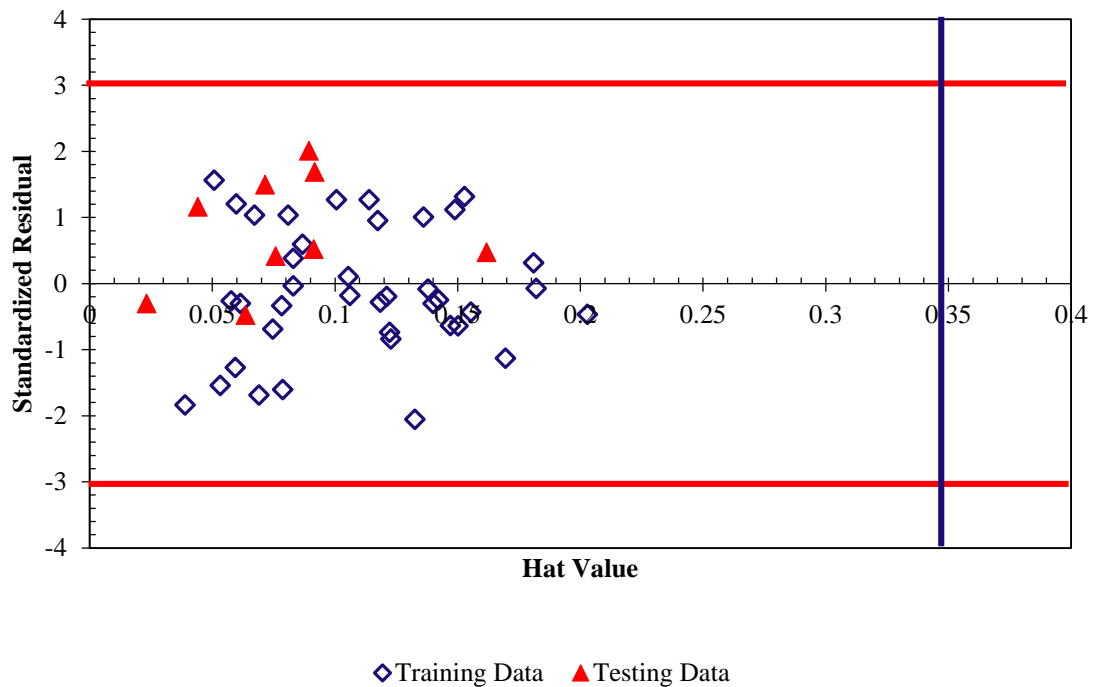

Figure 6-13: William plot for the results gained from the proposed proxy model for CO_2 miscible injection

6.4.3. Limitations of the Proxy Model

The proxy model developed in this study has the following conditions:

- The proxy model can be only applicable in the oil reservoir and geological circumstances similar to the synthetic model/system considered in this study.

185

- The model is valid within the ranges of the operating parameters mentioned in this study.

- It can be employed only to predict the performance of the CO_2 miscible injection operations.

References

[1].   Enick, R.M., Olsen, D., Ammer, J., Schuller, W., Mobility and conformance control for CO2 EOR via thickeners, foams, and gels e a literature review of 40 years of research and pilt tests. In: 18th SPE Improved Oil Recovery Symposium, April 14-18. 2012, SPE, Tulsa Oklahoma, USA.

[2].   Ding, M., Yuan, F., Wang, Y., Xia, X., Chen, W., Liu., D., Oil recovery from a CO2 injection in heterogeneous reservoirs: The influence of permeability heterogeneity, CO2-oil miscibility and injection pattern, Journal of Natural Gas Science and Engineering 2017, 44, 140-149

[3].   Ahmadi, M.A., Hasanvand, M.Z., Shokrollahzadeh Behbahani, S., Nourmohammad, A., Vahidi, A., Amiri, M., Ahmadi, G., Effect of operational parameters on the performance of carbonated water injection: Experimental and numerical modeling study, The Journal of Supercritical Fluids, 2016, 107, 542-548.

[4].   Ahmadi, M.A., Pouladi, B., Barghi, T., Numerical modeling of CO2 injection scenarios in petroleum reservoirs: Application to CO2 sequestration and EOR, Journal of Natural Gas Science and Engineering, 2016, 30, 38-49.

[5].   Zhang, R., Yin, X., Winterfeld, P.H., Wu, Y.-S., A fully coupled model of nonisothermal multiphase flow, geomechanics, and chemistry during CO_2 sequestration in brine aquifers. In: Proceedings of the TOUGH Symposium, 2012, pp. 838-848.

[6]. Zhang, R., Yin, X., Wu, Y.-S., Winterfeld, P.H., A Fully Coupled Model of Nonisothermal Multiphase Flow, Solute Transport and Reactive Chemistry in Porous Media, in SPE Annual Technical Conference and Exhibition. Texas, USA, San Antonio, 2012, pp. 8-10.

[7]. Wu, Y.-S., Chen, Z., Kazemi, H., Yin, X., Pruess, K., Oldenburg, C., Zhang, R., 2014. Simulation of Coupled Processes of Flow, Transport, and Storage of CO2 in Saline Aquifers. Trustees of the Colorado School of Mines.

[8]. Zhao, X., Rui, Z., Liao, X., Zhang, R., 2015a. The qualitative and quantitative fracture evaluation methodology in shale gas reservoir. Journal of Natural Gas Science and Engineering, 2015, 27, 486-495.

[9]. Zhao, X., Rui, Z., Liao, X., Zhang, R., 2015b. A simulation method for modified isochronal well testing to determine shale gas well productivity. Journal of Natural Gas Science and Engineering 2015, 27, 479-485.

[10]. Yao, Y., Wang, Z., Li, G., Wu, H., Wang, J., Potential of carbon dioxide miscible injections into the H-26 reservoir, Journal of Natural Gas Science and Engineering 34 (2016) 1085-1095

[11]. Zhang, R., Winterfeld, P.H., Yin, X., Xiong, Y., Wu, Y.-S., Sequentially coupled THMC model for CO2 geological sequestration into a 2D heterogeneous saline aquifer. Journal of Natural Gas Science and Engineering, 2015, 27, 579-615.

[12]. Wu, Y.-S., Fakcharoenphol, P., Zhang, R., et al., 2010. Non-darcy Displacement in Linear Composite and Radial Flow Porous Media, in SPE EUROPEC/EAGE Annual Conference and Exhibition. Society of Petroleum Engineers.

[13]. Xiong, Y., Fakcharoenphol, P., Winterfeld, P.H., Zhang, R., Wu, Y.-S., 2013. Coupled Geomechanical and Reactive Geochemical Model for Fluid and Heat Flow:

Application for Enhanced Geothermal Reservoir, in SPE Reservoir Characterization and Simulation Conference and Exhibition. SPE, Abu Dhabi, UAE, pp. 16-18.

[14].   Yao, Yuedong, Ji, Zemin, 2010. A quick evaluation model for CO2 flooding and sequestration. Petroleum Sci. 04, 515-523.

[15].   Zhang, R., Wu, Y.-S., Fakcharoenphol, P., 2014. Non-darcy displacement in linear composite and radial aquifer during CO2 sequestration, international journal of oil. Gas Coal Technol. 7 (3), 244-262.

[16].   Kovseek, A.R., Screening criteria for CO_2 storage in oil reservoir. Petroleum Science and Technology. 2003, 20 (7-8), 841-866

[17].   Mo, S., Akervoll I., Modeling long-term CO_2 storage in aquifer with a black-oil reservoir simulator. Paper SPE 93951 presented at SPE/ EPA/DOE Exploration and Production Environmental Conference held in Galveston, Texas, USA, 7- 9 March 2005

[18].   Wood, D.J., Lake, L.W., Johns, R.T., A screening model for CO2 flooding and storage in Gulf Coast reservoirs based on dimensionless groups. Paper SPE 100021 presented at SPE/DOE Symposium on Improved Oil Recovery held in Tulsa, Oklahoma, USA, 22-26 April 2006

[19].   Helaleh, A.H., Alizadeh, M., Performance prediction model of Miscible Surfactant-CO2 displacement in porous media using support vector machine regression with parameters selected by Ant colony optimization, Journal of Natural Gas Science and Engineering 30 (2016) 388-404

[20].   Jaber, A.K., Awang, M.B., Lenn, C.P., Box-Behnken design for assessment proxy model of miscible CO2-WAG in heterogeneous clastic reservoir, Journal of Natural Gas Science and Engineering 40 (2017) 236-248

[21].   Vapnik, V., Statistical learning theory, Wiley, New York, 1998.

[22]. Cortes, C., Vapnik, V., Support-Vector Networks, Machine Learning 20 (1995) 273–297.

[23]. Burges, C., A tutorial on support vector machines for pattern recognition, Data Min. Knowl. Disc. 2 (1998) 121–167.

[24]. Suykens, J., Gestel, T.V., Brabanter, J.D., Moor, B.D., Vandewalle, J., Least Squares Support Vector Machines, World Scientific Publishing Co. Pte. Ltd. K.U. Leuven, Belgium, 2002.

[25]. Ahmadi, M.A., Connectionist approach estimates gas–oil relative permeability in petroleum reservoirs: application to reservoir simulation, Fuel, 140C (2015), pp. 429–439.

[26]. Keerthi, S.S., Lin, C.J., Asymptotic behaviors of support vector machines with Gaussian kernel, Neural Comput. 15 (2003) 1667–1689.

[27]. Fazeli, H., Soleimani, R., Ahmadi, M.A., Badrnezhad, R., Mohammadi, A.H., Experimental Study and Modeling of Ultrafiltration of Refinery Effluents Using a Hybrid Intelligent Approach. Energy & Fuels 27 (6), 3523-3537

[28]. Ahmadi, M.A., Ebadi, M., Soleimani Marghmaleki, P., Mahboubi Fouladi, M., Evolving Predictive Model to Determine Condensate-to-Gas Ratio in Retrograded Condensate Gas Reservoirs, Journal of Fuel, 2014, 124, 241-245

[29]. Liu, H., Yao, X., Zhang, R., Liu, M., Hu, Z., Fan, B., Accurate Quantitative Structure−Property Relationship Model to Predict the Solubility of C60 in Various Solvents Based on a Novel Approach Using a Least-Squares Support Vector Machine, J. Phys. Chem. B 109 (2005) 20565–20571.

[30]. Liu, H.X., Yao, X.J., Zhang, R.S., Liu, M.C., Hu, Z.D., Fan, B.T., Prediction of the tissue/blood partition coefficients of organic compounds based on the molecular

structure using least-squares support vector machines, J. Comput.-Aided Mol. Des. 19 (2005) 499–508.

[31].   Ahmadi, M.A., Ebadi, M., Evolving Smart Approach for Determination Dew Point Pressure through Condensate Gas Reservoirs, Fuel (2014) 117 Part B, pp. 1074-1084

[32].   Baesens B., Viaene S., Van Gestel T., Suykens J.A.K., Dedene G., De Moor B., Vanthienen J., ``An Empirical assessment of Kernel Type Performance for Least Squares Support Vector Machine Classifiers'', in Proc. of the Fourth International Conference on Knowledge-Based Intelligent Engineering Systems and Allied Technologies (KES2000), Brighton, UK, Aug. 2000.

[33].   Suykens J.A.K., Vandewalle J., ``Training multilayer perceptron classifiers based on a modified support vector method'', IEEE Transactions on Neural Networks, vol. 10, no. 4, Jul. 1999, pp. 907-911.

[34].   Suykens, J., Gestel, T.V., Brabanter, J.D., Moor, B.D., Vandewalle, J., Least Squares Support Vector Machines, World Scientific Publishing Co. Singapour, 2002.

[35].   Suykens J.A.K., Vandewalle J., ``Recurrent least squares support vector machines'', IEEE Transactions on Circuits and Systems-I, vol. 47, no. 7, Jul. 2000, pp. 1109-1114.

[36].   Suykens J.A.K., De Brabanter J., Lukas L., Vandewalle J., ``Weighted least squares support vector machines : robustness and sparse approximation'', Neurocomputing, Special issue on fundamental and information processing aspects of neurocomputing, vol. 48, no. 1-4, Oct. 2002, pp. 85-105.

[37].   Suykens J.A.K., Vandewalle J., ``Multiclass Least Squares Support Vector Machines'', in Proc. of the International Joint Conference on Neural Networks (IJCNN'99), Washington DC, USA, Jul. 1999, pp. CD-ROM.

[38].	Ahmadi, M.A., Ebadi, M., Hosseini, S.M., Prediction Breakthrough Time of Water Coning in the Fractured Reservoirs by Implementing Low Parameter Support Vector Machine Approach, Fuel 117 (2014) 579–589.

[39].	Cullick, A. S., Johnson, W. D., Shi, G., Improved and More Rapid History Matching With a Nonlinear Proxy and Global Optimization. SPE Annual Technical Conference and Exhibition. 2006. San Antonio, Texas, USA: Society of Petroleum Engineers. SPE-101933-MS.

[40].	Jin, Y. 2005. A comprehensive survey of fitness approximation in evolutionary computation. Soft Computing – A Fusion of Foundations, Methodologies and Applications, 9, 3–12.

[41].	Jin, Y. Surrogate-assisted evolutionary computation: Recent advances and future challenges. Swarm and Evolutionary Computation, 2011, 1, 61–70.

[42].	Yaochu, J., Olhofer, M., Sendhoff, B., Managing approximate models in evolutionary aerodynamic design optimization. Evolutionary Computation, 2001. Proceedings of the 2001 Congress on, 2001 2001. 592–599 vol.1.

[43].	Razavi, S., Tolson, B. A., Burn, D. H., Review of surrogate modeling in water resources. Water Resources Research, 2012, 48, 6, 1-32.

[44].	Sayyafzadeh, M. History Matching by Online Metamodeling. PE Reservoir Characterisation and Simulation Conference and Exhibition held in Abu Dhabi, UAE, 14–16 September 2015. Society of Petroleum Engineers. SPE-175618-MS

[45].	Sayyafzadeh, M., Haghighi, M., Carter, J. N., Regularization in History Matching Using Multi-Objective Genetic Algorithm and Bayesian Framework. EAGE Annual Conference & Exhibition incorporating SPE Europec held in Copenhagen, Denmark, 4–7 June 2012. Society of Petroleum Engineers. SPE-154544-MS.

[46]. Zubarev, D. I., Pros and Cons of Applying Proxy-Models as a Substitute for Full Reservoir Simulations. SPE Annual Technical Conference and Exhibition. 2009. New Orleans, Louisiana: Society of Petroleum Engineers. SPE-124815-MS.

[47]. Silva, P. C., Maschio, C., Schiozer, D. J. Application of neural network and global optimization in history matching. 2008 500–5th Avenue SW, Suite 425, Calgary, Alberta, AB T2P 3L5, Canada. Petroleum Society, 22–25

[48]. Sampaio, T. P., Filho, V. J. M. F., Neto, A. D. S., An Application of Feed Forward Neural Network as Nonlinear Proxies for Use During the History Matching Phase. Latin American and Caribbean Petroleum Engineering Conference. 2009. Cartagena de Indias, Colombia: Society of Petroleum Engineers. SPE-122148-MS.

[49]. Rousseeuw, P. J.; Leroy, A. M., *Robust regression and outlier detection*. John Wiley & Sons: New York, 1987.

[50]. Gramatica, P., Principles of QSAR models validation: internal and external. *QSAR & Combinatorial Science* 2007, *26* (5), 694-701.

[51]. Goodall, C. R., *Computation Using the QR Decomposition*. Elsevier: Amsterdam, North-Holland, 1993; Vol. 9.

Chapter Seven: Conclusions and Recommendations

7.1. Conclusions

Considering the importance of thermodynamic and mass transfer parameters including equilibrium ratio, swelling factor, and minimum miscibility pressure (MMP), there have been efforts to make the performance of CO_2 based EOR methods reliable. Having deterministic tools provide easy-to-use methods to calculate parameters involved in CO_2 based EOR methods. This thesis provides easy-to-use connectionist models to determine parameters involved in CO_2 injection as well as reliable proxy model for performance prediction of CO_2 injection. The specific conclusions of this thesis are as follows:

7.1.1. Minimum Miscible Pressure (MMP) Determination

The performance and consequently ultimate oil recovery of a miscible gas injection process highly depend on the minimum miscible pressure (MMP) between the injected gas and reservoir oil. An attempt was made to develop an intelligent-based solution to calculate the MMP. Extensive measurements of miscibility data from Iranian oil fields (in addition to the literature data) were used to attain a reliable model. The following conclusions are drawn on the basis of the results of this study:

- Based on the previous works, four factors affecting the MMP of CO_2-oil system, including the reservoir temperature, C_{5+} molecular weight of oil, mole fractions of volatile components (CH_4 and N_2), and mole fractions of intermediate components (CO_2, H_2S, and C_2~C_6) of oil are considered for developing a new

correlation. Using the GEP approach, a four-parameter MMP predictive model for CO_2-oil systems was obtained.

- The new model has a higher accuracy compared to the models previously developed by Orr and Jensen, Yelling and Metcalfe, Lee [25], Glasø, and Alston et al. models. The new tool can predict the MMP within wider intervals of temperature and composition, compared to the other available correlations/techniques.

- The developed model was tested against the input variables such as temperature and compositions. It was found that the model is able to forecast the changes of the MMP with the input variables, implying a very good match between the predictions and experimental data.

- Compared to the conventional artificial neural network approaches, the GEP tool appears to be more effective and understandable for determination of MMP as a reliable and precise mathematical correlation is developed through employing this strategy.

- Estimation of MMP with a greater precision through the developed GEP model can considerably save time and money required to conduct experimental measurements. It also lowers the computational burden of mathematical methods for MMP determination that require strong knowledge in phase equilibria, transport phenomena, and computer code programming.

- The model is user-friendly and can be incorporated in commercial reservoir simulators such as ECLIPSE for miscible gas injection scenarios in oil

194

reservoirs. This modification can lead to a better design in terms of operating conditions and equipment sizing for CO_2 injection operations.

7.1.2. Equilibrium Ration Determination

A developed predictive model is introduced in this study to determine the thermodynamic equilibrium constant for hydrocarbons and non-hydrocarbons. Based on the outputs of this study, the following conclusions can be drawn:

- The high viability and capability of the LSSVM method with RBF kernel to estimate equilibrium ratio of hydrocarbons and non-hydrocarbons were successfully proven based on the available real data.

- σ^2 and γ values have significant effects on the LSSVM training results and generalization ability. Using genetic algorithm (GA), the optimal values of the σ^2 and γ were found to be 4.48527337 and 19067.1487, for hydrocarbons and 0.39915 and 3.8272 for non-hydrocarbons, correspondingly.

- A hybrid model of LSSVM and GA led to promising results for the equilibrium ratio of hydrocarbons and non-hydrocarbons. The LSSVM predictions are in very good agreement with the experimental data. The correlation coefficients and mean squared errors of the model are 0.9991 and 0.00074 for equilibrium ratio of hydrocarbons and 0.9979 and 0.044 for equilibrium ratio of non-hydrocarbons, respectively.

- The hybrid model proposed in this work is applicable within the wide ranges of thermodynamic conditions (e.g., low to high pressures and temperatures).

- The LSSVM technique was found to have favorable characteristics including generalization and efficiency. It is also a user-friendly approach, which makes it an appealing choice for modeling of highly nonlinear systems.

7.1.3. Determining CO_2-Oil Swelling Factor

We used the least square support vector machine (LSSVM) to estimate the oil swelling factor with CO_2 where the extensive experimental data were utilized. The genetic algorithm (GA) was employed to tune the model parameters. The following conclusions based on the research outputs are made:

- The feasibility and performance of LSSVM technique with RBF kernel function were evaluated using the available experimental data on estimating oil swelling factor by CO_2.

- GA was used to conduct the model parameter optimization—regularization factor and variance used in the kernel function which were obtained to be: $\gamma=33.4091$ and $\sigma^2= 0.268829$, respectively.

- The hybridized LSSVM-GA provided excellent results in predicting the CO_2-oil swelling factor. The performance of the hybrid model was evaluated by $R^2=0.9953$ and MSE= 0.0003, which shows high accuracy and reliability of the developed model.

- The relative importance of independent variables including API, temperature, pressure, and CO_2 solubility (mole fraction) on the CO_2-oil swelling factor was investigated using a promising statistical approach, called ANOVA. The API, temperature, pressure, and concentration have the highest to the lowest effect on the objective function in research study.

- The LSSVM features high efficiency, excellent generalization and routine computation methodology, which is suitable for nonlinear system identification such as the CO_2-oil system.

7.1.4. Proxy Model Development

This study presents a new simulation tool which is employed to model CO_2 miscible injection processes through a reliable and accurate manner. The main results obtained` from the present research work are as follows:

1.   The proposed proxy model to determine the ultimate recovery factor of miscible CO_2 injection method is simple, precise, and robust for the purposes of design of the EOR plants and optimal operating procedure.

2.   Based on the magnitudes of the statistical indexes including MSE, ARD, AARD, and residual values, the proxy model developed in this study provides reliable results, implying the model is statistically acceptable.

3.   The Leverage method was employed to validate the applicability range of the proxy model for miscible CO_2 injection processes and to evaluate the quality of the simulation outputs. According to the William plot, the hybridization of the LSSVM method and Box–Behnken design (BBD) approach for RF estimation of miscible CO_2 injection operations is statistically correct so that the hybrid model can forecast the production behavior/trend of the recovery technique.

4.   Employing a proxy model, a parametric sensitivity analysis was performed to study the impacts of important parameters (e.g., bottom-hole pressure, oil production rate, and CO_2 injection rate) on the target variable. It is concluded that CO_2 injection rate is the most important factor, affecting production performance. The outcomes are

satisfactory, as well. This phase of study again confirms the reliability and appropriateness of the developed model.

5. The model developed in this study can be linked to the commercial reservoir simulation packages such as computer modeling group (CMG) software to improve their performance and accuracy while forecasting the recovery factor for the miscible CO_2 injection processes.

7.2. Recommendations

In this thesis "Gene Expression Programming" was employed to develop a reliable correlation for MMP determination. It is recommended that applying this promising approach for proposing easy-to-use and accurate correlations for other thermodynamic parameters, i.e., solution gas to oil ratio, dew point pressure, equilibrium ratio, and binary interaction parameters in equation of sates. Also, incorporation of such a model with dynamic reservoir simulators might be an interesting work.

This work proposes low parameter model for predicting equilibrium ratio for both hydrocarbons and non-hydrocarbon gases. It is recommended to apply other statistical and stochastic methods to determine this parameter and compare the results with this work. Also, hybrid of other optimization algorithms including particle swarm optimization (PSO), imperialist competitive algorithm (ICA), and evolutionary methods for optimizing hyper parameters of LSSVM model is highly recommended.

Also, in a case of CO_2-oil swelling factor, it is suggested that optimization of oil production from immiscible CO_2 injection using optimizing CO_2-oil swelling factor and oil viscosity reduction could be part of future works.

Different intelligent based methods including fuzzy logic, adaptive neuro fuzzy interface system (ANFIS) and hybrid methods can be employed to develop a connectionist proxy model for performance prediction of CO_2 injection. Also, other types of CO_2 injection including simultaneous water alternating gas (SWAG) injection, water alternating gas (WAG) injection, and carbonated water injection could be selected as a base case scenario for proposing a proxy model. Finally, considering a real depleted oil reservoir with realistic costs (oil price, injection facilities, CO_2 price,..), i.e., one of the offshore reservoirs in Newfound and Labrador, might be good option for developing a predicitve proxy model.